Durham E-Theses

The Synthesis of Copolymers for Self-Assembly in Non-Polar Solvents and Tribological Testing

DAY, DANIEL

How to cite:

DAY, DANIEL (2021) *The Synthesis of Copolymers for Self-Assembly in Non-Polar Solvents and Tribological Testing*, Durham theses, Durham University. Available at Durham E-Theses Online: http://etheses.dur.ac.uk/14123/

Use policy

The Synthesis of Copolymers for Self-Assembly in Non-Polar Solvents and Tribological Testing

A thesis submitted in fulfilment of the degree of

Doctor of Philosophy

By

Daniel Day

Department of Chemistry

Durham University

2021

The Synthesis of Copolymers for Self-Assembly in Non-Polar Solvents and Tribological Testing

Abstract

The synthesis and properties of block copolymers have long been an important field of research. Recently, the self-assembly of block copolymers in a solvent selective for one block and the resultant formation of nano-objects with a variety of morphologies has attracted a lot of attention. Throughout this work, block copolymers comprising a block prepared using non-polar dienes such as 1,3-isoprene and 1,3-butadiene have been prepared such that a second block, comprising highly polar functionalities can be dispersed in non-polar solvents. Taking a very 'academic' approach, block copolymers of isoprene and various methacrylates have been prepared by a change of mechanism polymerisation (CHOMP) where living anionic polymerisation (LAP) was used to prepare end-capped polyisoprene which was then used as a macroinitiator for the atom-transfer radical polymerisation (ATRP) of methyl methacrylate (MMA) or *N,N*-(dimethylamino)ethyl methacrylate (DMAEMA). The block copolymers were then dispersed into non-polar solvents by solvent-switching resulting in self-assembly into micelles with different morphologies which were characterised by TEM and DLS. The same block copolymers of isoprene and the aforementioned methacrylates were investigated as potential friction modifiers in lubricant formulations by dispersion into non-polar base oils. PI-*b*-PDMAEMA was found to be an effective friction modifier both in neat base oil and full lubricant formulations where many other competing, surface-active additives are present. These results were used to guide the development of a more commercially feasible synthetic route towards structurally similar polymeric additives. Thus a series of microstructural block copolymers of homopolybutadiene, comprising 'blocks' rich in the 1,4- and 1,2-microstructures respectively, was prepared by LAP. A selective ene reaction was then carried out with maleic anhydride, resulting in blocky, amphiphilic copolymers which were then reacted by imidisation to impart a tertiary amine functionality pendant to the polymer chain. These maleinised and imidised polybutadienes were also found to be effective friction modifiers, offering a potential route to a new, commercially-viable class of polymeric friction modifier.

Table of Contents

List of Figures

List of Tables

List of Schemes

List of Abbreviations

ATRP	Atom transfer radical polymerisation
BHT	Butylated hydroxytoluene
BI	1-Butyl iodide
Bpy	2,2-Bipyripyl
BuLi	Butyllithium
CDCl$_3$	Deuterated chloroform
CHOMP	Change of mechanism polymerisation
CMC	Critical micelle concentration
CuBr	Copper(I) bromide
Đ	Dispersity
DCM	Dichloromethane
DLS	Dynamic light scattering
DMAPA	3-(Dimethylamino)-1-propylamine
DMSO-D$_6$	Deuterated dimethyl sulphoxide
DP	Degree of polymerisation
EI	Ethyl iodide
EO	Ethylene oxide
FTIR	Fourier-transform infrared spectroscopy
GMO	Glycerol monooleate
PBD-IM	Imidised polybutadiene
LAP	Living anionic polymerisation
PBD-MA	Maleinised polybutadiene
M$_n$	Number-average molar mass
MTM	Mini-traction machine
NMP	Nitroxide-mediated polymerisation
NMR	Nuclear magnetic resonance
OFM	Organic friction modifier
OI	1-Octyl iodide
PAO	Polyalphaolephin
PBD	Polybutadiene
PDMAEMA	Poly((*N,N*-dimethylamino) ethyl methacrylate)
PFM	Polymeric friction modifier
PI	Polyisoprene
PI-*Br*	Bromide-end-capped polyisoprene
PI-*OH*	Ethylene oxide-end-capped polyisoprene
PISA	Polymerisation-induced self-assembly
PMDETA	*N,N,N',N',N''*-pentamethyldiethylenetriamine
PMMA	Poly(methyl methacrylate)
PTFE	Poly(tetrafluoroethylene)

QDMAEMA	Quaternised (N,N-dimethylamino) ethyl methacrylate)
QISA	Quaternisation-induced self-assembly
RAFT	Reversible addition-fragmentation chain-transfer polymerisation
RDRP	Reversible-deactivation radical polymerisation
SEC	Size exclusion chromatography
TEM	Transmission electron microscopy
T_g	Glass transition temperature
THF	Tetrahydrofuran
TMEDA	N,N,N',N'-Tetramethylethylenediamine
VI	Viscosity index
wt%	Weight percentage
ZDDP	Zinc dialkyldithiophosphates
$\tilde{v}$	Wavenumber

Statement of Copyright

The copyright of this thesis rests with the author. No quotation from it should be published without the author's prior written consent and information derived from it should be acknowledged.

Acknowledgements

Firstly, I would like to thank Prof. Lian Hutchings for his supervision over the past 4 years. I honestly cannot envisage myself having managed to complete a PhD with any other supervisor, let alone enjoying it!

This project has been particularly dynamic and enjoyable thanks to the contributions of everyone at Synthomer and Croda. In particular I would like to acknowledge Paul Brooks and Dave Gillespie for their support which has been particularly important in the past 12 months. I hope we can work together again in the future.

Thank you to everyone I have worked with in the Hutchings group, particularly Antonella, Lloyd, Jon, Tash, Utku, Matt and Charles. Thank you also to everyone in SOFI CDT and my cohort. You have all been brilliant friends and colleagues.

Thank you to my Mum and Dad for their constant support and encouragement throughout my PhD and life in general! You both work harder in an average day than I have for this entire thesis, and I am unbelievably proud to have such wonderful role models.

Finally, thank you to my fiancée Natasha for all your support and love. I am endlessly in awe of you. The last 5 years have been the happiest of my life and I cannot wait for our future together…

1. Introduction

Almost exactly 100 years ago, Hermann Staudinger published the ground-breaking, 'Über Polymerisation' in which the key claim was that materials such as rubber are made up of repeat units connected by covalent bonds, rather than mixtures of small molecules held together by intermolecular forces, which was the prevailing theory at the time.[1] Industrial researchers such as Wallace Carothers widely accepted the hypothesis and Carothers went on to invent nylon by polycondensation, where the high molecular weight of the products could be inferred by the mass of the condensation by-product.[2] However, academics remained unconvinced by Staudinger's proposal until the evidence gathered from chemical modifications,[3] ultracentrifugation[4] and x-ray crystallography[5] became overwhelming. Staudinger's breakthrough was finally recognised when he was awarded the Nobel prize for chemistry in 1953.

Since the widespread acceptance of Staudinger's initial theory, research into polymers has exploded. Their unique properties and almost infinite variability has seen them exploited for many distinctive applications, for which other materials and additives are inadequate. The broad applicability of polymers has driven significant research into novel synthetic approaches whereby many different monomers can be polymerised into macromolecules with varying architectures and properties.

In particular, the synthesis of copolymers remains a significant area of interest because it enables the combination of diverse properties into a single polymer sample. This is particularly true of amphiphilic copolymers where monomers that produce homopolymers of differing solubility are combined, often to allow for the dissolution of a typically insoluble polymer into a specific solvent. For example, as described in this thesis, non-polar and polar monomers may be combined to prepare copolymers for the solubility and/or self-assembly of the latter in strongly non-polar solvents. In the context of this work, *amphiphilic* will be used to describe copolymers which are made up of monomers with different solubilities (rather than exclusively for molecules comprised, specifically, of hydrophilic and hydrophobic regions, as is common in academic literature).

The monomer sequence in a copolymer can be controlled to impart different properties on the final product. Typical arrangements of monomers in a linear copolymer

are shown below in Figure 1.1. The choice of synthetic method can be tailored to attain each of the 4 monomer sequences commonly targeted for linear copolymers. For example, a block copolymer would typically require sequential monomer additions and a living/controlled polymerisation mechanism.[6] Whereas the remaining 3 sequences of monomers would typically be produced by a 1-pot statistical process where both monomers are present in the reactor at the point of initiation. In this instance, the sequence is dictated by the reactivity ratios of the 2 monomers which defines the copolymerisation kinetics.[7]
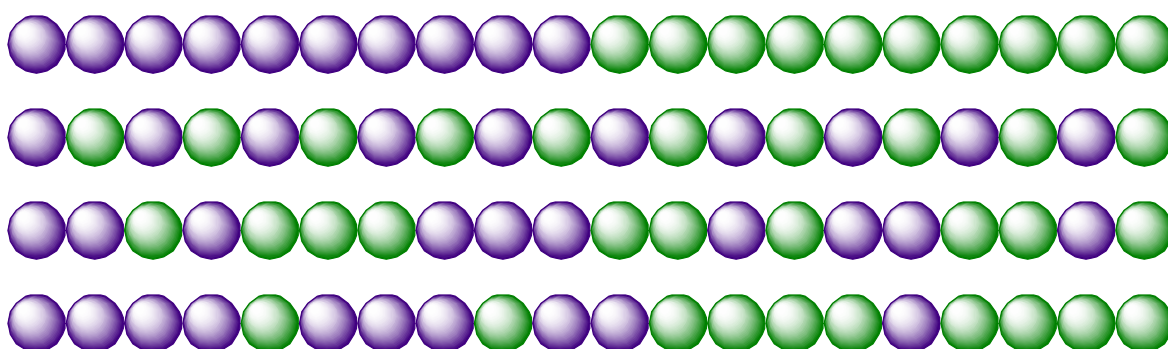
Figure 1.1: Diagram showing 4 common monomer sequences of linear copolymers. From top to bottom: block; alternating; random and gradient

1.1. Polymer Synthesis

There are 2 broad classes of polymer synthesis. The first is step growth, where multifunctional monomers react together to form oligomers which can then react further, building up the molecular weight in a stepwise fashion to generate polymers.[8] The 2 key types of step growth polymerisation are polyaddition, where the polymerisation mechanism has a 100 % atom economy (e.g. for polyurethanes) and polycondensation which involves the production of a small molecule by-product (e.g. water in polyester synthesis). A fundamental aspect of step growth polymerisation is the Carothers equation, which can be used to calculate the degree of polymerisation from the conversion of monomer to polymer.[9]

The alternative to step growth polymerisation is chain growth where the polymerisation only proceeds by monomer insertion at the chain end, one monomer unit at a time, and where the monomer is most commonly an alkene.[10, 11] Chain growth polymerisation is characterised by the occurrence of 3 distinct steps: initiation, which can

be achieved by chemical or energetic means to begin the polymerisation; propagation where monomers insert at the single, active site on the polymer chain and termination where the propagating site on the polymer chain is deactivated, preventing any further monomer insertion for that chain.[12] The main types of chain growth polymerisation are described in the following sections.

1.1.1. Free Radical Polymerisation

Free radical polymerisation (FRP) is a chain growth polymerisation mechanism where the active propagating species is a radical. FRP can generally be carried out under relatively benign conditions because the propagating radicals tolerate small amounts of air and water. For this reason, it is a facile, versatile and widely employed mechanism on a commercial scale.[13] FRP is compatible with a wide range of functional groups, and as such a very wide range of vinyl (alkene) monomers can be polymerised by this method.[14]

There are many mechanisms of initiation in free-radical polymerisation, but it is most commonly induced by a chemical initiator containing a peroxide, persulphate or azo functional group. The initiator undergoes homolytic bond fission (for example by thermal decomposition, photolysis or a simple redox reaction) to produce the active, initiating radicals. Other common methods of initiation are thermal- and photoinitiation.[13] In radical polymerisation, the rate of initiation is typically slow in comparison to the rate of propagation, contributing to a high dispersity in the products of the reaction.[15]

Competing with propagation are several termination mechanisms. These can involve reactions between two polymeric radicals such as combination (homolytic bond fusion) and disproportionation (hydrogen abstraction), or with other species such as oxygen or radical scavengers. Another common occurrence is chain transfer, where the radical on the propagating chain end is passed onto another species such as solvent or monomer. Following chain transfer, the newly produced radical can sometimes re-initiate chain growth. Termination and chain transfer reactions, that take place during the reaction also contribute to a wider dispersity and molecular heterogeneity in the final polymer architecture and molecular weight.[13]

In spite of the limitations, free radical polymerisation remains a significant method for industrial polymer synthesis, accounting for approximately 50 % of all synthetic plastics

produced since the 1980s.[14, 16] The main industrial methods exploiting FRP are emulsion, solution, suspension and bulk polymerisation, which are chosen depending on the polymer being prepared and its desired end-use.[13] There are countless applications of polymers prepared by free radical polymerisation, including polymer composites, adhesives, coatings and lubricant additives.[17]

1.1.2. Ionic Polymerisation

Ionic polymerisations are a form of chain growth polymerisation where the active, propagating species is either a cation or an anion.[15] Because of the high reactivity of ions, especially carbanions and carbocations, these polymerisations must often be carried out under inert conditions, using highly purified reagents. The most common monomers polymerised in this fashion are substituted alkenes, although heteroatom-containing cycles (e.g. siloxanes, epoxides, aziridines etc.) can also be polymerised in a controlled fashion by these mechanisms.[18, 19]

In ionic polymerisations, a fast rate of initiation (with respect to propagation) is crucial in giving a final product with predictable molecular weight and low dispersity. Also key in choosing the initiator, is the presence of a counter-ion to neutralise the charge. The association of the counter-ion (e.g. tightly with covalent character or as free ions) can be influenced by the solvent polarity, and as such can have a great impact on the nature of the polymer formed. This is also in contrast with radical polymerisation where the initiator does not influence the propagation step once consumed during initiation.[15]

1.1.2.1. Living Anionic Polymerisation

The discovery of living anionic polymerisation (LAP) by Szwarc in 1956 was instrumental in the history of polymer synthesis.[20] It was the first example of a living polymerisation, where the propagation proceeds in the absence of inherent termination mechanisms, opening up the possibility to produce well-defined block copolymers, a range of complex (branched) architectures, all with low dispersity and predictable molecular weights at 100 % conversion of the monomer.[21, 22] Whilst it remains a hugely important technique that has been widely exploited by industry, LAP suffers from the key drawback of being highly sensitive to impurities such as water, oxygen and carbon dioxide. This necessitates the use of highly inert conditions and stringently purified reagents.[23]

4

In order to qualify as a 'living' polymerisation, the kinetics must generally obey the following 2 conditions: $k_{initiation} \gg k_{propagation}$ and $k_{propagation} \ggg k_{termination}$. The latter shows that for a polymerisation to be truly 'living', it must proceed in the absence of inherent termination mechanisms. The anionic polymerisation of non-polar monomers typically meets these stipulations meaning that it qualifies as 'living' and there are many examples of cationic polymerisations which can also be classified in this fashion. This is not the case for radical polymerisation which contains self-termination mechanisms (see section 1.1.1). These termination steps compete with propagation, causing active chains to 'die' thus stopping the procession of the polymerisation causing a large variability in the final molecular weight.[15]

The range of monomers that can be easily polymerised by living anionic polymerisation is limited by the high reactivity of the propagating carbanion with electrophiles and acidic protons.[22, 24] Non-polar monomers such as 1,3-butadiene, 1,3-isoprene and styrene can be readily polymerised by conventional LAP at room temperature, and have been produced by this mechanism, on a commercial scale, for several decades. Polar monomers such as acrylates and methacrylates, which can be straightforwardly polymerised by other chain growth mechanisms, cannot be polymerised easily by LAP due to the anion undergoing competing nucleophilic attack on the carbonyl functionality (see mechanisms of termination in Figure 1.2).[25, 26] The high reactivity of the anion also prevents the polymerisation of monomers containing acidic hydrogens (such as acrylic acid) and the use of polar, protic reaction solvents.
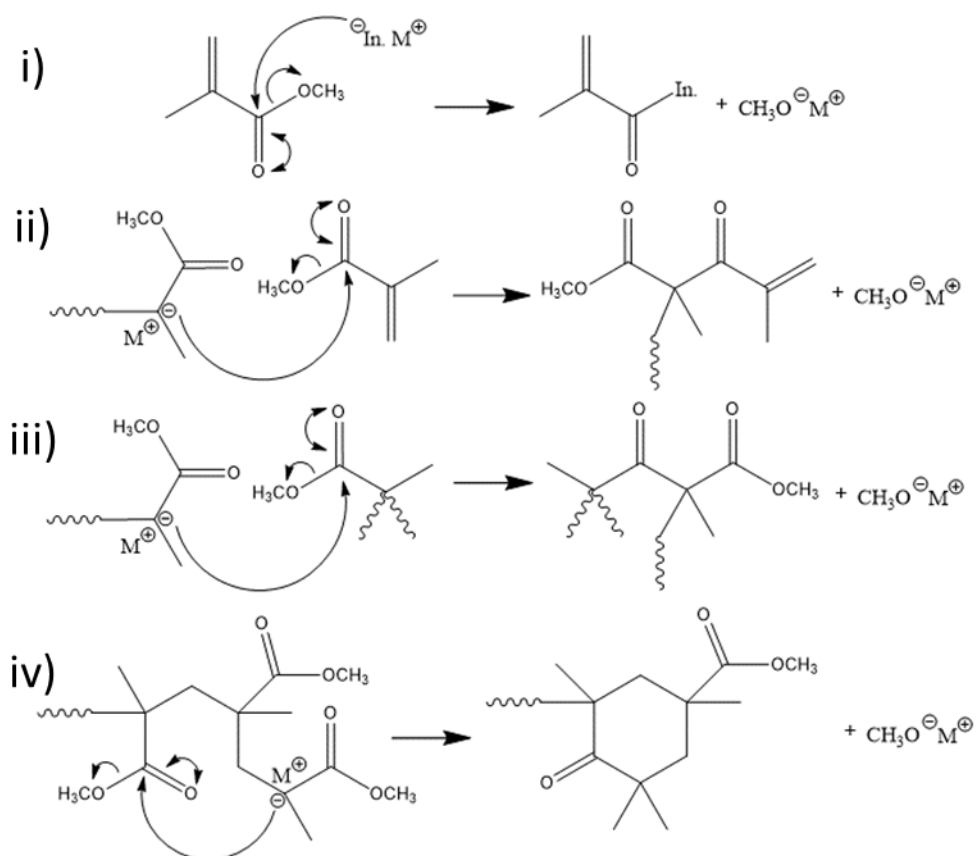
Figure 1.2: The 4 mechanisms of termination which may occur during the anionic polymerisation of alkyl methacrylate monomers (shown for MMA in all schemes). From top to bottom: i) Initiator destruction, ii) Monomer carbonyl attack, iii) Intermolecular polymer termination and iv) Intramolecular termination mechanism

In order to polymerise methacrylate monomers by an anionic mechanism, particular conditions must be used to eliminate the various termination reactions shown in Figure 1.2. Anionic polymerisation of methyl methacrylate was first reported by Szwarc, by use of a living polystyryl sodium initiator in THF at -78 °C.[26] However, the polymerisation was not truly 'living' because they were unable to polymerise styrene (or MMA) from the living poly(methyl methacrylate) in a second monomer addition step, because of what they described as self-termination of the polymer. This topic has been widely investigated over the past several decades with the aim of improving control and developing a truly living anionic polymerisation process for methacrylates.[25]

To eliminate the unfavourable side reactions, several issues must be addressed. The initiator used is critical because the carbonyl acts as a harder electrophile than the alkene double bond.[27, 28] For this reason, smaller, commonly-used initiators such as *sec*-butyllithium are undesirable because they are highly nucleophilic, meaning that attack on

the harder, electrophilic carbonyl to form lithium alkoxides is far more likely (Figure 1.2i).[29] For example, Szwarc's initial paper only successfully polymerised MMA from living polystryl sodium to prepare PS-*b*-PMMA block copolymers.[26] Other bulky initiators such as diphenylhexyllithium (formed by the reaction of butyllithium with *1,1*-diphenylethylene) are sterically-hindered nucleophiles, meaning that they attack the more sterically-available alkene double bond, initiating the polymerisation.[30] This allows for the preparation of PMMA homopolymers rather than blocks initiated from already living polymer chains.

One of the more prevalent termination reactions is the intramolecular, backbiting reaction, where the active propagating anion reacts with the carbonyl of the antepenultimate unit of the same chain (Figure 1.2iv). This reaction, first identified using IR spectroscopy by Goode *et al* in 1960, forms a 6-membered aliphatic ring with the expulsion of methoxide salt.[31] Unlike the other termination mechanisms that take place exclusively on the unconsumed monomer, this reaction remains problematic even at 100 % conversion. The 6-membered ring remains awkward once formed, because the carbonyls are capable of enolising which can terminate other (still living) chains.[22] The use of low temperatures (-78 °C in Szwarc's initial paper) have been found to virtually eliminate this intramolecular side reaction, however, such low temperatures are commercially impracticable due to the high cost, energy and health and safety concerns.[26] This means that other ways of limiting this side reaction need to be found before the reaction can be carried out industrially.

Another issue with the LAP of methacrylates is that the ion pair exists in an equilibrium that stabilises by resonance to form an enolate anion which can form aggregates with the counter-ion. The rate of propagation for the aggregated enolate is lower than for non-aggregated species.[32] The difference in rates of propagation across the equilibrated species causes a significant broadening in the dispersity of the product. A fast equilibrium between aggregated and non-aggregated species helps keep the overall rate of propagation constant, thus producing narrow dispersity. One way in which this can be accomplished is by use of more polar solvents where the equilibrium lies more towards the free ions.[33] Certain additives can also be useful in controlling the living anionic polymerisation of methacrylates. For example, Fayt *et al* used ^{7}Li NMR spectroscopy to show lithium chloride (LiCl) forms complexes with the active, propagating enolate anion

chain end to significantly reduce the dispersity in final molecular weight of PtBA.[34] No additives were used in the initial Szwarc paper which suggests that, although they achieved a good yield, the polymers likely had poor control in the molecular weight dispersity.[26]

The most successful, commercial reports for the anionic polymerisation of acrylates/methacrylates have been patents from Kuraray Co. Ltd. In 2001, Kuraray first patented the anionic polymerisation of block copolymers made up of different acrylates in toluene using a bulky trialkylaluminium additive.[35] These conditions allowed for a reasonable molecular weight (11600 g mol^{-1}) with a narrow dispersity (1.08) and a yield close to 100 %. However, the reaction still required a temperature of -60 $^{\circ}$C which remains difficult on an industrial scale. Since then, they have published several patents in the same field with iterations to the experimental procedure.[36, 37] The most recent is for the polymerisation of PMMA-*b*-PnBA-*b*-PMMA triblock copolymers, in which the methacrylate blocks were polymerised at room temperature in the presence of a bulky isobutyl bis(2,6-di-t-butyl-4-methylphenoxy)aluminium additive.[38] These block copolymers had a low dispersity (<1.10) up to a molar mass of 69 kg mol^{-1}, however the proportion of PMMA in the final product was less than 10 mol% in all cases, meaning that the majority of the product was the PnBA block which was polymerised at -30 $^{\circ}$C. The work by Kuraray represents significant progress in the field for the anionic polymerisation of acrylates/methacrylates, however, there clearly remains a need for progress for the process to be cost-effective on a large scale.

1.1.3. Reversible-Deactivation Radical Polymerisation

Reversible-Deactivation Radical Polymerisation (RDRP) is the IUPAC term that describes a group of controlled radical polymerisations that were developed in the 1990s.[39] The aim of RDRP is to give control to free radical polymerisation by suppressing termination and chain transfer mechanisms, such that the reaction becomes somewhat more 'living'. Unlike true living polymerisations the termination mechanisms remain, however, the active radical concentration is so low that such reactions are greatly suppressed.[40]

The synthetic procedures are designed to reversibly deactivate the propagating radical species. This deactivation equilibrium maintains a low concentration of radicals which decreases the rate of termination mechanisms overall. The small proportion of active

radicals can still undergo monomer insertion steps, increasing the molecular weight in a more controlled fashion than with free radical polymerisation.[41] The 3 most common RDRP mechanisms are reversible addition-fragmentation chain-transfer (RAFT) (see 1.1.3.1), nitroxide-mediated radical polymerisation (NMP) (see 1.1.3.2) and atom transfer radical polymerisation (ATRP) (see 1.1.3.3).

1.1.3.1. Reversible Addition-Fragmentation Chain-Transfer Polymerisation

First reported in 1998, reversible addition-fragmentation chain-transfer (RAFT) polymerisation is a metal-free RDRP mechanism where the radical deactivator is a covalently bound dithioester functional group (shown below in Figure 1.3).[42] This group acts to set up an equilibrium, with the dithioester reversibly adding to the active chain end.[43] RAFT has proven to be highly effective for the controlled polymerisation of a wide variety of monomers, often with a high end-group fidelity which lends itself to the preparation of block copolymers.[44, 45] RAFT polymerisation has frequently been used in the preparation of self-assembling diblock copolymers by polymerisation-induced self-assembly (PISA) (see 1.2.3).[46-49]
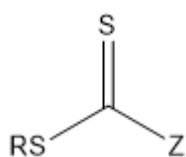
Figure 1.3: General chemical structure of a dithioester, reversible-addition fragmentation chain-transfer (RAFT) agent used to control RAFT polymerisations.

One of the key features of the RAFT agent in Figure 1.3 is the 'Z' group which acts to stabilise the dormant radical which forms on the central sp^2 carbon. Common examples are phenyl substituents, however, the choice of 'Z' group needs to be tailored, depending on the monomer being polymerised and/or the polymer structure desired. The 'R' group must also be chosen with care, such that it can be stabilise the radical formed on fragmentation of the dithioester, but also be reactive enough to rapidly re-initiate polymerisation to ensure a narrow dispersity in the final molecular weight. RAFT polymerisation can be used for wide ranges of monomers and solvents with good control of molecular weights and dispersity.[43]

The most obvious drawback to RAFT polymerisation is the RAFT agent itself. Clearly a universal RAFT agent would be preferable, however, different RAFT agents must often be

carefully selected depending on the reactivity of the monomer and the desired product.[50] The synthesis of dithioester molecules often requires multiple steps and rigorous purification, meaning that there are few examples of commercial scale-up,[51] which can be costly and time consuming. This cost is then passed on into the production of the polymers, which is particularly high for low molecular weights where more RAFT agent is required.[52] Furthermore, the RAFT agent is often malodorous and dark pink or red in colour. This renders the resulting polymers pink or red, unless the RAFT agent is removed by post-polymerisation purification. Producing polymers without removal of the RAFT agent significantly limits the scope of possible applications. Removal is practically simple and has been reported in several different ways, but it adds on extra steps and cost to the process.[53]

Recent research in RAFT polymerisation has focussed on practical methods for carrying out the process, including novel initiation procedures,[54] such as photoinitiation and redox initiation as opposed to the more conventional, thermal initiation which can be complicated by the prevalence of auto-initiation and chain transfer. The use of photo- and redox initiation can reduce the need for high temperature which limits these problems and can also allow for propagation to be switched 'on' and 'off' with ease, enabling the preparation of complex architectures.[55] There has also been significant research into finding sulphur-free, commercially-viable alternatives to the dithioester RAFT agent. One of the most commonly reported recently has been metal-catalysed chain transfer polymerisation (CCTP).[56] There are also reports of vinyl-terminated sulphur-free RAFT, which also avoids the use of metal catalysts during the polymerisation.[57]

1.1.3.2.　Nitroxide-Mediated Radical Polymerisation

Nitroxide-mediated radical polymerisation (NMP) employs a nitroxide which can reversibly bind to the propagating radical, giving a dormant chain end that prevents termination.[58] Nitroxides were initially used in radical polymerisation by Rizzardo and Solomon to investigate initiation by radical trapping.[59] The field of NMP gained significant interest when Georges *et al.* demonstrated that the use of nitroxides in the radical polymerisation of styrene allowed for conversions up to 90 % with a dispersity of <1.3.[60] The nitroxide forms a covalent bond with the propagating chain-end which renders the chain dormant. However, the formation of the key covalent bond is reversible at elevated temperatures and the nitroxide can break off from the chain end to re-generate the active

radical and allow for monomer insertion to take place. NMP is practically simple to carry out, however it is less versatile than RAFT and ATRP with respect to the choice of monomers that can be polymerised in a controlled fashion. NMP also suffers other limitations including slow polymerisation kinetics which greatly increases reaction times and can be challenging for the polymerisation of methacrylates because of side reactions that can take place.[61]

1.1.3.3. Atom Transfer Radical Polymerisation

Atom Transfer Radical Polymerisation (ATRP) was first reported simultaneously (and independently) by Sawamoto and Matyjaszewski in 1995.[62, 63] The reversible deactivation equilibrium between active and dormant radical, shown below in Figure 1.4, is established by the introduction of a transition metal catalyst with two easily accessible oxidation states which differ by 1 electron (frequently copper (I)/copper (II) because of its high activity). The exchange dynamics between the active and dormant radical are crucial in controlling an ATRP reaction. It is important that the rate of deactivation is far greater than the rate of activation ($k_{act.} \ll k_{deact.}$) as this maintains a low concentration of active radicals which suppresses the termination reactions.[64] At any point in an ATRP reaction it is commonly desirable for the proportion of active radical (compared to dormant) to be less than 0.1 %.[65] By tuning the nature of the metal catalyst, ligand, solvent, and temperature, the equilibrium can be pushed towards either the active or dormant state.[66] An alkyl halide that can undergo homolytic bond fission to form a radical is usually used as the initiator.[67]
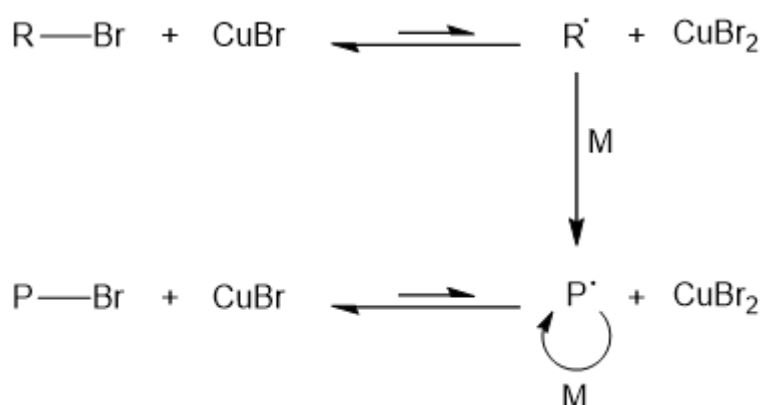
Figure 1.4: Mechanism of atom-transfer radical polymerisation (ATRP), showing the equilibrium formed between dormant (left) and active (right) propagating radical by introduction of a metal catalyst (in this case, CuBr)

ATRP has proven particularly useful for the polymerisation of polar monomers such as acrylates/methacrylates. Higher polarity monomers generally lead to higher equilibrium constants, caused by an increased rate of activation.[64, 66] Conversely, this means the use of ATRP in polymerisation of non-polar dienes is complicated. This is particularly because of the poor solubility of metal catalysts within the non-polar monomers/solvents and low rates of propagation, which are exacerbated by the diene competing with ligands to bind to the metal catalyst.[65] Slow reactions can often be compensated for by an increased temperature, however, butadiene and isoprene have very low boiling points (-4.4 and 34 °C respectively) meaning that high reaction temperatures are not easily or safely achievable. There are very few reports of the 'successful' polymerisation of isoprene or butadiene by ATRP. Moreover, where attempts to polymerise dienes by ATRP are reported, the polymerisations are poorly controlled in comparison to analogous results for other, more polar monomers, with low conversions and high dispersity in the final molecular weight.[68-71] For the preparation of non-polar polymers by ATRP, long-chain alkyl acrylates and methacrylates are more commonly used.[72, 73]

One of the key focusses of recent research in ATRP is to eliminate/reduce the high concentration of copper required to activate the dormant radicals, due to environmental and health concerns.[74, 75] A high concentration is required at the beginning of the reaction to compensate for chain termination steps which result in copper catalysts being 'trapped' as the deactivator, copper (II). Activator regeneration techniques such as Initiators for Continuous Activator Regeneration (ICAR) and Activator Regenerated by Electron Transfer (ARGET) ATRP both work on the principle of regenerating the activator, Cu(I) catalyst, from deactivator, Cu(II), by use of a reducing agent such as ascorbic acid.[76] In Supplemental Activation Reducing Agent (SARA) ATRP, the copper (I) catalyst is generated *in situ* by oxidation of copper (0) metal.[65, 77] The copper metal can also reduce Cu(II) to Cu(I) thus also acting as a regenerating agent.

1.1.4. Change of Mechanism Polymerisation (CHOMP)

Change of Mechanism Polymerisation (CHOMP) is a term first coined by Hillmyer in 1999,[78] however the concept had been applied prior to this, most commonly with an end-capped polymer prepared by living anionic polymerisation or ring-opening metathesis polymerisation (ROMP) as the first step.[79, 80] CHOMP is a means of combining

polymerisation mechanisms in the preparation of copolymers. The reason for using this method can vary, but it is most commonly used for synthesising copolymers where the constituent monomers are incompatible with a single polymerisation mechanism. For example, the polymerisation of polar monomers by anionic polymerisation can be complicated by the inherent self-termination mechanisms (see section 1.1.2.1) and as such, it can be simpler to use an end-capping procedure in the anionic polymerisation, followed by polymerisation of the polar monomer by an RDRP method.[81, 82]

Whilst CHOMP is a unique way of preparing block copolymers, it can be complicated, with several steps often needed to prepare the final copolymer. This makes it of limited viability for commercial scale due to cost and variability of polymerisation conditions. A more attractive approach for CHOMP has been reported where block copolymers were prepared by different mechanisms in a one-pot procedure. However, this is still practically more complicated than the preparation of block copolymers using a single mechanism, either by sequential monomer addition or a fire and forget process which utilises the reactivity ratios of the constituent monomers in reaction with each other.[83, 84]

1.1.5. Post-Polymerisation Modification

Another useful approach for controlling the chemistry, structure and architecture of polymers is by post-polymerisation functionalisation. This can be a useful and versatile strategy for preparing polymeric structures that ordinarily would not be possible to synthesise by a simple polymerisation method, broadening potential industrial applications.[85] For example, LAP is often highly complicated for monomers containing polar functionalities (see section 1.1.2.1), limiting its commercial use to non-polar monomers such as dienes and styrene. Although polydienes are highly non-polar, they most commonly polymerise into microstructures that leave double bonds either pendant to, or in the polymer backbone. These can be useful handles to introduce polar functionality (e.g. thiols and epoxides) whilst maintaining all of the initial benefits of living LAP.[86, 87]

The use of post-polymerisation modification simply requires the use of 'small molecule reactions' in macromolecules.[85]. An example of a modification reaction for polydienes is maleinisation (see scheme below in Figure 1.5) whereby the alkene bonds of polydienes can be reacted with maleic anhydride to directly attach the anhydride functionality. This can be achieved in several ways, most commonly through a radical mechanism.[88-90] Typically, maleinised polybutadienes have found commercial use as compatibilisers and adhesives. Similarly to epoxides, the presence of an anhydride allows for ring-opening to the diacid which can then be used to generate a wide variety of functional groups.
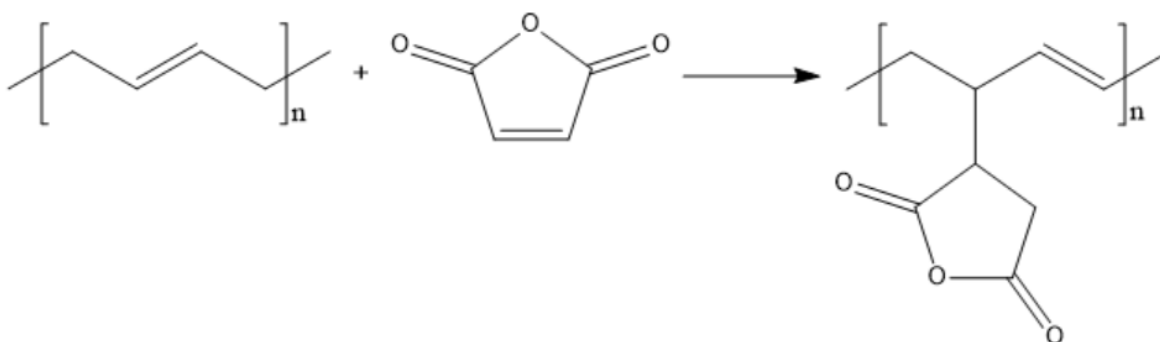
Figure 1.5: Reaction scheme showing the maleinisation reaction of polybutadiene

1.1.5.1.   Preparation of Quaternised Polymers

Cationic polymers are desirable for a number of applications such as flocculants, ion-exchange resins, and they also exhibit anti-microbial properties.[91, 92] There are few functional groups that can tolerate a permanent positive charge, with nitrogen-, phosphorus- and sulphur-based groups being the most common examples.[93] In particular, nitrogen-containing polymers (e.g. poly(*N,N*-(dimethylamino)ethyl methacrylate) (PDMAEMA)) have often been used for functionalisation by quaternisation with alkyl halides. This is attractive because quaternised PDMAEMA (PQDMAEMA) has increased polarity which can enhance solubility in water as is often advantageous for applications in drug delivery.[94]

Preparation of PQDMAEMA can be achieved in one of two ways. The monomer itself can be quaternised before polymerisation. This allows for a higher degree of charge within the final polymer, however, the monomer requires complicated purification and can act as a surfactant during the polymerisation which can make traditional processes

complicated. The alternative is by post-polymerisation functionalisation which is practically easier to do, however, the degree of quaternisation may be limited by steric and electronic effects.[93]

1.2. Phase Separation in Polymer Systems

Immiscible homopolymers can be blended in the melt by high shear mixing.[95-98] However, when this mixing is stopped, the blend will undergo macrophase separation to form discrete polymer domains which have morphologies and sizes that are dependent on the relative volume fractions of the constituent polymers, the Flory-Huggins interaction parameter (χ) and time.[99, 100] Although phase separation of polymers is thermodynamically favourable, the blend will never separate completely into 2 distinct phases because of the slow kinetics of the separation. Equation 1.1 shows the Flory-Huggins theorem for describing the enthalpic and entropic contributions of the Gibbs free energy of mixing for immiscible homopolymers.[101]

$$\Delta G_m = RT\left(n_A ln\phi_A + n_B ln\phi_B + n_A \phi_B \chi_{A,B}\right)$$

Equation 1.1: The Flory-Huggins equation for the Gibbs energy of mixing for immiscible homopolymers A and B.

Flory-Huggins theory was initially used to describe the dynamics of a polymer in solution, however it is commonly applied to polymer blends and also to block copolymers. The behaviour of polymer systems for many different applications, including in sensors, membranes and drug delivery, has been described using the equation.[102] The Gibbs energy is negative for spontaneous processes, meaning that for the process of mixing immiscible polymers (and therefore the Flory-Huggins equation) Gibbs energy is positive (i.e. not spontaneous).[103] The equation shows how de-mixing or phase separation is affected by the entropic and enthalpic terms. The Flory-Huggins interaction parameter (χ) is used to describe the non-ideal contributions to free energy and is made up of entropic and (temperature-dependent) enthalpic terms.[10] The enthalpic energy of dispersion can be positive or negative, depending on the choice of monomers, and can be used to predict if de-mixing is spontaneous.[104]

If 2 immiscible polymers are covalently bound to form a block copolymer, the phase separation is further constrained, meaning that the system instead undergoes microphase separation.[106] Figure 1.6 shows how the phase separation of linear diblock copolymers of immiscible blocks results in mesophases with distinctive morphologies, comprising regions of each block within the copolymer. The exact morphology formed depends on the degree of polymerisation, volume fraction of each block and the Flory-Huggins interaction parameter.[107] The size of domains depends upon the molar masses of the constituent blocks of the copolymer.[108] One of the most common examples of the commercial use of phase separated block copolymers is in thermoplastic elastomers, particularly using styrene-butadiene-styrene triblock copolymers, but block copolymers are also of interest for applications including fabrication of semiconductors and photovoltaics.[109-111]
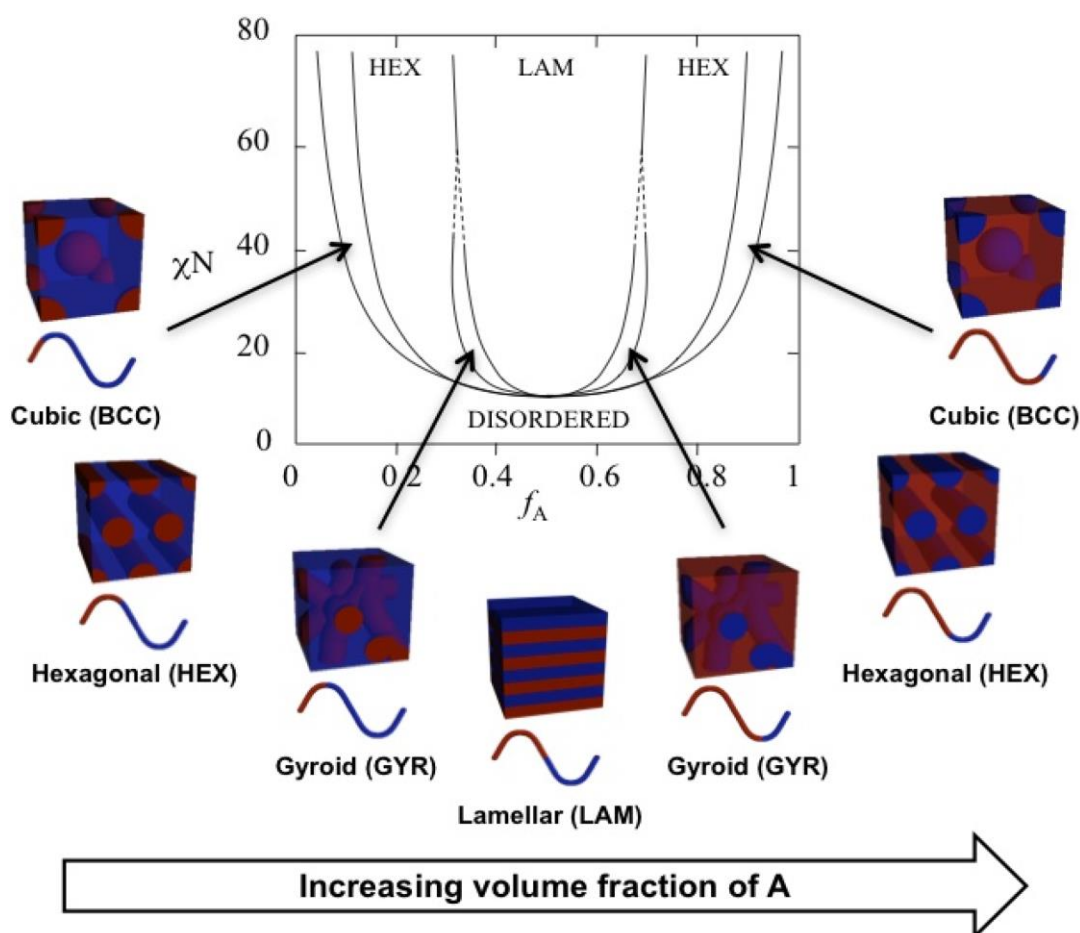
Figure 1.6: A phase diagram for a typical diblock copolymer, where χ is the Flory-Huggins Interaction parameter and f_A is the volume fraction of block A. Reprinted with permission under the Creative Commons Attribution License from reference[105]

The phase separation of immiscible blocks in a copolymer is enthalpically favourable. However, full separation of the blocks into 2 distinct environments is prevented

due to a loss of entropy as the system equilibrates. Entropy is lost via 2 components: localising the bonds between blocks at the interface and stretching of chains to maintain density.[112] The Flory-Huggins interaction parameter is temperature-dependent, meaning that the disorder within a sample can change upon heating.[113] A blend of diblock copolymers and the corresponding homopolymers leads to an intermediate phase separation where the block copolymers act like surfactants at the interface of the 2 immiscible phases.[114]

1.2.1. Self-Assembly of Amphiphilic Molecules in solution

The self-assembly of amphiphilic molecules, when dispersed into selective solvents, into micellar structures is well-known.[115-117] The formation of micelles from surfactants is a thermodynamically favourable process where the micellisation is driven by the increased stability gained from the insoluble portion of the molecule being shielded from unfavourable interactions with the solvent.[118] An important characteristic of surfactants within a solvent is the critical micelle concentration (CMC), above which, micelles will spontaneously form.[118-120]

Another important characteristic of surfactants is the Israelachvili packing parameter (see Equation 1.2).[121] This is a dimensionless number that that helps to rationalise how the dimensions of a given surfactant molecule can be represented by a simple shape (e.g. cone, truncated cone etc.), which will lead to self-assembly of said surfactant molecules into a specific micellar morphology (e.g. spherical micelles, vesicles etc.) when dispersed into the selective solvent.[122] The packing of surfactants can also vary depending on other factors such as the solvent and temperature which may alter the 3 values in Equation 1.2 at thermodynamic equilibrium and thus in turn, alter the packing parameter itself.[123]

$$p = \frac{v}{a_a l_c}$$

Equation 1.2: Formula for Israelachvili packing parameter (p) where v is the volume of the core-forming chain, a_a is the area per surface head group and l_c is the length of the core-forming chain.

The morphologies formed by self-assembled amphiphiles can be rationalised according to geometric calculations of simple 3D shapes such as spheres (p < 1/3), worms

or cylinders (1/3 < p < 1/2) and vesicles (1/2 < p < 1) (see Figure 1.7).[122] The Israelachvili packing parameter cannot be calculated easily because of the difficulty in measuring the relevant dimensions for the amphiphiles either in their free or self-assembled state. This makes it difficult to predict the morphology that will be formed upon self-assembly of a given surfactant. Nevertheless, it can be used as a useful model for describing the effect of tweaking the structure of surfactants, particularly in variations of the alkyl 'tail' group.
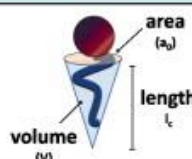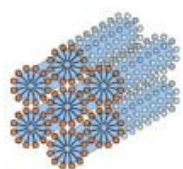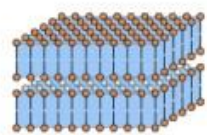
Aggregate type	Packing parameter	Surfactant geometry	Aggregate structure
Spherical Micelles	$\dfrac{V}{a_a l_c} < \dfrac{1}{3}$		
Cylindrical Micelles	$\dfrac{1}{3} < \dfrac{V}{a_a l_c} > \dfrac{1}{2}$		
Flexible Bilayers or Vesicles	$\dfrac{1}{2} < \dfrac{V}{a_a l_c} < 1$		
Planar Bilayers	$\dfrac{V}{a_a l_c} \sim 1$		
Inverted Micelles	$\dfrac{V}{a_a l_c} > 1$		

Figure 1.7: Diagram showing the morphologies of micelles formed in solution in relation to the Israelachvili packing parameter. Reprinted from reference.[124] Copyright 2020, with permission from Elsevier

1.2.2. Self-Assembly of Block Copolymers in Solution

The self-assembly of block copolymers when dispersed in a solvent that selectively dissolves just one of the constituent blocks has been studied extensively for the last 50 years.[125-127] Much like small, amphiphilic molecules, the self-assembly of block copolymers

will be into micellar structures. By varying parameters such as the relative molar mass of each block and the nature of the solvent, a wide range of morphologies can be formed. This is not dissimilar to the different morphologies that can form in bulk microphase separation of block copolymers with varying molecular weights of the constituent polymers (discussed above in section 1.2).[128]

Merrett first reported the formation of polymer colloids using branched copolymers formed by the graft polymerisation of MMA from natural rubber.[129] In an attempt to purify the polyisoprene-*graft*-poly(methyl methacrylate) (PI-*g*-PMMA) graft copolymer (by removal of unreacted rubber and PMMA homopolymer), the mixture was dissolved in benzene before adding a non-solvent (methanol) to precipitate the homopolymers. In doing so, Merrett reported the formation of a stable, colloidal sol which resembled a latex, presumably from self-assembly of the graft copolymer. Following this, Climie *et al*. investigated the aggregation of poly(acrylonitrile-*block*-(methyl methacrylate) (PAN-*b*-PMMA) block copolymers, prepared by free radical polymerisation in the presence of tertiary amines acting as chain transfer agents, in solvent mixtures of DMF/benzene.[125, 130] This method of synthesis leaves a terminal amine after the first stage of the a polymerisation which can then act as a 'macromolecular chain transfer agent' during the polymerisation of the 2nd monomer to produce a block copolymer. Light scattering measurements showed that, upon addition of benzene to a solution of the polymer in DMF, a 'critical concentration' was reached where the block copolymer formed aggregates. Since then, block copolymers for self-assembly have been prepared by many different chain-growth mechanisms, including LAP,[126, 131, 132] RDRP[133] and CHOMP.[134]

The self-assembly behaviour of block copolymer (surfactants) in solution is similar to small molecule surfactants, meaning that a choice between which to use depends on the desired properties for a particular application.[135] The use of block copolymers, rather than small molecule surfactants, to prepare self-assembled micelles in a selective solvent can be beneficial for a number of reasons. For example, polymers are structurally versatile with an almost infinite choice of monomers that can be combined via various polymerisation techniques, to give copolymers with different molecular weight, composition and dispersity.[136-138] All of these properties impact on the morphology and dimensions of the micelles formed and their stimuli-responsivity which is often very useful to investigate.[135]

Moreover, polymers have beneficial physical properties such as greater thermal and mechanical stability, and low volatility in comparison to smaller molecules, meaning that the range of operational temperatures and stresses under which block copolymer micelles can be exploited is very large.[139] A wide range of polymers is also thought to be benign to health, which makes polymer micelles highly desirable for encapsulation and drug delivery purposes.[140, 141]

The Israelachvili packing parameter shown in Equation 1.2 can also be applied to the self-assembly of block copolymers and is particularly useful because of how variable the block lengths are.[142-144] For example, from a fixed molar mass of a soluble, corona-forming block, an increasing molar mass of the insoluble core-forming polymer will increase the packing parameter, causing the micellar morphology to change from spherical to wormlike micelles and then vesicles.[46] It has also been reported extensively that the self-assembled morphology can vary depending on the concentration of block copolymer in the solvent, with the most prevalent theory used to describe this behaviour being that free energy is minimised by the formation of morphologies with a higher packing parameter at higher concentrations. Bhargava *et al* demonstrated this behaviour in their investigation of the self-assembly of PS-*b*-PEO block copolymers of fixed molecular weight at various concentrations in DMF/water – a solvent mixture which is selective for the PEO block.[145]

In many cases, for a copolymer of high molecular weight and in particular when the mole fraction of the insoluble block is high, it is often not possible to form micelles simply by addition to the solvent and mixing, as it is with small amphiphiles, e.g. surfactants. The self-assembly of such block copolymers has often been studied in systems where the block copolymer was initially fully dissolved in a good solvent for both blocks before the addition of a second (selective) solvent to induce self-assembly.[146-149] Whilst this approach can be successful in forming micelles, the use of solvent mixtures is often not desirable for commercial use. Solvent-switching has also been developed where the polymer is fully dissolved in a common, good solvent for both blocks in the polymer, before addition to the selective solvent and subsequent removal of the common solvent (e.g. by evaporation or dialysis).[150-152] This is a simple method for self-assembly of block copolymers on a small scale, and allows for purification of the polymers before self-assembly. However, it is commercially impractical due to the length of time and high costs involved.

1.2.3. Polymerisation-Induced Self-Assembly (PISA)

The application of block copolymer self-assembly has advanced notably in the past 10 years due to the development of polymerisation-induced self-assembly (PISA) by Armes *et al.*[47, 48] This is an *in situ* technique whereby the self-assembled nanostructures are prepared directly in the selective solvent as the polymerisation takes place (summarised schematically in Figure 1.8).[49] PISA is versatile technique which has been exploited for the synthesis of a wide range block copolymers that can self-assemble into a variety of morphologies .[46, 153]
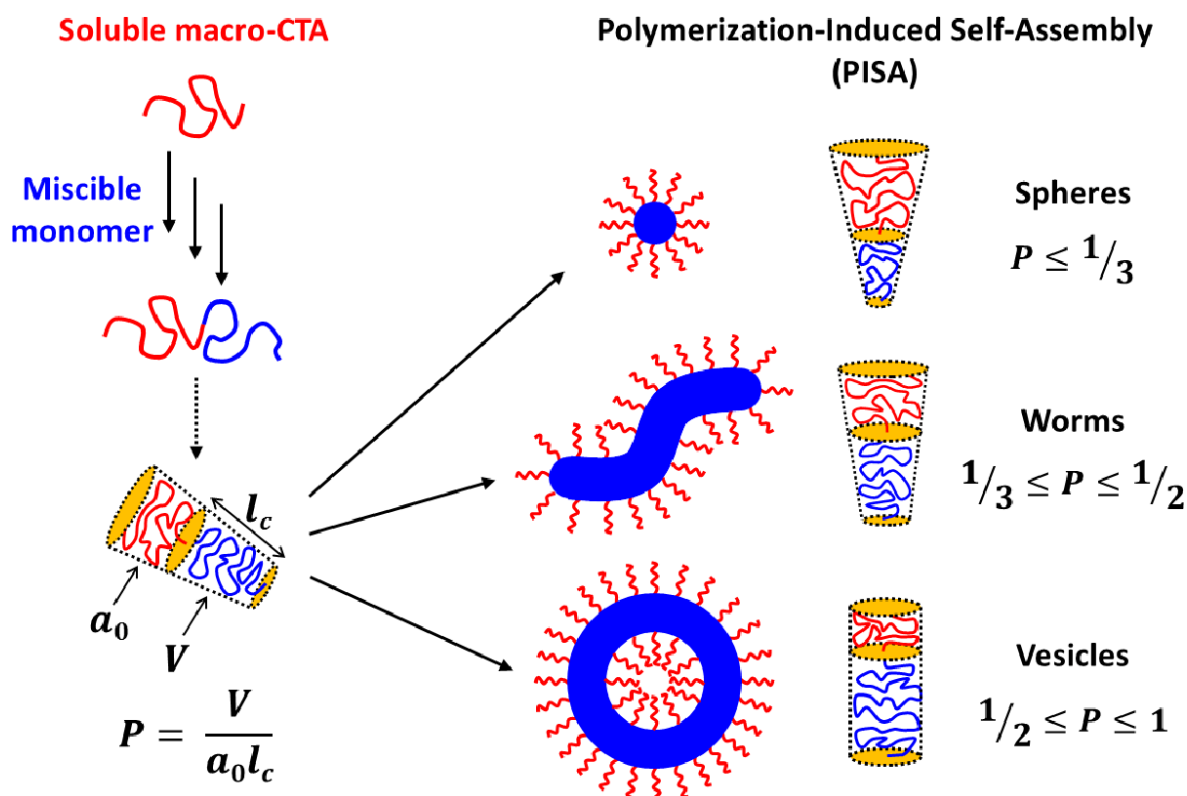
Figure 1.8: The mechanism of polymerisation-induced self-assembly (PISA) for preparing micelles directly within a selective solvent. Reprinted from reference[153] Copyright 2020, with permission from Elsevier

Research into PISA has increased massively since it was first reported and the topic has been advanced significantly by Armes (and others) over the past decade. PISA offers a significant advantage for the preparation of self-assembled nanostructures because it avoids the requirement for post-polymerisation self-assembly.[154] It is also robust, highly tailorable and can be performed at high polymer concentrations.[155, 156] PISA has predominantly been achieved using reversible-addition fragmentation chain-transfer polymerisation (RAFT), however it has also been reported using atom transfer radical

polymerisation (ATRP), nitroxide-mediated polymerisation (NMP), ring-opening metathesis polymerisation (ROMP), and recently, living anionic polymerisation.[157-161]

In PISA syntheses, the molar mass of the soluble (corona-forming) block is often kept constant by using the same macroinitiator to synthesise a series of block copolymers with varying molar masses of the insoluble block.[46, 158, 159, 162] In this case, the surface area of the corona-forming block (from the Israelachvili packing parameter in Equation 1.2) for the copolymer is constant, and the geometry of the core-forming block can then be systematically varied. Armes *et al.* first used a corona-forming block, of fixed molar mass for the preparation of a series of block copolymers. A water-soluble poly(2-(methacryloyloxy)ethyl phosphorylcholine) macroinitiator was used to initiate water-insoluble blocks of hydroxypropyl methacrylate (HPMA) of varying degree of polymerisation.[48] Self-assembly of the resulting block copolymers gave several different characteristic morphologies as a function of composition and concentration, which can be represented in the form of a phase diagram (see Figure 1.9).
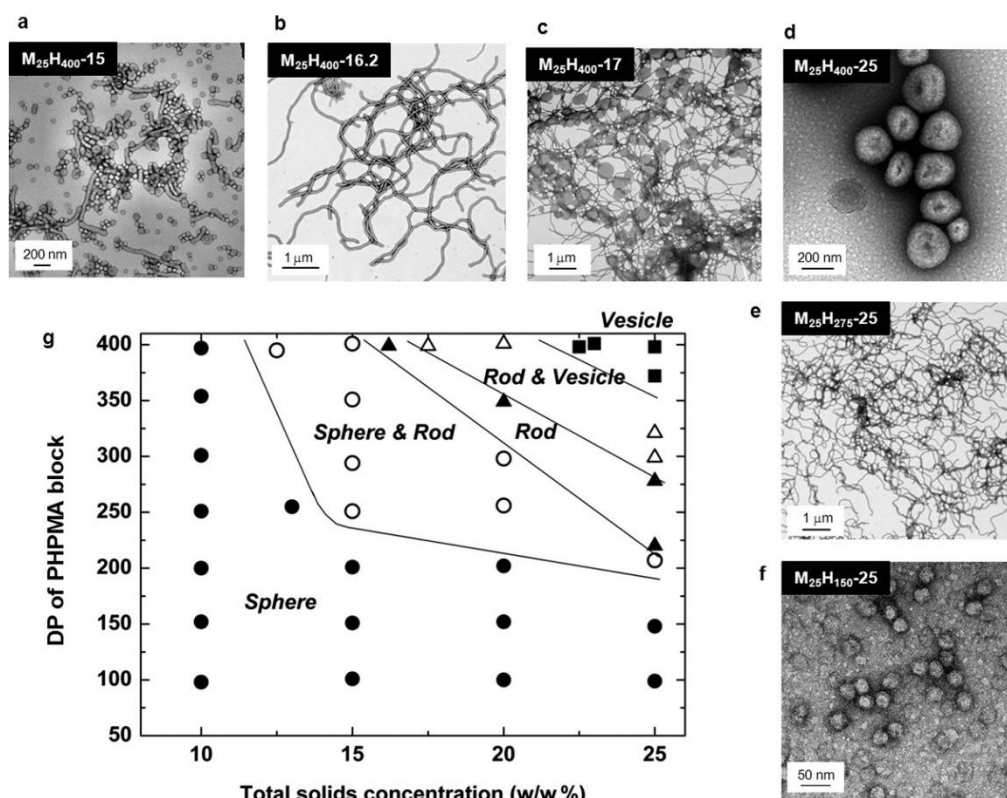
Figure 1.9: Phase diagram generated for the differing morphologies formed by varying the degree of polymerisation of HPMA and solids concentration from a fixed PMPC macroinitiator. Reprinted with permission from reference.[48]. Copyright (2020) American Chemical Society.

Figure 1.9 shows how different morphologies are formed as the DP_{HPMA} and total solids content change. At low DP_{HPMA} (150) the block copolymer forms spherical micelles (Figure 1.9f for inset TEM image), however a morphology of rods (or wormlike micelles) occurs at a DP_{HPMA} of 275 (Figure 1.9b and e) and vesicles at a DP_{HPMA} of 400 (Figure 1.9d). The reporting of such phase diagrams is now commonplace and one key characteristic of these phase diagrams is that the phase space within which wormlike micelles can be found is typically very narrow. This is another reason why PISA is useful, because the *in-situ* technique makes targeting the specific, often narrow, phases simpler. Another common feature of the phase diagrams is the presence of mixed phases (Figure 1.9a and c), which are comprised of 2 or more different morphologies and is particularly prevalent in the phase space close to the wormlike phase. It has previously been suggested that this is likely due the dispersity of the copolymers.[49] The vertical axis in such phase diagrams typically indicates the number average degree of polymerisation or number-average molar mass. The inherent dispersity in molar mass can cause the block copolymers in a single sample to have a range of packing parameters, resulting in mixed morphologies of micelles formed upon self-assembly. It is to be expected that this issue will be more prevalent where the dispersity is higher and it is of interest to explore the use of living anionic polymerisation, which typically yields polymers of predictable molar mass and narrower dispersity, to reduce or eliminate the presence of mixed phases in similar phase diagrams.

1.2.3.1.   PISA in Non-Polar Solvents

PISA has predominantly been reported for polymers produced using RDRP, particularly RAFT polymerisation, and as such polymerisations are most commonly carried out in polar solvents (particularly water), where the polymerisations are well-controlled and have favourable kinetics. There are far fewer reported examples of PISA in non-polar solvents where the first (corona-forming) block is a non-polar polymer and the core-forming block is a polar polymer.[46, 153, 163-165]

However, there are some reports of PISA in non-polar solvents. For example RAFT has been used with various long-chain acrylates and methacrylates e.g. lauryl methacrylate, as the soluble, corona-forming block prepared in a non-polar solvent such as isododecane or an *n*-alkane, with an insoluble polymer (e.g. benzyl methacrylate) as the core-forming block.[164, 166] Upon self-assembly, these block copolymers form the typical physical

structures and morphologies seen for PISA formulations in polar solvents, and likewise vary with the degree of polymerisation of the core-forming block and solids content (see phase diagram in Figure 1.10).[46]
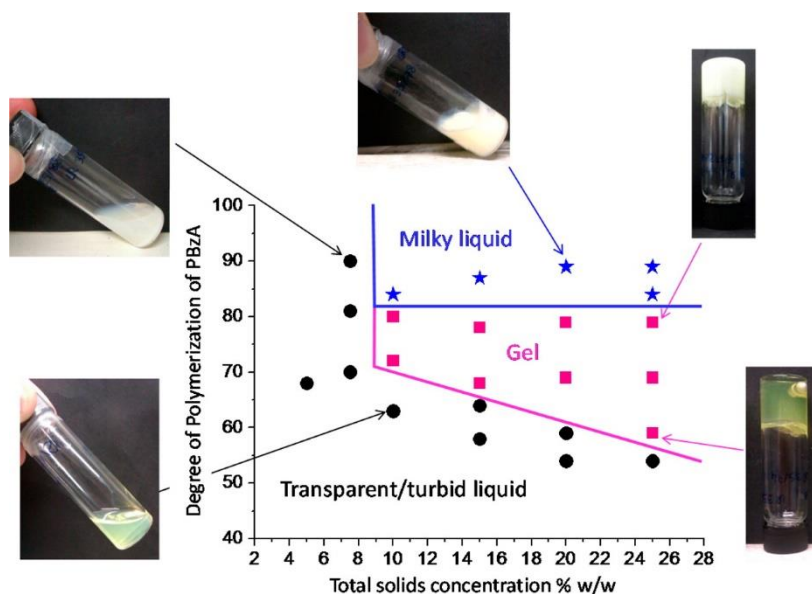
Figure 1.10: Phase diagram generated for block copolymers of PLA$_{14}$-b-PBzA$_x$, prepared by RAFT-mediated PISA in n-heptane from a fixed PLA macroinitiator by varying DP$_{PBzA}$ and solids content. Reprinted with permission from reference[46]. Copyright (2020) American Chemical Society. Further permissions related to the material excerpted should be directed to the ACS.

The different physical structures and morphologies shown in the phase diagrams in Figure 1.9 and Figure 1.10 can be useful for different applications and studies. For example, Derry *et al*. have previously reported that poly(stearyl methacrylate-*block*-benzyl methacrylate) (PSMA-*b*-PBzMA) self-assembles into vesicles in *n*-dodecane and undergo a thermal transition to wormlike micelles at 130 °C, which drastically increases the viscosity of the solution.[167] Variable temperature NMR data indicated that this transition was caused by plasticisation of the core-forming PBzMA block at the PSMA/PBzMA interface. This has potential applications as a novel thickener of engine oils to maintain viscosity at high temperature. However, the same group also reported that a similar, PLMA-*b*-PBzMA block copolymer that forms wormlike micelles in *n*-dodecane undergoes a thermal transition to spherical micelles at 50 °C which causes a decrease in the viscosity.[165] These contrasting behaviours for different morphologies formed by almost identical copolymers shows how it is critical to be able to reproducibly target a particular morphology when a particular

stimuli-responsivity is necessary. The reporting of phase diagrams for a given block copolymer allows for the reproducibility in targeting of the phases.

There are also examples of RAFT-mediated PISA where the corona-forming, soluble blocks were polymerised by a different mechanism (i.e. CHOMP). Lopez-Oliva *et al.* prepared poly((dimethyl siloxane)-*block*-(benzyl methacrylate)) (PDMS-*b*-PBzMA) block copolymers in *n*-heptane, a selective solvent for the PDMS block.[168] The PDMS macroinitiator was prepared from monocarbinol-terminated PDMS which is typically prepared by anionic ring-opening polymerisation. The utilisation of CHOMP allowed for the facile preparation of self-assembled PDMS-*b*-PBzMA block copolymers, which typically would not be possible by a single polymerisation mechanism. Recently, a similar method of synthesis has been published by Darmau *et al,* where hydrogenated poly(butadiene-*block*-benzyl methacrylate) (PhBD-*b*-BzMA) block copolymers were prepared by RAFT polymerisation of BzMA from a PhBD macroinitiator.[169] The polymerisation took place in *n*-dodecane, a selective solvent for the PhBD block. The PhBD used in the study was supplied by Kraton Polymers LLC but would typically be synthesised by living anionic polymerisation of 1,3-butadiene and subsequent hydrogenation of the polymer. Once more, this paper demonstrated the unique ability of CHOMP to prepare self-assembled block copolymers where the constituent polymers cannot be polymerised in a controlled fashion by a single polymerisation mechanism.

1.2.3.2.   Critical Appraisal of PISA

PISA is a useful means of directly preparing self-assembled block copolymers *in-situ*. It is versatile and can be used with a wide variety of solvents, monomers and polymerisation techniques and can be utilised across a range of solids contents. It is a simple method for accessing the different micellar morphologies that can form in diblock copolymers, particularly the wormlike micelles which are typically found in a very narrow parameter space between spherical micelles and vesicles.

However, there are limitations/disadvantages with PISA, both as a technique and with the commonly used RAFT polymerisation.[154] RAFT-mediated PISA necessitates the use of a RAFT agent, which imparts control to the polymerisation. These agents are expensive, malodorous and highly coloured. This means that the resultant self-assembled structures are often pink, which could be unappealing depending on the final use of the self-assembly (see images of self-assemblies in Figure 1.11). In theory, the RAFT agent (coloured) residue can easily be removed from the chain end of polymers but this is not practical for polymers that are already self-assembled into micelles.[170] Even if it can be done, it is likely to add extra time and cost in any industrial commercialisation. Moreover, RAFT-mediated PISA is generally limited to the use of methacrylates and acrylates, meaning that highly non-polar commercial monomers such as butadiene and isoprene have not been used in RAFT-mediated PISA. Even so, PISA has been transformative in the field of block copolymer self-assembly and continues to be studied for a wide variety block copolymers, solvents and potential applications.
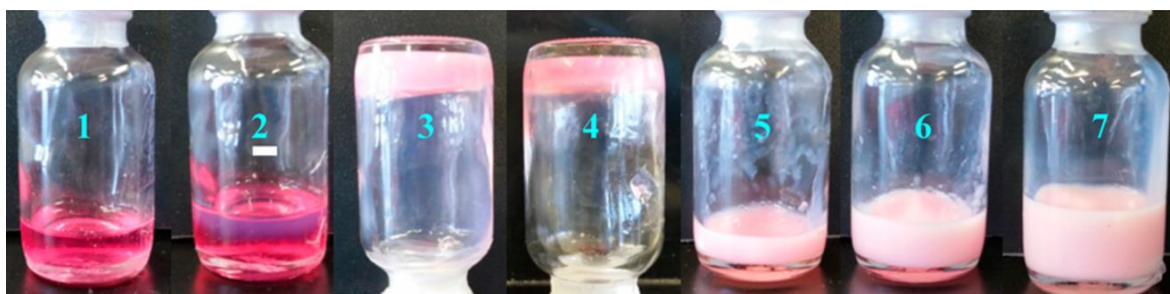
Figure 1.11: Picture showing several different self-assembled structures formed from the RAFT-mediated PISA of PPPMA from fixed PSMA macroinitiators. From left to right, the DP$_{PPPMA}$ increases, causing a change from transparent liquids to opaque gels. All self-assemblies are pink due to the contamination with the RAFT agent (CPDB) Reprinted with permission from reference.[171] Copyright (2020) American Chemical Society

1.3. Lubricants

Lubrication is vital for fulfilling a wide variety of objectives, most importantly in reducing friction and wear of solid surfaces which are in close contact. In nearly all machinery, there are moving solid-solid interfaces, in contact, which generate large frictional forces. This causes problems such as damage/wear at the interface, generation of excessive heat and loss of efficiency. An effective lubricant can reduce or eliminate these problems and the development of novel lubricant technologies is critically important to a wide variety of applications and industries.[172]

The most familiar example of a machine with solid-solid contact is the internal combustion engine which allows for transfer of energy from chemical combustion to kinetic motion through the motion of cast iron pistons within cylinders. The movement of the metal pistons against the metal casing is lubricated by an engine oil which reduces energy loss due to friction, improving fuel efficiency.[173] Metal-metal contact is also encountered in the transmission and differential of automobiles and as such, choosing a suitable lubricant can hugely improve efficiency and performance.[174]

As well as improving fuel economy, lubricants perform other functions in internal combustion engines, including the removal of particulates to prevent corrosion and acting as a seal to prevent the escape of generated gases. When formulating a lubricant, it is vitally important to consider all of these functions, and as such, formulations often contain many ingredients dispersed within a base oil. The interactions between these ingredients and the metal surface must be considered, but also the interactions between the constituent components of the formulation to ensure the best possible performance.[175]

1.3.1. Friction Modifiers

One of the most important components of a lubricant formulation is the friction modifier which helps reduce friction, improving fuel efficiency and reducing CO_2 emissions.[176] Friction modifiers bind to the metal surfaces and, as such, are often chemically designed to have a strongly polar functionality. However, because of the non-polar nature of the base oil, it is also necessary for friction modifiers to be highly non-polar for long-term solubility. Previous studies of organic friction modifiers have found that the design of the lipophilic, oil-soluble part of the molecule is also highly important to ensure the best possible friction performance with strong variations in performance being observed, even with 1 carbon atom difference on an alkyl chain.[177, 178]

There are 4 common classes of friction modifier: organic friction modifiers (OFMs), organo-molybdenum compounds, nanoparticles and polymeric friction modifiers (PFMs).[176] OFMs were the first to be conventionally used for lubricity with very early descriptions of an increased 'oiliness' in olive oil from 1886.[179] In the modern day, OFMs are most commonly amphiphilic molecules, (e.g. fatty acids, amides and amines) to combine solubility and surface binding. The mode of action is self-assembly into tribofilms at metal surfaces by interaction of the polar 'head' group.[180] One of the most commonly used OFMs in current use is glycerol monooleate (GMO), first patented as a rust inhibitor in 1949 (Figure 1.12),[181] which is similar in structure to fatty acids.[182] GMO self-assembles into micelles when dispersed into either polar solvents such as water or non-polar solvents, with the core being comprised of the non-polar alkyl chain or the polar glycerol moiety, respectively.[183, 184] The formation of micelles by GMO when dispersed into base oil is likely to be key in the performance as a friction modifier, however, the mechanism by which it interacts with metal surfaces is poorly understood.[185]
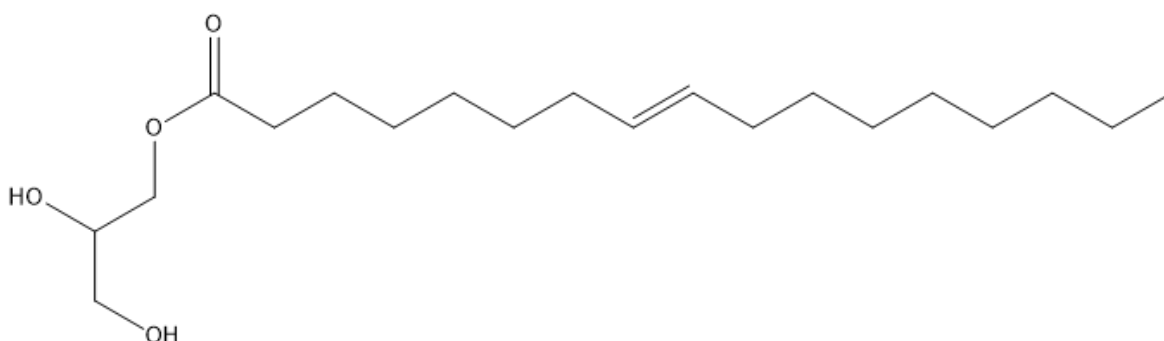
Figure 1.12: Chemical structure of glycerol mono-oleate (GMO), a commercial organic friction modifier (OFM), commonly used in lubricant formulations.

More recently, PFMs have been investigated as friction modifiers. The shear thinning property of polymers means they can be useful as friction modifiers even without a specific chemical functionality, which was first recognised in polymers used as viscosity modifiers (see section 1.3.2). In 1961, Okrent first reported a significant reduction in friction by introduction of so-called 'multifunctional polymers' in comparison to unfunctionalised polyisobutylene, that could not be explained solely by shear thinning.[186, 187] Optical interferometry has since been used on similar systems to show thick tribofilms forming on metal surfaces.[188, 189]

Since this early work, there has been considerable focus on functionalised polymers that can interact strongly with metal surfaces. A comprehensive study into the use of amphiphilic copolymers comprising methacrylate blocks found that polymers with strongly polar amine or hydroxyl functionalities e.g. poly(*N,N*-dimethylaminoethyl methacrylate) (PDMAEMA) or poly(2-hydroxyethyl methacrylate) (PHEMA), in lubrication formulations gave significantly reduced friction in all cases, in comparison with other, less polar polymers.[190] Ultrathin film interferometry showed that these polymers in particular formed very thick tribofilms at metal surfaces.[191] This behaviour is not unexpected given that many ligands that strongly binding to metals contain these functional groups.

The introduction of polar functional groups can render polymeric structures analogous to OFMs. This enhanced friction reduction of shear-thinning polymers which, combined with their potential to increase the viscosity index at high temperatures, can make them very useful additives. When introducing functionality into copolymers, there is also the opportunity to systematically vary the monomer sequence (see Figure 1.1), which can change how polymers interact with surfaces. For example, statistical copolymers will have binding sites distributed throughout the polymer chain and, as such, bind more tightly to the surface (pancake) than blocky/end-capped polymers which can form polymer brushes (or mushrooms if the solubility of the polymer in the oil is poor).[192] These shapes of polymers adsorbed onto solid surfaces are shown below in Figure 1.13.

Figure 1.13: Diagram showing the variations in adsorption to solid surfaces of polymers with different monomer sequences. Reprinted with permission from reference.[193] Copyright Elsevier (2020)

The effect of monomer sequence and polymer architecture on friction reduction has also been investigated. A study of polymers made from HEMA, DMAEMA and DMAPMA found that block copolymers form thicker films and reduce friction more than analogous statistical copolymers.[191] This suggests that the formation of 'brush-like' structures, where polar binding functionalities are grouped together is preferable. The same study also

showed that an increase in molar mass (in chemically identical polymers) form thicker films and reduced friction.

1.3.1.1.   Stribeck Curves

The most commonly used way to measure the friction of a given lubricant formulation is a Stribeck curve which is a graph of the friction coefficient experienced between two solid surfaces vs. rotational speed. The rotational speed can be reported in several different ways (e.g. entrainment speed, Hersey number or Gumbel number).[194] First discussed by Stribeck in 1902, these are important plots which show that the relationship between friction and entrainment speed is non-linear.[195-197] This is a fundamental tribological concept which means that performance across all rotational speeds can be difficult to predict even with extensive recordings of data.

The Stribeck curve is generally broken down into 3 distinct regimes: i) boundary lubrication where entrainment speed is low, there is minimal lubricant present and solid parts are in very close contact; ii) mixed lubrication where some lubricant is present at intermittent speed and there is some solid-solid contact and iii) hydrodynamic lubrication, which occurs at higher speeds, with a thicker film of lubricant present and minimal solid contact.[194, 198] The breakdown of the lubrication regimes can be very clear and is shown on a Stribeck Curve in Figure 1.14.
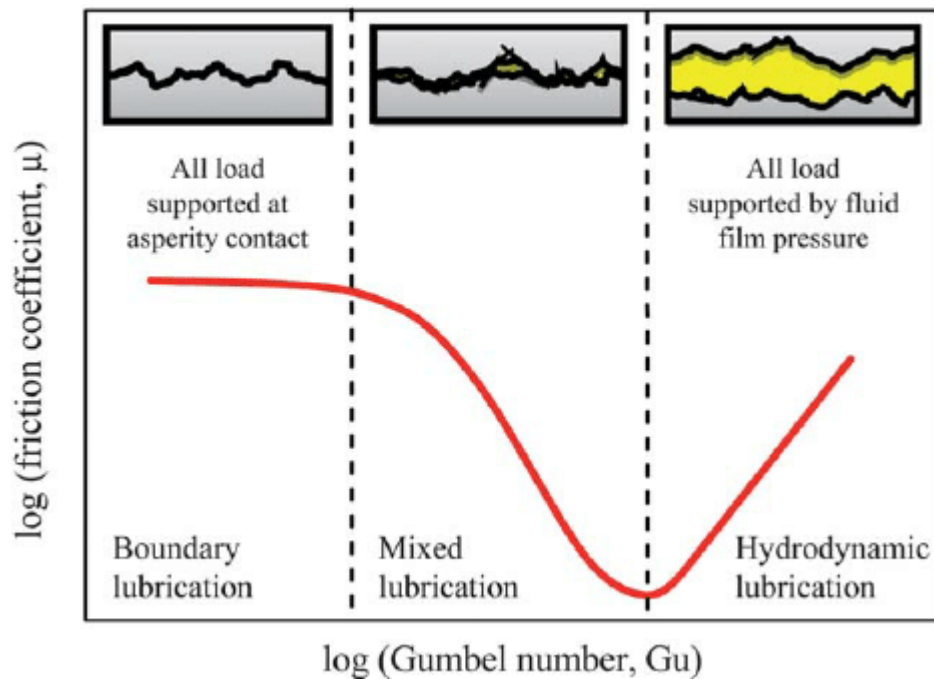
Figure 1.14: Typical Stribeck curve with the 3 different regimes of lubrication indicated and inset images of the typical lubricant film at that rotational speed. Reprinted from reference[199]. Copyright 2020, with permission from RSC

Figure 1.14 shows a typical Stribeck curve with the 3 different regimes of lubrication indicated. The friction is particularly high in the boundary regime where the metal contacts are in close proximity. The hydrodynamic regime shows lower friction, because as entrainment speed increases, the lubricant film generally becomes thicker. It is important that a lubricant reduces friction across all 3 regimes shown in Figure 1.14 so that the best possible efficiency is achieved, however, lubricity in the boundary regime, where friction is inherently high is of most interest. In an internal combustion engine, this is where metal parts are in closest proximity and where damage and performance inefficiencies are most likely to occur.[200, 201] The boundary regime replicates when an engine is first turned on, when there may be very little lubricant present between surfaces. It is vitally important that friction modifiers present at the surface from previous use, show a strong affinity to the metal surface so as to remain bound at this point. Moreover, in the mixed and hydrodynamic regimes the lubricant film thickness can be tailored by the choice of oil among other things, whereas boundary regime lubrication relies on the chemical properties of the friction modifiers.[202]

1.3.2. Viscosity Modifiers

Another critically important factor to consider when formulating a lubricant is the performance over the full working temperature range, from when the engine is first turned on up to when it is fully operational. A key physical change over these temperature ranges is the viscosity of the liquid.[203] The viscosity of a fluid generally experiences a significant decrease as temperature increases. Therefore, it is important to use additives that maintain the viscosity at high temperature without significantly increasing viscosity at colder temperatures.

The viscosity can be maintained by use of viscosity modifiers which are most commonly polymeric additives of a specific architecture and/or monomer sequence that can change in solubility as the temperature is increased.[204] For example, star shaped hydrogenated styrene-diene copolymers (HSDCs) in which the styrene block is insoluble at room temperature, are known to increase in solubility at high temperatures. This causes the star architecture to 'unfold', resulting in a higher radius of gyration and therefore a higher viscosity.[205-207] This higher viscosity offsets the expected reduction observed for the oil as it is heated, giving a lubricant that performs consistently across the temperature range.

The use of multifunctional additives that can meet multiple requirements of a lubricant formulation is highly desirable, because they can reduce cost and overcomplicated recipes by reducing ingredients.[208] One recent report suggests the use of organic-inorganic hybrid star polymers could be useful for friction and wear reduction and viscosity modification.[209] Whilst the additive showed the expected improvement in viscosity index (for a star polymer) and some friction reduction, it did not undergo comprehensive friction testing meaning that it was not tested towards the boundary condition. Nevertheless, the future of multifunctional additives will most likely require polymeric additives because of the improvement to viscosity index that cannot be addressed easily with small molecules.

1.3.3. Amphiphilic Block Copolymers in Lubricant Formulations

The presence of amphiphilic molecules (both small-molecule and polymeric) in lubricant formulations that combine polar components for binding to metal surfaces and

non-polar components to ensure solubility in base oils is crucial for fulfilling requirements such as friction reduction and wear reduction.[210-213] There are a few examples of copolymers in use as commercial lubricant additives (particularly as viscosity modifiers). Zheng *et al* investigated the use of block copolymers prepared by ATRP in which the soluble, corona-forming block comprised of a random copolymer of ethyl hexyl acrylate and *tert*-butyl acrylate, and the core-forming block was 2-cinnamoyloxyethyl acrylate (P((EXA-*r*-tBA)-*b*-CEA)).[214] The block copolymer was dispersed into dodecane at 1.5 wt%, and imaged by TEM, to show the formation of spherical micelles. The controlled, partial hydrolysis of tBA repeat units to acrylic acid was shown to enhance binding of the aggregates to a stainless steel surface using AFM to observe the topography of the surface before and after being exposed to the micelles.[215]

A further investigation by the same group, using the same polymers dispersed in base oil, found that micelles with larger cores performed better in lubrication tests.[216] They also investigated the photo-crosslinking of the PCEA block in the core of the micelles following their self-assembly in cyclohexane. Once crosslinked, the spherical nanoparticles were recovered from the solvent and re-dispersed into base oil; a method chosen because of the photosensitive compounds present in the base oil. This study concluded that the partial crosslinking of micelles was somewhat beneficial for friction reduction. Fully-crosslinked cores were found to increase friction, due to the decreased mobility at the surface and the decreased shear thinning effect.

More recently, Derry *et al*. conducted a similar investigation using PISA to prepare PSMA-*b*-PBzMA block copolymers, directly in mineral oil. These underwent self-assembly to form spherical micelles, which were imaged by TEM.[217] They also prepared core-crosslinked spherical micelles by introduction of EGDMA, following the PISA of BzMA, which showed good friction performance compared to neat base oil and GMO within base oil, particularly at the boundary condition. However, the authors also draw attention to the potential limitations posed by the presence of the RAFT agent, which is costly to remove, particularly on a commercial scale and the difficulty in core-crosslinking micelles in larger batches for commercial production.

In each of the limited number of reports on the testing of self-assembled block copolymers described above, there are promising results for friction reduction and/or

viscosity modification. However, testing was only carried out on solutions of polymer in neat base oil rather than in full lubricant formulations, meaning that it is not possible to assess how effectively the spherical micelles could actually perform. Because lubricant formulations are complex mixtures containing many components including a variety of surface active agents such as detergents for particulate and debris removal, the performance of all additives can change greatly under these conditions.[185, 218] During the current investigation, the performance of block copolymers in a neat base oil will be tested to allow comparison to results published in previous reports. Following this, the same samples will be tested in full formulations to assess the effectiveness of tested copolymers in the presence of multiple ingredients, many of which are also surface-active.

1.4. Aims and Objectives

The aims of this project are to prepare block copolymers, by a variety of synthetic techniques including living anionic polymerisation, atom-transfer radical polymerisation and post-polymerisation modifications, that can be dispersed into non-polar solvents. The resulting copolymers will be investigated both in 'academic' and 'industrial' contexts with a feedback loop between the synthetic approach and the results of applications testing to allow optimisation of structure. The first two results chapters will focus on an 'academic' study of the synthesis and self-assembly of polyisoprene-based block copolymers in selective, non-polar solvents. The following two results chapters will describe the applications testing of polyisoprene-based block copolymers and explore alternative synthetic routes towards analogous copolymers which are more suited to industrial scale-up. The aims of each chapter are described below:

Chapter 3 will describe an investigation into the preparation of homologous families of poly(isoprene-*block*-(methyl methacrylate) (PI-*b*-PMMA) block copolymers by a change of mechanism polymerisation (CHOMP). LAP will be used to prepare end-capped lipophilic, PI blocks with fixed molar mass and ATRP to prepare the PMMA block. The block copolymers will then be dispersed into non-polar solvents, which are selective for the PI block, by solvent-switching, and the resulting self-assembled morphologies will be investigated by DLS and TEM. The thermal responsivity of the self-assembled block copolymers will be investigated by variable temperature rheology.

Chapter 4 will describe a similar CHOMP procedure to prepare poly(isoprene-*block*-(*N,N*-(dimethylamino)ethyl methacrylate) (PI-*b*-PDMAEMA) block copolymers. The self-assembly into micelles in non-polar solvents will be investigated and the behaviour compared to analogous PI-*b*-PMMA samples from the previous chapter. The amine functionality of PDMAEMA allows for further derivatisation of the polymeric structure through a post-polymerisation quaternisation with alkyl iodides to prepare PI-*b*-PQDMAEMA which will also be self-assembled into non-polar solvents. The change in solubility upon quaternisation of PDMAEMA in THF could cause an *in situ* self-assembly (quaternisation-induced self-assembly) which will also be investigated by TEM.

In chapter 5, PI-*b*-PMMA and PI-*b*-PDMAEMA block copolymers will be tested as friction modifiers and viscosity modifiers by dispersing them into a common base oil. Promising candidates will also be tested in several different full, lubricant formulations to see if the block copolymers retain their performance in the presence of other surface-active ingredients.

Chapter 6 will describe the results of a preliminary investigation into the synthesis and applications testing of novel copolymers, prepared by protocols considered more feasible for industrial scale up. Guided by the results from the applications testing of PI-*b*-PMMA and PI-*b*-PDMAEMA in the previous chapter, the aim is to prepare copolymers with similar structural features by the selective maleinisation of homopolybutadiene. By controlling the conditions of the LAP, the microstructure of polybutadiene will be tailored, such that the maleinisation reaction allows for the preparation of amphiphilic, 'blocky' copolymers. Imidisation of the anhydride groups will allow for further derivatisation of the chemical structure with an aim of introducing functional groups capable of binding to metal surfaces. These samples will then be tested as lubricant additives, as before, to see if they perform similarly to the previous additives.

1.5. References

1. H. Staudinger, *Ber. Dtsch. Chem. Ges.*, 1920, **53**, 1073-1085.
2. *US Pat.*, US2071250A, 1937.
3. H. Staudinger, J. Fritschi, *Helv. Chim. Acta*, 1922, **5**, 785-806.
4. T. Svedberg, H. Rinde, *J. Am. Chem. Soc.*, 1924, **46**, 2677-2693.
5. K. H. Meyer, H. Mark, *Ber. Dtsch. Chem. Ges.*, 1928, **61**, 593-614.
6. E. J. Goethals, *Telechelic Polymers*, Taylor & Francis, 1988.
7. J. W. Nicholson, *The Chemistry of Polymers*, Royal Society of Chemistry, 2006.
8. W. H. Carothers, *J. Am. Chem. Soc.*, 1929, **51**, 2548-2559.
9. W. H. Carothers, *Trans. Faraday Soc.*, 1936, **32**, 39-53.
10. P. J. Flory, *Principles of polymer chemistry*, Cornell University Press, 1953.
11. G. Odian, *Principles of polymerization*, John Wiley & Sons, New Jersey, 2004.
12. P. J. Flory, *J. Am. Chem. Soc.*, 1937, **59**, 241-253.
13. G. Moad, D. H. Solomon, *The Chemistry of Radical Polymerization*, Elsevier Science, 2006.
14. C. Craver, C. Carraher, *Applied Polymer Science: 21st Century*, Elsevier Science, 2000.
15. M. Szwarc, M. Van Beylen, *Ionic polymerization and living polymers*, Springer Science & Business Media, 2012.
16. D. Braun, *Int. J. Polym. Sci.*, 2009, **893234**, 1-10.
17. P. Nesvadba, *Encyclopedia of Radicals in Chemistry, Biology and Materials*, 2012.
18. E. Rieger, A. Manhart, F. R. Wurm, *ACS Macro Lett.*, 2016, **5**, 195-198.
19. B. Obermeier, F. Wurm, C. Mangold, H. Frey, *Angew. Chem.-Int. Edit.*, 2011, **50**, 7988-7997.
20. M. Szwarc, *Nature*, 1956, **178**, 1168-1169.
21. M. Szwarc, M. Levy, R. Milkovich, *J. Am. Chem. Soc.*, 1956, **78**, 2656-2657.
22. H. Hsieh, R. P. Quirk, *Anionic polymerization: principles and practical applications*, CRC Press, 1996.
23. N. Hadjichristidis, H. Iatrou, S. Pispas, M. Pitsikalis, *J. Polym. Sci. Pol. Chem.*, 2000, **38**, 3211-3234.
24. D. Baskaran, A. H. E. Muller, *Prog. Polym. Sci.*, 2007, **32**, 173-219.
25. D. Baskaran, *Prog. Polym. Sci.*, 2003, **28**, 521-581.
26. M. Szwarc, A. Rembaum, *J. Polym. Sci.*, 1956, **22**, 189-191.
27. S. Bywater, *Pure Appl. Chem.*, 1962, **4**, 319-332.
28. D. M. Wiles, S. Bywater, *Polymer*, 1962, **3**, 175-185.
29. D. M. Wiles, S. Bywater, *J. Phys. Chem.*, 1964, **68**, 1983-1987.
30. D. M. Wiles, S. Bywater, *Trans. Faraday Soc.*, 1965, **61**, 150-158.
31. W. Goode, F. Owens, W. Myers, *J. Polym. Sci.*, 1960, **47**, 75-89.
32. D. Kunkel, A. H. E. Muller, M. Janata, L. Lochmann, *Makromol. Chem., Macromol. Symp.*, 1992, **60**, 315-326.
33. R. Kraft, A. H. E. Muller, H. Hocker, G. V. Schulz, *Makromol. Chem. Rapid. Comm.*, 1980, **1**, 363-368.
34. R. Fayt, R. Forte, C. Jacobs, R. Jerome, T. Ouhadi, P. Teyssie, S. K. Varshney, *Macromolecules*, 1987, **20**, 1442-1444.
35. *US Pat.*, US6329480B1, 2001.
36. *US Pat.*, US20090118450A1, 2012.

37. *US Pat.*, US6555637B1, 2003.
38. *CA Pat.*, CA2975070A1, 2016.
39. A. D. Jenkins, R. G. Jones, G. Moad, *Pure Appl. Chem.*, 2010, **82**, 483-491.
40. K. Matyjaszewski, T. P. Davis, *Handbook of Radical Polymerization*, Wiley, 2003.
41. M. J. Zhong, K. Matyjaszewski, *Macromolecules*, 2011, **44**, 2668-2677.
42. J. Chiefari, Y. K. Chong, F. Ercole, J. Krstina, J. Jeffery, T. P. T. Le, R. T. A. Mayadunne, G. F. Meijs, C. L. Moad, G. Moad, E. Rizzardo, S. H. Thang, *Macromolecules*, 1998, **31**, 5559-5562.
43. S. Perrier, *Macromolecules*, 2017, **50**, 7433-7447.
44. *US Pat.*, US6153705A, 2000.
45. D. J. Keddie, *Chem. Soc. Rev.*, 2014, **43**, 496-505.
46. L. P. D. Ratcliffe, B. E. McKenzie, G. M. D. Le Bouedec, C. N. Williams, S. L. Brown, S. P. Armes, *Macromolecules*, 2015, **48**, 8594-8607.
47. Y. T. Li, S. P. Armes, *Angew. Chem.-Int. Edit.*, 2010, **49**, 4042-4046.
48. S. Sugihara, A. Blanazs, S. P. Armes, A. J. Ryan, A. L. Lewis, *J. Am. Chem. Soc.*, 2011, **133**, 15707-15713.
49. A. Blanazs, A. J. Ryan, S. P. Armes, *Macromolecules*, 2012, **45**, 5099-5107.
50. G. Moad, E. Rizzardo, S. H. Thang, *Aust. J. Chem.*, 2009, **62**, 1402-1472.
51. A. J. Brzytwa, J. Johnson, *Polym. Prepr. (Am. Chem. Soc., Div. Polym. Chem.)*, 2011, **52**, 533-534.
52. M. Destarac, *Polym. Chem.*, 2018, **9**, 4947-4967.
53. S. Perrier, P. Takolpuckdee, C. A. Mars, *Macromolecules*, 2005, **38**, 2033-2036.
54. X. Y. Tian, J. J. Ding, B. Zhang, F. Qiu, X. D. Zhuang, Y. Chen, *Polymers*, 2018, **10**, 318.
55. M. Chen, M. Zhong, J. A. Johnson, *Chem. Rev.*, 2016, **116**, 10167-10211.
56. A. H. Soeriyadi, G. Z. Li, S. Slavin, M. W. Jones, C. M. Amos, C. R. Becer, M. R. Whittaker, D. M. Haddleton, C. Boyer, T. P. Davis, *Polym. Chem.*, 2011, **2**, 815-822.
57. N. G. Engelis, A. Anastasaki, G. Nurumbetov, N. P. Truong, V. Nikolaou, A. Shegiwal, M. R. Whittaker, T. P. Davis, D. M. Haddleton, *Nat. Chem.*, 2017, **9**, 171-178.
58. G. Moad, E. Rizzardo, *The History of Nitroxide-mediated Polymerization*, Royal Soc Chemistry, Cambridge, 2016.
59. E. Rizzardo, D. H. Solomon, *Polym. Bull.*, 1979, **1**, 529-534.
60. M. K. Georges, R. P. N. Veregin, P. M. Kazmaier, G. K. Hamer, *Macromolecules*, 1993, **26**, 2987-2988.
61. R. B. Grubbs, *Polym. Rev.*, 2011, **51**, 104-137.
62. J. S. Wang, K. Matyjaszewski, *J. Am. Chem. Soc.*, 1995, **117**, 5614-5615.
63. M. Kato, M. Kamigaito, M. Sawamoto, T. Higashimura, *Macromolecules*, 1995, **28**, 1721-1723.
64. K. Matyjaszewski, J. Xia, *Chem. Rev.*, 2001, **101**, 2921-2990.
65. K. Matyjaszewski, *Macromolecules*, 2012, **45**, 4015-4039.
66. T. G. Ribelli, F. Lorandi, M. Fantin, K. Matyjaszewski, *Macromol. Rapid Commun.*, 2019, **40**, 1800616.
67. Y. N. Zhou, Z. H. Luo, *Aiche J.*, 2015, **61**, 1947-1958.
68. Y. F. Zhu, F. J. Jiang, P. P. Zhang, J. Luo, H. D. Tang, *Chin. Chem. Lett.*, 2016, **27**, 910-914.
69. J. Wootthikanokkhan, M. Peesan, P. Phinyocheep, *Eur. Polym. J.*, 2001, **37**, 2063-2071.

70. S. U. Heo, G. H. Rhee, D. H. Lee, J. H. Kim, D. S. Choi, D. W. Lee, *J. Ind. Eng. Chem.*, 2006, **12**, 241-247.

71. J. Hua, J. T. Geng, X. Wang, J. Zhao, L. Xu, *J. Macromol. Sci. Part A-Pure Appl. Chem.*, 2009, **46**, 1156-1161.

72. S. H. Qin, J. Saget, J. R. Pyun, S. J. Jia, T. Kowalewski, K. Matyjaszewski, *Macromolecules*, 2003, **36**, 8969-8977.

73. F. Dutertre, P. Y. Pennarun, O. Colombani, E. Nicol, *Eur. Polym. J.*, 2011, **47**, 343-351.

74. N. V. Tsarevsky, K. Matyjaszewski, *Chem. Rev.*, 2007, **107**, 2270-2299.

75. Y. Q. Shen, H. D. Tang, S. J. Ding, *Prog. Polym. Sci.*, 2004, **29**, 1053-1078.

76. K. Min, H. F. Gao, K. Matyjaszewski, *Macromolecules*, 2007, **40**, 1789-1791.

77. N. Ayres, *Polym. Rev.*, 2011, **51**, 138-162.

78. M. Hillmyer, *Curr. Opin. Solid State Mat. Sci.*, 1999, **4**, 559-564.

79. J. Feldthusen, B. Ivan, A. H. E. Muller, *Macromolecules*, 1998, **31**, 578-585.

80. W. Risse, R. H. Grubbs, *Macromolecules*, 1989, **22**, 1558-1562.

81. S. Mahajan, B. K. Cho, A. Allgaier, L. J. Fetters, G. W. Coates, U. Wiesner, *Macromol. Rapid Commun.*, 2004, **25**, 1889-1894.

82. J. D. Tong, S. R. Ni, M. A. Winnik, *Macromolecules*, 2000, **33**, 1482-1486.

83. L. R. Hutchings, P. P. Brooks, D. Parker, J. A. Mosely, S. Sevinc, *Macromolecules*, 2015, **48**, 610-628.

84. L. R. Hutchings, P. P. Brooks, P. Shaw, P. Ross-Gardner, *J. Polym. Sci. Pol. Chem.*, 2019, **57**, 382-394.

85. E. Blasco, M. B. Sims, A. S. Goldmann, B. S. Sumerlin, C. Barner-Kowollik, *Macromolecules*, 2017, **50**, 5215-5252.

86. J. Justynska, H. Schlaad, *Macromol. Rapid Commun.*, 2004, **25**, 1478-1481.

87. D. Zuchowska, *Polymer*, 1980, **21**, 514-520.

88. S. F. Thames, S. Gupta, *J. Appl. Polym. Sci.*, 2001, **81**, 754-761.

89. L. Iancu, P. Ghioca, B. Spurcaciu, R. M. Grigorescu, C. A. Nicolae, R. A. Gabor, *Mater. Plast.*, 2013, **50**, 137-140.

90. F. Ferrero, *Prog. Org. Coat.*, 2005, **53**, 50-55.

91. Y. H. Fu, C. L. Lin, L. F. Chen, Y. Song, H. C. Ma, *Preparation of Cationic Rice Husk Flocculant and its flocculating characteristics*, Trans Tech Publications Ltd, Stafa-Zurich, 2012.

92. Y. F. Pan, Q. Y. Xia, H. N. Xiao, *Polymers*, 2019, **11**, 1283.

93. W. Jaeger, J. Bohrisch, A. Laschewsky, *Prog. Polym. Sci.*, 2010, **35**, 511-577.

94. T. Manouras, E. Koufakis, S. H. Anastasiadis, M. Vamvakaki, *Soft Matter*, 2017, **13**, 3777-3782.

95. L. Jiang, M. P. Wolcott, J. W. Zhang, *Biomacromolecules*, 2006, **7**, 199-207.

96. G. Y. Choi, H. G. Kim, Y. H. Kim, C. W. Seo, J. H. Choi, D. H. Han, D. H. Oh, K. E. Min, *J. Appl. Polym. Sci.*, 2002, **86**, 917-924.

97. A. Karami, S. T. Balke, *Polym. Eng. Sci.*, 2000, **40**, 2342-2355.

98. E. Kim, E. J. Kramer, J. O. Osby, *Macromolecules*, 1995, **28**, 1979-1989.

99. P. J. Flory, *J. Chem. Phys.*, 1941, **9**, 660-661.

100. M. L. Huggins, *J. Chem. Phys.*, 1941, **9**, 440-440.

101. K. Binder, *Phase-Transitions in Polymer Blends and Block-Copolymer Melts - Some Recent Developments*, Springer-Verlag Berlin, Berlin, 1994.

102. T. H. Russell, B. J. Edwards, B. Khomami, *Eur. Polym. J.*, 2014, **108**, 66003.

103. P. W. Atkins, J. De Paula, J. Keeler, *Atkins' physical chemistry*, Oxford university press, 2018.
104. D. J. Kozuch, W. L. Zhang, S. T. Milner, *Polymers*, 2016, **8**, 241.
105. J. M. G. Swann, P. D. Topham, *Polymers*, 2010, **2**, 454-469.
106. L. Leibler, *Macromolecules*, 1980, **13**, 1602-1617.
107. R. A. Farrell, T. G. Fitzgerald, D. Borah, J. D. Holmes, M. A. Morris, *Int. J. Mol. Sci.*, 2009, **10**, 3671-3712.
108. M. Motoyama, N. Yamazaki, M. Nonomura, T. Ohta, *J. Phys. Soc. Jpn.*, 2003, **72**, 991-994.
109. I. W. Hamley, *Nanotechnology*, 2003, **14**, 39-54.
110. S. B. Darling, *Energy Environ. Sci.*, 2009, **2**, 1266-1273.
111. G. Holden, *Understanding thermoplastic elastomers*, Hanser, 2000.
112. F. S. Bates, *Science*, 1991, **251**, 898-905.
113. R. Koningsveld, L. A. Kleintjens, H. M. Schoffeleers, *Pure Appl. Chem.*, 1974, **39**, 1-32.
114. M. W. Matsen, *Macromolecules*, 1995, **28**, 5765-5773.
115. A. E. Alexander, P. Johnson, *Colloid science*, Clarendon Press, 1949.
116. J. W. McBain, *Colloid science*, Reinhold Publishing Corporation, New York, 1950.
117. H. R. KRUYT, L. C. JACKSON, *Colloid Science. Edited by H.R. Kruyt. (English Translations by L.C. Jackson.)*, Elsevier Publishing Company, 1952.
118. Y. Moroi, *Micelles: Theoretical and Applied Aspects*, Springer US, 1992.
119. R. Nagarajan, E. Ruckenstein, *Langmuir*, 1991, **7**, 2934-2969.
120. J. N. Israelachvili, *Intermolecular and Surface Forces, 3rd Edition*, Elsevier Academic Press Inc, San Diego, 2011.
121. J. N. Israelachvili, D. J. Mitchell, B. W. Ninham, *J. Chem. Soc., Faraday Trans. 2*, 1976, **72**, 1525-1568.
122. R. Nagarajan, *Langmuir*, 2002, **18**, 31-38.
123. P. J. Missel, N. A. Mazer, G. B. Benedek, C. Y. Young, M. C. Carey, *J. Phys. Chem.*, 1980, **84**, 1044-1057.
124. A. Ballesteros-Gomez, M. D. Sicilia, S. Rubio, *Anal. Chim. Acta*, 2010, **677**, 108-130.
125. I. E. Climie, E. F. T. White, *J. Polym. Sci.*, 1960, **47**, 149-156.
126. G. M. Burnett, C. Paton, P. Meares, *Trans. Faraday Soc.*, 1962, **58**, 737-746.
127. S. Krause, *J. Phys. Chem.*, 1964, **68**, 1948-1955.
128. L. H. Radzilowski, B. O. Carragher, S. I. Stupp, *Macromolecules*, 1997, **30**, 2110-2119.
129. F. M. Merrett, *Trans. Faraday Soc.*, 1954, **50**, 759-767.
130. C. H. Bamford, E. F. T. White, *Trans. Faraday Soc.*, 1956, **52**, 716-727.
131. F. Caldérara, Z. Hruska, G. Hurtrez, T. Nugay, G. Riess, M. A. Winnik, *Makromol. Chem. Rapid. Comm.*, 1993, **194**, 1411-1420.
132. M. Antonietti, S. Heinz, M. Schmidt, C. Rosenauer, *Macromolecules*, 1994, **27**, 3276-3281.
133. B. S. Sumerlin, A. B. Lowe, D. B. Thomas, C. L. McCormick, *Macromolecules*, 2003, **36**, 5982-5987.
134. M. Ranger, M. C. Jones, M. A. Yessine, J. C. Leroux, *J. Polym. Sci. Pol. Chem.*, 2001, **39**, 3861-3874.
135. T. Zinn, L. Willner, R. Lund, V. Pipich, M. S. Appavou, D. Richter, *Soft Matter*, 2014, **10**, 5212-5220.
136. F. Meng, Z. Zhong, J. Feijen, *Biomacromolecules*, 2009, **10**, 197-209.

137. B. M. Discher, Y. Y. Won, D. S. Ege, J. C. M. Lee, F. S. Bates, D. E. Discher, D. A. Hammer, *Science*, 1999, **284**, 1143-1146.
138. P. A. Beales, S. Khan, S. P. Muench, L. J. C. Jeuken, *Biochem. Soc. Trans.*, 2017, **45**, 15-26.
139. M. Schulz, W. H. Binder, *Macromol. Rapid Commun.*, 2015, **36**, 2031-2041.
140. J. Z. Du, R. K. O'Reilly, *Soft Matter*, 2009, **5**, 3544-3561.
141. H. R. Marsden, C. B. Quer, E. Y. Sanchez, L. Gabrielli, W. Jiskoot, A. Kros, *Biomacromolecules*, 2010, **11**, 833-838.
142. R. Fenyves, M. Schmutz, I. J. Horner, F. V. Bright, J. Rzayev, *J. Am. Chem. Soc.*, 2014, **136**, 7762-7770.
143. S. Svenson, *Curr. Opin. Colloid Interface Sci.*, 2004, **9**, 201-212.
144. S. R. Prabhu, G. B. Dutt, *J. Phys. Chem. B*, 2013, **117**, 5868-5874.
145. P. Bhargava, J. X. Zheng, P. Li, R. P. Quirk, F. W. Harris, S. Z. D. Cheng, *Macromolecules*, 2006, **39**, 4880-4888.
146. M. Villacampa, E. D. Deapodaca, J. R. Quintana, I. Katime, *Macromolecules*, 1995, **28**, 4144-4149.
147. J. R. Quintana, E. Hernaez, I. Inchausti, I. Katime, *J. Phys. Chem. B*, 2000, **104**, 1439-1446.
148. J. R. Quintana, M. Villacampa, I. A. Katime, *Macromolecules*, 1993, **26**, 601-605.
149. T. Rager, W. H. Meyer, G. Wegner, *Macromol. Chem. Phys.*, 1999, **200**, 1672-1680.
150. Y. Y. Mai, A. Eisenberg, *Chem. Soc. Rev.*, 2012, **41**, 5969-5985.
151. L. F. Zhang, A. Eisenberg, *J. Am. Chem. Soc.*, 1996, **118**, 3168-3181.
152. L. I. Atanase, G. Riess, *Polymers*, 2018, **10**, 62.
153. M. J. Derry, L. A. Fielding, S. P. Armes, *Prog. Polym. Sci.*, 2016, **52**, 1-18.
154. S. L. Canning, G. N. Smith, S. P. Armes, *Macromolecules*, 2016, **49**, 1985-2001.
155. M. Semsarilar, E. R. Jones, A. Blanazs, S. P. Armes, *Adv. Mater.*, 2012, **24**, 3378-3382.
156. E. R. Jones, M. Semsarilar, A. Blanazs, S. P. Armes, *Macromolecules*, 2012, **45**, 5091-5098.
157. N. J. W. Penfold, J. Yeow, C. Boyer, S. P. Armes, *ACS Macro Lett.*, 2019, **8**, 1029-1054.
158. G. Wang, M. Schmitt, Z. Y. Wang, B. Lee, X. C. Pan, L. Y. Fu, J. J. Yan, S. P. Li, G. J. Xie, M. R. Bockstaller, K. Matyjaszewski, *Macromolecules*, 2016, **49**, 8605-8615.
159. A. Darabi, P. G. Jessop, M. F. Cunningham, *Macromolecules*, 2015, **48**, 1952-1958.
160. D. B. Wright, M. A. Touve, L. Adamiak, N. C. Gianneschi, *ACS Macro Lett.*, 2017, **6**, 925-929.
161. J. Wang, M. Y. Cao, P. Zhou, G. W. Wang, *Macromolecules*, 2020, **53**, 3157-3165.
162. M. Y. Cao, Y. X. Zhang, J. Wang, X. S. Fan, G. W. Wang, *Macromol. Rapid Commun.*, 2019, **40**, 1900296.
163. M. J. Derry, L. A. Fielding, N. J. Warren, C. J. Mable, A. J. Smith, O. O. Mykhaylyk, S. P. Armes, *Chem. Sci.*, 2016, **7**, 5078-5090.
164. L. A. Fielding, M. J. Derry, V. Ladmiral, J. Rosselgong, A. M. Rodrigues, L. P. D. Ratcliffe, S. Sugihara, S. P. Armes, *Chem. Sci.*, 2013, **4**, 2081-2087.
165. L. A. Fielding, J. A. Lane, M. J. Derry, O. O. Mykhaylyk, S. P. Armes, *J. Am. Chem. Soc.*, 2014, **136**, 5790-5798.
166. L. Houillot, C. Bui, M. Save, B. Charleux, C. Farcet, C. Moire, J. A. Raust, I. Rodriguez, *Macromolecules*, 2007, **40**, 6500-6509.
167. M. J. Derry, O. O. Mykhaylyk, S. P. Armes, *Angew. Chem.-Int. Edit.*, 2017, **56**, 1746-1750.

168. A. P. Lopez-Oliva, N. J. Warren, A. Rajkumar, O. O. Mykhaylyk, M. J. Derry, K. E. B. Doncom, M. J. Rymaruk, S. P. Armes, *Macromolecules*, 2015, **48**, 3547-3555.

169. B. Darmau, M. J. Rymaruk, N. J. Warren, R. Bening, S. P. Armes, *Polym. Chem.*, 2020, **11**, 7533-7541.

170. H. Willcock, R. K. O'Reilly, *Polym. Chem.*, 2010, **1**, 149-157.

171. Y. Pei, L. Thurairajah, O. R. Sugita, A. B. Lowe, *Macromolecules*, 2015, **48**, 236-244.

172. T. Mang, W. Dresel, *Lubricants and Lubrication*, Wiley, 2007.

173. D. Bonneau, A. Fatu, D. Souchet, *Internal Combustion Engine Bearings Lubrication in Hydrodynamic Bearings*, Wiley, 2014.

174. A. S. f. Testing, Materials, A. International, *Chapter 5: Combustion Engine Lubricants*, ASTM International, 2009.

175. D. M. Pirro, M. Webster, E. Daschner, *Lubrication Fundamentals, Revised and Expanded*, CRC Press, 2016.

176. H. Spikes, *Tribol. Lett.*, 2015, **60**, 1-26.

177. W. Hardy, I. Bircumshaw, *Proc. R. soc. Lond. Ser. A-Contain. Pap. Math. Phys. Character*, 1925, **108**, 1-27.

178. F. P. Bowden, J. N. Gregory, D. Tabor, *Nature*, 1945, **156**, 97-101.

179. O. Reynolds, *Philos. T. R. Soc. B.*, 1886, **177**, 157-234.

180. I. Langmuir, *Trans. Faraday Soc.*, 1920, **15**, 62-74.

181. *US Pat.*, US2482517A, 1949.

182. M. Kano, Y. Yasuda, Y. Okamoto, Y. Mabuchi, T. Hamada, T. Ueno, J. Ye, S. Konishi, S. Takeshima, J. M. Martin, M. I. D. Bouchet, T. Le Mogne, *Tribol. Lett.*, 2005, **18**, 245-251.

183. J. L. Bradley-Shaw, P. J. Camp, P. J. Dowding, K. Lewtas, *J. Phys. Chem. B*, 2015, **119**, 4321-4331.

184. P. Pitzalis, M. Monduzzi, N. Krog, H. Larsson, H. Ljusberg-Wahren, T. Nylander, *Langmuir*, 2000, **16**, 6358-6365.

185. G. Tsagkaropoulou, C. P. Warrens, P. J. Camp, *ACS Appl. Mater. Interfaces*, 2019, **11**, 28359-28369.

186. E. H. Okrent, *A S L E Transactions*, 1961, **4**, 257-262.

187. E. H. Okrent, *A S L E Transactions*, 1961, **4**, 97-108.

188. M. Smeeth, H. Spikes, S. Gunsel, *Tribol. Trans.*, 1996, **39**, 726-734.

189. G. Guangteng, H. A. Spikes, *Tribol. Trans.*, 1996, **39**, 448-454.

190. J. Fan, M. Müller, T. Stöhr, H. Spikes, *Tribol. Lett.*, 2007, **28**, 287-298.

191. M. Muller, K. Topolovec-Miklozic, A. Dardin, H. A. Spikes, *Tribol. Trans.*, 2006, **49**, 225-232.

192. W. J. Brittain, S. Minko, *J. Polym. Sci. Pol. Chem.*, 2007, **45**, 3505-3512.

193. W. Yang, F. Zhou, *Biosurf. Biotribol.*, 2017, **3**, 97-114.

194. X. B. Lu, M. M. Khonsari, E. R. M. Gelinck, *J. Tribol.-Trans. ASME*, 2006, **128**, 789-794.

195. R. Stribeck, *Z. VDI.*, 1902, **46**, 1341-1348.

196. R. Stribeck, *Z. VDI.*, 1902, **46**, 1432-1438.

197. R. Stribeck, *Z. VDI.*, 1902, **46**, 1463-1470.

198. M. Woydt, R. Wasche, *Wear*, 2010, **268**, 1542-1546.

199. E. Andablo-Reyes, R. Hidalgo-Alvarez, J. de Vicente, *Soft Matter*, 2011, **7**, 880-883.

200. M. A. Nicholls, T. Do, P. R. Norton, M. Kasrai, G. M. Bancroft, *Tribol. Int.*, 2005, **38**, 15-39.

201. J. Zhang, Y. G. Meng, *Friction*, 2015, **3**, 115-147.
202. P. Kapsa, J. M. Martin, *Tribol. Int.*, 1982, **15**, 37-42.
203. A. Martini, U. S. Ramasamy, M. Len, *Tribol. Lett.*, 2018, **66**, 1-14.
204. G. Verstrate, M. J. Struglinski, *ACS Symp. Ser. Am. Chem. Soc.*, 1991, **462**, 256-272.
205. N. N. Petrukhina, O. N. Tsvetkov, A. L. Maksimov, *Russ. J. Appl. Chem.*, 2019, **92**, 1179-1189.
206. P. Ghosh, A. V. Pantar, U. S. Rao, A. S. Sarma, *Indian J. Chem. Technol.*, 1998, **5**, 309-314.
207. D. Erickson, F. Z. Lu, D. Q. Li, T. White, J. Gao, *Exp. Therm. Fluid Sci.*, 2002, **25**, 623-630.
208. L. Cosimbescu, J. W. Robinson, Y. Zhou, J. Qu, *RSC Adv.*, 2016, **6**, 86259-86268.
209. B. G. P. van Ravensteijn, R. B. Zerdan, D. Seo, N. Cadirov, T. Watanabe, J. A. Gerbec, C. J. Hawker, J. N. Israelachvili, M. E. Helgeson, *ACS Appl. Mater. Interfaces*, 2019, **11**, 1363-1375.
210. J. L. Mansot, J. M. Martin, S. J. Candau, *Colloids Surf.*, 1983, **7**, 301-310.
211. S. Plaza, L. Margielewski, *Surfactants Lubricating Oil Additives*, Tsinghua University Press, Beijing, 2009.
212. N. J. Mosey, M. H. Muser, T. K. Woo, *Science*, 2005, **307**, 1612-1615.
213. N. N. Gosvami, J. A. Bares, F. Mangolini, A. R. Konicek, D. G. Yablon, R. W. Carpick, *Science*, 2015, **348**, 102-106.
214. R. H. Zheng, G. J. Liu, T. C. Jao, *Polymer*, 2007, **48**, 7049-7057.
215. R. H. Zheng, J. D. Wang, G. J. Liu, T. C. Jao, *Macromolecules*, 2007, **40**, 7601-7608.
216. R. H. Zheng, G. J. Liu, M. Devlin, K. Hux, T. C. Jao, *Tribol. Trans.*, 2010, **53**, 97-107.
217. M. J. Derry, T. Smith, P. S. O'Hora, S. P. Armes, *ACS Appl. Mater. Interfaces*, 2019, **11**, 33364-33369.
218. Z. Pawlak, *Tribochemistry of Lubricating Oils*, Elsevier Science, 2003.

2. Experimental

2.1. Materials

2.1.1. Materials for Chapters 3 and 4

Isoprene (Sigma-Aldrich; 99 %, containing <1000 ppm 4-tert-butylcatechol (4-TBC)), toluene (Fisher; ≥99.9 %), dichloromethane (Fisher; ≥99.8 %) and benzene (Sigma-Aldrich; 99.8 %) were dried with calcium hydride (Acros; ca. 93 %, 0-2 mm grain size) and degassed by a series of freeze-pump-thaw cycles. Tetrahydrofuran (for quaternisation reactions) (Fisher; AR grade) was distilled prior to use, following drying with sodium (Fisher; Sticks in mineral oil, 99 %) and benzophenone (Fisher, 99 %) and degasssing by a series of freeze-pump-thaw cycles. 1,4-Dioxane (Fisher; ≥99 %), tetrahydrofuran (for ATRP reactions) (Fisher; GPC grade, stabilised with 0.025 % BHT) and methyl methacrylate (Sigma- Aldrich; 99 %, containing ≤ 30 ppm MEHQ) were each passed through neutral aluminium oxide (Fisher; Brockmann I, 60 Å) before use. *N,N*-dimethylaminoethyl methacrylate (Fisher; 99 %, stabilised) was passed through basic aluminium oxide (Fisher; Brockmann I, 60 Å) before use. *Sec*-Butyllithium (Sigma-Aldrich; 1.4 M in cyclohexane), butylated hydroxytoluene (Sigma-Aldrich; ≥99 %), chloroform-*d* (Apollo; 99.96 atom% D), α-bromoisobutyryl bromide (Sigma-Aldrich; 98 %), methanol (Fisher; AR grade), triethylamine (Sigma-Aldrich; 99.5 %), copper (I) bromide (Acros; 98 %, extra pure), 2-2'-bipyridyl (Sigma-Aldrich; ≥99 %), *N,N,N',N'',N''*-pentamethyldiethylenetriamine (Tokyo Chemical Industry; >99.0 %), ethyl iodide (Sigma-Aldrich; 99 %, contains copper as stabiliser), 1-butyl iodide (Fisher; 98 %, stabilised), 1-octyl iodide (Fisher; >98 %, stabilised with copper) and *n*-decane (Fisher; >99 %) were all used as received. Ethylene oxide (Sigma-Aldrich; ≥99.5 %) was dried and purified by passing through columns of Carbosorb (Sigma-Aldrich) and further dried and purified by stirring for 30 minutes at 0 °C over calcium hydride immediately prior to use.

2.1.2. Materials for Chapters 5 and 6

For dispersion of the block copolymers in base oil and full, lubricant formulations, the following materials were used. Dichloromethane (Fisher) and *n*-heptane (Fisher) were used as received. Yubase 4 (SK Lubricants), Irganox L135 (BASF), Perfad 3050, glycerol monooleate (both Croda) Synfluid Polyalphaolefin (PAO) 4 (Chevron Phillips Chemical Company), SV261L, SV203, P6003 (all Infineum), VM410 (Aerzen) were all provided by

Croda and used as received. Full formulations of Mobil Delvac 5W30, Motul 0W16 and Motul 5W30 were also provided by Croda and used as received.

The synthesis of microstructural block copolymers of polybutadiene was carried out in part using commercial processes and some materials have been omitted to maintain confidentiality. The following chemicals were used. Butadiene (Air Liquide), butyllithium (Sigma-Aldrich; solution in cyclohexane), maleic anhydride (Alfa Aesar, 98+ %), 3-(dimethylamino)-1-propylamine (Sigma-Aldrich, 99 %) and methanol (Fisher; AR grade) were used as received.

2.2. Measurements

2.2.1. Size Exclusion Chromatography (SEC)

Molecular weight analysis was carried out by size exclusion chromatography (SEC) using a Viscotek TDA 302 with detectors for refractive index, light scattering and viscosity. Two 300 mm PLgel 5 μm mixed C-columns were used with a linear molecular weight range of 200 – 2 000 000 g mol^{-1}. THF was used as the eluent at a flow rate of 1.0 mL min^{-1} at a temperature of 35 $^{\circ}$C. For all polymers, triple detection SEC was utilised for molecular weight determination with light scattering, using dn/dc values of 0.085 mL g^{-1} for poly(methyl methacrylate) (PMMA), 0.130 mL g^{-1} for polyisoprene (PI), 0.084 m Lg^{-1} for poly(N,N-dimethylaminoethyl methacrylate) (PDMAEMA) and 0.124 mL g^{-1} for polybutadiene (PBd). Samples were prepared for SEC analysis by dissolving c. 2 mg of the polymer in 2 mL THF for a concentration of ca. 1 mg mL^{-1}.

2.2.2. Nuclear Magnetic Resonance (NMR)

^{1}H NMR spectra were recorded using a Bruker DRX-400 (400 MHz, 298 K) spectrometer with chloroform-d or dimethyl sulphoxide-d$_6$ as the solvent. The spectra were referenced to the trace proton signals present in chloroform-d (7.26 ppm) or dimethyl sulphoxide-d$_6$ (2.50 ppm).

2.2.3. Fourier-Transform Infrared (FTIR)

FTIR measurements were made using a PerkinElmer Frontier spectrometer. The polymer was applied directly to the mounted top-plate and scanned from 4000 cm^{-1} – 400 cm^{-1}.

2.2.4. Rheology

Rheological characterisation of self-supporting gels was performed using a TA AR-2000 rheometer, equipped with a 25 mm parallel plate geometry and a Peltier plate for thermal analysis. Free-flowing liquids were analysed in the same way, but with a concentric cylinder geometry. Angular frequency (ω) sweeps were conducted at 25 °C and from these, a constant angular frequency of 1 rad s^{-1} and strain of 0.2 were used for the temperature sweep experiments. Complex viscosity (η*) was calculated from: $\eta^* = \frac{\sqrt{G'^2 + G''^2}}{\omega}$

2.2.5. Transmission Electron Microscopy (TEM)

High resolution transmission electron microscopy (TEM) images were obtained using a JEOL 2100F FEG TEM operating at 200 kV. For free-flowing copolymer morphologies, holey carbon grids (Agar scientific; holey carbon film on 300 mesh copper grids) were dipped in the liquid polymer dispersion, prepared at 15 wt% in decane (or 0.1 wt% for the diluted samples) and blotted with filter paper to remove the excess solvent. For self-supporting gels, a thin film was spread on a glass slide, onto which the holey carbon grid was dipped and then blotted on filter paper. To investigate the thermal-responsivity that was known to be reversible at high concentration a 'kinetic trapping' method was used. This was achieved by by dilution to 0.1 wt%, as descried above, however the sample was held to 150 °C for 10 minutes and diluted with *n*-decane of the same temperature before being allowed to cool to room temperature. For sample preparation of QISA solutions in THF, samples were taken *in situ* from the reaction. The holey carbon grids were dipped in the solution (either liquid or gel) and excess solvent was blotted on filter paper.

2.2.6. Dynamic Light Scattering (DLS)

Particle size analysis of self-assembled structures was carried out using a Malvern Panalytical Zetasizer μV (scattering angle θ = 90°). Values reported herein are the intensity-average hydrodynamic radius with the PDI obtained using the cumulant analysis embedded in the software. Samples were prepared by dispersion of polymer samples at 10 wt% in *n*-decane, followed by dilution with decane to 0.72 wt%. Dispersions in *n*-decane (≈1 mL) were added to a 1 cm quartz cuvette, by injection through a 0.2 μm PTFE syringe filter. Each experiment was repeated three times with 13 measurements recorded in each case.

2.2.7. Mini-Traction Machine (MTM)

Friction testing was carried out using a PCS Instruments mini-traction machine (MTM), a diagram of which is shown below in Figure 2.1. Standard, stainless steel, ¾" ball and disc specimens (PCS Instruments) were sonicated 3 times in fresh *n*-heptane for 15 minutes. The metal parts of the MTM were also cleaned in the same way. The lubricant to be tested was poured into the chamber of the MTM, before the cleaned metal parts were fitted, and the entire chamber sealed with a PTFE cap.
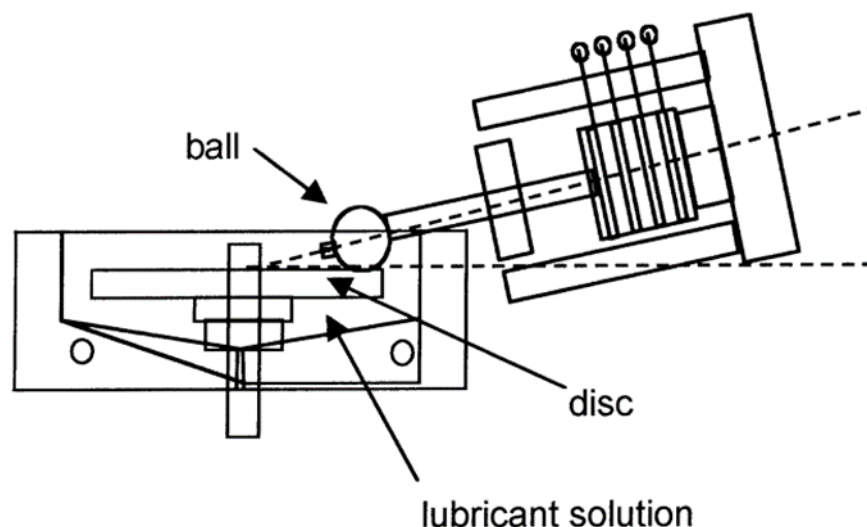
Figure 2.1: Diagram showing the mini-traction machine (MTM) used for testing the friction of lubricants at varying entrainment speed. Reprinted from reference[1] with permission from Springer (copyright 2021).

Different procedures were used for testing the block copolymers in base oil and in full, lubricant formulations. These MTM testing protocols are described below in sections 2.2.7.1. and 2.2.7.2. respectively.

2.2.7.1. Protocol for Measuring the Coefficient of Friction for Polymer in Base Oil

For solutions of 1 wt% friction modifier in Yubase 4 (base oil), the following procedure was used. Step 2 was found to be necessary to allow the system to fully equilibrate.

1. Stribeck curve (see Section 1.3.1.1.) from 3000 mm s^{-1} – 1 mm s^{-1} at 80 $^{\circ}$C, 36 N.
2. Sample held for 2 hours at 60 $^{\circ}$C, 50 mm s^{-1}, 30 N.
3. Stribeck curve from 3000 mm s^{-1} – 3 mm s^{-1} (10 repeats at each entrainment speed) at 80 $^{\circ}$C, 36 N.

The results reported from this test are the mean of the 10 repeated measurements of coefficient of friction in step 3. Outliers were excluded using the μ ± 4σ rule.

2.2.7.2. Protocol for Measuring the Coefficient of Friction for Polymer in Full Formulations

For full formulations containing friction modifiers, a more industrially relevant procedure was used. This test is a more intense process that seeks to elucidate the ongoing effect of wear on the metal specimens in contact.

1. Stribeck curve from 3000 mm s^{-1} – 5 mm s^{-1} at 80 ^{o}C, 36 N.
2. Rubbing of disc and ball in the presence of lubricant for 5 minutes at 50 mm s^{-1}, 80 ^{o}C, 30 N.
3. These steps were then repeated with Stribeck curves (identical to step 1) taken after longer rubbing intervals (10, 15, 30, 60 mins) until the sample had been rubbed for 2 hours, at which point a final Stribeck curve was run as per Step 1.

For certain full formulations (Motul 5W30 and Mobil Delvac 5W30), a slightly different protocol was used, where the temperature throughout was 135 ^{o}C. This is specified in all figure captions for the relevant Stribeck curves in the results and discussion chapters. Unless stated, the data illustrated in the discussion all show the final Stribeck curve after 2 hours rubbing, as this result always showed the highest friction coefficient across all entrainment speeds after wearing. For each formulation, the polymer being investigated was tested at 1 wt% with respect to the full formulation.

2.3. Synthetic Protocols

2.3.1. Ethylene Oxide-End-Capped Polyisoprene (PI-*OH*)

Living anionic polymerisation was employed to prepare a series of end-capped polyisoprene ATRP macroinitiators, of varying molar mass, using standard high vacuum techniques and trap-to-trap distillation. Thus, in a typical reaction, the synthesis of PI-*OH* with a target molar mass of 3500 g mol^{-1} was carried out as follows: toluene (≈50 mL) and isoprene (8.1 g, 120 mmol) were distilled into the reactor. *s*-BuLi (1.4 M in cyclohexane; 1.64 mL, 2.3 mmol) was injected via a rubber septum, causing the reaction mixture to turn pale yellow. The propagation of isoprene was allowed to proceed with stirring at room temperature for 2 hours. Meanwhile, ethylene oxide (1.1 mL; 0.97 g, 22 mmol) was distilled onto calcium hydride, cooled to 0 ^{o}C with an ice-water bath, and stirred for 30 minutes. The

EO was then distilled into the reactor, causing the contents to turn colourless within 1 minute of stirring. The reaction was left overnight to ensure quantitative end-capping before the reaction was terminated by the injection of a 1:1 HCl (37 wt% in water)/MeOH by volume for an HCl concentration of 6 M (0.38 mL, 2.3 mmol). The polymer was recovered by addition of the polymer solution to methanol (400 mL). The viscous liquid polymer was allowed to settle before the supernatant liquor was decanted away to yield a colourless, sticky viscous liquid, which was dried *in vacuo* to constant mass, to yield PI$_{55}$-*OH* (6.7 g, 83 %). The polymer was stored in a freezer until further use.

SEC: M_n (PI$_{55}$-*OH*) = 3730 g mol^{-1}, M_w = 3880 g mol^{-1}; M_w/M_n = 1.04. ^1H-NMR (400 MHz, CDCl$_3$, 298 K, ppm): δ = 1.62-1.70 CH$_2$-CH=C(CH$_3$)-CH$_2$), 1.90-2.07 (**CH$_2$**-CH=C(CH$_3$)-**CH$_2$**), 2.38 (-**CH$_2$**-CH$_2$-OH), 3.51 (-CH$_2$-**CH$_2$**-OH), 3.63 (-CH$_2$-CH$_2$-O**H**), 4.67-5.15 (CH$_2$-C**H**=C(CH$_3$)-CH$_2$).

2.3.2. Bromide-End-Capped Polyisoprene (PI-*Br*)

The hydroxyl end-group of PI$_{55}$-*OH* was converted to a bromide end-group for use as an ATRP macroinitiator according to the following procedure: PI-*OH* (3730 g mol^{-1}) (6.0 g, 1.6 mmol) was charged to a Schlenk flask containing a magnetic stirrer bar, which was sealed with a rubber septum and placed under high vacuum. Dichloromethane (≈30 mL) was then distilled into the flask. The temperature was lowered to 0 °C, before the injection of triethylamine (0.67 mL; 0.49 g, 4.8 mmol) and α-bromoisobutyryl bromide (0.60 mL; 1.11 g, 4.8 mmol) via the rubber septum. After 3 hours of stirring at 0 °C, the reaction mixture (which had turned pale brown) was warmed to room temperature and left stirring. After 18 hours, the contents had turned dark brown. At this point, the polymer was precipitated by addition of the polymer solution to methanol (400 mL). The viscous liquid polymer was allowed to settle before being recovered by pouring off the supernatant liquor to yield a clear, brown, sticky viscous liquid. PI$_{55}$-Br (Yield = 5.1 g, 81 %)

SEC: M_n = 3710 g mol^{-1}; M_w = 3860 g mol^{-1}; M_n/M_w = 1.04. ^1H-NMR (400 MHz, CDCl$_3$, 298 K, ppm): δ = 1.62-1.70 CH$_2$-CH=C(CH$_3$)-CH$_2$), 1.95 (C(C**H$_3$**)$_2$), 1.90-2.07 (**CH$_2$**-CH=C(CH$_3$)-**CH$_2$**), 4.67-5.15 (CH$_2$-C**H**=C(CH$_3$)-CH$_2$).

2.3.3. Poly(isoprene-*block*-methyl methacrylate) (PI-*b*-PMMA)

The following describes a typical procedure for the preparation of one of a family of PI-*b*-PMMA block copolymers prepared by ATRP. PI$_{55}$-*Br* was used to make a series of

block copolymers with PMMA blocks of varying molar mass. Thus, in a typical reaction, for a target molecular weight for PMMA of 25000 g mol^{-1}, PI$_{55}$-Br (3710 g mol^{-1}; 0.38 g, 0.10 mmol) and 2,2'-bipyridyl (66 mg, 0.42 mmol) were charged to a Schlenk flask, along with MMA (2.55 g, 25 mmol) and 1,4-dioxane ($\approx$10 mL) (both of which were passed through columns of neutral aluminium oxide immediately prior to use). The reactor was sealed with a rubber septum, and the contents were then degassed by freeze-pump-thaw cycles before raising the flask to atmospheric pressure with nitrogen gas. Meanwhile, copper (I) bromide (17 mg, 0.12 mmol) was charged to a separate Schlenk flask, containing a magnetic stirrer bar, which was also sealed with a rubber septum. This was evacuated and backfilled with nitrogen gas; a process repeated 3 times to remove any oxygen. The dioxane solution of macroinitiator, monomer and ligand was then added to the copper bromide flask by injection via a rubber septum before the mixture was degassed with freeze-pump-thaw cycles. The dark brown reaction mixture was raised to atmospheric pressure with nitrogen gas and the mixture stirred magnetically overnight at 90 °C. The following morning, the contents had turned green, indicating the presence of copper (II) salts. The solution was cooled to room temperature, passed through a column of neutral aluminium oxide to remove the copper salts and the copolymer was recovered by addition to methanol (250 mL) containing BHT (5 g). The precipitated polymer was collected by filtration to yield a white powder (2.3 g, 79 %).

SEC: M_n = 24690 g mol^{-1}; M_w = 31850 g mol^{-1}; M_n/M_w = 1.29. ^1H-NMR (400 MHz, CDCl$_3$, 298 K, ppm): δ = 0.86-1.15 (-C$\mathbf{H_3}$), 1.62-1.69 CH$_2$-CH=C(CH$_3$)-CH$_2$), 1.83 (-C$\mathbf{H_2}$), 1.90-2.05 (C$\mathbf{H_2}$-CH=C(CH$_3$)-C$\mathbf{H_2}$), 3.61 (-O-C$\mathbf{H_3}$), 4.67-5.14 (CH$_2$-C$\mathbf{H}$=C(CH$_3$)-CH$_2$).

2.3.4. Poly(isoprene-block-(N,N-dimethylaminoethyl methacrylate) (PI-b-PDMAEMA)

The following describes a typical procedure for the preparation of one of a family of PI$_{37}$-b-PDMAEMA$_x$ block copolymers prepared by ATRP of DMAEMA. PI$_{37}$-Br was used to make a series of block copolymers with PDMAEMA blocks of varying molar mass. Thus, in a typical reaction, for a target molecular weight for PDMAEMA of 10000 g mol^{-1}, PI$_{37}$-Br (3070 g mol^{-1}; 0.50 g, 0.16 mmol) and PMDETA (34 μL; 28 mg, 0.16 mmol) were charged to a glass reactor (see photograph in Figure 2.2), along with DMAEMA (1.6 g, 10 mmol) and THF ($\approx$25 mL) (both of which were passed through columns of aluminium oxide; basic and

neutral, respectively, immediately prior to use). The reactor was sealed with a rubber septum, and the contents were then degassed by freeze-pump-thaw cycles. Meanwhile, copper (I) bromide (23 mg, 0.16 mmol) was charged to the adjacent Schlenk flask (connected by a glass tube), containing a magnetic stirrer bar, which was also sealed with a rubber septum. The 2-flask reactor was evacuated and backfilled with nitrogen gas; a process repeated 3 times to remove any oxygen. The THF solution of macroinitiator, monomer and ligand was then decanted along the connecting, glass tube into the copper bromide flask before the mixture was degassed with freeze-pump-thaw cycles. The turbid, bright green reaction mixture was raised to atmospheric pressure with nitrogen gas and the mixture stirred magnetically overnight at 30 $^{\circ}$C. The following morning, the liquid contents remained green, with small, green solid particles present. The solution was passed through a column of basic aluminium oxide to remove the copper salts and the copolymer recovered by rotary evaporation of the solvent and drying *in vacuo* to yield a thick, sticky, dark yellow gel (1.5 g, 71 %).

SEC: M_n = 7030 g mol^{-1}; M_w = 7870 g mol^{-1}; M_w/M_n = 1.12.

^{1}*H*-NMR (400 MHz, CDCl$_3$, 298 K, ppm): δ = 0.69-1.31 (C-C**H**$_3$), 1.62-1.69 C**H**$_2$-CH=C(CH$_3$)-CH$_2$), 1.76-1.98 (C-C**H**$_2$), 1.90-2.05 (C**H**$_2$-CH=C(CH$_3$)-C**H**$_2$), 2.30 (N-(C**H**$_3$))$_2$, 2.57 (N-C**H**$_2$) 4.06 (O-C**H**$_2$), 4.67-5.14 (CH$_2$-C**H**=C(CH$_3$)-CH$_2$).
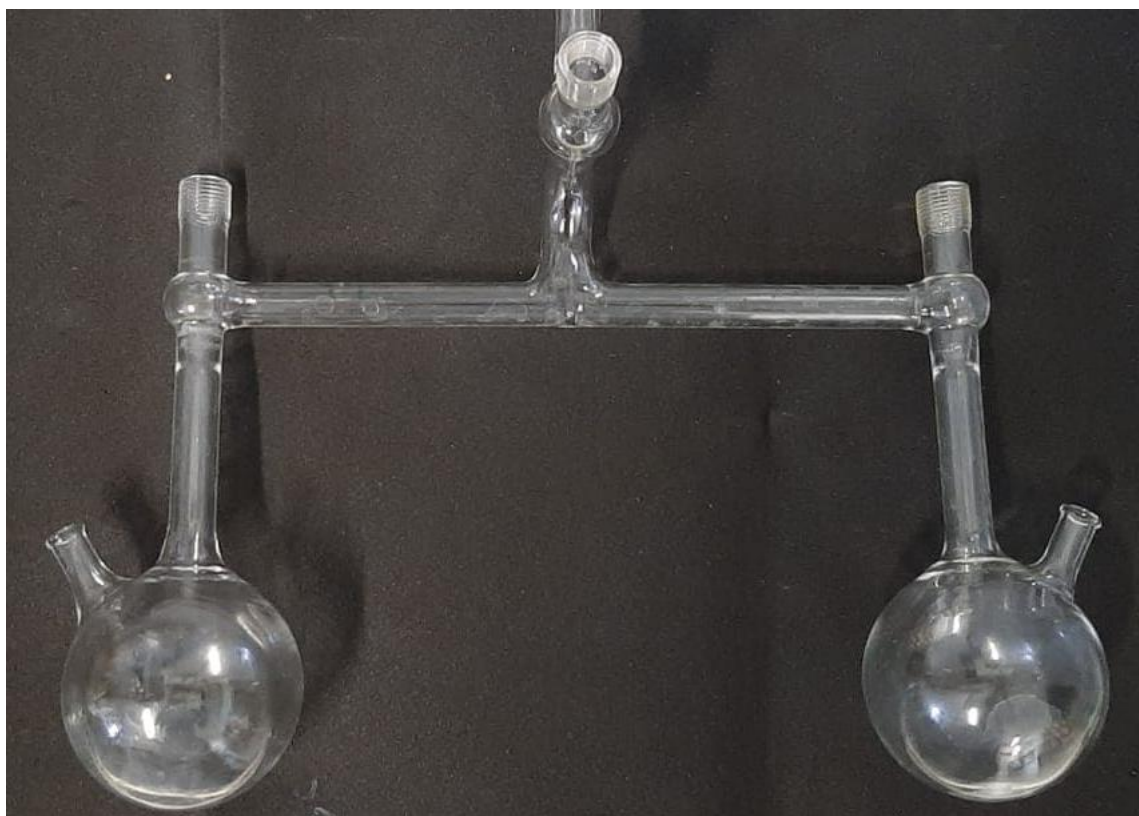
Figure 2.2: Reactor used for the ATRP of DMAEMA from a PI-Br macroinitiator

2.3.5. Quaternisation of PDMAEMA in PI-*b*-PDMAEMA Block Copolymers

The quaternisation of PI-*b*-PDMAEMA to produce PI-*b*-PQDMAEMA was carried out with 3 different alkyl iodides: ethyl iodide, 1-butyl iodide and 1-octly iodide, all at varying mol% with respect to PDMAEMA. The same protocol was used for all such reactions from the same PI$_{37b}$-*b*-PDMAEMA$_{35}$ block copolymer. The following describes a typical quaternisation reaction to a target conversion of 40 mol% with ethyl iodide.

The PI-*b*-PDMAEMA was first dissolved in DCM (a common solvent for PI and PDMAEMA) for transfer into a reactor flask. PI$_{37b}$-*b*-PDMAEMA$_{35}$ (7390 g mol^{-1}; 10.31 g, 1.40 mmol) was fully dissolved in DCM (45.73 g, 538 mmol) with magnetic stirring. A portion of this solution (3.18 g) was added to a Schlenk flask containing a magnetic stirrer bar, which was then sealed with a rubber septum. The solution was degassed by freeze-pump-thaw cycles and the DCM was distilled off under reduced pressure. The polymer (7390 g mol^{-1}; 0.65 g, 0.09 mmol) was left drying overnight under high vacuum. THF (≈60 mL) was distilled into the Schlenk flask under reduced pressure to dissolve the PI$_{37b}$-*b*-PDMAEMA$_{35}$ block copolymer, forming a clear, yellow solution. Ethyl iodide (0.09 mL; 0.18 g, 1.2 mmol) was injected via rubber septum. The solution was left for 24 hours at room temperature

with magnetic stirring, following which, the solution had changed into a turbid, pale yellow, loose gel. At this point, ≈8 mL was poured into a separate vial for TEM analysis. The remaining reaction mixture had the solvent removed by rotary evaporation and the product was dried *in vacuo* to yield a pale yellow, brittle, solid (0.74 g, 89 %).

^1H-NMR (400 MHz, CDCl$_3$, 298 K, ppm): δ = 0.72-1.33 (C-**CH$_3$**), 1.52-1.66 CH$_2$-CH=C(CH$_3$)-**CH$_2$**), 1.66-1.96 (C-**CH$_2$**), 1.96-2.15 (**CH$_2$**-CH=C(CH$_3$)-**CH$_2$**), 2.30 (N-(**CH$_3$**))$_2$, 2.59 (N-**CH$_2$**), 3.54 (N$^+$-(**CH$_3$**)$_2$), 3.91 (N$^+$-**CH$_2$**) 4.07 (O-**CH$_2$**), 4.64-5.21 (CH$_2$-**CH**=C(CH$_3$)-CH$_2$).

2.3.6. Microstructural Block Copolymers of Polybutadiene

Polybutadiene samples were prepared by living anionic polymerisation in a non-polar aprotic solvent. The polymers were synthesised using a commercial process and the details of the following procedure, for the preparation of PBD2, have been omitted.

SEC: M_n = 11100 g mol^{-1}; M_w = 11700 g mol^{-1}; M_w/M_n = 1.05.

^1H-NMR (400 MHz, CDCl$_3$, 298 K, ppm): δ = 1.03-1.63 (C-**CH$_3$**), 1.85-2.23 (**CH$_2$**-CH=CH-**CH$_2$**), 4.98 (CH=**CH$_2$**), 5.28-5.48 (CH$_2$-**CH**=CH-CH$_2$) 5.57 (**CH**=CH$_2$), 5.82 ((CH$_2$)$_2$-CH-**CH**=CH$_2$).

2.3.7. Maleinisation of Polybutadiene

The maleinisation of polybutadiene was carried out according to a commercial process and some details have been omitted to ensure confidentiality. Each polymer was maleinised to 5 and 10 wt%. The following describes the maleinisation of PBD2 to 10 wt% to produce PBD2-10MA. PBD2 (400 g), a commercial antioxidant package (2 g) and maleic anhydride (43 g, 10 wt%) were charged to a 5 L glass reactor containing a mechanical stirrer blade under an inert atmosphere. The reaction mixture was heated for a pre-determined amount of time (according to the industrial procedure), such that the reaction went to high conversion. The product was collected with no additional work-up.

FTIR: $\tilde{v}$ (C=O stretch) = 1784 cm^{-1} (asymmetric), 1863 cm^{-1} (symmetric)

^1H-NMR (400 MHz, CDCl$_3$, 298 K, ppm): δ = 1.04-1.65 (C-**CH$_3$**), 1.84-2.21 (**CH$_2$**-CH=CH-**CH$_2$**), 2.62-2.84 (CH-**CH$_2$**-C(O)-O-C(O)), 3.19 (**CH**-CH$_2$-C(O)-O-C(O)) 4.98 (CH=**CH$_2$**), 5.25-5.51 (CH$_2$-**CH**=CH-CH$_2$) 5.58 (**CH**=CH$_2$), 5.82 ((CH$_2$)$_2$-CH-**CH**=CH$_2$).

2.3.8. Imidisation of Maleinised Polybutadiene

Maleinised polybutadiene was further modified by imidisation. The imidisation reaction was carried out as described below for the imidisation of PBD2-10MA to produce PBD2-10IM.

PBD2-10MA (9.65 g) was charged to a 2-necked round-bottom flask fitted with a rubber septum and a condenser. The polymer was dissolved in dry toluene (≈100 mL) with magnetic stirring. The solution was sparged with dry nitrogen for 15 minutes, followed by the injection of DMAPA (1.13 mL, 0.918 g; 8.98 mmol) via rubber septum into the reactor. The contents were heated to 110 °C in an oil bath and left stirring under reflux and a blanket nitrogen flow for 24 hours. The solution was cooled to room temperature and poured into methanol (≈500 mL) to precipitate the brown viscous product which was allowed to sink to the bottom of the beaker before being collected and dried *in vacuo*.

FTIR: $\tilde{v}$ (C=O stretch) = 1701 cm^{-1}

^1H-NMR (400 MHz, CDCl$_3$, 298 K, ppm): δ = 1.01-1.62 (C-C**H**$_3$), 1.86-2.17 (C**H**$_2$-CH=CH-C**H**$_2$), 2.22 (N-(C**H**$_3$)$_2$ 2.54-2.80 (CH-C**H**$_2$-C(O)-N-C(O)), 2.86 (C**H**-CH$_2$-C(O)-N-C(O)) 4.98 (CH=C**H**$_2$), 5.27-5.50 (CH$_2$-C**H**=C**H**-CH$_2$) 5.58 (C**H**=CH$_2$), 5.82 ((CH$_2$)$_2$-CH-C**H**=CH$_2$).

2.4. Dispersion of Copolymers in Non-Polar Solvents

2.4.1. Self-Assembly of PI-*b*-PMMA in n-Decane

A typical procedure for the self-assembly of the PI-*b*-PMMA in *n*-decane was carried out as follows. PI$_{32}$-*b*-PMMA$_{73}$ (1.00 g) was dissolved in dichloromethane (6.50 g), a good solvent for both blocks, in a sample vial with magnetic stirring, to give a colourless solution. Meanwhile, *n*-decane (0.50 g) was weighed into a separate sample vial, containing a magnetic stirrer. The block copolymer solution (see Table 2.1 for mass added for each wt%) was added dropwise to the *n*-decane with fast magnetic stirring. The slightly turbid solution was then heated to 60 °C with magnetic stirring to evaporate off DCM until the mass of solution reached that of *n*-decane plus polymer added.

Table 2.1: Masses used for self-assembly of PI$_{32}$-b-PMMA$_{73}$ in n-decane at the designated wt%. The initial polymer solution in DCM (1.00 g in 6.50 g) was added in the mass ratios described below to the selective solvent, n-decane (0.50 g)

Wt% PI32-*b*-PMMA73	Mass of soln. added/ g	Mass of polymer added/ g
5	0.195	0.026
10	0.435	0.058
15	0.660	0.088
20	0.938	0.125
25	1.215	0.162
30	1.62	0.216

2.4.2. Dispersion of Block Copolymers in Yubase 4

For testing of neat solutions and the 0W20 formulation, a similar solvent-switching procedure for dispersing the block copolymers to the one described above in Section 2.4.1 was used. For example, PI$_{79}$-*b*-PMMA$_{256}$ (21.0 g) was fully dissolved in dichloromethane (507 g). This solution was then added dropwise over 1 hour to Yubase 4 (399 g, for a 5 wt% solution of polymer in oil) under fast mechanical stirring. Once complete, the solution was rotary evaporated to remove the DCM, leaving an opaque, white solution of PI-*b*-PMMA dispersed in Yubase 4 at 5 wt%. Finally, Irganox L135 (0.84 g, 2000 ppm) was added to act as an antioxidant.

The neat solutions of block copolymer in Yubase 4 were all tested at varying concentrations to reflect the typical loadings of friction and viscosity modifiers. Dilutions of the 5 wt% solutions described above were carried out in accordance with the masses described in Table 2.2.

Table 2.2: Tabulated data showing the masses of 5 wt% polymer stock solution and Yubase 4 used in the preparation of samples of varying concentration for testing of neat solutions.

Target Concentration/ wt%	Mass of 5 wt% solution/ g	Mass of Yubase 4/ g
2.5	12.5	12.5
1.0	5.0	20.0
0.5	2.5	22.5

2.4.3. Fully Formulated Sample Preparation

For the dispersion of polymers into a standard Shell 0W20 full formulation, a typical preparation was carried out as follows. Infineum SV261L (4.00 g), Synfluid PAO 4 (40.00 g),

Yubase 4 (24.50 g)* and the block copolymer (5 wt% solution in Yubase 4 as described in Section 2.4.2; 20.20 g)* were weighed out into a beaker. The mixture was stirred mechanically at 90 °C for 30 minutes to ensure complete dissolution of the viscosity and friction modifiers. The solution was cooled to room temperature before the addition of Infineum P6003 additive package (12.3 g). The solution was stirred mechanically at 50 °C for a further 30 minutes until fully homogenised.

*Where the friction modifier was a commercial standard (and therefore not made up as a 5 wt % solution in Yubase 4), 1.01 g of the friction modifier and 43.70 g of Yubase 4 were used.

For Mobil Delvac 5W30, Motul 0W16 and Motul 5W30, all friction modifiers were dispersed directly into already prepared full formulations as follows. Friction modifier (1.00 g) was weighed out into a beaker with formulation (99.00 g). The mixture was stirred mechanically at 90 °C for 1 hour until fully homogenised (110 °C, 2 hours for all PI-*b*-PDMAEMA polymers).

2.5. References

1. S. Lee, M. Muller, M. Ratoi-Salagean, J. Voros, S. Pasche, S. M. De Paul, H. A. Spikes, M. Textor, N. D. Spencer, *Tribol. Lett.*, 2003, **15**, 231-239.

3. Synthesis and Self-Assembly of Poly(isoprene-*block*-methyl methacrylate) Block Copolymers in Selective, Non-Polar Solvents

3.1. Introduction

The self-assembly of diblock copolymers (BCPs) in solution to form micellar structures has been widely studied for the last 60 years.[1-3] This area of research has advanced significantly in the past decade with the breakthrough of polymerisation-induced self-assembly (PISA) to produce block copolymer micelles *in situ*.[4, 5] The majority of this research has exploited the use of reversible-deactivation radical-polymerisation (RDRP) for polymer synthesis, and in particular reversible addition-fragmentation chain-transfer (RAFT) polymerisation in aqueous or polar solvents.[6-8] However, there is also a limited number of reported examples of PISA being carried out in non-polar solvents.[9-12] These reports have primarily made use of long chain alkyl acrylates or methacrylates as the non-polar, soluble block as these can be polymerised easily by RDRP.

Dienes (such as 1,3-butadiene and isoprene) are widely used in industry as highly non-polar monomers, because of their availability and low cost. The preparation of these polymers is often achieved by living anionic polymerisation (LAP) because the use of RDRP techniques for these monomers is not very effective.[13-16] Conversely, the polymerisation of polar monomers by LAP is not industrially viable because of the prevalence of unwanted side reactions leading to termination competing with propagation during syntheses.[17-19] In this chapter, a change of mechanism polymerisation (CHOMP) procedure is described in which a non-polar, polyisoprene (PI) block is prepared by LAP and end-capped with ethylene oxide. This functionality was then converted to a bromide, allowing the polymer to be used as a macroinitiator for the atom-transfer radical polymerisation (ATRP) of a polar, methyl methacrylate (MMA) block (also a commercially-relevant, cheap and widely available monomer). Similar methods for preparing block copolymers have previously been reported.[20] In this context, CHOMP was advantageous because it allowed for the preparation of homologous families of PI-*b*-PMMA block copolymers with varying molecular weights of PMMA and polyisoprene blocks of fixed molecular weight.

The PI-*b*-PMMA block copolymers that were prepared underwent self-assembly in *n*-decane, a selective solvent for the non-polar, PI block. PISA was not employed for the

preparation of micelles, instead the block copolymers underwent self-assembly following dispersion using an alternative, post-polymerisation, solvent-switching method.[21-25] Depending on the molecular weight of the PMMA block, a variety of physical structures was formed, including free-flowing liquids and self-supporting gels. These were probed with TEM and DLS and found to arise as a result of the formation of different micellar morphologies (e.g. spherical and wormlike micelles). Finally, the thermoresponsivity of the various self-assembled morphologies was explored by variable-temperature rheology and TEM. The dispersibility of these heteroatom-containing block copolymers in non-polar solvents suggests that they could be useful as additives in lubricant formulations. This was subsequently investigated and is discussed in Chapter 5.

3.2. Results and Discussion

For the past decade, reports on the self-assembly of diblock copolymers have predominantly focussed on polymerisation-induced self-assembly (PISA).[4, 26, 27] Before this technique became widely established, the most common means of self-assembling block copolymers was by using solvent mixtures or solvent switching.[28, 29] While RAFT-mediated PISA is an extremely useful and relatively simple technique for preparing self-assembled nano-structures *in situ*, there are also significant drawbacks, including the fact that the dithioester RAFT agent, which is expensive, also renders the resulting polymers deeply coloured and is not easy to remove from self-assembled micelles.[30] There are also expected to be practical difficulties in the industrial scale-up for direct preparation of block copolymers via PISA.[31] The block copolymers in this study were prepared by an alternative, change-of-mechanism polymerisation (CHOMP) and redispersed post-polymerisation, as described herein.

3.2.1. Polymer Synthesis

A two-step CHOMP approach was adopted for the synthesis of PI-*b*-PMMA BCPs. In the first step, LAP was used to produce ethylene oxide end-capped polyisoprene (PI-*OH*) which, following conversion to an ATRP macroinitiator (PI-*Br*) was used for the polymerisation of MMA by ATRP.

3.2.1.1. Synthesis of Bromide-end-capped Polyisoprene (PI-*Br*) Macroinitiator

Ethylene oxide end-capped polyisoprene (PI-*OH*) was prepared by living anionic polymerisation according to a previously published method as illustrated in Scheme 3.1.[32] Ethylene oxide was used in (at least) a 10-fold excess with respect to *s*-BuLi to ensure quantitative end-capping, in the knowledge that ethylene oxide is unable to propagate when using a lithium counter-ion.[33]
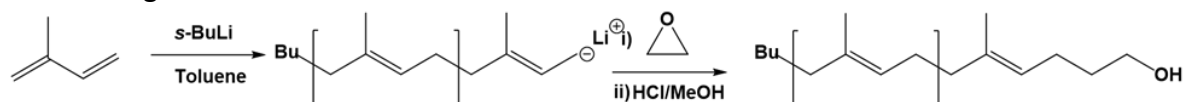
Scheme 3.1: Reaction scheme for the living anionic polymerisation of isoprene and its subsequent end-capping with ethylene oxide to yield PI-OH

Using the reaction protocol described in Scheme 3.1, a series of 3 PI-*OH* polymers with different molecular weights was synthesised (see Figure 3.1 and Table 3.1). In all cases the molar mass obtained by SEC was in excellent agreement with the predicted values and dispersities are low. This is typical for the living anionic polymerisation of isoprene which takes place in the absence of inherent self-termination mechanisms.[34]
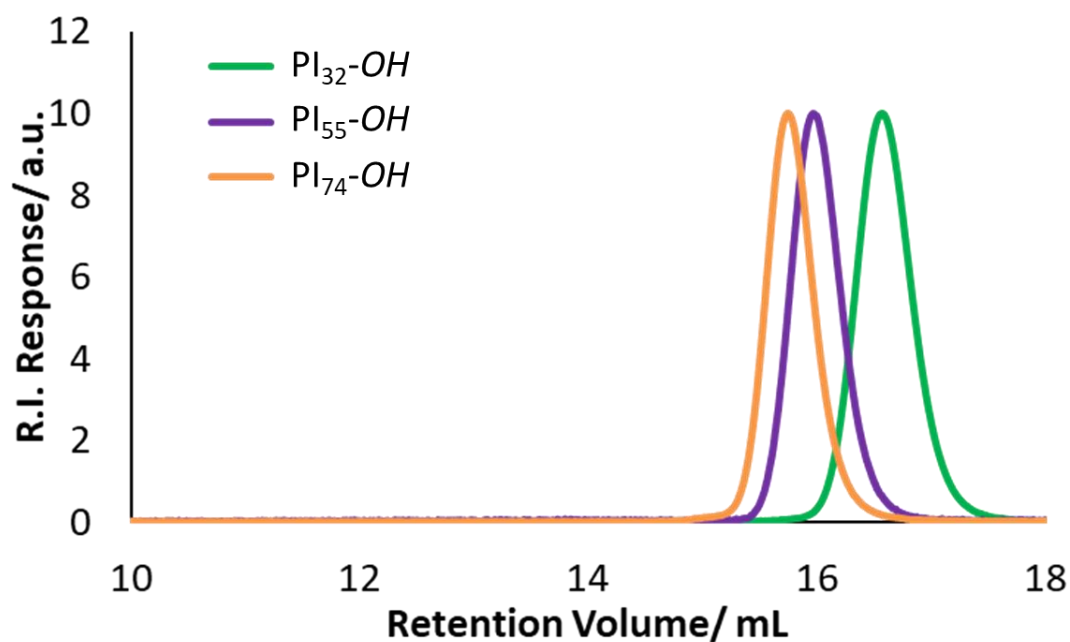
Figure 3.1: SEC Chromatograms for PI$_{32}$-OH, PI$_{55}$-OH and PI$_{74}$-OH prepared by living anionic polymerisation

59

Table 3.1: Molar mass data for 3 PI-OH samples prepared according to Scheme 3.1, obtained using triple detection SEC in THF (dn/dc = 0.13 mL g⁻¹).

Polyisoprene$_{DP}$ [a]	M_n (theo) / g mol^{-1}	M_n (expt) / g mol^{-1}	Đ
PI$_{32}$	2040	2150	1.07
PI$_{55}$	3540	3730	1.04
PI$_{74}$	5040	5030	1.06

[a]DP of PI block calculated from SEC data

^{1}H-NMR was used to measure the degree of end-capping of polyisoprene chains with ethylene oxide. A characteristic proton NMR spectrum for ethylene oxide end-capped polyisoprene is shown in Figure 3.2. By comparing the integration values of the peaks at δ3.56 – 3.79 ppm representing the CH$_2$ adjacent to the hydroxyl end-group, with those of polyisoprene, the degree of end-capping can be estimated to be 100 %. This is consistent with reports in the literature which suggests that living polystyryl lithium in benzene reacts quantitatively with ethylene oxide.[33]
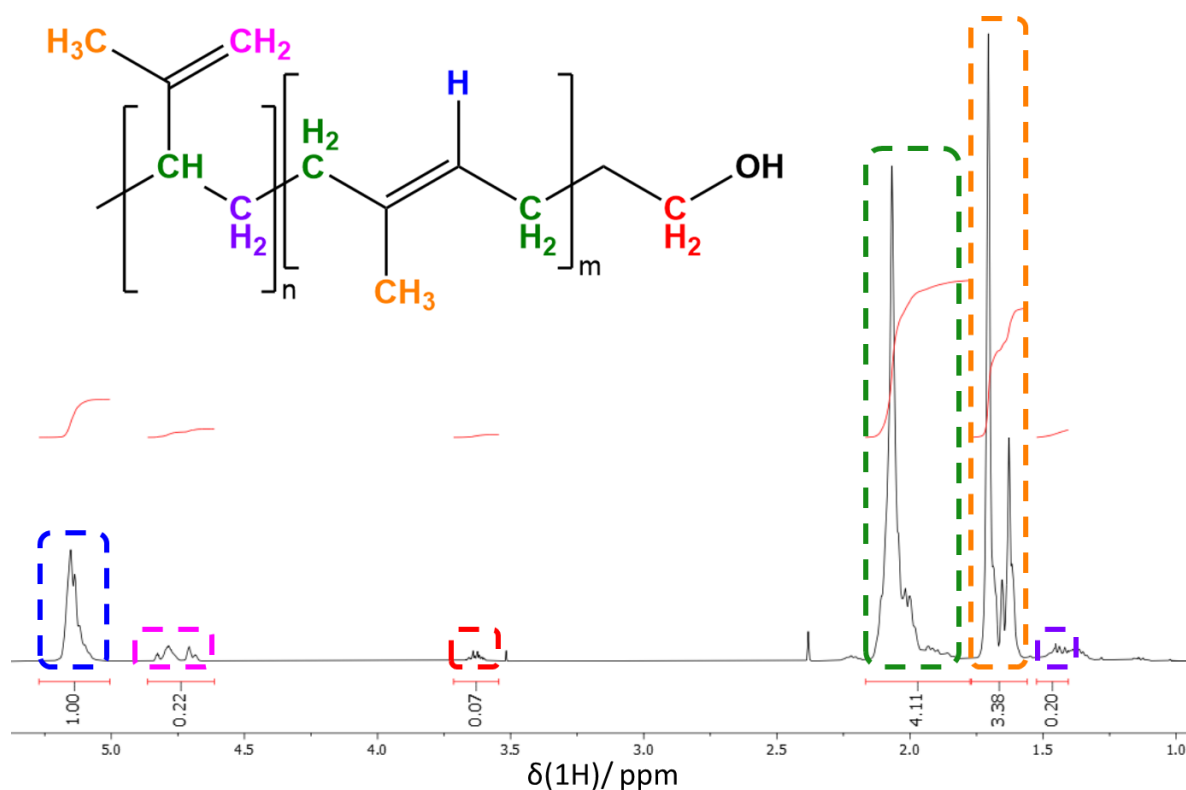
Figure 3.2: ^1H NMR spectrum of PI$_{32}$-OH.

In order to prepare an ATRP macroinitiator, bromoacetylation of PI-*OH* was carried out using an excess of α-bromoisobutyryl bromide in the presence of triethylamine, in a similar fashion to previous reports.[35] The ^1H NMR spectrum of the bromide-end-capped polyisoprene (PI-*Br*) macroinitiator is shown in Figure 3.3. The emergence of a peak at δ1.95 ppm is characteristic of the methyl groups (highlighted in gold) introduced following end-capping with bromoisobutyryl bromide. It is not possible to ascertain the degree of end-capping using this peak because of the overlap with the peak of the protons adjacent to the double bond of polyisoprene (highlighted in green). However, the success of this reaction is also indicated by the disappearance of the C**H**$_2$-*OH* peak at δ3.56 – 3.79 ppm, which has shifted downfield to δ4.05 – 4.21 ppm following conversion to the ester (highlighted in red). By comparing the integrals of this peak with those of polyisoprene, the degree of end-capping with the bromide functionality can be shown to be quantitative.
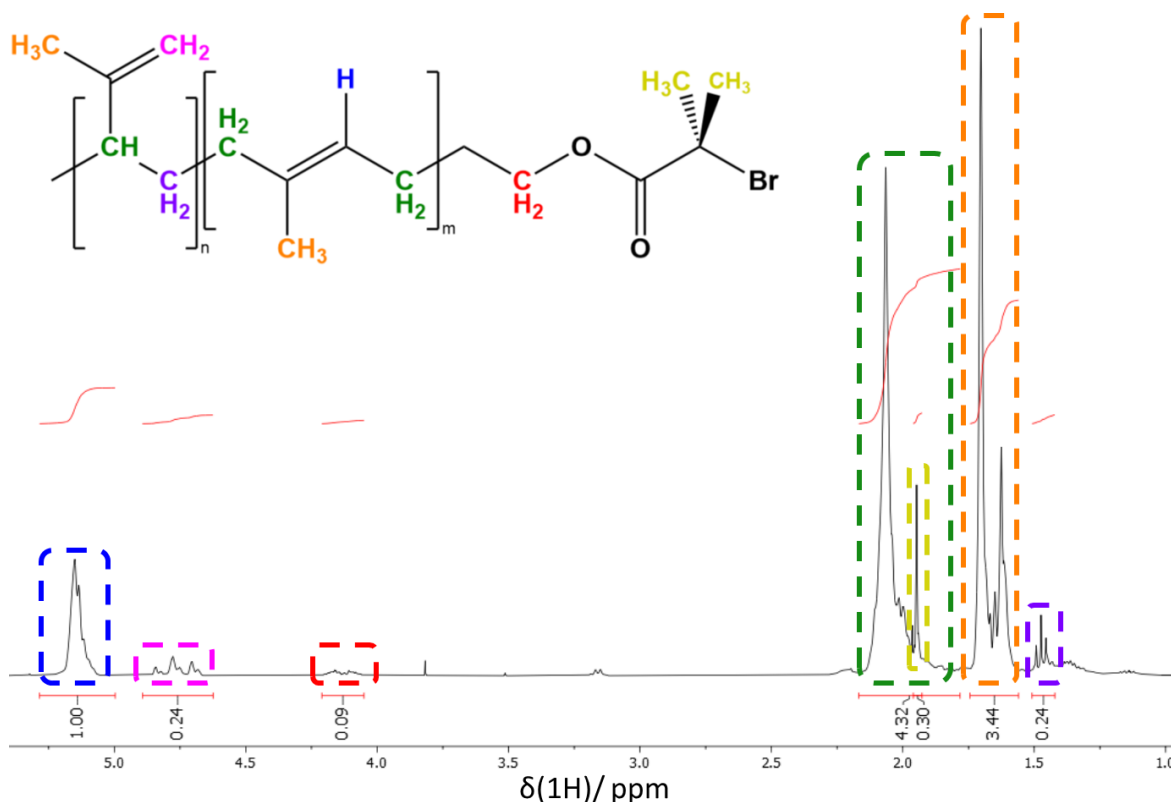
Figure 3.3: ^{1}H NMR spectrum of PI$_{32}$-Br ATRP macroinitiator.

3.2.1.2. Synthesis of Block Copolymers by ATRP of MMA

ATRP of MMA has been widely reported using a range of conditions and a variety of initiators, ligands, solvents etc.[36-38] For this study, a system with copper (I) bromide catalyst, 2,2-bipyridyl ligand and 1,4-dioxane as the solvent, at 90 °C was used to prepare (PI-*b*-PMMA). Exemplar SEC chromatograms for PI$_{55}$-*Br* and the respective PI$_{55}$-*b*-PMMA$_x$ block copolymers are shown in Figure 3.4 and the chromatogram for all PI$_{55}$-*b*-PMMA block copolymers show a significant shift to lower retention volumes (higher molar mass) for the block copolymers compared to the respective PI-*Br* macroinitiator.
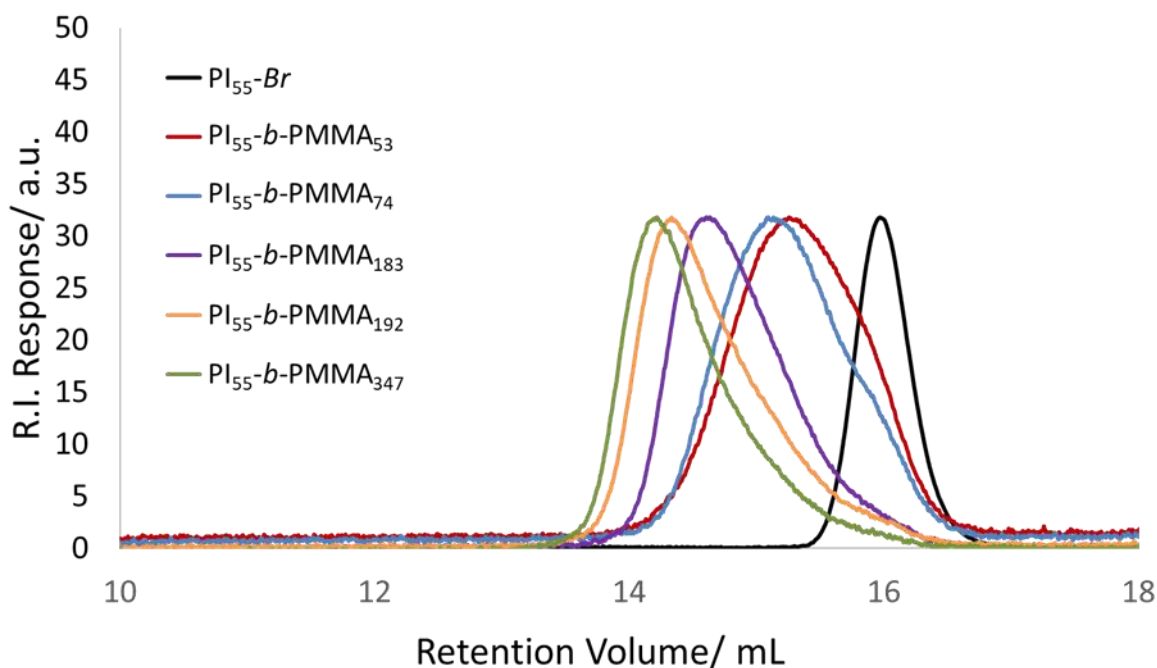
Figure 3.4: Overlaid size exclusion chromatography (SEC) RI traces for the PI$_{55}$-Br macroinitiator (black line) and the resulting PI-b-PMMA block copolymers.

It is worth noting that the chromatograms in Figure 3.4 for PMMA blocks with a low DP (PI$_{55}$-*b*-PMMA$_{53}$ and PI$_{55}$-*b*-PMMA$_{74}$), show the presence of a shoulder, at a retention volume which is coincident with the peak corresponding to the macroinitiator, indicating the presence of residual polyisoprene homopolymer in the final product. The proton NMR spectrum (Figure 3.3) for PI-*Br* macroinitiator suggests quantitative end-capping of polyisoprene with the initiating bromide moiety, therefore the most likely reason for the presence of PI in the SEC is a slow rate of initiation by PI-*Br* in the ATRP of MMA. This would also explain why the shoulder does not appear for the block copolymers with a higher DP$_{PMMA}$.

Because of the differences in the refractive index increment (dn/dc) of PI (0.13 mL g^{-1}) and PMMA (0.085 mL g^{-1}) homopolymers in THF, the molar mass of the PMMA blocks prepared by ATRP using PI-*Br* macroinitiators, cannot be accurately calculated by triple-detection SEC. Instead, the molar mass of PMMA was calculated from the integrals of the NMR spectra of the block copolymers (example in Figure 3.5). The method of calculation used was based on the degree of polymerisation of PI (DP$_{PI}$), calculated from the number

average molecular weight ($M_{n,PI(SEC)}$) obtained by SEC. This is shown below Figure 3.5 with a worked example for PI$_{32}$-b-PMMA$_{107}$.
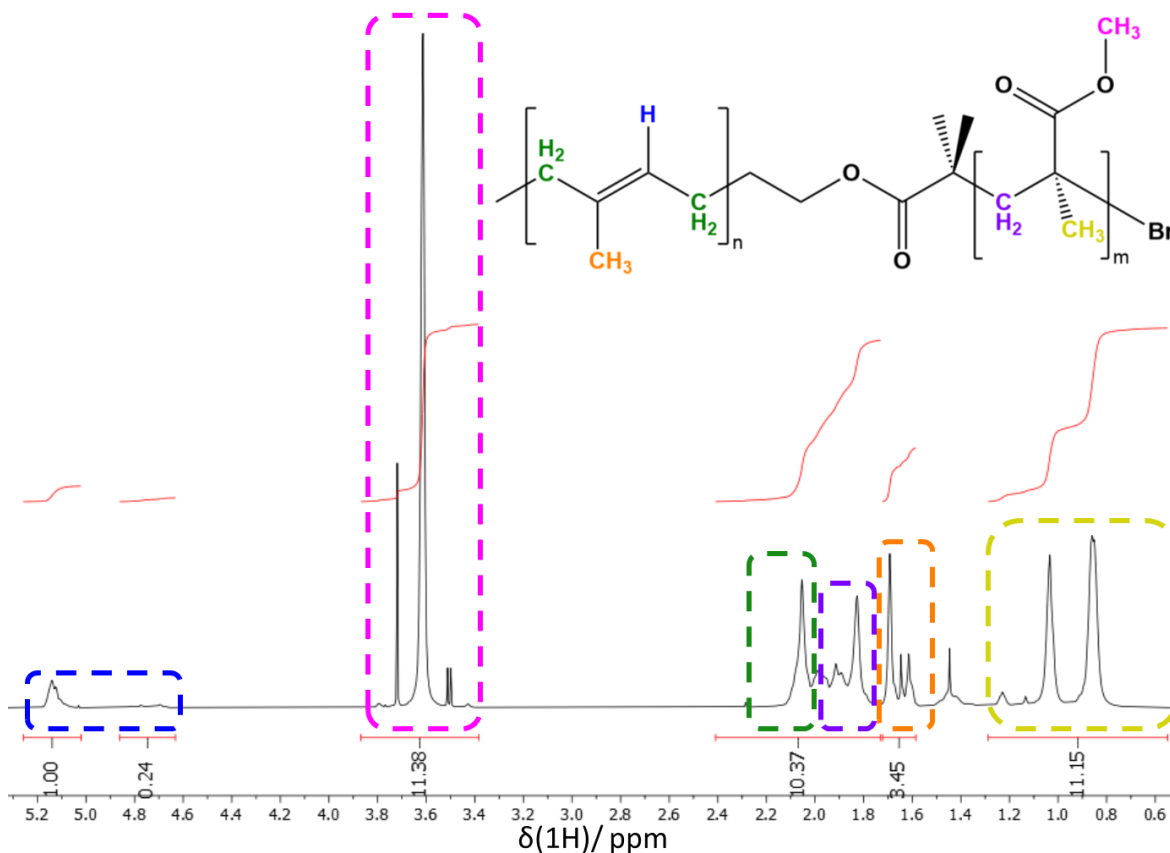
Figure 3.5: ^1H NMR spectrum for a PI-b-PMMA block copolymer. In this instance the sample shown is PI$_{32}$-b-PMMA$_{107}$, prepared by ATRP of MMA from the PI$_{32}$-Br macroinitiator.

$$DP_{PI} = \frac{M_{n,PI(SEC)}}{M_{r,Isoprene}} = \frac{2150 \ gmol^{-1}}{68.12 \ gmol^{-1}} = 31.6$$

DP$_{PI}$ was used with the integrals for the alkene protons (considering the different environments for the 1,4 and 1,2 microstructures) to calculate the integration per proton (∫ per H$_{PI}$) in the spectrum.

$$\int per \ H_{PI} = \frac{\int_{5.14 \ ppm} + \frac{\int_{4.85 \ ppm-4.62 \ ppm}}{2}}{DP_{PI}} = \frac{1.00 + \frac{0.24}{2}}{31.6} = 0.035$$

The integral for the peak for the methyl ester in PMMA was divided by ∫ per H$_{PI}$ to calculate the molar mass of the PMMA block.

$$M_{n,PMMA} = \frac{\int_{3.61 \ ppm}}{\int per \ H_{PI} \times 3} \times M_{r,MMA} = \frac{11.38}{0.035 \times 3} \times 100.12 \ gmol^{-1} = 10700 \ gmol^{-1}$$

Using the respective values from the SEC of PI-*OH* (Table 3.) and the proton NMR spectra of PI-*b*-PMMA (Figure 3.5), the calculations described above were carried out for all PI-*b*-PMMA block copolymers to determine the molar mass of each PMMA block. The molar mass data for the PI-*b*-PMMA block copolymers are summarised below in Table 3.2.

Table 3.2: Molar mass data for PI$_x$-b-PMMA$_y$ block copolymers where x and y are degree of polymerisation obtained by SEC for PI block and NMR for PMMA block, respectively.

Sample Name	$M_{n,}$(theo)[a] / g mol^{-1}	$M_{n,}$(expt) / g mol^{-1}	$M_{n,}$ (NMR)[b] / g mol^{-1}	Đ
PI$_{32}$	2040	2150	-	1.07
PI$_{32}$-*b*-PMMA$_{71}$	22000	15100	9290	1.19
PI$_{32}$-*b*-PMMA$_{73}$	9540	11700	9460	1.50
PI$_{32}$-*b*-PMMA$_{96}$	14500	13300	11800	1.48
PI$_{32}$-*b*-PMMA$_{107}$	12000	15500	12900	1.46
PI$_{32}$-*b*-PMMA$_{161}$	22200	22700	18300	1.24
PI$_{55}$	3540	3730	-	1.04
PI$_{55}$-*b*-PMMA$_{53}$	8540	11400	9060	1.29
PI$_{55}$-*b*-PMMA$_{74}$	11000	12200	11100	1.31
PI$_{55}$-*b*-PMMA$_{183}$	23500	20400	22100	1.21
PI$_{55}$-*b*-PMMA$_{192}$	28500	24700	23000	1.29
PI$_{55}$-*b*-PMMA$_{347}$	38500	29600	38500	1.27
PI$_{74}$	5040	5030	-	1.06
PI$_{74}$-*b*-PMMA$_{69}$	25000	15100	11900	1.19
PI$_{74}$-*b*-PMMA$_{154}$	75000	24000	20400	1.21
PI$_{74}$-*b*-PMMA$_{169}$	45000	28200	22000	1.22
PI$_{74}$-*b*-PMMA$_{172}$	30000	25100	22200	1.26
PI$_{74}$-*b*-PMMA$_{198}$	35000	29000	24900	1.26
PI$_{74}$-*b*-PMMA$_{233}$	50000	30700	28400	1.35
PI$_{74}$-*b*-PMMA$_{250}$	40000	33000	30100	1.38
PI$_{74}$-*b*-PMMA$_{356}$	70000	54700	41000	1.19
PI$_{74}$-*b*-PMMA$_{467}$	95000	50400	51800	1.39

[a] Molar mass PI + theoretical molar mass of PMMA

[b] $M_{n,}$(NMR) calculated using molar mass by SEC for PI block and NMR data for PMMA block according to method explained in supporting information.

The molar mass data are entirely in line with expectations for a successful block copolymer synthesis. It is also clear from the chromatograms (Figure 3.4) and the data in Table 3. that the dispersity value for the block copolymers is higher than that of the precursor macroinitiator. This is not unexpected given that termination reactions may still occur in ATRP reactions and ATRP routinely results in broader molar mass distributions than LAP.

It is clear from the molar mass data in Table 3.2 that there is a discrepancy between the molar mass obtained from NMR data and the molar mass obtained by SEC. As discussed above, triple detection SEC analysis requires the use of an accurate value for the refractive index increment (dn/dc), which varies according to the polymer. In the current study a dn/dc value of 0.085 mL g^{-1} was used, which is the dn/dc of PMMA. Thus, an error will be expected for a block copolymer, which is particularly evident when the PMMA block is shorter. For this reason, it is believed that the molar mass of the copolymers in this study is more accurately determined using NMR data, also reported in Table 3.2.

3.2.2. Self-Assembly of PI-*b*-PMMA in non-polar Solvents

Recently, polymerisation-induced self-assembly (PISA) has been widely reported, predominantly using RAFT polymerisation.[39-41] Whilst there are many benefits of this technique, including relative simplicity and scalability, there are also associated difficulties such as purification of the subsequently self-assembled block copolymer.[42] However, PISA is not the only viable process to enable BCPs to self-assemble. In the current study, BCPs were dissolved in a common solvent and subsequently exposed to a solvent switching method (i.e. by evaporation) to drive self-assembly, as has been described in the literature.[43-45] Thus, a solution of the block copolymer in dichloromethane was added dropwise into *n*-decane, a selective solvent for the PI block, with rapid stirring, before evaporation of the common solvent. The self-assembly of three homologous series of PI-*b*-PMMA BCPs in *n*-decane was studied. In each series the molar mass of the PI-block remains constant and the molar mass of the PMMA block is systematically varied. Each BCP was dispersed in *n*-decane at a variety of concentrations, from 5 – 30 wt%, resulting in the formation of stable nanoparticle dispersions. Self-assembly of block copolymers at high solids content has previously been cited as a distinct benefit of the RAFT-mediated PISA process[42, 46] and it is therefore notable that the post-polymerisation, solvent-switching

approach was successful, even for solids contents as high as 30 wt%. Three distinctive self-assembled nanostructures were observed, which manifested themselves as free-flowing liquids, transparent gels, and opaque gels, depending on the molar mass of the PMMA block and/or solids content. These are shown in a "phase diagram" below for BCPs based on the PI$_{32}$-*Br* macroinitiator (Figure 3.6).
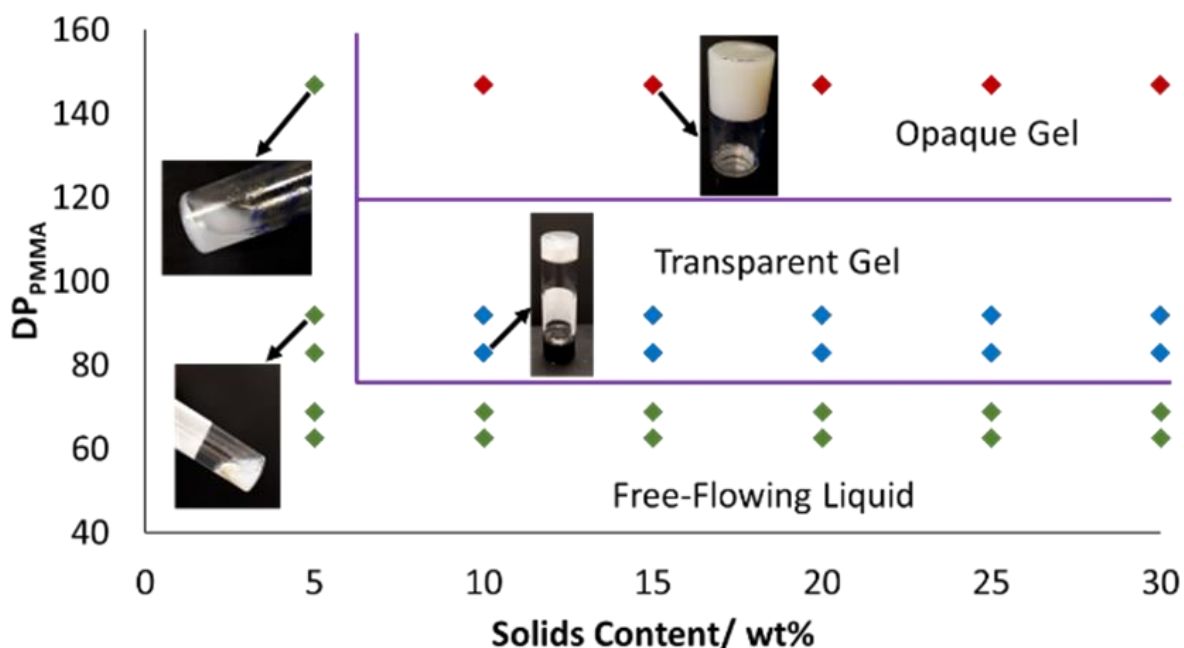
Figure 3.6: Phase diagram generated for PI$_{32}$-b-PMMA$_y$ block copolymers, with varying degree of polymerisation, prepared by LAP-ATRP CHOMP, dispersed in n-decane.

The phase diagram in Figure 3.6 shows that for PI-*b*-PMMA block copolymers formed from PI$_{32}$-*Br*, with a PMMA block of DP < 73, the self-assembled structures form free-flowing liquids at all solids contents up to 30 wt%. It is also clear that at 5 wt%, all BCPs in this series self-assemble into free-flowing liquids, regardless of the DP of the PMMA block. However, at 10 wt% (and above), the BCP with PMMA DP = 86 formed self-supporting transparent gels and as the PMMA block DP increases to 161, self-supporting opaque gels were observed above 10 wt% solids content. The impact of molar mass, composition, and solids content on the self-assembly of BCPs prepared via PISA has been represented in similar phase diagrams in previously published reports[5, 47-49] which also discuss the different self-assembled morphologies that give rise to the various physical behaviours. Analogous phase diagrams were also generated for the PI-*b*-PMMA BCPs prepared from PI$_{55}$-*Br* and PI$_{74}$-*Br* macroinitiators, dispersed in *n*-hexane and *n*-decane respectively (see Figure 3.7).
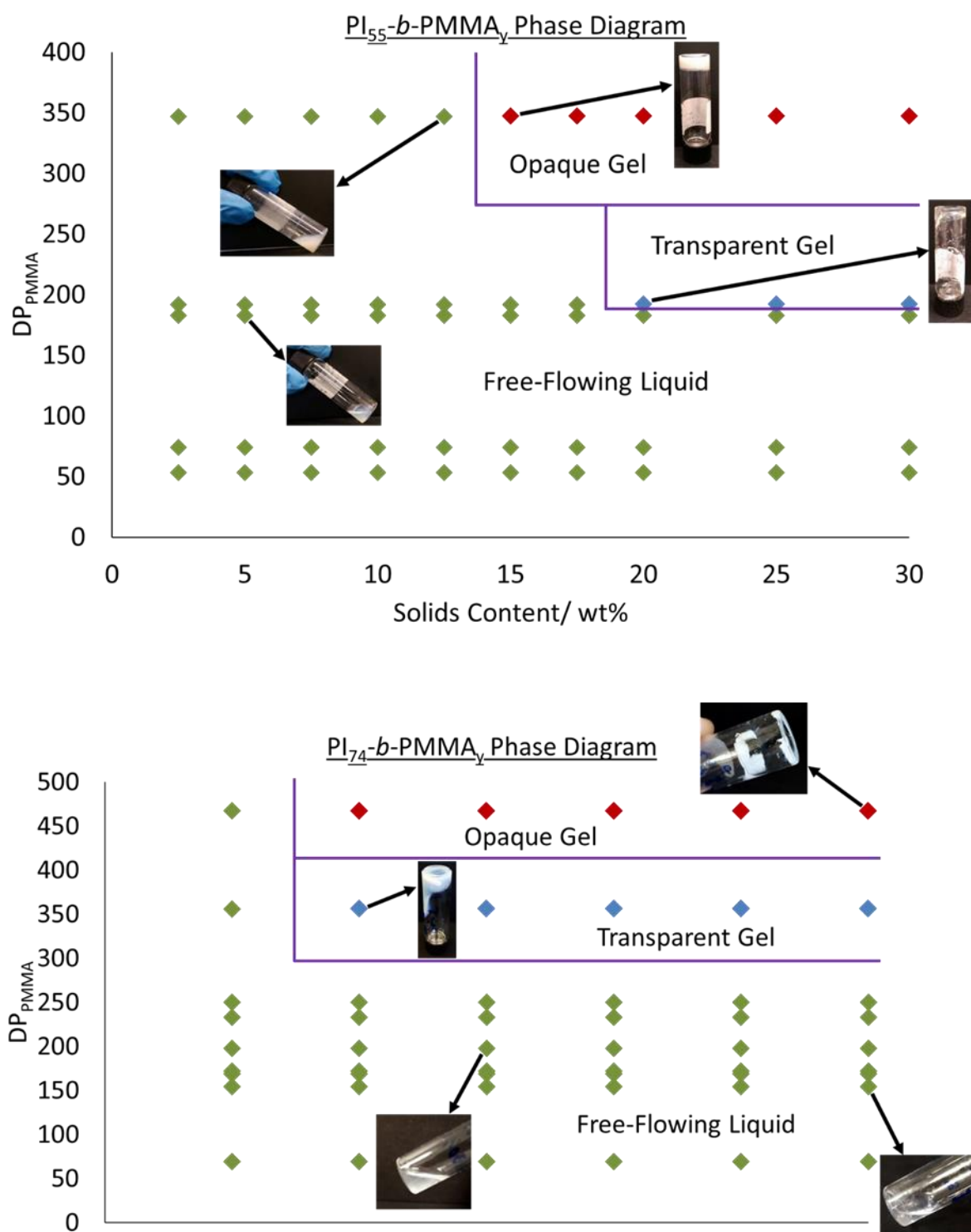
Figure 3.7: Phase diagrams generated for homologous families of PI-b-PMMA block copolymers, prepared by ATRP from polyisoprene macroinitiators and dispersed in selective, non-polar solvents for PI. Top: PI$_{55}$-b-PMMA$_y$ in n-hexane and bottom PI$_{74}$-b-PMMA$_y$ in n-decane

Characterisation of all PI-*b*-PMMA dispersions by TEM was not possible because of time constraints, however, one can hypothesise that the equivalent physical properties are caused by the same morphologies of micelles. A direct comparison between the phase

diagrams of PI_{32}-b-$PMMA_x$ and PI_{74}-b-$PMMA_x$ suggests that there is not a linear correlation between an increase in the molar mass of PI block and the increase in molar mass of PMMA required to achieve the equivalent phases in the phase diagram. This can be rationalised according to the Israelachvili packing parameter, whereby an increase in area per surface head group (i.e. MW_{PI}) causes a decrease in the packing parameter. This decrease can be offset to maintain the packing parameter by an increase in the volume of the core-forming block (i.e. MW_{PMMA}). However, this is not a scalar change because it will also cause an increased length of the core-forming block, decreasing the packing parameter further. To compensate for this, the volume must be increased further by an increase in the volume of the core-forming block (i.e. a greater proportional increase in MW_{PMMA}).

3.2.2.1. Characterisation of PI-b-PMMA Dispersions by TEM and DLS

Transmission electron microscopy (TEM) and dynamic light scattering (DLS) are commonly utilised to identify and measure the particle sizes of self-assembled morphologies and the reports cited above describe the presence of mixed phases where different morphologies appear in the same solution. However, it is not entirely clear whether this is caused by dispersity in block length resulting in BCPs samples which span the phase boundaries. Mixed phases are particularly common at lower dispersion concentrations because, for example, the spherical micelles have a reduced likelihood of fusing to form the longer wormlike micelles.[50, 51]

Transmission electron microscopy (TEM) was used in the current study to identify the self-assembled morphologies giving rise to the differing dispersion properties observed and micrographs are shown below in Figure 3.8. It can be challenging to image self-assembled block copolymers in which the core-forming block has a T_g below room temperature[47] although in some cases cryoTEM has been used to overcome these difficulties. In this study however, the core-forming PMMA block has a high T_g (105 °C) whilst the corona-forming PI block has a T_g of −67 °C. As such the use of cryoTEM was not required, as has been shown to be the case in analogous studies of block copolymers with phenyl acrylate (T_g = 50 °C) as the core-forming block.[52] TEM images of the different self-assembled morphologies of PI_{32}-b-$PMMA_y$ are shown in Figure 3.8. In each case the molar mass of the PI block remains constant with a DP of 32 and each image corresponds to a

solids content of 15 wt%. Thus, the different morphologies arise purely as a function of the block length of the core-forming PMMA block.
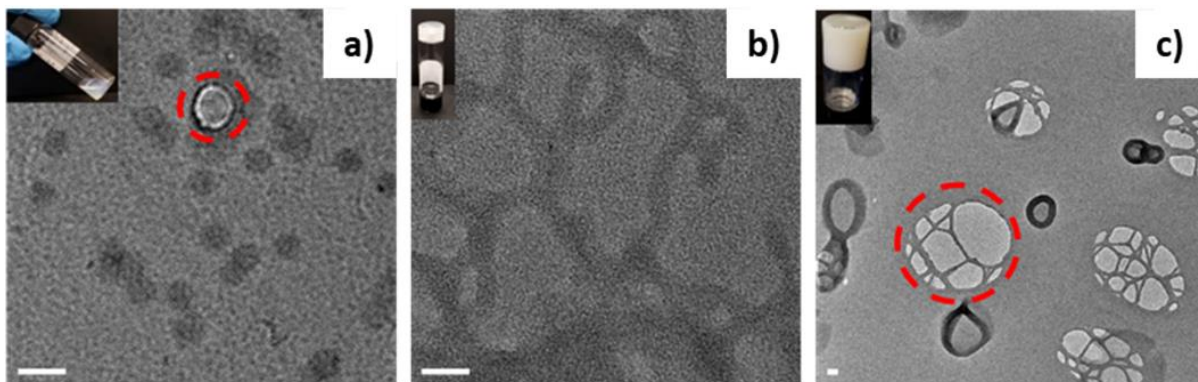
Figure 3.8: High resolution TEM images of the 3 different self-assembled structures dispersed at 15 wt% in n-decane; a: PI$_{32}$-b-PMMA$_{73}$, b: PI$_{32}$-b-PMMA$_{96}$, c: PI$_{32}$-b-PMMA$_{161}$. Scale bar = 50 nm. It should be noted that the features indicated with the red circle in a and c are part of the TEM grid and not a micelle

The sample with the lowest DP PMMA block (PI$_{32}$-*b*-PMMA$_{73}$) forms spherical micelles with uniform diameters of approximately 30 nm (Figure 3.8a), which accounts for the free-flowing liquid. This observation is consistent with expectations as a block copolymer comprising a lower mole fraction of the insoluble core-forming (PMMA) block would be expected to form spherical micelles in solution.[53] It should be noted that the feature indicated with the red circle is part of the grid and NOT a micelle. The TEM micrograph of PI$_{32}$-*b*-PMMA$_{96}$ (Figure 3.8b), with a larger core-forming block, clearly illustrates a different morphology and suggests that the self-supporting transparent gel is made up of wormlike micelles with diameters of a similar size to the spherical micelles formed from PI$_{32}$-*b*-PMMA$_{73}$. The TEM image (Figure 3.8c) of PI$_{32}$-*b*-PMMA$_{161}$, shows that the block copolymer with the largest PMMA block, formed vesicles which are approximately 200 nm in diameter, an order of magnitude larger than the size of the spherical micelles. The TEM images can be used to infer how the physical properties of each dispersion arise. The spherical micelles observed in Figure 3.8a are relatively small and therefore can flow past one another easily, hence forming a free-flowing liquid. The phase diagram in Figure 3.6 shows that the same polymer sample remains mobile even at 30 wt%. The vesicles formed by PI$_{32}$-*b*-PMMA$_{161}$ at 15 wt% (Figure 3.8c) are also spherical but, being (at least) an order of magnitude larger that the spherical micelles, results in clustering, inhibiting their ability to flow at such a solids content. The formation of free-flowing liquids

of unentangled wormlike micelles, has been reported but such observations were made for low dispersion concentrations (i.e. below the critical gelation concentration).[54] The wormlike micelles formed in the current study from PI_{32}-b-$PMMA_{96}$ at 15 wt% are dimensionally anisotropic with a length which is far greater than the diameter. This results in significant entanglement and prevents the wormlike micelles from flowing on a short timescale, accounting for the formation of a self-supporting gel. These observations are consistent with reports in the literature.[47, 55]

Having established (using TEM) the relationship between PMMA block length and/or concentration and morphology, dynamic light scattering (DLS) measurements were made on the free-flowing spherical micelles to ascertain particle size. DLS is a well-established technique for the characterisation of spherical particles because the mathematics underpinning the calculation of particle size assumes all scattering events are from isotropic materials.[56] While it is also possible to use DLS for the characterisation of particles with anisotropic dimensions – e.g. worm-like micelles, it can be difficult to distinguish between sample anisotropy and size dispersity.[57] The DLS analysis of a dispersion of PI_{32}-b-$PMMA_{73}$ in n-decane (self-assembled at 15 wt%, but diluted to 0.72 wt% for DLS) is shown in Figure 3.9, which shows a single, monomodal peak with intensity-weighted diameter of 62.35 nm (PDI = 0.117). This is a reasonably similar result to the TEM image for the same sample (Figure 3.8a) which showed spherical micelles with a diameter of approximately 30 nm. Obtaining a larger particle size from DLS than TEM is common because of the differences in the measurement techniques. In particular, the hydrodynamic shell[58] and increased light scattering of larger particles has been shown to shift the results of intensity-weighted particle size towards larger values.[59] The same phenomenon has also been observed for polymeric particles and micelles.[60, 61] Moreover, the DLS particle size distribution has a relatively narrow dispersity which suggests that the combination of living anionic polymerisation and ATRP to prepare BCPs with a reasonably low dispersity in molar mass can be useful for preparing near-monodisperse self-assembled nanostructures.
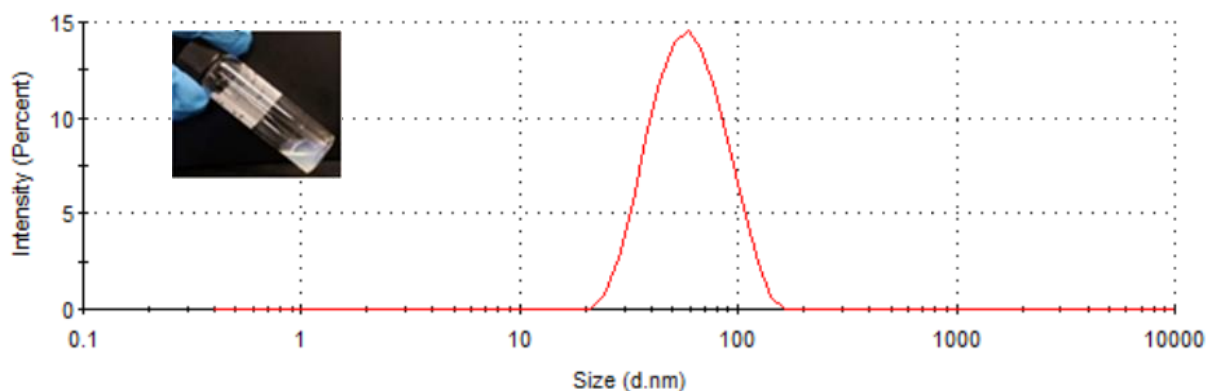
Figure 3.9: DLS analysis of the spherical micelles formed by a dispersion of PI$_{32}$-b-PMMA$_{73}$ in n-decane, self-assembled at 15 wt% and diluted to 0.72 wt%

3.2.2.2. Thermal-Responsivity Testing of PI-*b*-PMMA Dispersions

The response of self-assembled micellar structures to environmental stimuli such as temperature, salinity, pH etc. has been reported for micelles of both surfactants and block copolymers.[62] For example, cetyltrimethylammonium hydroxynaphthalene carboxylate (CTAHNC) is a surfactant that forms vesicles at room temperature, which undergo a vesicle to worm transition upon heating to 70 °C, or a vesicle to worm transition upon the addition of cetyltrimethylammonium bromide (CTAB), a co-surfactant.[63] Similar phenomena have been observed for micelles formed from diblock copolymers.[64-66] The rheological properties of self-assembled structures are also of significant interest for many applications, providing information both on performance and processing properties.[67, 68] The impact of temperature on the rheological properties of such systems is inherently interesting and has been previously reported.[54, 69] In the current study, the self-supporting gels arising from wormlike micelles and vesicles are expected to exhibit more solid-like rheological properties, but may be expected to exhibit modified behaviour as the temperature is increased, particularly if the packing parameter changes with respect to temperature as previously discussed. A decreasing viscosity (with increasing temperature) can be very useful for mechanical processing, whilst an increasing viscosity can be useful for applications such as in viscosity modifiers.[70] Rheology curves illustrating the impact of temperature on the complex viscosity for the self-supporting gels formed by both wormlike micelles (a) and vesicles (b) are shown in Figure 3.11. The conditions for the temperature sweep (angular frequency = 1 rad s^{-1} and strain = 0.2) were derived from exploratory frequency sweeps (also shown below in Figure 3.11) for the samples which showed a

constant gradient in complex viscosity across all angular frequencies, indicating that any changes in viscosity would only be a result of the change in temperature.
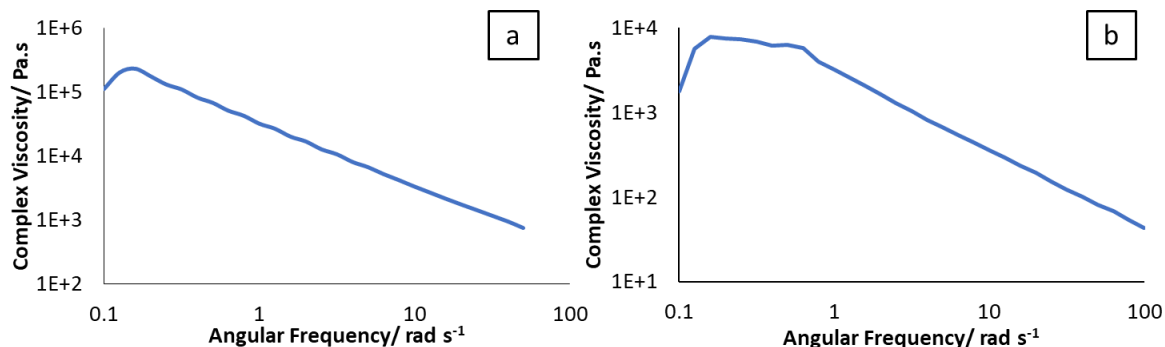
Figure 3.11: Logarithmic plot of complex viscosity versus angular frequency for 15 wt% dispersions in n-decane of a) PI$_{32}$-b-PMMA$_{96}$, and b) PI$_{32}$-b-PMMA$_{161}$
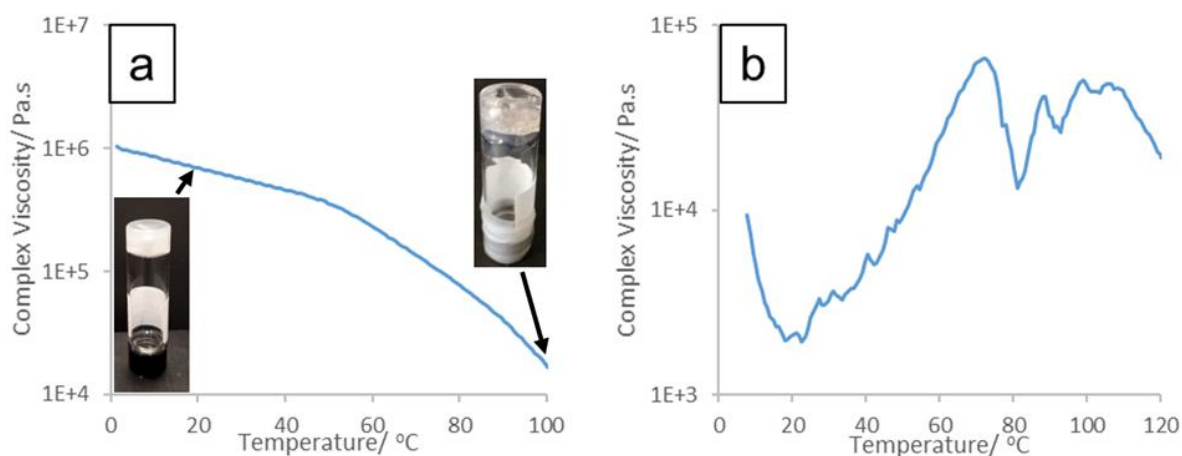
Figure 3.10: Logarithmic plot of complex viscosity versus temperature for 15 wt% dispersions in n-decane of a) PI$_{32}$-b-PMMA$_{96}$, and b) PI$_{32}$-b-PMMA$_{161}$. Inset photographs in a) of sample dispersions at temperatures indicated on graph. Complex viscosity calculation described in experimental chapter.

A plot of the log(complex viscosity) versus temperature for PI$_{32}$-*b*-PMMA$_{96}$ (Figure 3.11a), which at 15 wt% forms a self-supporting gel of worm-like micelles at room temperature, shows an almost linear, but shallow, decrease in log complex viscosity from 0 - 50 °C, at which temperature the plot shows an abrupt change in gradient. The likely explanation for this phenomenon is a slight increase in solubility of the core-forming PMMA block in *n*-decane at higher temperature, which results in interfacial plasticisation of the core of the micelles (i.e. the PMMA segments closest to the polyisoprene block). The phenomenon of interfacial plasticisation arising due to increased solubility of the core-forming block in BCP micelles has been previously reported.[64, 71-73] This enhanced solubility can cause the ratio of soluble polymer : insoluble polymer, in the BCP to increase, with a concomitant change in the packing parameter. The abrupt change in the gradient of log

complex viscosity versus temperature for PI$_{32}$-*b*-PMMA$_{96}$ at 50 °C is difficult to rationalise with certainty without *in situ* TEM characterisation. However, the inset photographs of the sample in Figure 3.11a show that the sample becomes far more transparent at higher temperatures and begins to show some signs of flow, which would suggest the onset of a change in morphology. Similar observations have previously been reported by Fielding *et al.* for the reversible gelation of a poly(lauryl methacrylate)$_{16}$-*block*-poly(benzyl methacrylate)$_{37}$ copolymer.[64] Upon heating above 50 °C, de-gelation occurred because of a partial transition from wormlike to spherical micelles which reduces the extent of entanglement of the remaining worms in the dispersion. Ratcliffe *et al.* reported similar behaviour[47] for a poly(lauryl acrylate)–poly(benzyl acrylate) block copolymer which was a stiff gel at 4 °C that became softer at 20 °C and finally a free-flowing liquid at 80 °C. This behaviour was explained by i) a change in properties of the core-forming PBzA block with a T_g of 6 °C and ii) "debranching" leaving "free", disentangled worms that form a softer gel before a full transition to spherical micelles. The results in the current study for PI$_{32}$-*b*-PMMA$_{96}$ (Figure 3.11a) would suggest that the latter (debranching) explanation is more plausible given that the T_g of the core-forming PMMA block (105 °C) in the current work is far higher than the transition point observed in the rheology (50 °C). It is unlikely that a full morphological transition from wormlike to spherical micelles has taken place at 100 °C because the storage and loss moduli did not cross over and the complex viscosity remains several orders of magnitude higher than that of the PI$_{32}$-*b*-PMMA$_{73}$ sample which self-assembled into spherical micelles at 15 wt% in *n*-decane (see Figure 12). The evidence therefore points towards the onset of a transition at 50 °C from entangled wormlike micelles to shorter, partially disentangled worms accompanied by a pronounced decline in the viscosity. It is likely that the sample exists as a mixture of wormlike micelles, some of which remain entangled in a 3D network, and also a small proportion of spherical micelles at 100 °C. This is also consistent with the observed convergence of the storage and loss moduli in the rheology plot. It is likely that if the temperature was increased further, a steeper decline in the complex viscosity would result, as the free worms complete the transition to spherical micelles.

At ambient temperature, a 15 wt% dispersion of PI$_{32}$-*b*-PMMA$_{161}$ in *n*-decane forms vesicles. The plot of log complex viscosity against temperature is shown in Figure 3.11b. At

10 °C the complex viscosity of PI_{32}-b-$PMMA_{161}$ is about 2 orders of magnitude lower than that seen for PI_{32}-b-$PMMA_{96}$ (Figure 3.11a) which exists as wormlike micelles at the same temperature. The lower viscosity of dispersions of vesicles, compared to worms, has been particularly well-demonstrated recently by Ratcliffe et $al.$ for a single sample of (thermoresponsive) block copolymer that can form spheres, worms and vesicles at different temperatures.[74] In this paper, the rheological analysis showed a maximum in the complex viscosity at 14 °C, arising due to the formation of wormlike micelles, with a complex viscosity which is approximately 2 orders of magnitude greater than that of spherical micelles (formed upon cooling) and vesicles (formed upon heating). In the current work, the data in Figure 3.11b illustrates that as the temperature was increased from 20 to 70 °C the complex viscosity of PI_{32}-b-$PMMA_{161}$ rises by almost 2 orders of magnitude, which could reasonably be assumed to arise due to a transition in morphology from vesicles to wormlike micelles, as the PMMA undergoes interfacial plasticization and an increase in the area of the corona-forming head group. Similar observations of a higher viscosity with increasing temperature were made by Derry et $al.$ for self-assembled PSMA-b-PBzMA BCPs dispersed in a non-polar base oil.[70] In that case, TEM characterisation of samples before and after heating, and variable temperature SAXS, were used to illustrate the transition in morphology. The authors concluded that the transition was due to increased solvation of the insoluble PBzMA core-forming block. Above 70 °C, the complex viscosity data for PI_{32}-b-$PMMA_{161}$ (Figure 3.11b) become erratic, however, one might tentatively suggest that the apparent maximum in viscosity at 70 °C, followed by a (noisy) decrease in complex viscosity above that temperature, is due to the onset of a transition of the wormlike micelles towards spherical micelles.

For completeness, the analogous rheology curve for the dispersion in n-decane of 15 wt% of PI_{32}-b-$PMMA_{73}$, which formed a free-flowing liquid dispersion of spherical micelles, is shown in Figure 3.12. In this case the complex viscosity was constant at 0.020 Pa.s across the entire temperature range from 25 – 115 °C and very much lower than the complex viscosity of both samples illustrated in Figure 3.11, which is to be expected for a free-flowing liquid.
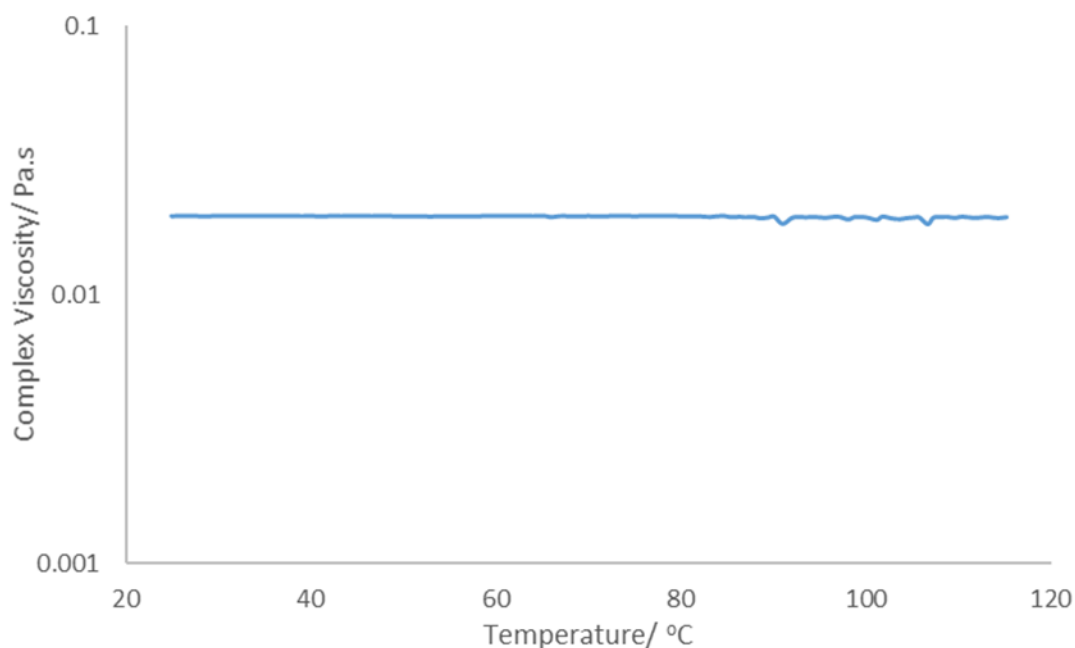
Figure 3.12: Logarithmic plot of complex viscosity versus temperature of a 15 wt% dispersion of PI$_{32}$-b-PMMA$_{73}$ in n-decane. The dispersion exists as a free-flowing liquid of spherical micelles as illustrated in Figure 3.8a.

3.2.2.3. Characterisation of Thermally Responsive PI-*b*-PMMA Dispersions by TEM

With the aim of providing further evidence to support the hypothesis that an increase in temperature drives a change in self-assembled morphology, TEM was used to image a dispersion of PI$_{32}$-*b*-PMMA$_{96}$ (15 wt% in *n*-decane), that exists as wormlike micelles at room temperature (Figure 3.8b), after heating to 150 $^{\circ}$C for 10 minutes, which is well above the temperature at which a change in the complex viscosity was observed (Figure 3.11a). We hypothesised that at this elevated temperature the morphology should switch from worms to spherical micelles. The heated sample was then diluted to 1 wt% in *n*-decane, at the elevated temperature. Whilst the formation of wormlike micelles is thermodynamically favoured (for this sample) at room temperature, and one might expect any heat-induced transition in morphology to be reversed upon cooling, drastic dilution of the dispersion after any potential transition in morphology to spherical micelles decreases the probability of the spherical micelles colliding in order to re-fuse into wormlike micelles. In effect, dilution kinetically traps any newly-formed morphology upon heating, and is in keeping with previous reports of imaging of thermally-induced morphology transitions.[64, 70, 75] The diluted dispersion was allowed to cool to room temperature. A control sample

was also prepared by diluting (without heating) the same sample from 15 wt% to 1 wt% at room temperature. TEM images of the 2 samples are shown below in Figure 3.13.
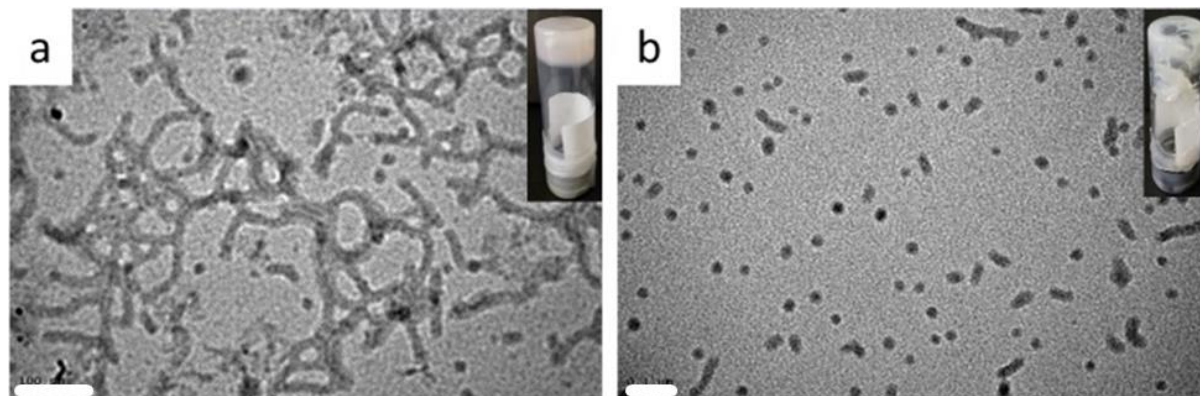
Figure 3.13: High resolution TEM images of PI_{32}-b-$PMMA_{96}$, dispersed at 15 wt% in n-decane at room temperature before a) dilution with n-decane to 1 wt% at room temperature and b) dilution to 1 wt% at 150 °C by the addition of n-decane, followed by cooling to room temperature. Scale bar = 100 nm.

The TEM image of PI_{32}-*b*-$PMMA_{96}$ which was diluted to 1 wt% at room temperature (Figure 3.13a) shows a mixed morphology which is dominated by wormlike micelles, and displays a very similar morphology to the same sample at 15 wt%, prior to dilution (see Figure 3.8b). This clearly illustrates that the wormlike morphology is conserved upon dilution at room temperature, confirming that dilution alone does not lead to a change in morphology. The TEM image in Figure 3.13b shows PI_{32}-*b*-$PMMA_{96}$ after heating to 150 °C, followed by dilution to 1 wt% (at 150 °C) before cooling to room temperature to allow characterisation. This clearly shows a morphology of predominantly spherical micelles and a few short wormlike micelles (c. 100 nm in length). Having established that the initial worm-like morphology is unaffected by dilution alone, this image suggests a change in morphology from worms to spheres occurs upon heating, with the second morphology being trapped by dilution to 1 wt%. The change in morphology at high temperature is consistent with the observed decrease in complex viscosity shown in Figure 3.11a. The most plausible explanation for a transition in morphology, as suggested above, is partial solvation of the core-forming PMMA in *n*-decane. A thermally-induced transition from worm-like to spherical micelles of PDMAEMA-*b*-PPMA BCPs dispersed in ethanol has previously been described by Pei *et al.*, who used TEM characterisation coupled with 'hot dilution' to trap the newly formed spherical morphology.[76] Pei also used variable temperature proton NMR and showed that the peaks for the core-forming PPMA block

increased in intensity at high temperature, suggesting increased solvation of the core-forming block in agreement with the hypothesis proposed above.

The effect of hysteresis upon heating/cooling was also investigated by heating a 15 wt% dispersion in n-decane of PI$_{32}$-b-PMMA$_{96}$ and then cooling without dilution. Thus, the sample which self-assembles into wormlike micelles at room temperature was heated to 150 °C, the temperature previously shown to induce a change in morphology to spherical micelles (Figure 3.13), held for 15 minutes in a sealed system to prevent any loss of solvent, before cooling to room temperature. TEM images of the cooled sample gel (Figure 3.14) showed a morphology consisting of worm-like micelles of diameter approximately 20 nm, which is practically identical to the TEM image (Figure 3.8b) of the sample prior to being heated. This would appear to confirm that the worm-like micelles of PI$_{32}$-b-PMMA$_{96}$ in n-decane transition to spherical micelles upon heating to 150 °C, which, if not trapped by dilution, revert back to the thermodynamically-favoured worm-like morphology upon cooling to room temperature. In this respect the behaviour of the PI-b-PMMA block copolymers is analogous to that previously reported by Blanazs *et al* for thermoresponsive PGMA-b-PHPMA diblock copolymers, dispersed in water.[77]
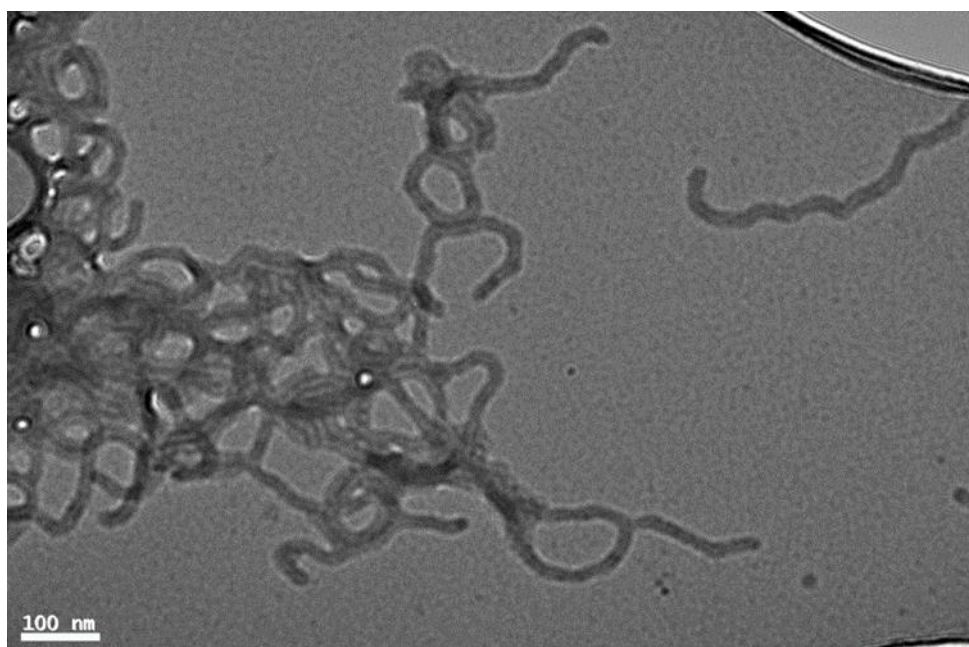
Figure 3.14: TEM image of PI$_{32}$-b-PMMA$_{96}$, from 15 wt% dispersion in n-decane heated to and held at 150 °C for 15 minutes before being allowed to cool to room temperature.

3.3. Conclusions

A family of polyisoprene-*block*-poly(methyl methacrylate) block copolymers has been prepared, using cheap and readily-available monomers, by a change of mechanism polymerisation in which an ATRP polyisoprene macroinitiator was synthesised by living anionic polymerisation. The use of living anionic polymerisation enables the scalable and quantitative polymerisation of isoprene with well-controlled molar mass and a narrow dispersity. Moreover, by fixing the molar mass of the polyisoprene block, and varying the molar mass of PMMA, three homologous series of block copolymers were prepared and fully characterised using ^{1}H NMR spectroscopy. The resulting block copolymers were dispersed in *n*-decane, a selective solvent for the polyisoprene block, at high solids contents of up to 30 wt% enabling an exhaustive investigation into the impact of molar mass, composition, and solids content on the self-assembly of this block copolymer system.

Systematically varying the molar mass of the core-forming PMMA block resulted in the formation of a variety of morphologies. These were characterised by DLS and TEM and identified as spherical micelles, wormlike micelles, and vesicles. The thermoresponsive properties of the resulting nano-objects have been demonstrated in so much that it is possible to transition between different self-assembled morphologies by varying the temperature. In particular it has been shown that for a 15 wt% dispersion of PI$_{32}$-b-PMMA$_{96}$ in *n*-decane, an increase in temperature results in the onset of a transition from worm-like to spherical micelles, as evidenced by an abrupt change in complex viscosity above 50 °C and TEM analysis of the newly formed spherical micelles was performed on micelles that were trapped by dilution at 150 °C. The conclusion that a transition in morphology arises due to enhanced solubility of the core-forming block, and a change in the Israelachvili packing parameter, is supported by the literature. Control experiments unambiguously show that the transition is not triggered by dilution alone and that cooling without dilution causes the spherical micelles to revert to initial worm-like morphology – thereby also demonstrating thermoreversibility. Furthermore, complex viscosity data suggest analogous behaviour for PI$_{32}$-*b*-PMMA$_{161}$ which transitions from (lower viscosity) vesicles at room temperature to (higher viscosity) worm-like micelles at 70 degrees.

Although the current study focusses on the synthesis and characterisation of PI-*b*-PMMA block copolymers, the use of living anionic polymerisation in combination with ATRP

offers an extraordinarily versatile and scalable approach for the preparation of block copolymers, with almost infinite variability in terms of molar mass and composition. This versatility will be explored in the subsequent chapter where a similar mechanism will be used to prepare polyisoprene-based block copolymers with a different methacrylate polymer (*N,N*-dimethylaminoethyl methacrylate) (DMAEMA). The self-assembly in *n*-decane will also be carried out in the same way, enabling the effect of increased polarity and differing dimensions of the core-forming block on the self-assembly behaviour to be investigated. The samples prepared in this chapter will also be investigated in applications testing as lubricant additives in Chapter 5.

3.4. References

1. Z. S. Gao, S. K. Varshney, S. Wong, A. Eisenberg, *Macromolecules*, 1994, **27**, 7923-7927.
2. I. E. Climie, E. F. T. White, *J. Polym. Sci.*, 1960, **47**, 149-156.
3. S. Krause, *J. Phys. Chem.*, 1964, **68**, 1948-1955.
4. Y. T. Li, S. P. Armes, *Angew. Chem.-Int. Edit.*, 2010, **49**, 4042-4046.
5. A. Blanazs, A. J. Ryan, S. P. Armes, *Macromolecules*, 2012, **45**, 5099-5107.
6. N. J. Warren, O. O. Mykhaylyk, D. Mahmood, A. J. Ryan, S. P. Armes, *J. Am. Chem. Soc.*, 2014, **136**, 1023-1033.
7. E. R. Jones, M. Semsarilar, P. Wyman, M. Boerakker, S. P. Armes, *Polym. Chem.*, 2016, **7**, 851-859.
8. E. R. Jones, O. O. Mykhaylyk, M. Semsarilar, M. Boerakker, P. Wyman, S. P. Armes, *Macromolecules*, 2016, **49**, 172-181.
9. L. A. Fielding, M. J. Derry, V. Ladmiral, J. Rosselgong, A. M. Rodrigues, L. P. D. Ratcliffe, S. Sugihara, S. P. Armes, *Chem. Sci.*, 2013, **4**, 2081-2087.
10. L. A. Fielding, J. A. Lane, M. J. Derry, O. O. Mykhaylyk, S. P. Armes, *J. Am. Chem. Soc.*, 2014, **136**, 5790-5798.
11. M. J. Derry, L. A. Fielding, S. P. Armes, *Polym. Chem.*, 2015, **6**, 3054-3062.
12. L. P. D. Ratcliffe, B. E. McKenzie, G. M. D. Le Bouedec, C. N. Williams, S. L. Brown, S. P. Armes, *Macromolecules*, 2015, **48**, 8594-8607.
13. D. Benoit, E. Harth, P. Fox, R. M. Waymouth, C. J. Hawker, *Macromolecules*, 2000, **33**, 363-370.
14. V. Jitchum, S. Perrier, *Macromolecules*, 2007, **40**, 1408-1412.
15. Y. F. Zhu, F. J. Jiang, P. P. Zhang, J. Luo, H. D. Tang, *Chin. Chem. Lett.*, 2016, **27**, 910-914.
16. J. W. Bartels, S. I. Cauet, P. L. Billings, L. Y. Lin, J. H. Zhu, C. Fidge, D. J. Pochan, K. L. Wooley, *Macromolecules*, 2010, **43**, 7128-7138.
17. D. Baskaran, *Prog. Polym. Sci.*, 2003, **28**, 521-581.
18. M. Szwarc, A. Rembaum, *J. Polym. Sci.*, 1956, **22**, 189-191.
19. D. Kunkel, A. H. E. Muller, M. Janata, L. Lochmann, *Makromol. Chem., Macromol. Symp.*, 1992, **60**, 315-326.
20. M. H. Acar, K. Matyjaszewski, *Macromol. Chem. Phys.*, 1999, **200**, 1094-1100.
21. L. F. Zhang, A. Eisenberg, *J. Am. Chem. Soc.*, 1996, **118**, 3168-3181.
22. Y. Y. Mai, A. Eisenberg, *Chem. Soc. Rev.*, 2012, **41**, 5969-5985.
23. R. K. O'Reilly, C. J. Hawker, K. L. Wooley, *Chem. Soc. Rev.*, 2006, **35**, 1068-1083.
24. Y. S. Jung, C. A. Ross, *Adv. Mater.*, 2009, **21**, 2540-2545.
25. S. P. Paradiso, K. T. Delaney, C. J. Garcia-Cervera, H. D. Ceniceros, G. H. Fredrickson, *ACS Macro Lett.*, 2014, **3**, 16-20.
26. M. J. Derry, L. A. Fielding, S. P. Armes, *Prog. Polym. Sci.*, 2016, **52**, 1-18.
27. D. Zehm, L. P. D. Ratcliffe, S. P. Armes, *Macromolecules*, 2013, **46**, 128-139.
28. D. J. Adams, C. Kitchen, S. Adams, S. Furzeland, D. Atkins, P. Schuetz, C. M. Fernyhough, N. Tzokova, A. J. Ryan, M. F. Butler, *Soft Matter*, 2009, **5**, 3086-3096.
29. S. Valkama, T. Ruotsalainen, A. Nykanen, A. Laiho, H. Kosonen, G. ten Brinke, O. Ikkala, J. Ruokolainen, *Macromolecules*, 2006, **39**, 9327-9336.
30. S. L. Canning, G. N. Smith, S. P. Armes, *Macromolecules*, 2016, **49**, 1985-2001.

31. M. J. Derry, T. Smith, P. S. O'Hora, S. P. Armes, *ACS Appl. Mater. Interfaces*, 2019, **11**, 33364-33369.

32. J. Bowers, A. Zarbakhsh, J. R. P. Webster, L. R. Hutchings, R. W. Richards, *Langmuir*, 2001, **17**, 131-139.

33. J. Herzberger, K. Niederer, H. Pohlit, J. Seiwert, M. Worm, F. R. Wurm, H. Frey, *Chem. Rev.*, 2016, **116**, 2170-2243.

34. M. Szwarc, M. Van Beylen, *Ionic polymerization and living polymers*, Springer Science & Business Media, 2012.

35. B. Liu, F. Liu, N. Luo, S. K. Ying, Q. Liu, *Chin. J. Polym. Sci.*, 2000, **18**, 39-43.

36. G. H. Zhu, L. F. Zhang, Z. B. Zhang, J. Zhu, Y. F. Tu, Z. P. Cheng, X. L. Zhu, *Macromolecules*, 2011, **44**, 3233-3239.

37. Y. Kwak, K. Matyjaszewski, *Polym. Int.*, 2009, **58**, 242-247.

38. J. L. Wang, T. Grimaud, K. Matyjaszewski, *Macromolecules*, 1997, **30**, 6507-6512.

39. H. Tanaka, K. Yamauchi, H. Hasegawa, N. Miyamoto, S. Koizumi, T. Hashimoto, *Physica B Condens. Matter.*, 2006, **385**, 742-744.

40. G. Wang, M. Schmitt, Z. Wang, B. Lee, X. Pan, L. Fu, J. Yan, S. Li, G. Xie, M. R. Bockstaller, K. Matyjaszewski, *Macromolecules*, 2016, **49**, 8605-8615.

41. J. Wu, C. Tian, L. Zhang, Z. Cheng, X. Zhu, *RSC Adv.*, 2017, **7**, 6559-6564.

42. S. L. Canning, G. N. Smith, S. P. Armes, *Macromolecules*, 2016, **49**, 1985-2001.

43. L. F. Zhang, A. Eisenberg, *J. Am. Chem. Soc.*, 1996, **118**, 3168-3181.

44. Y. Mai, A. Eisenberg, *Chem. Soc. Rev.*, 2012, **41**, 5969-5985.

45. L. I. Atanase, G. Riess, *Polymers*, 2018, **10**, 62-87.

46. M. J. Derry, L. A. Fielding, S. P. Armes, *Polym. Chem.*, 2015, **6**, 3054-3062.

47. L. P. D. Ratcliffe, B. E. McKenzie, G. M. D. Le Bouëdec, C. N. Williams, S. L. Brown, S. P. Armes, *Macromolecules*, 2015, **48**, 8594-8607.

48. P. C. Yang, L. P. D. Ratcliffe, S. P. Armes, *Macromolecules*, 2013, **46**, 8545-8556.

49. L. A. Fielding, M. J. Derry, V. Ladmiral, J. Rosselgong, A. M. Rodrigues, L. P. D. Ratcliffe, S. Sugihara, S. P. Armes, *Chem. Sci.*, 2013, **4**, 2081-2087.

50. A. Blanazs, J. Madsen, G. Battaglia, A. J. Ryan, S. P. Armes, *J. Am. Chem. Soc.*, 2011, **133**, 16581-16587.

51. N. J. Warren, O. O. Mykhaylyk, D. Mahmood, A. J. Ryan, S. P. Armes, *J. Am. Chem. Soc.*, 2014, **136**, 1023-1033.

52. S. L. Canning, V. J. Cunningham, L. P. D. Ratcliffe, S. P. Armes, *Polym. Chem.*, 2017, **8**, 4811-4821.

53. J. N. Israelachvili, D. J. Mitchell, B. W. Ninham, *J. Chem. Soc., Faraday Trans. 2*, 1976, **72**, 1525-1568

54. J. R. Lovett, M. J. Derry, P. C. Yang, F. L. Hatton, N. J. Warren, P. W. Fowler, S. P. Armes, *Chem. Sci.*, 2018, **9**, 7138-7144.

55. V. Ladmiral, A. Charlot, M. Semsarilar, S. P. Armes, *Polym. Chem.*, 2015, **6**, 1805-1816.

56. J. F. Gohy, S. K. Varshney, R. Jérôme, *Macromolecules*, 2001, **34**, 3361-3366.

57. G. Guérin, J. Raez, I. Manners, M. A. Winnik, *Macromolecules*, 2005, **38**, 7819-7827.

58. S. Pabisch, B. Feichtenschlager, G. Kickelbick, H. Peterlik, *Chemical Physics Letters*, 2012, **521**, 91-97.

59. T. G. F. Souza, V. S. T. Ciminelli, N. D. S. Mohallem, *J. Phys.: Conf. Ser.*, 2016, **733**.

60. A. Bootz, V. Vogel, D. Schubert, J. Kreuter, *European Journal of Pharmaceutics and Biopharmaceutics*, 2004, **57**, 369-375.

61.   Q. H. Xu, C. Tian, L. F. Zhang, Z. P. Cheng, X. L. Zhu, *Macromol. Rapid Commun.*, 2019, **40**, 1800327-1800333.
62.   Y. Feng, Z. Chu, C. A. Dreiss, *Smart Wormlike Micelles*, Springer, Heidelberg, 2015.
63.   P. A. Hassan, B. S. Valaulikar, C. Manohar, F. Kern, L. Bourdieu, S. J. Candau, *Langmuir*, 1996, **12**, 4350-4357.
64.   L. A. Fielding, J. A. Lane, M. J. Derry, O. O. Mykhaylyk, S. P. Armes, *J. Am. Chem. Soc.*, 2014, **136**, 5790-5798.
65.   S. L. Canning, T. J. Neal, S. P. Armes, *Macromolecules*, 2017, **50**, 6108-6116.
66.   M. E. Seitz, W. R. Burghardt, K. T. Faber, K. R. Shull, *Macromolecules*, 2007, **40**, 1218-1226.
67.   S. R. Bhatia, A. Mourchida, M. Joanicot, *Curr. Opin. Colloid Interface Sci*, 2001, **6**, 471-478.
68.   A. P. Lopez-Oliva, N. J. Warren, A. Rajkumar, O. O. Mykhaylyk, M. J. Derry, K. E. B. Doncom, M. J. Rymaruk, S. P. Armes, *Macromolecules*, 2015, **48**, 3547-3555.
69.   M. J. Derry, O. O. Mykhaylyk, S. P. Armes, *Angew Chem Int Ed*, 2017, **56**, 1746-1750.
70.   C. M. Beliciu, C. I. Moraru, *J. Dairy Sci.*, 2009, **92**, 1829-1839.
71.   E. L. Michor, J. C. Berg, *Langmuir*, 2015, **31**, 9602-9607.
72.   D. Bendedouch, S. H. Chen, W. C. Koehler, *J. Phys. Chem.*, 1983, **87**, 153-159.
73.   L. P. D. Ratcliffe, M. J. Derry, A. Ianiro, R. Tuinier, S. P. Armes, *Angew. Chem.-Int. Edit.*, 2019, **58**, 18964-18970.
74.   C. G. Clarkson, J. R. Lovett, J. Madsen, S. P. Armes, M. Geoghegan, *Macromol. Rapid Commun.*, 2015, **36**, 1572-1577.
75.   Y. W. Pei, N. C. Dharsana, J. A. Van Hensbergen, R. P. Burford, P. J. Roth, A. B. Lowe, *Soft Matter*, 2014, **10**, 5787-5796.
76.   A. Blanazs, R. Verber, O. O. Mykhaylyk, A. J. Ryan, J. Z. Heath, C. W. I. Douglas, S. P. Armes, *J. Am. Chem. Soc.*, 2012, **134**, 9741-9748.

4. Preparation of Poly(isoprene-*block*-((*N,N*-dimethylamino)ethyl methacrylate)) Block Copolymers for Self-Assembly and Quaternisation-Induced Self-Assembly (QISA)

4.1. Introduction

The use of nitrogen-containing polymers such as poly((*N,N*-dimethylamino)ethyl methacrylate) (PDMAEMA) is highly desirable for a number of bespoke applications including gene delivery and drug delivery.[1, 2] PDMAEMA is a water-soluble, pH-responsive polymer that can be prepared simply by conventional free radical and reversible-deactivated radical polymerisation (RDRP) methods.[3-5] There are also reported examples of the successful living anionic polymerisation of DMAEMA, albeit with stringently controlled and commercially unviable reaction conditions (i.e. -78 °C, bulky initiator, lithium chloride additive etc.) to avoid side reactions and self-termination reactions at the methacrylate functionality during propagation.[6, 7] Following on from the PI-*b*-PMMA investigation described in the previous chapter, herein, the use of a PDMAEMA block in place of the PMMA block in a series of PI-*b*-PDMAEMA block copolymers is discussed. The aim was to investigate the self-assembly behaviour of such block copolymers when dispersed into selective, non-polar solvents. The different dimensions of the PDMAEMA repeat unit in comparison with PMMA, and the increased polarity because of the tertiary amine functionality are expected to have pronounced effects on the self-assembly behaviours in non-polar solvents.[8, 9]

Furthermore, the use of nitrogen-containing polymers is of interest for applications as friction modifiers in lubricant formulations because of the nitrogen atom's ability to bind, via the lone pair, to metal surfaces and form co-operative tribofilms with other friction modifiers such as zinc dialkyldithiophosphates (ZDDP).[10, 11] Reports in the literature describe how PDMAEMA-based copolymers have been shown to reduce friction of base oils by forming thick tribofilms on the surfaces.[12, 13] Because base oils are strongly non-polar solvents, it is necessary to combine PDMAEMA in copolymers with non-polar monomers to ensure dispersibility. Hence the investigation described in this chapter focusses on PI-*b*-PDMAEMA block copolymers. By first investigating the synthesis and self-assembly of PI-*b*-PDMAEMA block copolymers in *n*-decane, a greater understanding of the properties of

PDMAEMA-based dispersions in non-polar solvents will be gained before carrying out applications testing, the results of which will be described in the following chapter.

The previously described change of mechanism polymerisation (CHOMP) approach will again be used for the preparation of PI-*b*-PDMAEMA block copolymers. The benefit of this method for the preparation of block copolymers is in its versatility for the polymerisation of different monomers particularly via the atom-transfer radical polymerisation (ATRP) of different methacrylates.[14] Direct comparisons will be drawn between the self-assembly behaviours of PI-*b*-PMMA and PI-*b*-PDMAEMA whereby any observed differences should purely be a result of the different lipophobic methacrylate block. The self-assembly in *n*-decane was undertaken by a conventional solvent switching process[15, 16] and the resulting physical structures were studied by TEM, to observe the resulting morphologies.

Moreover, the amine functionality of DMAEMA in the block copolymer allows for further derivatisation of the polymeric structure. By a simple organic quaternisation reaction with a haloalkane, an ammonium salt can be formed on the PDMAEMA repeat unit.[17] Quaternisation not only results in the formation of a polyelectrolyte block, but also changes the size/molar mass of the insoluble, core-forming block which in turn should change the self-assembly behaviour when dispersed into non-polar solvents.[18] The cationic polymers produced via quaternisation reactions are often desirable for their antimicrobial properties and their applications as ion-exchange resins and flocculants,[19, 20] and they could also have potential in lubricant applications.

For this study, the quaternised versions of PI-*b*-PDMAEMA (PI-*b*-PQDMAEMA) will be investigated with a view towards observing any differences in behaviour upon self-assembly into *n*-decane. The quaternisation of PDMAEMA with different alkyl iodides of varying molar mass will change the charge density and dimensions of the core-forming block to different extents, which means that the self-assembled morphologies of a single block copolymer may vary, depending on the alkyl halide quaternising agent. Moreover, the degree of quaternisation of the PDMAEMA block can also be varied thereby offering another independent variable to influence the self-assembly and offer control over the resulting morphology.

Finally, the quaternisation of PI-*b*-PDMAEMA in THF was also found to change the solubility of the PDMAEMA block to such an extent that self-assembly was induced during the quaternisation reaction. The formation of micelles in THF during quaternisation was confirmed by TEM and is believed to be the first example of a quaternisation-induced self-assembly (QISA). QISA was found to be highly specific to the quaternisation of PI-*b*-PDMAEMA with ethyl iodide, and the resulting morphology was dependent upon the degree of quaternisation. QISA could be a useful tool for the facile preparation of different morphologies from a single block copolymer. A comprehensive study of self-assembled PDMAEMA-based block copolymers (and their quaternised versions) in non-polar solvents shows unique behaviour that could be extremely potent for the future preparation of self-assembled block copolymer micelles and possibly for their use as lubricant additives.

4.2. Results and Discussion

A change of mechanism polymerisation (CHOMP) procedure was again used for the preparation of PI-*b*-PDMAEMA block copolymers. A bromide-end-capped polyisoprene macroinitiator was prepared by living anionic polymerisation, as has previously been reported.[21] This was then used as a macroinitiator for the ATRP of DMAEMA to prepare a homologous series of block copolymers with a varying molar mass of PDMAEMA from a polyisoprene block of constant molar mass, as described before for PI-*b*-PMMA. This CHOMP methodology has previously been reported for the preparation of poly(butadiene-*b*-DMAEMA) block copolymers.[22] The PI-*b*-PDMAEMA block copolymers were subsequently dispersed in *n*-decane and characterised by TEM, to investigate the effect of PDMAEMA block molar mass on the resulting morphology and to compare to analogous PI-*b*-PMMA block copolymers.

Additionally, the presence of the tertiary amine group on PDMAEMA allowed for further (post-polymerisation) functionalisation by quaternisation[23] and three alkyl iodides (ethyl, butyl and octyl) of different molar masses were used as quaternising agents, at different degrees of quaternisation, to investigate the impacts of the length of alkyl group and extent of quaternisation on the self-assembly behaviours in *n*-decane. Any differences in morphology following quaternisation were also observed by TEM.

4.2.1. Polymer Synthesis

Previously, PI-*b*-PMMA block copolymers were prepared by a change of mechanism polymerisation (CHOMP) procedure so that the molecular weight of PMMA could be varied whilst maintaining a constant molar mass of polyisoprene. CHOMP has previously been shown to be a useful approach for preparing mechanistically incompatible copolymers, offering great versatility in the polymers that can be prepared and the mechanisms used in their synthesis.[24-26] In this instance, living anionic polymerisation was used to prepare ethylene oxide-end-capped polyisoprene (PI-*OH*) and the end-group was converted to a bromide by a bromoacetylation reaction. This was then used as a macroinitiator for the ATRP of DMAEMA. The degree of polymerisation of PDMAEMA was varied to study the effect on the self-assembly behaviour in *n*-decane, both relatively, and in comparison to that of PI-*b*-PMMA as discussed in the previous chapter. The synthetic method used for the preparation of PI-*b*-PDMAEMA was almost identical to that of PI-*b*-PMMA; the only slight difference being the conditions for the ATRP reaction. This demonstrates some of the potential for the CHOMP mechanism to be used in preparing diverse families of block copolymers with different chemistries and molar masses.

4.2.1.1. Synthesis of Bromide-end-capped Polyisoprene (PI-*Br*) Macroinitiator

The preparation of PI-*Br* was carried out according to the procedure described in chapter 3. Table 4.1 shows the molar mass data obtained by size exclusion chromatography for the sample of unfunctionalised polyisoprene taken from the reaction before the addition of ethylene oxide.

Table 4.1: Molecular weight values of the PI sample taken from the anionic polymerisation to prepare PI-OH. Data obtained using triple detection SEC in THF (dn/dc = 0.13 mL g^{-1}).

Polyisoprene$_{DP}$ [a]	$M_{n,Calc}$/ g mol^{-1}	$M_{n,SEC}$/ g mol^{-1} [b]	Đ [c]
PI$_{37}$	2000	2540	1.03

a: DP calculated from SEC for PI from PI-Br macroinitiator
b: $M_{n,SEC}$ calculated using dn/dc = 0.13 mL g^{-1},
c: Dispersity from $M_{w,SEC}/M_{n,SEC}$

Table 4.1 shows that the molar mass of PI$_{37}$ was in reasonable agreement with the target molar mass. The slight discrepancy most likely suggests the *s*-BuLi solution used to initiate the polymerisation was of a lower concentration than expected. This is not

uncommon for butyllithium which over time succumbs to the fact that it is highly air- and water-sensitive.

4.2.1.2. Synthesis of Block Copolymers by ATRP of DMAEMA

To prepare PI-*b*-PDMAEMA block copolymers from the PI$_{37}$-*Br* macroinitiator, ATRP of DMAEMA was carried out. ATRP is a complex process where slight differences to any of the conditions (e.g. temperature, solvents, initiator etc.) can result in significant variation in molar mass and dispersity in the polymers produced.[27] In particular, a change in the monomer being polymerised, e.g. in this case DMAEMA instead of MMA often means that entirely different reaction conditions are required for a controlled polymerisation.[28] In particular, the tertiary amine functionality of DMAEMA can bind to copper, thus competing with the ligands used to solubilise the catalyst. The reversible binding of the monomer to the metal affects the chemical environment of the double bond which decreases the reactivity of DMAEMA and therefore decreases the rate of propagation.[29] To compensate for this, the ATRP of DMAEMA from PI-*Br* was carried out using PMDETA as the ligand instead of Bpy, as previously reported.[30] Furthermore, the ATRP was performed at a lower temperature (30 °C) in THF, as summarised below in Scheme 4.1. These conditions were adopted from a previous report for the ATRP of DMAEMA from a bromide-end-capped polybutadiene macroinitiator.[22]
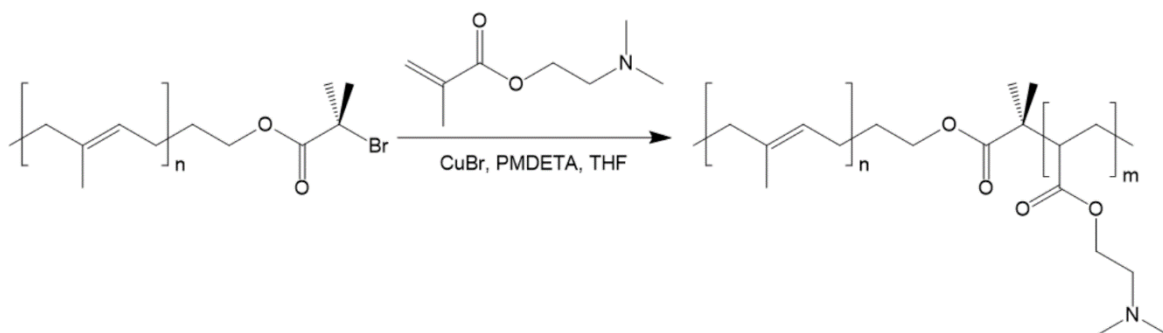
Scheme 4.1: Reaction scheme for the preparation of PI$_{37}$-b-PDMAEMA$_x$ block copolymers by ATRP of DMAEMA from the fixed PI$_{37}$-Br macroinitiator, prepared by living anionic polymerisation

Previously, Tang *et al* reported the effect of various ligands on metal centres and the resulting impact on the kinetics of ATRP.[31] In general, for copper(I) catalysts, tridentate ligands such as PMDETA result in a higher rate of activation ($k_{act.}$) than bidentate ligands such as Bpy. A high $k_{act.}$ for catalysts means a higher equilibrium constant (K_{ATRP}), a higher

concentration of active radicals and therefore a higher rate of propagation in ATRP. However, a high concentration of active radicals, particularly in the early stages of the reaction, can also result in a higher rate of termination, which in time reduces the rate of propagation and gives broad dispersities in the final polymer. Therefore, it is critically important to consider the impact of rates of activation and deactivation on termination. As well as the choice of ligand, the choice of metal catalyst, and reaction conditions, such as solvent and temperature, can also be varied to change the rates of activation and deactivation of the copper catalyst.[27]

Because of the large differences in the dn/dc values of PDMAEMA and PI in THF (0.084 and 0.13 mL g^{-1}, respectively), it is not possible to accurately determine the number-average molar mass of the PDMAEMA block in each block copolymer solely by triple detection SEC. Therefore, ^1H-NMR was also used to determine the final molar mass of all PI_{37}-*b*-PDMAEMA$_x$ block copolymers, based on the known molar mass of the polyisoprene block obtained by SEC and reported in Table 4.1. Figure 4.1 shows an exemplar proton NMR spectrum, for PI_{37}-*b*-PDMAEMA$_{27}$, used for molar mass determination.
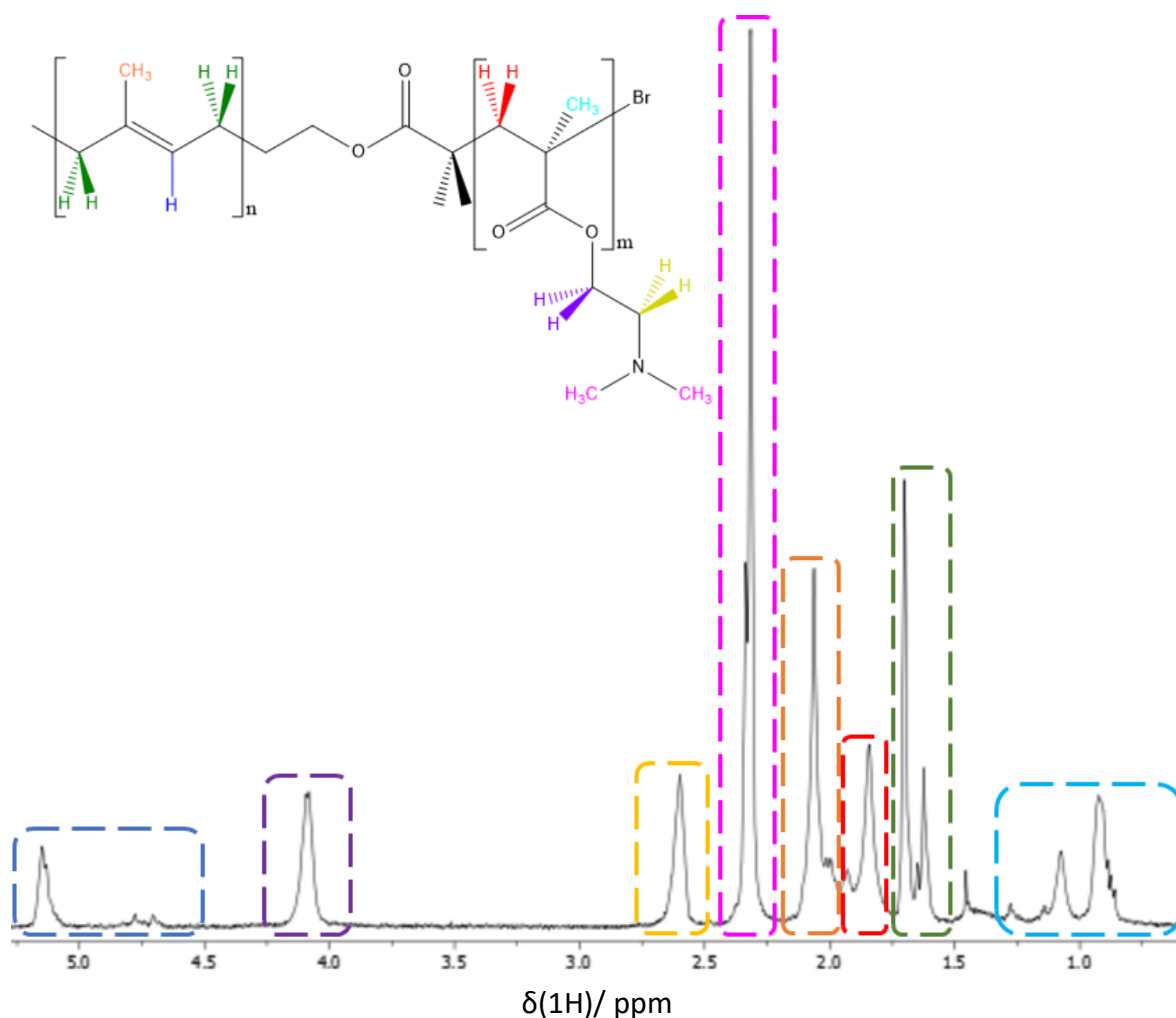
Figure 4.1: ^1H NMR spectrum for a PI-b-PDMAEMA block copolymer. In this instance the sample shown is PI$_{37}$-b-PDMAEMA$_{27}$. NMR spectrum referenced to the solvent, CDCl$_3$, peak at 7.26 ppm

The NMR spectrum in Figure 4.1 shows the presence all of the expected peaks for PDMAEMA.[32] In particular, the peaks arising due to CH$_2$ protons adjacent to the ester, and the nitrogen (shown in purple and gold at 4.06 and 2.57 ppm respectively), and the sharp peak for the dimethylamino methyl protons (shown in pink at 2.30 ppm) are all very characteristic. These peaks, specifically, also do not overlap with other peaks for polyisoprene, and therefore the integrals can be used in the determination of the molar mass with respect to the polyisoprene (for example the peak for the alkene proton at 4.67 – 5.14 ppm, highlighted in dark blue) of a known molar mass from the triple detection SEC of the macroinitiator.

Table 4.2 below shows molar mass data for the polyisoprene ATRP macroinitiator, and for the family of PI$_{37}$-b-PDMAEMA$_x$ block copolymers – obtained by both SEC and NMR.

The block copolymers had varying target molar masses of PDMAEMA allowing any variation in the self-assembly behaviour to be correlated with PDMAEMA block length.

Table 4.2: Molecular weight data for all PI$_{37}$-b-PDMAEMA$_x$ block copolymers prepared by ATRP from the PI$_{37}$-Br macroinitiator of fixed degree of polymerisation

Sample Name$_{DP}$ [a]	M$_{n,Calc}$/ g mol^{-1} [b]	M$_{n,SEC}$/ g mol^{-1} [c]	M$_{n,NMR}$/ g mol^{-1} [d]	Đ [e]
PI$_{37}$	2000	2540	-	1.03
PI$_{37}$-*b*-PDMAEMA$_{34}$	10500	8150	7960	1.19
PI$_{37}$-*b*-PDMAEMA$_{38}$	12500	7030	8460	1.12
PI$_{37}$-*b*-PDMAMEA$_{58}$	17500	9900	11800	1.12
PI$_{37}$-*b*-PDMAEMA$_{61}$	18000	12600	12200	1.06
PI$_{37}$-*b*-PDMAEMA$_{62}$	22500	11500	12300	1.13
PI$_{37}$-*b*-PDMAEMA$_{77}$	32500	11800	14700	1.09

a: DP calculated from SEC for PI block and from NMR for PDMAEMA block,
b: Calculated molecular weight from DP PI + theoretical molecular weight of PDMAEMA,
c: M$_{n,SEC}$ calculated using dn/dc = 0.084 mL g^{-1},
d: M$_{n,NMR}$ calculated from comparing integrals for PDMAEMA to values for the PI$_{37}$-Br macroinitiator + M$_{n,SEC,}$
$_{PI,}$
e: Dispersity from M$_{n,SEC}$/M$_{w,SEC}$

In the case of the PI-*b*-PDMAEMA block copolymers, there is a reasonably good agreement between the number average molecular weight determined by NMR and from triple detection SEC. The PI-*b*-PDMAEMA block copolymers described in Table 4.2 are all relatively low in molecular weight which is most probably the reason for the similarity in the total values. Because of the difference in dn/dc for the constituent homopolymers (0.13 and 0.084 mL g^{-1} for PI and PDMAEMA respectively), the M$_n$ from SEC is unlikely to be as accurate as the value obtained by NMR. Therefore, the value for M$_n$ from NMR will be used in all subsequent discussions, as was the case with PI-*b*-PMMA block copolymers. The data in Table 4.2 also show that there is agreement between the final molar mass of the block copolymer and the target molar mass, especially for the lower target molar masses where in most cases the measured block copolymer molar mass is approximately two-thirds of the target molar mass. However, where the target molar mass is greater than 20 kg mol^{-1} the difference between target and experimental molar mass becomes significantly greater. The yields for all ATRP reactions were above 60 %, suggesting that conversion levels were limited, and this is particularly so for the higher target molar masses. It is difficult to achieve

high molar masses and high conversion with high accuracy and low dispersity by RDRP techniques such as ATRP, because of the high likelihood of side reactions that terminate chain growth. These side reactions are less prevalent during the analogous polymerisation to lower molar mass.[33, 34] In general, the longer the reaction proceeds, the more opportunity the active radicals have to undergo termination events.[35] A similar trend was previously observed with the preparation of PI$_{74}$-*b*-PMMA$_x$ block copolymers in Chapter 3.

All of the PI-*b*-PDMAEMA block copolymers reported in Table 4.2 show narrow molecular weight distributions, which suggest high degrees of control in the ATRP reactions as was expected for the high rate of activation for the CuBr/PMDETA system. The PI-*b*-PMMA block copolymers described in chapter 3 had higher dispersities in their final molar masses, which can be rationalised because of the 'less active' catalyst system with the bidentate ligand, Bpy. The results in Table 4.2 show that the block copolymers have lower dispersities than the literature reports for ATRP of DMAEMA using the same reaction conditions, to prepare both PDMAEMA homopolymers and block copolymers from a PB-*Br* macroinitiator. Their results showed dispersities of 1.30 and 1.27, albeit with the latter having a higher molar mass of PDMAEMA (38.5 kg mol^{-1})[22, 30]. The differences are not dramatic in either case, and still show good levels of control in the polymerisation of DMAEMA in our work.

Exemplar SEC traces for PI$_{37}$-*Br* macroinitiator and 2 PI$_{37}$-*b*-PDMAEMA$_x$ block copolymers prepared according to the ATRP reaction shown in Scheme 4.1 using PI$_{37}$-Br are shown in Figure 4.2.
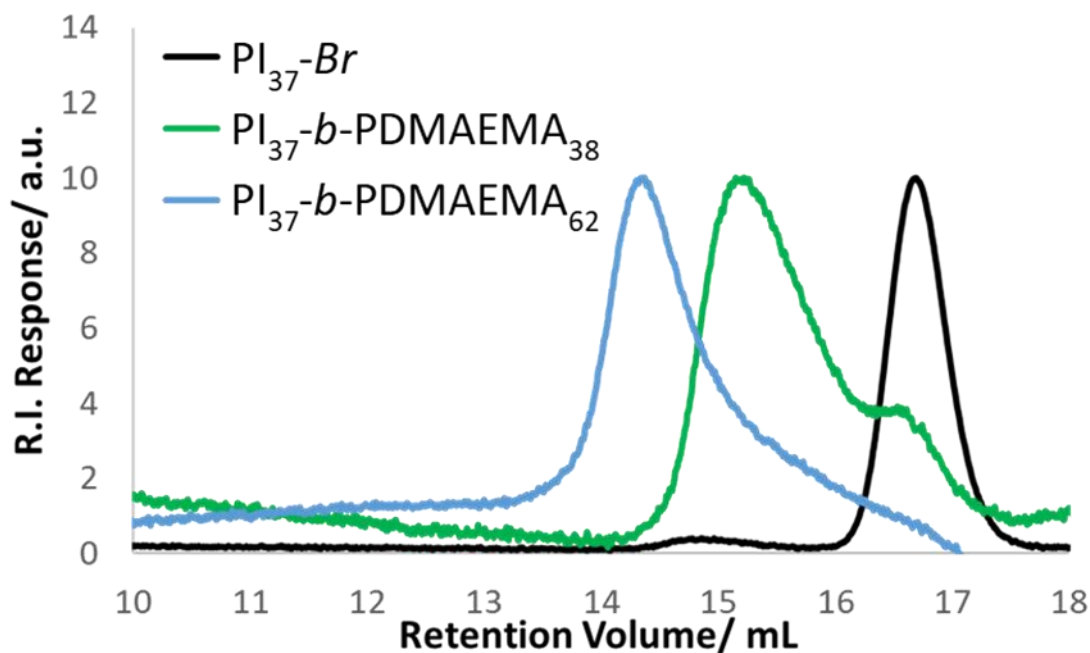
Figure 4.2: SEC traces from the RI detector used in triple-detection SEC in THF for the PI_{37}-Br macroinitiator and 2 PI_{37}-b-PDMAEMA$_x$ block copolymers

The SEC chromatogram of PI_{37}-*Br* (16.8 mL retention volume) shows a narrow peak, as expected for a polymer produced by anionic polymerisation. The peaks in the chromatograms of the block copolymers in Figure 4.2 are shifted to lower retention volumes indicating successful ATRP of DMAEMA from the PI_{37}-*Br* macroinitiator. PI_{37}-*b*-PDMAEMA$_{38}$ and PI_{37}-*b*-PDMAEMA$_{62}$ had target molar masses for the PDMAEMA block, of 10.0 and 20.0 kg mol^{-1}, respectively. The elution of these analytes at 15.1 and 14.2 mL in the SEC, along with the previously reported molar mass data (Table 4.2), shows that there is some degree of control over the final experimental molar mass. The chromatograms for each block copolymers show slight broadening in the molar mass distributions, compared to the macroinitiator, which is characteristic for RDRP reactions in comparison to polymers prepared by living anionic polymerisation. [34]

In the SEC chromatogram of PI_{37}-*b*-PDMAEMA$_{38}$, there is a shoulder at 16.6 mL which overlaps perfectly with that of the PI_{37}-*Br* macroinitiator. The NMR previously showed complete conversion of PI-*OH* to PI-*Br* suggesting that there would not be unreacted PI-*OH* present in the block copolymer. Instead, the shoulder is most likely caused by a slow rate of ATRP initiation. The conditions for ATRP (i.e., ligand, solvent etc.) could be changed to increase the rate of activation relative to deactivation. However, because the

block copolymers are to be self-assembled in *n*-decane, which is selective for the polyisoprene block, a small amount of unreacted polyisoprene is not anticipated to affect the self-assembly behaviour being investigated.

4.2.2. Self-Assembly of PI-*b*-PDMAEMA in *n*-Decane

Following the synthesis of a family of PI_{37}-*b*-$PDMAEMA_x$ block copolymers with a varying degree of polymerisation of the PDMAEMA block, samples were dispersed in *n*-decane, a selective solvent for the polyisoprene block, at varying wt%. The solvent-switching method of dispersion was identical to the procedure previously described in chapter 3. This method is in contrast to the commonly-employed polymerisation-induced self-assembly (PISA), which is a method of preparing self-assembled block copolymers *in-situ* and has been widely reported in the last 10 years.[36-38]

As with the self-assembly of PI-*b*-PMMA in *n*-decane, a variety of solution properties was formed on dispersion of the PI-*b*-PDMAEMA samples. These can be represented in a 'phase diagram' (Figure 4.3) of $DP_{PDMAEMA}$ vs. solids content, allowing comparisons to be drawn with the previous phase diagrams of PI-*b*-PMMA.
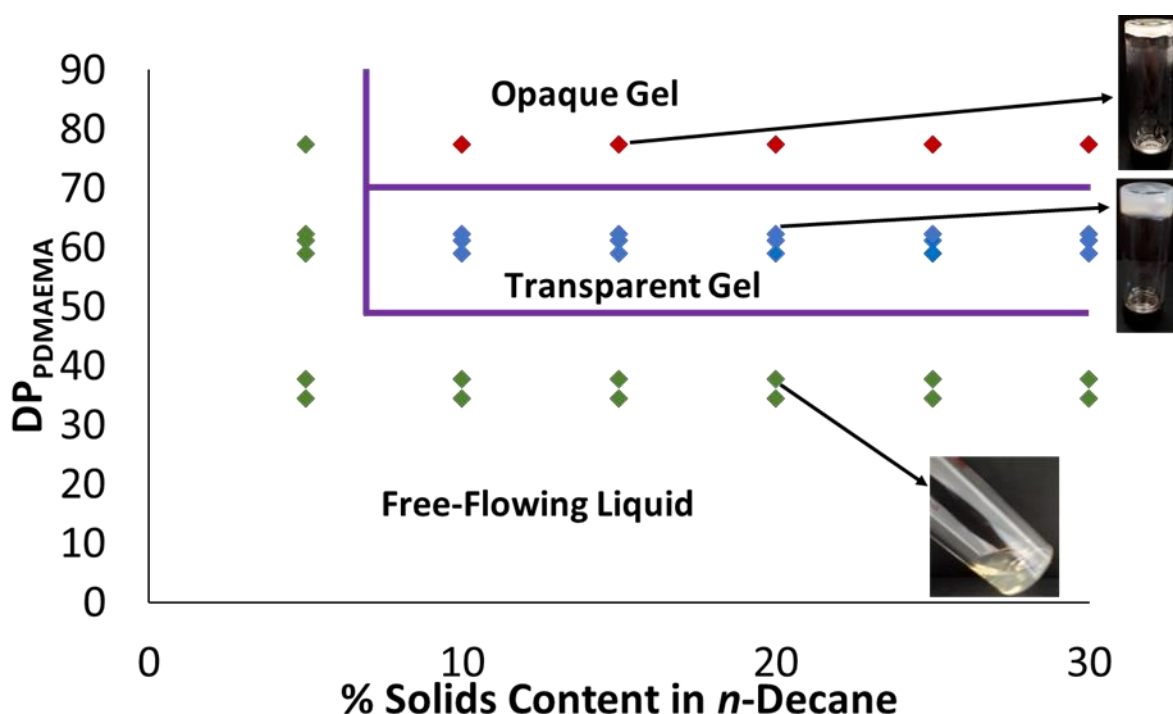
Figure 4.3: Phase diagram illustrating the results of self-assembly of PI_{37}-b-$PDMAEMA_x$ in n-decane at varying solids content.

The phase diagram in Figure 4.3 shows how different physical structures emerge (as a function of block copolymer composition and solids content) which are reminiscent of those of PI-*b*-PMMA dispersions (i.e. free-flowing liquids, transparent gels and opaque gels) and to those previously reported as a result of the self-assembly of other block copolymers in selective solvents.[38, 39] The dispersions take on distinctly different physical forms as the degree of polymerisation of PDMAEMA increases. These characteristic physical forms have previously been identified by TEM and DLS as being the result of different self-assembled morphologies i.e., spherical micelles, wormlike micelles and vesicles for liquids, transparent gels, and opaque gels, respectively. The observation of these physical structures for the PI-*b*-PDMAEMA system strongly suggests self-assembly into the same morphologies as was observed with PI-*b*-PMMA.

Comparing Figure 4.3, based on PI_{37}-*b*-$PDMAEMA_x$, to the phase diagram of PI_{32}-*b*-$PMMA_x$ (Chapter 3, Figure 3.6), which has a PI block of similar molar mass (2540 g mol^{-1} and 2040 g mol^{-1}, respectively), key differences in the self-assembly behaviour can be observed. Most notably, the characteristic physical structures that form upon self-assembly of PI-*b*-PDMAEMA emerge at far shorter methacrylate (core-forming) block lengths. This can be rationalised by the greater molar mass of the DMAEMA repeat unit. However, the PI_{32}-*b*-$PMMA_{83}$ block copolymer described in the previous chapter, which formed a free-flowing liquid, had a PMMA block molar mass which is in between the PDMAEMA block molar mass of PI_{37}-*b*-$PDMAEMA_{58}$ and PI_{37}-*b*-$PDMAEMA_{61}$ i.e., 8150 g mol^{-1} compared to 7560 and 8560 g mol^{-1} respectively), both of which formed transparent gels. This result suggests that the resulting self-assembled morphology is not only correlated with molar mass of the core-forming block. Looking at the repeat units comprising the PMMA and PDMAEMA blocks, it is clear that there are differences in their chemical structures, functionality, and molar mass, which in turn will result in different chain dimensions for PMMA and PDMAEMA blocks of the same molar mass. Both repeat units contain 2 carbon atoms in the polymer backbone, however, the size and molar mass of the PDMAEMA repeat unit is significantly larger because of the amine moiety on the ester group. This will result in a greater volume in the core-forming block which is known to affect the Israelachvili packing parameter, meaning that higher values for the packing parameter would be obtained for PDMAEMA, even with an equivalent degree of polymerisation.[8] An

increase in packing parameter can cause different morphologies of micelles to form upon self-assembly (i.e. wormlike micelles instead of spherical micelles or vesicles instead of wormlike micelles).

Additionally, the differences in chemical structure of the two methacrylate polymers must be considered. Clearly, both groups contain an ester, however, the presence of the tertiary amine in PDMAEMA may be expected to change the solubility in non-polar solvents. The difference in solubility between PDMAEMA and PMMA could drive the micellisation of PI-*b*-PDMAEMA block copolymers to occur at lower concentrations and also into different morphologies. This could also have a significant role in the following investigation into the quaternisation of PDMAEMA in PI-*b*-PDMAEMA block copolymers. Plainly, it is not possible to change the chemistry of the polymer without also significantly changing the dimensions, so studying the individual effects of each would be challenging, and instead both factors must be considered during this investigation.

4.2.2.1 Characterisation of Self-Assembled PI-*b*-PDMAEMA by TEM

To investigate the nature of the self-assembled morphologies giving rise to the different physical forms observed, TEM was used to study the various dispersions. In the case of PI-*b*-PMMA block copolymers, cryo-TEM was not required because of the high glass transition temperature of the core-forming PMMA block (105 °C).[40] The T_g of PDMAEMA is about room temperature (20 °C) meaning that cryo-TEM could be beneficial for PI-*b*-PDMAEMA block copolymers. However, initially, for reasons of simplicity and higher throughput, standard TEM sample preparation was exploited. The only difference was that the PI-*b*-PDMAEMA dispersions were diluted to 0.1 wt% following their initial self-assembly at 15 wt% in *n*-decane. In the study of PI-*b*-PMMA described in the previous chapter, dilution was not found to affect self-assembled morphology of micelles, therefore dilution was used because of the ease of sample preparation of the gels for TEM imaging. This has also been used as common practice for TEM imaging of similar self-assembled block copolymers.[41, 42] Figure 4.4 shows TEM images of block copolymers self-assembled at 15 wt% (then diluted to 0.1 wt% where they become free-flowing liquids) in *n*-decane; Figure 4.4a is the TEM of PI$_{37}$-*b*-PDMAEMA$_{38}$ – a free-flowing liquid; 4.4b is the TEM of PI$_{37}$-*b*-PDMAEMA$_{62}$ – a transparent gel and 4.4c is the TEM of PI-*b*-PDMAEMA$_{77}$ – an opaque gel.

These physical structures have previously been shown to be the result of self-assembly into micelles of the different morphologies.
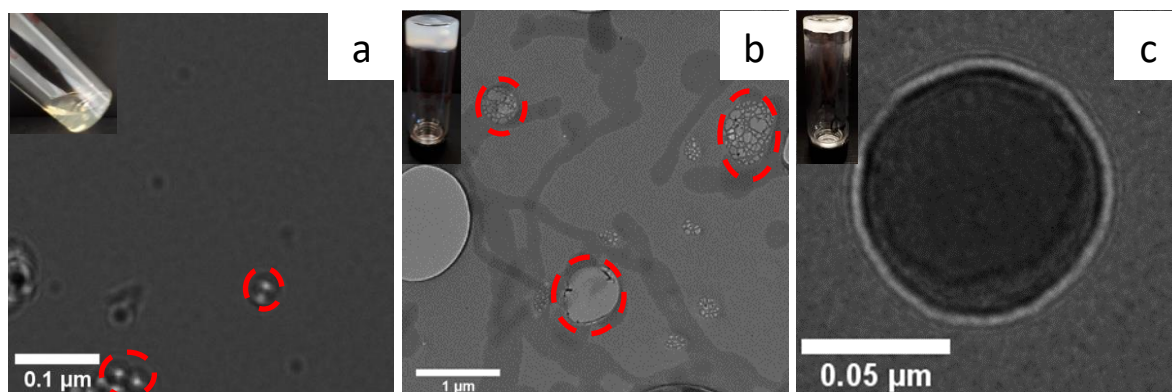
Figure 4.4: High resolution TEM images of the 3 different self-assembled structures of PI$_{37}$-b-PDMAEMA$_x$ block copolymers in n-decane; a: PI$_{37}$-b-PDMAEMA$_{38}$, b: PI$_{37}$-b-PDMAEMA$_{62}$, c: PI$_{37}$-b-PDMAEMA$_{77}$, self-assembled at 15 wt% in n-decane. Scale bar = 100 nm. Images taken of samples at 0.1 wt% following dilution in n-decane. Objects highlighted in red are part of the holey carbon grid used for sample preparation.

TEM images of the self-assembled morphologies of PI$_{37}$-b-PDMAEMA$_x$ (Figure 4.4) show the expected characteristic micellar morphologies.[38] PI$_{37}$-b-PDMAEMA$_{38}$ forms a free-flowing liquid in decane, due to the presence of spherical micelles of diameter approximately 25 nm, which can freely move past each other in solution, resulting in the formation of a low viscosity liquid. PI$_{37}$-b-PDMAEMA$_{62}$ forms a transparent gel, mostly made up of wormlike micelles. This is to be expected with a larger core-forming block relative to corona-forming PI block, which is known to increase the Israelachvili packing parameter.[8] One surprising observation for the wormlike micelles is the large diameter of approximately 100 nm. Previously, for PI-b-PMMA, the diameters of spherical micelles and wormlike micelles were almost identical, so a 4x increase in this instance is somewhat unexpected. One explanation could be the position of PI$_{37}$-b-PDMAEMA$_{62}$ on the phase diagram (Figure 4.3) in that it is very close to the 'boundary' between wormlike micelles and vesicles. Blanazs et al have previously reported the formation of intermittent phases between pure wormlike micelles and pure vesicles in PGMA-b-HPMA block copolymers self-assembled by RAFT-mediated PISA in aqueous solution. Specifically, they imaged 'octopi' and jellyfish' morphologies among wormlike micelles and vesicles. The image in Figure 4.4b shows some larger spherical objects and some bundles of wormlike micelles which could be showing the formation of these intermediates. Zehm et al have previously investigated the effects of variations in block composition of PHEMA-b-BzMA block

copolymers, self-assembled in ethanol by PISA, on the final micellar morphology and particle size.[43] They imaged the dispersions by cryo-TEM to show intermittent phases between pure wormlike micelles and pure vesicles. Specifically, they observed mixtures of wormlike micelles and vesicles with the presences of 'jellyfish' which are believed to be a key intermediate in the formation of vesicles. The increase in diameters of micelles as DP increases has also previously been explored for spherical micelles made up of different DP in the core-forming block to show different diameters that form. For example, Bagheri *et al* investigated the self-assembly of poly((ethylene glycol)-*block*-(*N*-benzoyloxypropyl methacrylamide)) (PEG-*b*-(PHPMA-Bz)) in aqueous solution and measured the diameter of spherical micelles from cryo-TEM images.[44] They reported an increase in the diameter of spherical micelles from 4 to 14 nm as the molar mass of the core-forming PHPMA-Bz block increased from 2200 to 18500 g mol^{-1}, demonstrating the influence of the relative molar mass on the packing parameter. Evidence for this reasoning applying in the current study can be gained from Figure 4.3 where the commonly narrow transparent gel phase is populated by 3 different PI$_{37}$-*b*-PDMAEMA$_x$ block copolymers. The sample imaged in Figure 4.4b had the highest DP$_{PDMAEMA}$ of the 3 samples that populate the transparent gel phase, suggesting it could be close to the phase boundary where larger diameters could be expected. Additional experiments to prepare block copolymers near to this phase boundary or to image the other block copolymers in this phase could be used to further explore this hypothesis. Finally, the opaque gel arising from the self-assembly of PI$_{37}$-*b*-PDMAEMA$_{77}$ is shown to be made up of vesicles with a diameter of approximately 90 nm. Again, the formation of vesicles is expected as the core-forming block length increases, which causes an increase in the packing parameter relative to wormlike micelles.

4.2.3. Quaternisation Reaction of PDMAEMA in PI-*b*-PDMAEMA

Following the preparation and self-assembly of PI-*b*-PDMAEMA block copolymers in *n*-decane, it was of interest to investigate the impact of quaternisation of the PDMAEMA block on the self-assembly behaviour of the resultant quaternised block copolymers. Quaternisation with an alkyl halide is not only expected to introduce charge via the formation of a cationic polyelectrolyte,[18, 45] but will also lead to a pronounced increase in the overall molar mass and tube diameter of the core-forming block. A change in the molar mass/size of the core-forming block has previously been shown to change the morphology

of the self-assembled structures formed and the overall physical structure.[8] Cationic polymers are useful in their own right as they have antimicrobial properties, particularly as amphiphilic block copolymers, due of their disruptive interaction with amphiphilic lipid membranes.[46] They also have further potential applications as flocculants and ion-exchange resins.[47, 48]

4.2.3.1. Preparation of a Large Batch of PI-*b*-PDMAEMA

To investigate the effect of quaternisation with different alkyl iodides and different degrees of quaternisation, a large batch of PI-*b*-PDMAEMA block copolymer was required. For this, a new PI-*Br* macroinitiator was prepared by the same living anionic polymerisation and bromoacetylation procedure previously described in section 3.2.1.1. The target molar mass of PI was identical to the one used previously (and reported in Table 4.1 -2540 g mol^{-1}). A single ATRP reaction of DMAEMA using the new PI-*Br* macroinitiator was then carried out as described in Scheme 4.1. The target molar mass of the PDMAEMA block was chosen to replicate a block copolymer that had previously been shown to self-assemble into spherical micelles, specifically PI$_{37}$-*b*-PDMAEMA$_{38}$. This was because the quaternisation reaction should increase the molar mass of the insoluble block relative to the soluble polyisoprene, which was shown in Figure 4.3 (in the case of unquaternised samples) to cause the morphology to change from spheres to wormlike micelles and then vesicles. Unlike the unquaternised samples illustrated in Figure 4.3, quaternisation will not result in an increase in molar mass due to an increase in the degree of polymerisation, but instead as a result of an increase in the molar mass of each quaternised repeat unit. By starting with a PI-*b*-PDMAEMA block copolymer that forms spherical micelles, it may be possible to induce the formation of different morphologies (and conceivably to generate a new phase diagram) simply by quaternisation (to varying degrees) of a single block copolymer. The molar mass data for the polyisoprene precursor and the PI-*b*-PDMAEMA block copolymer are reported in Table 4.3.

Table 4.3: Molecular weight data for PI_{37b}-b-PDMAEMA_{35} block copolymer.

Sample Name$_{DP}$ [a]	$M_{n,Calc}$/ g mol^{-1} [b]	$M_{n,SEC}$/ g mol^{-1} [c]	$M_{n,NMR}$/ g mol^{-1} [d]	Đ [e]
PI$_{37b}$	2500	2510	-	1.04
PI$_{37b}$-b-PDMAEMA$_{35}$	12500	18100	7390	1.12

a: DP calculated from SEC for PI block and from NMR for PDMAEMA block,
b: Calculated molecular weight from DP PI + theoretical molecular weight of PDMAEMA,
c: $M_{n,SEC}$ calculated using dn/dc = 0.084 mL g^{-1},
d: $M_{n,NMR}$ calculated from comparing the respective integrals for PDMAEMA to values for the PI$_{37}$-Br macroinitiator + $M_{n,SEC, PI}$,
e: Dispersity from $M_{n,SEC}$/$M_{w,SEC}$

The molecular weight data in Table 4.3 shows that the polyisoprene, prepared by living anionic polymerisation had, as expected, an almost identical number average molecular weight to the polyisoprene previously prepared for the initial PI-b-PDMAEMA study (see Table 4.1). For this reason, the sample has been given the name PI$_{37b}$ to differentiate it from the previous PI$_{37}$ sample. The degree of polymerisation (DP) of the PDMAEMA block (DP = 35) is between the DP of the 2 lowest molecular weight PDMAEMA block polymers (DP = 34 and 38) previously reported in Table 4.2. Both of those earlier samples formed free-flowing liquids of spherical micelles following self-assembly in n-decane. Spherical micelles was the target morphology for the newly prepared PI-b-PDMAEMA block copolymer, with the expectation that quaternisation of the core-forming PDMAEMA block should dramatically change the packing parameter and result in a change in morphology to wormlike micelles and/or vesicles.

4.2.3.2. Quaternisation of PI-b-PDMAEMA in THF

Classically, the preparation of cationic polymers can be achieved via 2 routes: post-polymerisation modification and polymerisation of a cationic monomer.[49] The former route was chosen for this investigation because it was desirable to prepare a homologous series of block copolymers, by systematically varying the degree of quaternisation using a single PI-b-PDMAEMA block copolymer. To prepare the required series of samples by polymerisation of a quaternised monomer would require a high degree of reproducibility in the molar mass that is not possible by any polymerisation technique. However, one possible consequence of the post-polymerisation route could be difficulties in achieving a high degree of quaternisation, particularly for the bulkier alkyl iodides. Scheme 4.2 shows the reaction used for the quaternisation of PI-b-PDMAEMA with alkyl iodides. The product

shown is that of the theoretical, quantitatively quaternised product. The solvent and temperature choices (room temperature) for the reaction were based on literature reports for the quaternisation of PDMAEMA.[18]
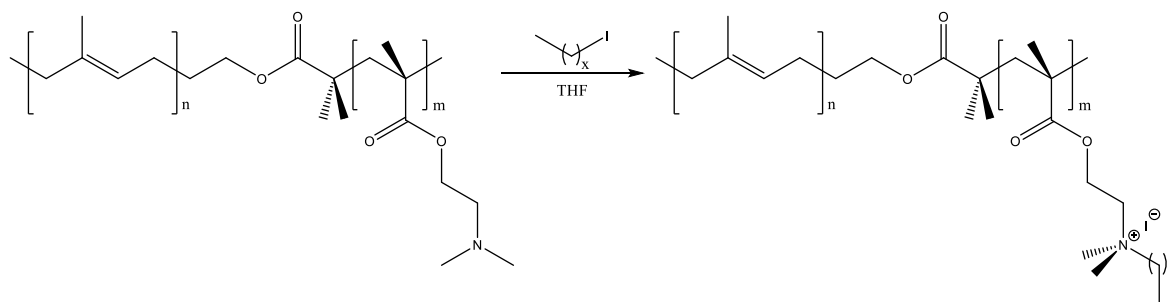
Scheme 4.2: Reaction scheme for the preparation of PI$_{37b}$-b-PQDMAEMA$_{35}$ from PI$_{37b}$-b-PDMAEMA$_{35}$ by quaternisation of PDMAEMA with different alkyl halides. In the example shown, the quaternisation is to 100 mol% with respect to PDMAEMA. For ethyl iodide, n-butyl iodide and n-octyl iodide, x = 1, 3 and 7, respectively.

In the case of PI$_{37b}$-*b*-PDMAEMA$_{35}$, a solid gel, was first dissolved in DCM (a common solvent for PI and PDMAEMA) for transfer into a reactor flask. The DCM was then removed by distillation and the polymer was dried *in vacuo* overnight. Initially, for an investigation into the synthesis of PI-*b*-PQDMAEMA by quaternisation, a preliminary reaction using a different PI-*b*-PDMAEMA block copolymer was carried out with a target degree of quaternisation of 100 mol% using ethyl iodide. This reaction was carried out in THF at ≈10 wt% and resulted in the formation of strong, solid gel after 15 hours. The formation of the gel stopped the magnetic stirring and gave a product that could not be worked up. Therefore, subsequent quaternisation reactions were carried out at a lower polymer concentration (≈1 wt%) in THF.

During the subsequent quaternisation reactions at 1 wt% in THF with ethyl iodide, the physical properties of the solution changed with time such that after 15 hours, loose gels had formed during reactions with a target degree of quaternisation of 40, 60 and 80 %. The reason for the change in physical properties (gelation) was subsequently investigated by TEM (See section 3.2.3.3) and it was concluded that the PDMAEMA block becomes insoluble in THF upon quaternisation, which induces a self-assembly into micelles – Quaternisation Induced Self-Assembly (QISA). This was most unexpected given that previous literature reports for the quantitative quaternisation of PDMAEMA homopolymers were carried out in THF, with no mention of the quaternised polymer

having reduced solubility. We believe this is the first reported case of QISA of block copolymers in solution.

The quaternisation reaction illustrated in Scheme 4.2 indicates that different alkyl iodides were investigated. Specifically, ethyl iodide, n-butyl iodide and n-octyl iodide (where x = 1, 3 and 7, respectively) were used to quaternise PI$_{37b}$-b-PDMAEMA$_{35}$. Quaternisation with each of these alkyl iodides results in significant changes to the block copolymer, including the chemistry of the final PI-b-PQDMAEMA block copolymer and also the molar mass of the DMAEMA repeat unit and therefore the core-forming block. The molar mass of the repeat unit and the degree of polymerisation both change the dimensions of the core-forming block and therefore both cause a difference in the packing parameter.[8] As well as the different alkyl iodides used in this investigation, the target degree of quaternisation with each alkyl iodide was also varied from 20 -100 mol%.

The outcomes of the quaternisation reactions were not analysed by size exclusion chromatography because of concerns about strong interactions between the charged polymer and the column packing which would render any analysis inaccurate and cause damage to the column.[50] Therefore, the products of the quaternisation reactions were analysed using proton NMR. An exemplar NMR spectrum for PI$_{37b}$-b-PQDMAEMA$_{35}$(EI-19%) is shown below in Figure 4.5b, while Figure 4.5a shows the spectrum of the unquaternised PI$_{37b}$-b-PDMAEMA$_{35}$ block copolymer for comparison. The sample naming system encompasses the key molecular parameters of the quaternised product. Thus PI$_{37b}$-b-PQDMAEMA$_{35}$(EI-19%) indicates that PI$_{37b}$-b-PDMAEMA$_{35}$ was quaternised (Q) with ethyl iodide (EI) such that 19 mol% of PDMAEMA repeat units were quaternised, as calculated by NMR. Likewise (see later) BI indicates butyl iodide and OI, octyl iodide.
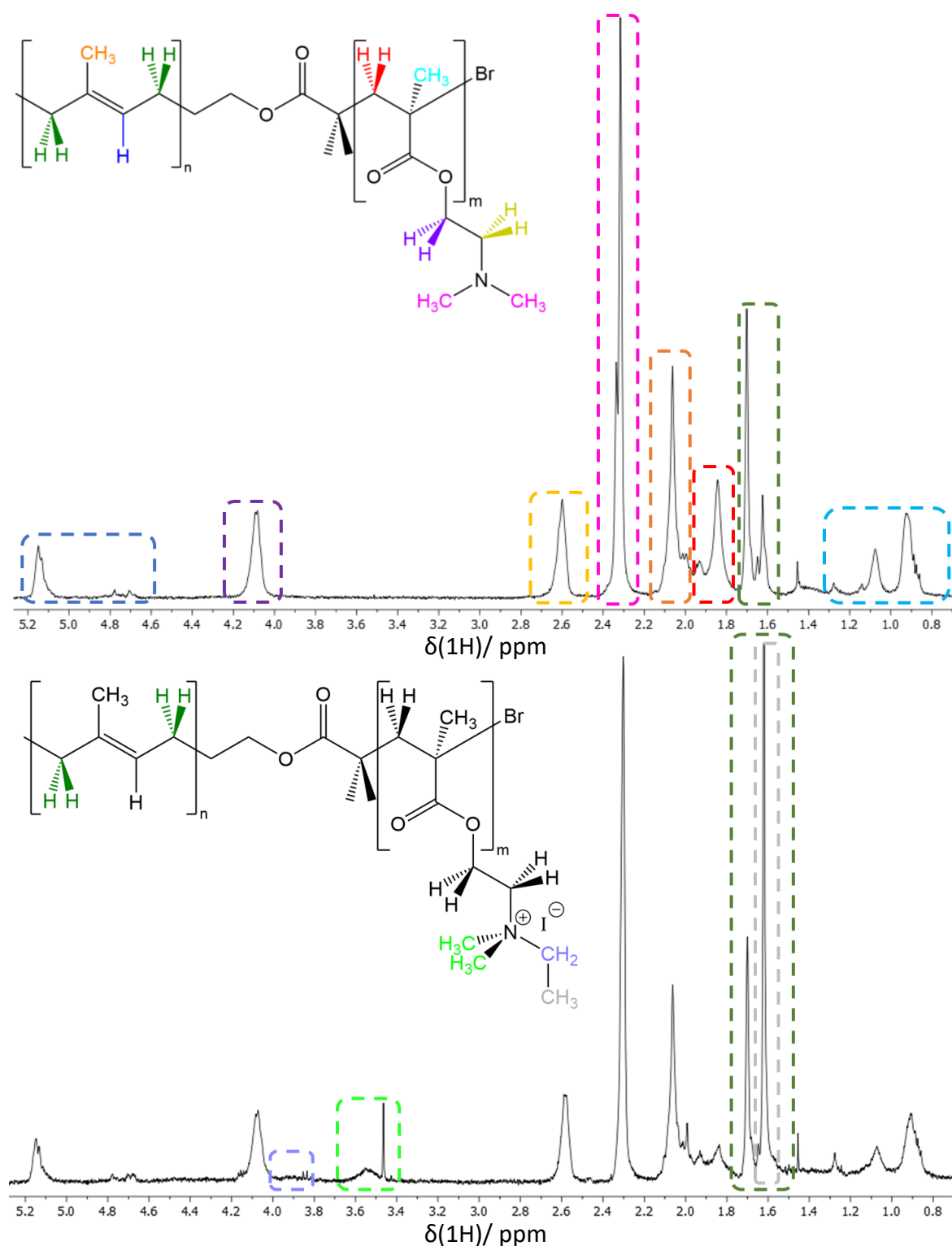
Figure 4.5: Characteristic ^1H NMR spectra for a) unquaternised PI_{37b}-b-$PDMAEMA_{35}$ and b) PI_{37b}-b-$PQDMAEMA_{35}$(EI-19%). NMR spectra referenced to the solvent, $CDCl_3$, peak at 7.26 ppm

The exemplar proton NMR spectrum in Figure 4.5a shows the characteristic peaks for polyisoprene and PDMAEMA.[32] Because the target conversion of the quaternisation reaction with ethyl iodide was 40 mol% of the DMAEMA repeat units, the NMR spectrum

for the product (Figure 4.5b) comprises of both quaternised and unquaternised repeat units and there is significant overlap between the proton signals for PQDMAEMA and PDMAEMA (e.g. for the peaks for the methyl group attached to the methacrylate backbone at 0.82 – 1.31 ppm). The key difference in the quaternised spectrum is the emergence of the peak at 3.40 – 3.67 ppm (highlighted in light green) which is characteristic of the methyl protons attached to the nitrogen of the ammonium iodide. This is also borne out by the peak at 2.30 ppm (highlighted in pink in Figure 4.5a) which is depleted (relative to those of polyisoprene from 4.63 – 5.18 ppm (highlighted in dark blue) for the equivalent methyl protons of the unquaternised PDMAEMA repeat unit. Comparison of the integral for the aforementioned peak at 3.40 – 3.67 ppm with those of unquaternised PDMAEMA at 2.30 ppm can be used to calculate the degree of quaternisation. In this case, the mol% of quaternised PDMAEMA in the polymer is 19 mol%. This is significantly below the target degree of quaternisation which was 40 mol%, however, as is discussed in more detail below, this was not unexpected because of steric repulsion that inhibits higher degrees of quaternisation under these conditions for the reaction.[45] There is also the possibility that the decreased solubility of the product in THF which resulted in the changing physical properties of the reaction medium impacted the conversion of the reaction. However, this would be more likely to result in a general plateau where the degree of quaternisation reaches a maximum and the solubility of the polymer changes. Because the degree of quaternisation increases with the target, this suggests that solubility is not the biggest issue.

The extent of quaternisation data for all PI_{37b}-b-$PQDMAEMA_{35}$ block copolymers is reported in Table 4.4. The quaternisation levels for the PI_{37b}-b-$PQDMAEMA_{35}$(BI) and PI_{37b}-b-$PQDMAEMA_{35}$(OI) block copolymers were also calculated in the same fashion from the proton NMR, however, dimethyl sulphoxide-d_6 was used as the solvent because they were insoluble in chloroform-d.

Table 4.4: The target and experimental degrees of quaternisation for the quaternisation of PI$_{37b}$-b-PDMAEMA$_{35}$ with different alkyl iodides

Sample	Target Degree of Quaternisation/ mol%	Experimental Degree of Quaternisation/mol%
PI$_{37b}$-*b*-PQDMAEMA$_{35}$(EI-16%)	20	16
PI$_{37b}$-*b*-PQDMAEMA$_{35}$(EI-19%)	40	19
PI$_{37b}$-*b*-PQDMAEMA$_{35}$(EI-25%)	60	25
PI$_{37b}$-*b*-PQDMAEMA$_{35}$(EI-26%)	80	26
PI$_{37b}$-*b*-PQDMAEMA$_{35}$(EI-27%)	100	27
PI$_{37b}$-*b*-PQDMAEMA$_{35}$(BI-10%)	20	10
PI$_{37b}$-*b*-PQDMAEMA$_{35}$(BI-21%)	40	21
PI$_{37b}$-*b*-PQDMAEMA$_{35}$(BI-22%)	60	22
PI$_{37b}$-*b*-PQDMAEMA$_{35}$(BI-25%)	80	25
PI$_{37b}$-*b*-PQDMAEMA$_{35}$(BI-27%)	100	27
PI$_{37b}$-*b*-PQDMAEMA$_{35}$(OI-8%)	20	8
PI$_{37b}$-*b*-PQDMAEMA$_{35}$(OI-10%)	40	10
PI$_{37b}$-*b*-PQDMAEMA$_{35}$(OI-12%)	60	12
PI$_{37b}$-*b*-PQDMAEMA$_{35}$(OI-15%)	80	15
PI$_{37b}$-*b*-PQDMAEMA$_{35}$(OI-19%)	100	19

The results in Table 4.4 show that, for equal target degree of quaternisation, the experimental degree of quaternisation achieved decreased as the molecular weight of the alkyl iodide increased. This was expected because the larger alkyl iodides will naturally experience greater steric repulsion with the reacted PDMAEMA repeat units as the reaction progresses. The disparity in target and actual degrees of quaternisation is particularly clear for the 100 % target where the conversions were 27 mol% for ethyl and butyl iodide, and 19 mol% for octyl iodide. There is little difference between ethyl and butyl iodide which are more similar in molecular weight than butyl and octyl iodide. These results are in excellent agreement with a recent kinetic investigation by De Jésus-Téllez *et al*. for the quaternisation of a PDMAEMA homopolymer (with a target of 100 % quaternisation) under similar conditions with butyl iodide (33 mol%), hexyl iodide (24 mol%) and decyl iodide (20 mol%), where the degree of quaternisation was also measured by proton NMR in CDCl$_3$.[45] The slightly lower values of quaternisation in our investigation are most likely the result of the quaternisation reactions being performed at room temperature rather than 30 °C, and on a PI-*b*-PDMAEMA block copolymer rather than a PDMAEMA homopolymer. De Jésus-Téllez went on to show that the degree of quaternisation for the 3 alkyl iodides could be

increased to 94, 90 and 87 mol% when the reactions (with the same target of 100 % quaternisation) were carried out at 60 °C for 48 hours. These conditions were not replicated for our investigation because, the self-assembly behaviour is hypothesised to show the greatest differences at low degrees of quaternisation.

Furthermore, the data reported in Table 4.4 show that the measured degree of quaternisation increases as the target degree of quaternisation increases. This is expected because of the increased frequency of molecular collisions and suggests that a higher degree of quaternisation could be attained by using an excess of alkyl iodide. However, in each case, the degree of quaternisation appears to reach a plateau, so significant increases in conversion would be unlikely without a concurrent increase in the temperature of the reaction, as has previously been demonstrated by De Jesús-Téllez *et al*.[45] They rationalised the increased conversion at higher temperatures as being caused by an increase in the frequency of molecular collisions between the reagents.

4.2.3.3. Characterisation of the Products of Quaternisation-Induced Self-Assembly (QISA)

During the quaternisation reactions of PI$_{37b}$-*b*-PDMAEMA$_{35}$ with ethyl iodide, there were noticeable differences in the appearance of the reaction mixture as the reaction progressed. In several cases the reaction mixture changed colour and/or formed gels *in-situ* in the reaction solvent, THF. This type of behaviour had not been observed in any of the previous reactions carried out in this study, for example during the ATRP of MMA or DMAEMA, which were carried out, by design, in a good solvent for both blocks. Samples of the gel-like quaternised block copolymers in THF were collected for further investigation. Images of samples taken directly from the quaternisation of PI$_{37b}$-*b*-PDMAEMA$_{35}$ with ethyl iodide, with degrees of quaternisation from 16 – 27 mol% in THF are shown below in Figure 4.6.
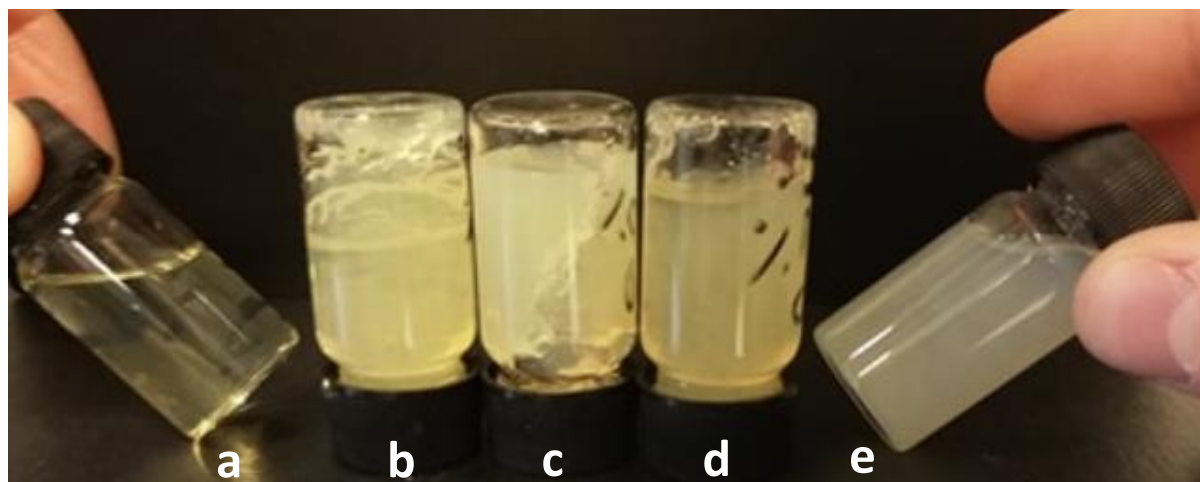
Figure 4.6: Images of samples formed by quaternisation of PI$_{37b}$-b-PDMAEMA$_{35}$ with ethyl iodide in THF at varying degrees of quaternisation a-e represent the different degrees of quaternisation of 16, 19, 25, 26 and 27 %, dispersed at 1 wt% in THF

The image in Figure 4.6 shows the differing nature of the products (in THF) formed during the quaternisation of PI$_{37b}$-b-PDMAEMA$_{35}$ with ethyl iodide. Figure 4.6a shows that PI$_{37b}$-*b*-PQDMAEMA(EI-16%) remained as a transparent, free-flowing liquid at 1 wt% in THF. The reactions with a degree of quaternisation of 19, 25 and 26 mol% (Figure 4.6b-d) all formed loose gels which were capable of 'bulk flow', but partially held their shapes like solids. The sample with a degree of quaternisation of 27 mol% formed an opaque white free-flowing liquid (Figure 4.6e) which was quite different to the transparent liquid of unquaternised PI-*b*-PDMAEMA block copolymers, which dissolved fully in THF. Previously, different physical properties have arisen for dispersions of PI-based block copolymers in *n*-decane, as a result of self-assembly into various morphologies. The structures illustrated in Figure 4.6 are somewhat reminiscent of those previously observed physical structures which could suggest self-assembly of the quaternised block copolymer in THF.

In order to investigate the hypothesis of quaternisation-induced self-assembly, aliquots from each quaternisation reaction were imaged by TEM. TEM images for samples of PI$_{37b}$-*b*-PQDMAEMA$_{35}$(EI) in THF, quaternised at 16, 19 and 25 mol % respectively, are shown in Figure 4.7.
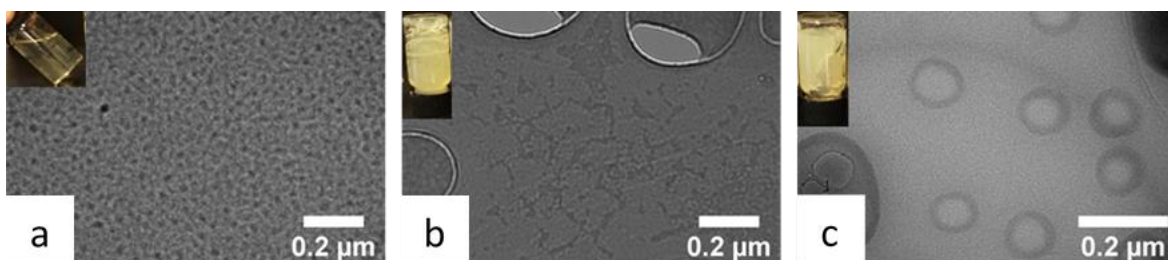
Figure 4.7: TEM images of PI-b-QPDMAEMA(EI-X%) quaternised with ethyl iodide in THF at varying degrees of quaternisation. a: X = 16, b: X = 19 and c: X = 25. Scale bar = 200 nm

The images in Figure 4.7 for the dispersions of PI_{37b}-*b*-PQDMAEMA(EI) in THF show evidence of self-assembly into micelles in a similar fashion to that of previous TEM images of PI-*b*-PMMA and PI-*b*-PDMAEMA (see Figure 4.4) block copolymers when dispersed in *n*-decane and previous literature studies for self-assembled block copolymers.[38, 51] This confirms the hypothesis of a quaternisation-induced self-assembly (QISA) in THF. The TEM of PI_{37b}-*b*-PQDMAEMA$_{35}$(EI-16%) (Figure 4.7a) shows spherical micelles. This is expected for self-assembled block copolymers with a core-forming block of low degree of polymerisation relative to the soluble corona-forming block. However, in this instance, it is a low degree of quaternisation which renders the PDMAEMA block insoluble and causes self-assembly into spherical micelles. The spherical micelles have a diameter of approximately 25 nm which is in good agreement with the dimensions of previously imaged spherical micelles formed from PI_{32}-*b*-PMMA$_{73}$ (20 nm) and PI_{37}-*b*-PDMAEMA$_{38}$ (25 nm) which clearly have similar chain dimensions for the corona-forming PI block and also the core-forming methacrylate where the M_n is 7.31 and 5.97 kg mol^{-1} for PMMA and PDMAEMA, respectively.

Figure 4.7b shows that, upon increasing the degree of quaternisation to 19 mol% PI_{37b}-*b*-PQDMAEMA$_{35}$(EI-19%), the impact upon solubility and chain dimensions of the quaternised block result in the formation of a mixture of wormlike micelles, with a diameter of approximately 20 nm, and a small proportion of spherical micelles with the same diameter. The reason for the mixed phases is most likely the low concentration of the polymer in THF ($\approx$1 wt%), and similar observations have previously been reported for PISA formulations at low solids content.[52] This low concentration is also the most probable reason for the weak nature of the gel. It would be expected that increasing the solids content to 10 wt%, which was previously needed to form self-supporting gels, would result

in a higher proportion (and concentration) of wormlike micelles and the formation of a much stronger, self-supporting gel.

PI$_{37b}$-*b*-PQDMAEMA$_{35}$(EI-25%) (Figure 4.7c) self-assembles into vesicles with a diameter of 100 nm. This diameter is similar to that of PI$_{37}$-*b*-PDMAEMA$_{77}$ (90 nm) which had similar chain dimensions and also self-assembled into vesicles. The thickness of the polymer bilayer is approximately 20 nm, which is similar to the diameter of the spherical micelles. The self-assembly of block copolymers into vesicles to form a turbid gel typically occurs when the DP of the insoluble core-forming block is high relative the DP of the soluble block.[38] In this case, it is the higher degree of quaternisation of the PDMAEMA block which causes self-assembly into vesicles. The vesicles in Figure 4.7c appear very monodisperse which (on the basis of a small sample size in this single sample) might suggest that QISA could be a useful technique for preparing uniform, self-assembled vesicles. The dispersity of nano-objects, particularly vesicles, is difficult to control, with several papers investigating possible methods, both mechanical and synthetic, for preparing monodisperse unilamellar vesicles.[53-55] This preliminary image could offer some potential in that regard.

The images in Figure 4.7 for the dispersions of PI$_{37b}$-*b*-PQDMAEMA$_{35}$(EI) in THF all appear to illustrate self-assembled structures which are not dissimilar to the TEM images of PI-*b*-PMMA and PI-*b*-PDMAEMA (see Figure 4.4) block copolymers in *n*-decane and previous literature studies for self-assembled block copolymers.[38, 51] PI and PDMAEMA are both soluble in THF and the PI-*b*-PDMAEMA block copolymer was initially dissolved in THF for the reaction, as has been reported as common practice for quaternisation of PDMAEMA.[23, 45] However, it is clear that during the quaternisation reaction, the methacrylate block becomes increasing insoluble which causes the block copolymer to self-assemble with the PI block at the corona of the micelles.

The self-assembly of PDMAEMA-based block copolymers as a result of quaternisation has been previously reported in a single study by Fan *et al*., however, self-assembly occurred by quaternisation and crosslinking of block copolymers not in solution, but tethered to the surface of silica particles, as is summarised schematically in Figure 4.8.[56]
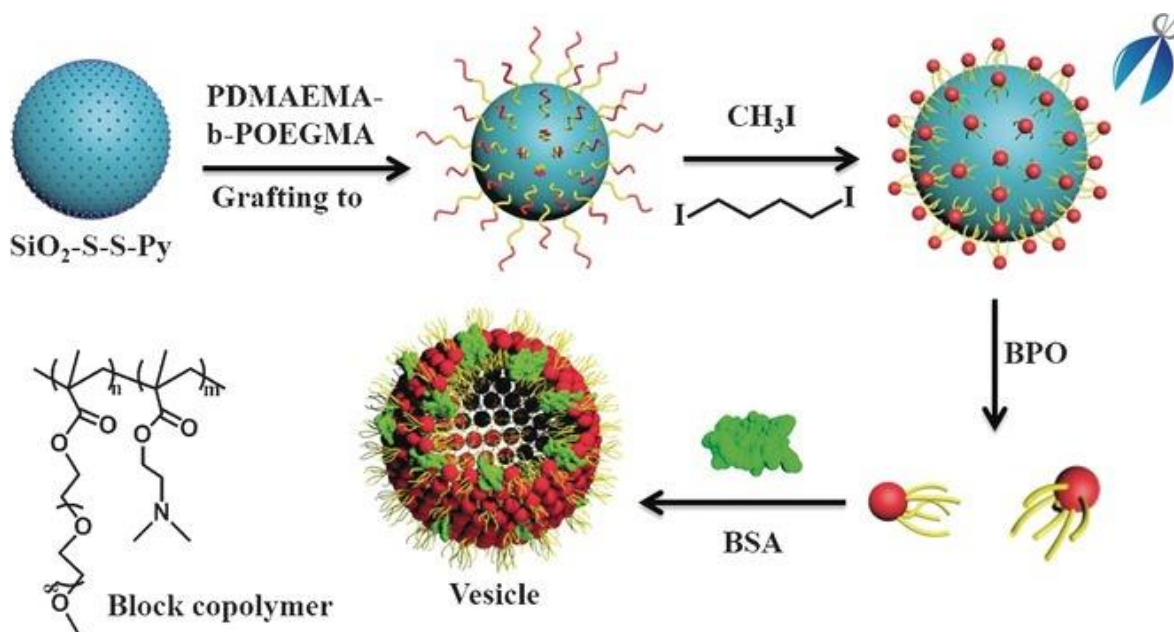
Figure 4.8: Scheme used for the preparation of pinned micelles on silica particles and their subsequent co-assembly with BSA protein. Reprinted with permission under the Creative Commons Attribution License from reference[56]

A following paper from the same group described the preparation of block copolymers of PDMAEMA with poly(oligo(ethylene glycol) monomethyl ether methacrylate) (PDMAEMA-*b*-POEGMA) by RAFT polymerisation.[57] They then covalently tethered the block copolymers to the surface of silica particles to form PDMAEMA-*b*-POEGMA block copolymer brushes (with POEGMA at the silica surface) attached by a thiol-disulphide exchange reaction in THF. Following this, the PDMAEMA was partially quaternised with methyl iodide and core-crosslinked with 1,4-diiodobutane to form 'pinned micelles' (*s*-micelles), which resulted in fused silica particles, as shown by SEM imaging. The crosslinked s-micelles were then cleaved from the surface by a reaction with benzoyl peroxide (BPO) which induced the formation of 'patchy' spherical micelles in THF with a small diameter (<5 nm), as proven by TEM imaging. The crosslinked micelles were then re-dispersed into a (10:1) THF:water solvent mixture leading to assembly of the micelles themselves to reversibly form vesicles for their eventual use in a study in which they were subjected to ultrasound irradiation to show reversible dissociation of the vesicles. Whilst this paper demonstrates the use of quaternisation to self-assemble and crosslink block copolymer brushes into pinned micelles, it is believed that quaternisation has not previously been used to self-assemble free block copolymers *in-situ* before now.

Moreover, the group did not investigate the preparation of micelles with different morphologies, as this was not the focus of the study. In this regard, QISA of a single PI-*b*-PDMAEMA block copolymers in THF is unique because the free polymers can be self-assembled into spherical micelles, wormlike micelles, or vesicles by a simple variation in the degree of quaternisation with ethyl iodide.

There are also further reports describing the quaternisation of PDMAEMA-based block copolymers in solution, however, no observation of self-assembly was mentioned. Most notably, Baines *et al.* reported the preparation, by group transfer polymerisation, of diblock copolymers of PDMAEMA with different alkyl methacrylates.[23] The PDMAEMA block was subsequently quaternised with methyl iodide in THF. The resulting block copolymers were self-assembled in water to measure the surface tensions and particle size. This paper reports that the quaternised block copolymer was insoluble in organic solvents such as methanol and THF and mentions that the polymers precipitated from solution during the quaternisation reaction. There are a number of possible reasons why the quaternised PDMAEMA-alkyl methacrylate block copolymers precipitated from solution rather than undergoing self-assembly. Firstly, the block copolymer solution concentration during the quaternisation reaction (which is not explicitly mentioned in the paper) may have been relatively high compared to the 1 wt% concentration used in the current study. High concentrations/solids contents have been reported previously to cause difficulties in the self-assembly of certain block copolymers.[58] Secondly, the unquaternised PDMAEMA-*b*-PMMA block copolymers had a different composition and molar mass to those used in the current study. Not only was the total molar mass significantly higher, > 30000 g mol^{-1} c.f 7390 g mol^{-1} for the PI-*b*-PDMAEMA studied here, but in the previous study, all the (insoluble) block copolymers had a much higher mole fraction of PDMAEMA than the PI-*b*-PDMAEMA used here – 61-81 mol% c.f. 46 mol%. Quaternisation of the (major) PDMAEMA block would undoubtedly have a more dramatic impact upon the solubility of the resulting block copolymer. Self-assembled structures would likely not be stabilised by the much shorter (soluble) alkyl methacrylate block resulting in precipitation. Finally, the use of methyl iodide differs to the use of ethyl iodide and the degree of quaternisation was reported as 'near-quantitative' in comparison to a maximum of 27 mol% in the current

study. Quantitative quaternisation was achieved because of the fast rate of reaction for methyl iodide and also because a 3-mol excess (w.r.t. DMAEMA) of methyl iodide was used.

A similar study by Sentoukas *et al*. reported the preparation of PDMAEMA-*b*-PHPMA block copolymers, also for self-assembly in water.[59] They also quaternised the block copolymers quantitatively with methyl iodide in THF at a polymer solution concentration of 2 wt%. However, Sentoukas made no mention of precipitation or any change in the physical properties during the quaternisation reaction. To the best of our knowledge, we maintain that the results described above are the first reported example of quaternisation-induced self-assembly in solution, whereby the degree of quaternisation not only induces self-assembly, but also dictates the nature of the self-assembled morphology.

The variation in self-assembled morphologies, arising due to QISA of PI_{37b}-*b*-$PDMAEMA_{35}$ with ethyl iodide, enables the construction of a crude phase diagram. The phase diagram in Figure 4.9 shows the different phases that emerge with varying degree of quaternisation with ethyl iodide during QISA at solids content of 1 wt% in THF.
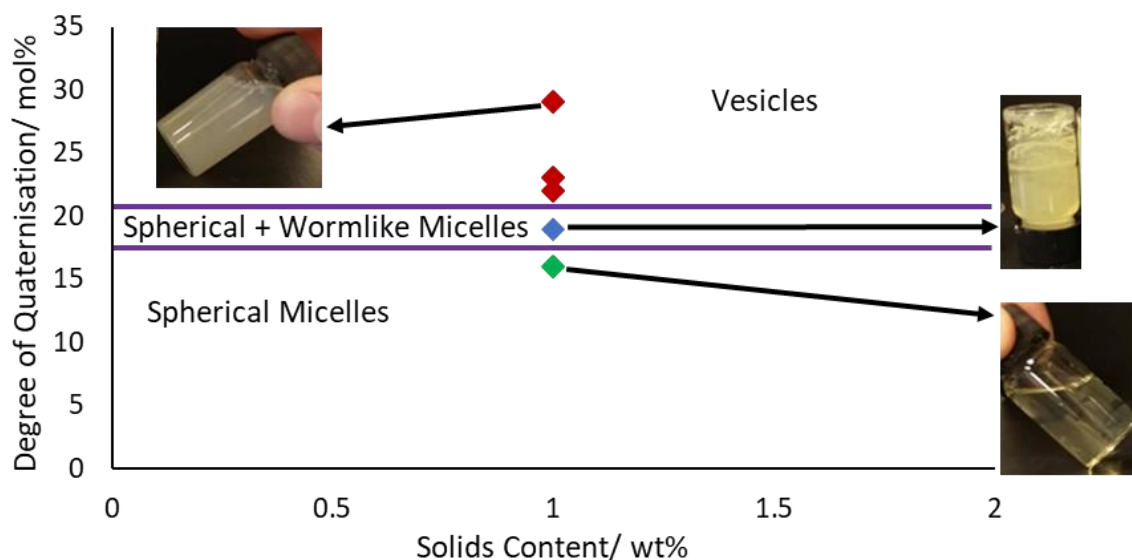
Figure 4.9: Phase diagram generated for the quaternisation-induced self-assembly (QISA) of PI_{37b}-b-$PQDMAEMA_{35}$(EI-X%) in THF. For all dispersions, the solids content is that of the quaternisation reactions carried out (≈1 wt%)

The diagram is profoundly under-populated, particularly with respect to the solids content on the x-axis because the reactions were only carried out at 1 wt%. It would obviously be desirable to carry out a more thorough investigation by varying the wt% of polymer used for the quaternisation reaction. This would possibly cause different physical

structures to emerge, particularly for the mixed wormlike/spherical micelles phase and for the vesicles phase which have previously been shown to form strong, self-supporting gels at solids contents ≥10 wt%. However, the morphology of micelles formed at higher solids content would most likely be similar to that of the block copolymers at 1 wt% shown in Figure 4.9, but with pure rather than mixed phases.

Parallels can be drawn between the observed variation in morphology of self-assembled PI_{37b}-*b*-$PQDMAEMA_{35}$(EI) as a function of degree of quaternisation and the variation in the self-assembly in *n*-decane of PI-*b*-PMMA (Chapter 3) and PI-*b*-PDMAEMA (Figure 4.3), as a function of the DP of the insoluble, core-forming methacrylate block. In this case, the degree of quaternisation appears to induce the formation of micelles with all different morphologies. The remarkable ability of a single block copolymer to form all of the characteristic phases of self-assembled block copolymers at room temperature appears to be unique. This provides more evidence for QISA being directly related to variation in the Israelachvili packing parameter which, in itself, is strong evidence for self-assembly behaviour.[8]

The quaternisation in THF of PI_{37b}-*b*-$PDMAEMA_{35}$ was also carried out (in an identical fashion) using 1-butyl iodide and 1-octyl iodide. However, PI_{37b}-*b*-$PQDMAEMA_{35}$(BI), with degrees of quaternisation in the range of 10-27 mol% and PI_{37b}-*b*-$PQDMAEMA_{35}$(OI) in the range 8-19 mol% showed no obvious differences in physical properties during the quaternisation reaction. The solutions remained as transparent, yellow liquids throughout. Although time did not allow for any characterisation of these solutions by TEM or DLS, one might speculate that either self-assembly into spherical micelles or no self-assembly at all occurred. Previously, the self-assembly of PI-*b*-PDMAEMA and block copolymers in *n*-decane to form spherical micelles resulted in transparent free-flowing liquids (see Figure 4.3). A simple DLS measurement for these solutions should be suitable for determining if there are or are not self-assembled particles present in the free-flowing liquids, or if the block copolymers are acting as free polymer chains in solution. The second potential reason for the dispersion forming a free-flowing liquid is that there was not self-assembly during quaternisation with the longer alkyl halides. As hypothesised previously, the longer alkyl chain attached to the nitrogen (i.e., butyl and octyl rather than ethyl) will impact upon the solubility of the quaternised block

due to a decrease in charge density of the quaternised block, which in turn could explain why, upon quaternisation, the PQDMAEMA remained soluble in THF and the diblock copolymer will remain as free polymer in solution rather than self-assembled micelles.

As a technique, QISA clearly has similarities to polymerisation-induced self-assembly (PISA). A comparison of the two methods reveals benefits and limitations of each technique. PISA is highly versatile and robust to different solvents and monomers, particularly because of the different polymerisation mechanisms that have been used, including RAFT, ATRP and LAP.[38, 60, 61] QISA is less obviously versatile because of the need for a nitrogen-containing block that can be quaternised. Furthermore, in the current study, self-assembly was only demonstrated for block copolymers quaternised with ethyl iodide. It is possible that changes to the molar mass or composition of the block polymer before quaternisation, quaternisation agent and solvent polarity could result in self-assembly, however thus far QISA has only been demonstrated for a rather narrow set of system variables. Another potential constraint could be precipitation of the polymer upon quaternisation, as was previously reported by Baines *et al.* for PDMAEMA-*b*-PMMA block copolymers when quantitatively quaternised with methyl iodide in THF.[23] This would likely mean that the degree of quaternisation must also be carefully controlled to prevent precipitation in future studies.

However, the outstanding benefit of QISA in comparison to PISA is the ability to access different, self-assembled morphologies by a simple variation in the degree of quaternisation of a single block copolymer sample. This is a particularly useful feature of quaternisation reactions in general when compared to RDRP which are typically less predictable for precisely accessing target molecular weights.[34] Another advantage is the potential for complete conversion of the quaternisation reaction which, although not achieved in this study, can commonly be accomplished by raising the temperature of the reaction. RDRP reactions often do not reach 100 % conversion meaning that the self-assembled product has unreacted monomer present which can be extremely harmful to health, blocking commercialisation.[62]

4.2.4. Self-Assembly of PI-*b*-PQDMAEMA in *n*-Decane

As discussed in section 3.2.3, the quaternisation of PDMAEMA is expected to cause significant differences in the chemistry and volume of the core-forming block which, in turn are known to change the packing parameter.[8] This was unexpectedly shown during the quaternisation reactions in THF with ethyl iodide, which underwent quaternisation-induced self-assembly into micelles with different morphologies, as the degree of quaternisation increased from 16-27 mol%. Herein we describe the self-assembly behaviour of PI-*b*-PQDMAEMA samples in *n*-decane, which was achieved by re-dispersing the products of the quaternisation reactions described above, by a conventional solvent switching approach, whereby the samples were first dissolved in DCM, a common solvent for the constituent blocks.[15, 16] The precursor, (unquaternised) PI_{37b}-*b*-$PDMAEMA_{35}$ was also dispersed in *n*-decane for comparison. An image of the PI_{37b}-*b*-$PQDMAEMA_{35}$(OI) block copolymer dispersions, with varying degrees of quaternisation, in *n*-decane at 15 wt% is shown in Figure 4.10.
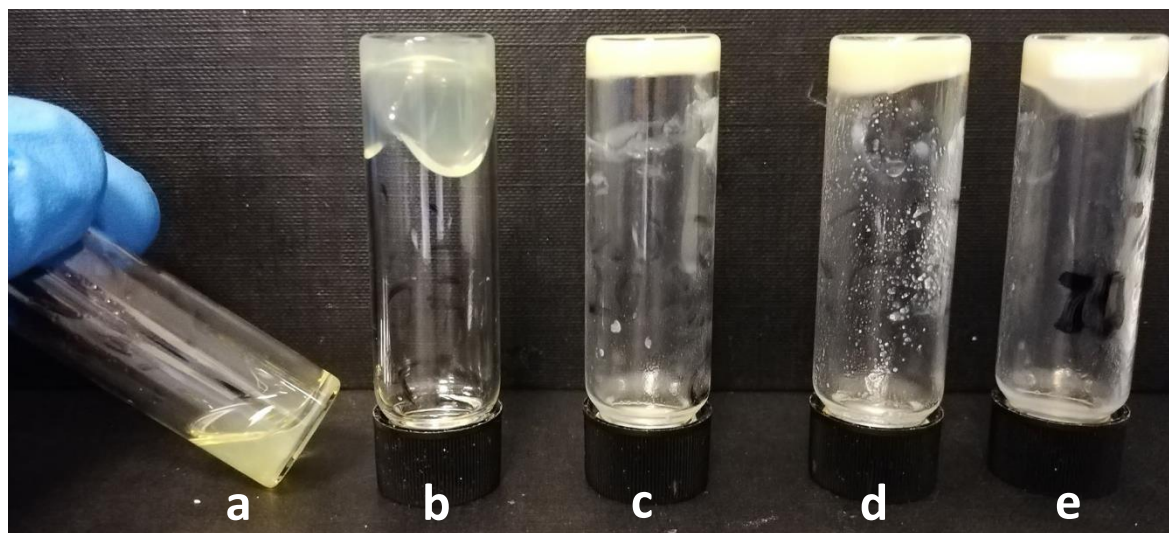
Figure 4.10: Image of PI_{37b}-b-$PQDMAEMA_{35}$(OI-X%) at 15 wt% in n-decane. For a-e: X = 8, 10, 12, 15 and 19 with respect to PDMAEMA in PI_{37b}-b-$PDMAEMA_{35}$

Figure 4.10a shows that PI_{37b}-*b*-$PQDMAEMA_{35}$(OI-8%) (where OI indicates quaternised with octyl iodide) formed a transparent free-flowing liquid, similar in nature to the unquaternised PI_{37}-*b*-$PDMAMEA_{38}$ self-assembled at 15 wt% in *n*-decane (see Figure 4.3). Upon increasing the degree of quaternisation to 10 mol%, the block copolymer dispersion forms a transparent gel (Figure 4.10b) which was similar in nature to the dispersion of PI_{37}-*b*-$PDMAEMA_{61}$. Finally, dispersions of the 3 polymers with degrees of

quaternisation of 12, 15 and 19 mol% (Figure 4.10c-e) all resembled opaque gels in *n*-decane, which is similar to that of the PI$_{37}$-*b*-PDMAEMA$_{77}$ dispersion. The described physical structures formed upon the dispersion of PI$_{37}$-*b*-PDMAEMA$_x$ in *n*-decane were previously imaged by TEM and were shown to be caused by self-assembly into different morphologies i.e., spherical micelles, wormlike micelles, and vesicles (see Figure 4.4). Dispersions of PI$_{37b}$-*b*-PDMAEMA$_{35}$, which formed a free-flowing liquid at 15 wt% in *n*-decane, and PI$_{37b}$-*b*-PQDMAEMA$_{35}$(OI-19%), which formed an opaque, self-supporting gel, were investigated by TEM; the images are shown below in Figure 4.11.
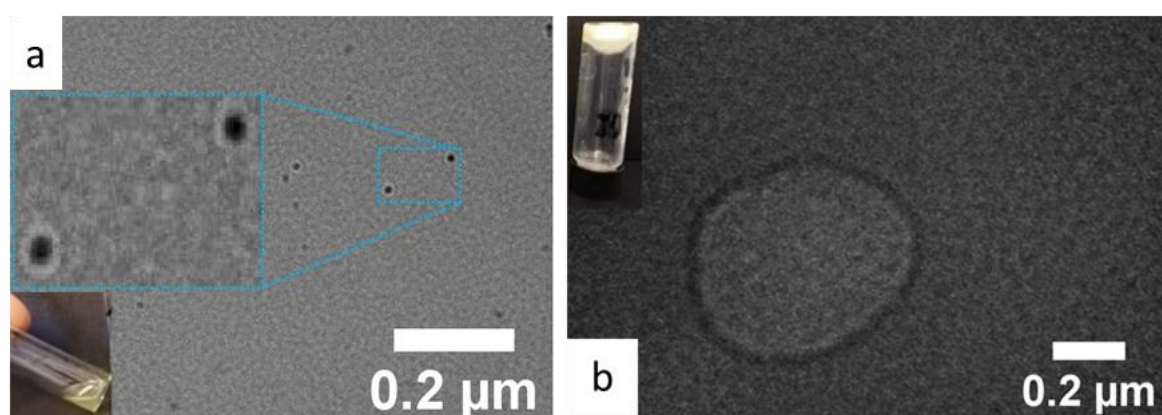
Figure 4.11: High resolution TEM images for the self-assembled morphologies of a: PI$_{37b}$-b-PDMAEMA$_{35}$ and b: PI$_{37b}$-b-PQDMAEMA$_{35}$(OI-19%) both at 15 wt % in n-decane (images inset of the respective free-flowing liquid and opaque gel formed). Scale bar = 200 nm.

The TEM images Figure 4.11 show a clear difference in morphology between the unquaternised PI$_{37b}$-*b*-PDMAEMA$_{35}$ (Figure 4.11a) and the quaternised PI$_{37b}$-*b*-PQDMAEMA$_{35}$(OI-19%) (Figure 4.11b) when self-assembled at 15 wt% in *n*-decane. Figure 4.11a shows that, before quaternisation, PI$_{37b}$-*b*-PDMAEMA$_{35}$ forms spherical micelles with a diameter of approximately 20 nm. This is (as expected) the same result as seen previously in TEM images of PI$_{37}$-*b*-PDMAEMA$_{35}$ (Figure 4.4), and the relatively small size of the spheres, which allows them to freely move past one another, explains why a free-flowing liquid is formed. Figure 4.11b shows that the opaque gel formed by PI$_{37b}$-*b*-PQDMAEMA$_{35}$(OI-19%) arises due to the formation of vesicles with a diameter of approximately 570 nm and a bilayer thickness of 30 nm. These vesicles are double the diameter of the vesicles formed upon self-assembly of PI$_{37}$-*b*-PDMAEMA$_{77}$, which also formed an opaque gel. The increase in size could be the result of the bulkier side groups

upon quaternisation with octyl iodide. The increased volume of the core-forming block upon quaternisation would result in an increase to the packing parameter, meaning that it could be further from the worm/vesicle phase boundary than previous examples. Bagheri *et al* have previously found that spherical micelles formed by poly(ethylene glycol-*block*-(*N*-2-benzoyloxypropyl methacrylamide)) (PEG-*b*-PHPMA-Bz) block copolymers in water increased in particle size from 9.2 to 28.2 nm, as evidenced by cryo-TEM images, as the molar mass of the core-forming PHPMA-Bz block increased from 2.2 to 18.5 kg mol^{-1}.[44] It is reasonable to assume that the effect of an increased packing parameter on particle size for spherical micelles, also applies to vesicles such as the one imaged above in Figure 4.11b. TEM images of the samples quaternised to 12 and 15 mol% with octyl iodide (which also both formed opaque gels) could prove which of these hypotheses is the case, however these were not obtained due to time constraints.

The TEM images in Figure 4.11 supports the hypothesis that quaternisation of the PDMAEMA, which changes the dimensions of the core-forming block, increases the packing parameter. In the case of quaternisation with octyl iodide, the morphology changes from spherical micelles to vesicles, which is indicative of an increased packing parameter. The observed morphologies, which correlate with and give rise to the physical structures (e.g., free flowing liquid, gel) seen for dispersions of the quaternised block copolymers are in excellent agreement with previous observations of self-assembled block copolymers discussed in this investigation and other literature reports.[38]

The confirmation by TEM of the fact that PI$_{37b}$-b-PDMAEMA$_{35}$ (free-flowing liquid) and PI$_{37b}$-b-PQDMAEMA$_{35}$(OI-19%) (opaque gels) arise due to the formation of spherical micelles and vesicles respectively, could suggest that the transparent gel formed by PI$_{37b}$-*b*-PQDMAEMA$_{35}$(OI-10%) (Figure 4.10) is made up of a different morphology of micelles. As previously mentioned, for PI-*b*-PMMA and PI-*b*-PDMAEMA, the transparent gel formed at intermediate DP of the core-forming block was shown to be made up of wormlike micelles. Therefore, the most likely conclusion would be that the transparent gel in Figure 4.10 is also made up of wormlike micelles. A phase diagram can be plotted for PI$_{37b}$-*b*-PQDMAEMA$_{35}$(OI) at varying solids contents. Previously, phase diagrams for self-assembled PI-*b*-PMMA and PI-*b*-PDMAEMA have been plotted with the degree of polymerisation of the insoluble core-forming methacrylate block on the y-axis. However, for this investigation

into the impact of the degree of quaternisation, the DP of each block is fixed and molar mass of the core forming block only varies as a function of the degree of quaternisation. Thus, the mol% of quaternisation with octyl iodide formed the y-axis in Figure 4.12.
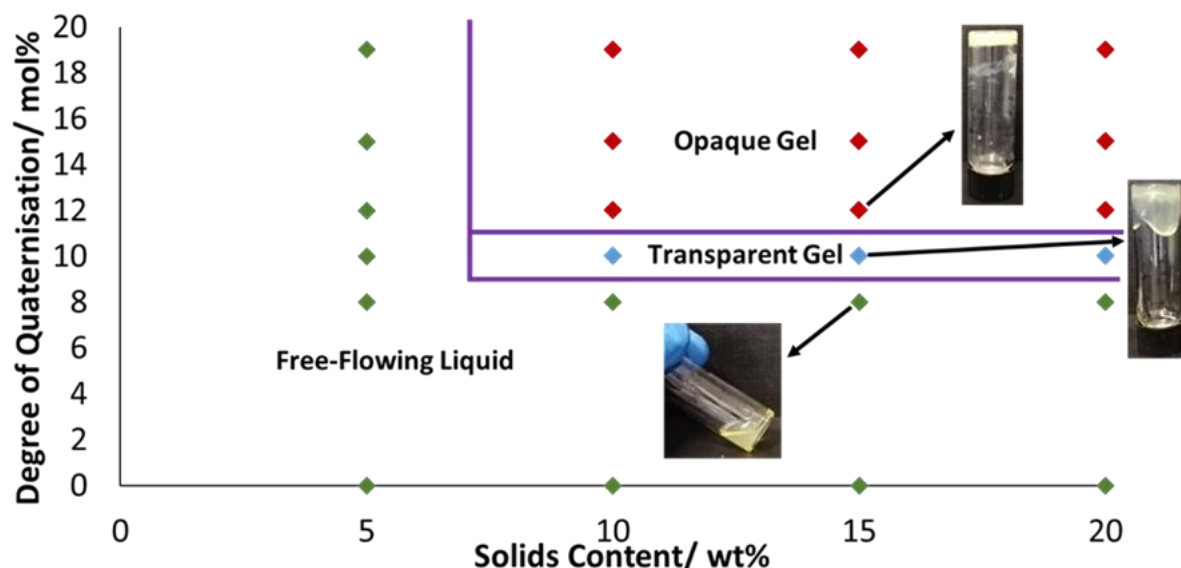
Figure 4.12: Phase diagram for the self-assembly in n-decane at varying solids content of PI$_{37b}$-b-PQDMAEMA$_{35}$(OI)

The phase diagram in Figure 4.12 for PI$_{37b}$-b-PQDMAEMA$_{35}$(OI) is similar to those that have previously been plotted in this investigation and most likely suggests that different morphologies can be achieved from a single block copolymer, simply by varying the degree of quaternisation. Similar behaviour was observed upon in-situ quaternisation-induced self-assembly of the same block copolymer, using ethyl iodide in THF, to give polymers with a degree of quaternisation from 16-27 mol% (see Figure 4.9). Previously, variable temperature rheology was used to show that the physical properties of all the different structures formed upon self-assembly differ greatly, which means that they can be useful for applications such as viscosity modifiers.[41] The quaternisation reaction can easily be carried out to different degrees of conversion which allows access to different self-assembled morphologies from a single block copolymer. The control of the quaternisation reaction could be improved further if the reaction were carried out in a good solvent for the quaternised PDMAEMA rather than becoming insoluble in THF. This could be particularly useful for accessing the transparent gel phase, typically made up of wormlike micelles, which often occupies a narrow parameter space in the phase diagram, as is also the case in Figure 4.12.[37, 63]

Recently, Ratcliffe *et al* have reported the formation of the 3 characteristic micellar morphologies from a single, thermoresponsive poly(*N*-(2-hydroxypropyl)methacrylamide)-*block*-(2-hydroxypropyl methacrylate) (PHPMAC-*b*-PHPMA) block copolymer self-assembled in aqueous solution.[64] At 50 °C, an opaque solution was formed, which was found by TEM to be made up of vesicles. This solution was cooled to 22 °C resulting in a transformation into a soft gel made up of wormlike micelles and then into a slightly turbid fluid formed by spherical micelles at 4 °C. Variable temperature ^{1}H NMR was used to show that this behaviour was caused by partial solvation of the core-forming PHPMA block upon heating. A unique feature of the study was the results of variable-temperature rheology which showed a peak in the viscosity (*type of viscosity not specified in the paper*) at 14 °C, approximately 2 orders of magnitude above a flat baseline on either side of the peak. This is strongly characteristic of the formation of wormlike micelles, resulting in an entangled network and a viscous dispersion. The discrepancy between the formation of wormlike micelles (22 °C) and the peak in the viscosity (14 °C) was ascribed to the slow kinetics of forming wormlike micelles from spherical micelles. The authors pointed out that hysteresis was achieved by heating, albeit on long timescales, however, the data were not included in the report. In comparison, an advantage to the quaternisation technique for preparing different morphologies from a single block polymer is that the different morphologies are accessible at room temperature which could be advantageous in applications where the temperature must remain constant.

Following the investigation into the self-assembly of PI$_{37b}$-*b*-PQDMAEMA$_{35}$(OI) in *n*-decane, PI$_{37b}$-*b*-PQDMAEMA$_{35}$(EI) and PI$_{37b}$-*b*-PQDMAEMA$_{35}$(BI) block copolymers were also dispersed in *n*-decane. Photographs for the dispersions at 15 wt% in *n*-decane are shown in Figure 4.13a and b respectively. Figure 4.13a1 also shows (unquaternised) PI$_{37b}$-*b*-PDMAEMA$_{35}$ dispersed at 15 wt% in *n*-decane which formed a free-flowing liquid.
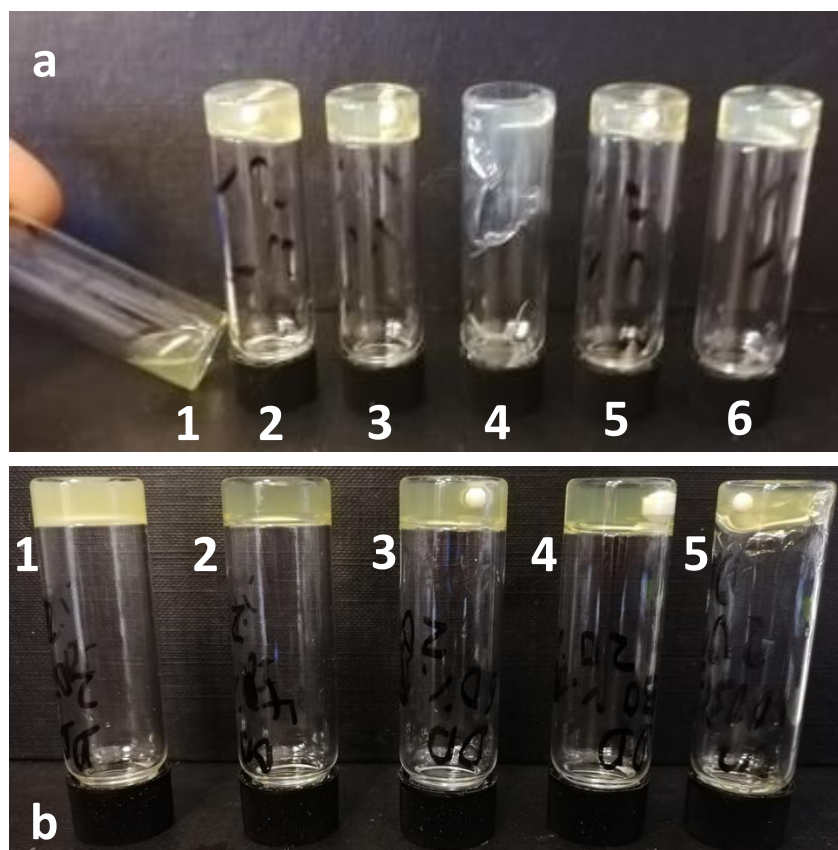
Figure 4.13: Images of a) PI$_{37b}$-b-PQDMAEMA$_{35}$(EI-X%) and b) PI$_{37b}$-b-PQDMAEMA$_{35}$(BI-Y%) all dispersed at 15 wt% in n-decane From left to right: X = 0, 16, 19, 25, 26 and 27 and Y = 10, 21, 22, 25, 27

When quaternised with ethyl iodide to 16 mol% w.r.t. PDMAEMA, the resulting block copolymer formed a transparent self-supporting gel when in *n*-decane at 15 wt% (Figure 4.13a2). The transition from free-flowing liquid to gel upon quaternisation to 16 mol% suggests a different self-assembled morphology following quaternisation compared to the unquaternised PI$_{37b}$-*b*-PDMAEMA$_{35}$ block copolymer (Figure 4.13a1) . The change in physical properties of the dispersion upon quaternisation could be a result of the increase in molar mass of the core-forming PDMAEMA block arising from quaternisation or reduced solubility of the cationic polyelectrolyte in the non-polar solvent. Either of these changes could result in a change in morphology of the micelles, most likely to wormlike micelles which would typically be expected to result in a transparent gel. This is consistent with the Israelachvili packing parameter.

Further to the discussion related to PI$_{37b}$-*b*-PQDMAEMA$_{35}$(EI), the vials in Figure 4.13b also show that the dispersions of PI$_{37b}$-*b*-PQDMAEMA$_{35}$(BI), quaternised to varying extents from 10-27 mol% all formed transparent gels. This is consistent with the result seen

for PI$_{37b}$-*b*-PQDMAEMA$_{35}$(EI) (Figure 4.13) and suggests that the dimensions and/or chemistry of the core-forming block do not change significantly between having a butyl or ethyl group. Assuming that these transparent gels are the result of self-assembly into wormlike micelles, as might be expected from previous results, it would be of interest to investigate whether the dimensions of the worms differ significantly either as a function of degree of quaternisation and/or the nature of the quaternisation agent. The effect of increased DP of the core-forming block on the particle size of spherical micelles has previously been explored by Sugihara *et al*. for poly(2-(methacryloyloxy)ethylphosphorylcholine-*block*-2-hydroxypropyl methacrylate) (PMPC-*b*-PHPMA) block copolymers dispersed in water at 10 wt%. By maintaining a constant DP for PMPC of 25, they showed by DLS and TEM that an increase in DP$_{PHPMA}$ from 100 to 400 resulted in an increase in the diameter of micelles from 12 to 58 nm, respectively.[51]

The quaternisation reaction with different alkyl iodides has been shown to result in significant differences in the physical structures formed at similar degrees of quaternisation because of the different alkyl chain lengths attached to the core-forming methacrylate. Therefore, an additional phase diagram has been plotted below in Figure 4.14 to illustrate these changes - in this case the y-axis is the molar mass of the alkyl group of the alkyl iodide.
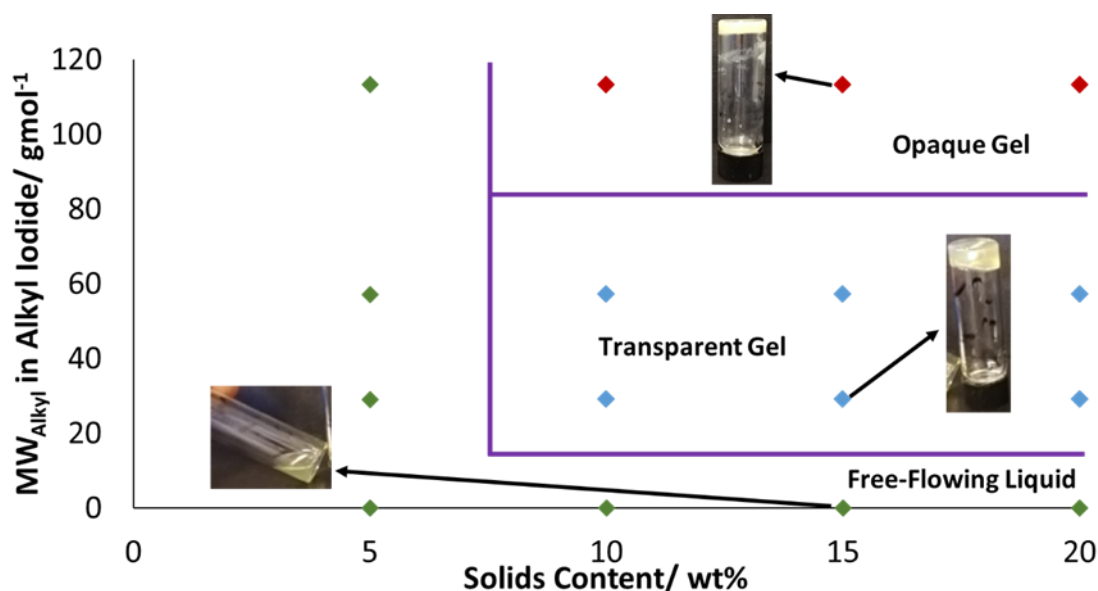
Figure 4.14: Phase diagram generated for the PI$_{37b}$-b-PQDMAEMA$_{35}$ at varying molecular weight of the alkyl in alkyl iodides and solid content of the self-assembly in n-decane at a similar degree of quaternisation (16, 10 and 12 mol %, respectively)

The phase diagram in Figure 4.14 looks very similar to the previous phase diagrams where the y-axes had DP$_{PDMAEMA}$ (Figure 4.3) and mol% quaternisation with octyl iodide (Figure 4.12), in that free-flowing liquids transition to transparent gels and opaque gels as the y-axis value is increased. Figure 4.14 can be used to infer that different alkyl iodides react with PDMAEMA to give polymers with significantly different dimensions, which in turn self-assemble into different morphologies in agreement with the concept of the Israelachvili packing parameter.[8] However, it should also be considered that the samples highlighted in Figure 4.14 do have slightly different degrees of quaternisation (16, 10 and 12 mol% for EI, BI and OI respectively). We have shown previously in Figure 4.12 that small changes in the degree of quaternisation with the same alkyl iodide can result in different physical structures forming, so it should be taken into account that the slight differences for these samples may be the sole cause of the different physical structures forming.

4.3. Conclusions

In conclusion, the preparation and self-assembly of PI-*b*-PDMAEMA block copolymers has been extensively studied. Previously, self-assembled PDMAEMA-based block copolymers have predominantly been studied in aqueous and/or polar media however, in the current study, poly(isoprene-*block*-(*N,N*-(dimethylamino)ethyl methacrylate (PI-*b*-PDMAEMA) block copolymers were self-assembled into non-polar solvents for self-assembly investigations. PI-*b*-PDMAEMA was prepared by a change of mechanism polymerisation (CHOMP) procedure in which bromide-end-capped polyisoprene was synthesised by living anionic polymerisation. This was then used as a macroinitiator for the ATRP of DMAEMA to prepare a homologous series of well-controlled block copolymers with a fixed molecular weight of the soluble, PI block. The PI-*b*-PDMAEMA block copolymers were re-dispersed into *n*-decane, a selective solvent for the PI block, by solvent switching and found to self-assemble into micelles. The polymers were imaged by TEM which showed that the morphology of the micelles varied depending on the molecular weight of the insoluble, core-forming PDMAEMA block.

Following on from the investigation of PI-*b*-PDMAEMA block copolymers, the amine of the methacrylate was quaternised with different alkyl iodides at varying mol% with respect to PDMAEMA. During the quaternisation of PI-*b*-PDMAEMA in THF with ethyl iodide, a range of physical structures including gels and turbid liquids was found to form *in*

situ in THF. These structures were analysed by TEM and found to be caused by self-assembly into different morphologies. This is believed to be the first example of a quaternisation-induced self-assembly (QISA). QISA could offer several benefits over the more conventional polymerisation-induced self-assembly (PISA), including the simplicity of the reaction and high degree of control which can be achieved by varying the target degree of quaternisation. QISA was not observed during the quaternisations of PI-*b*-PDMAEMA with butyl iodide or octyl iodide which suggests that the reagents with which QISA can take place may occupy a narrow window. However, the morphology formed upon QISA may also be shown to be tailorable by making tweaks to the molar mass and/or composition of the PI-*b*-PDMAEMA block copolymer or using different alkyl iodides at varying degrees of quaternisation.

The PI-*b*-PQDMAEMA block copolymers were subsequently re-dispersed in *n*-decane, as was done with the unquaternised analogues, to explore the potential for self-assembly. Remarkably, quaternisation was shown to cause significant changes in self-assembly behaviour with morphologies of a higher packing parameter (i.e., wormlike micelles and vesicles) being formed, in comparison to the unquaternised PI-*b*-PDMAEMA. This was particularly evident for sample quaternised with octyl iodide, with all 3 characteristic physical structures being observed with varying mol% quaternisation. TEM was used to show that for 1 of the opaque gels, the quaternisation caused a change in the morphology from spherical micelles to vesicles. So far, the effect of quaternisation changing the morphology of PI-*b*-PDMAEMA upon self-assembly in *n*-decane has been proven for 1 PI-*b*-PDMAEMA block copolymer. It would be expected for different block copolymers to show similar changes in the self-assembly behaviour following quaternisation with alkyl iodides.

4.4. References

1. S. Agarwal, Y. Zhang, S. Maji, A. Greiner, *Mater. Today*, 2012, **15**, 388-393.
2. Y. L. Lo, G. J. Chen, T. H. Feng, M. H. Li, L. F. Wang, *RSC Adv.*, 2014, **4**, 11089-11098.
3. J. Y. Zheng, M. J. Tan, P. Thoniyot, X. J. Loh, *RSC Adv.*, 2015, **5**, 62314-62318.
4. Q. F. Xiong, P. H. Ni, F. Zhang, Z. Q. Yu, *Polym. Bull.*, 2004, **53**, 1-8.
5. S. B. Lee, A. J. Russell, K. Matyjaszewski, *Biomacromolecules*, 2003, **4**, 1386-1393.
6. J.-F. Gohy, S. Antoun, R. Jérôme, *Macromolecules*, 2001, **34**, 7435-7440.
7. S. Antoun, J. S. Wang, R. Jerome, P. Teyssie, *Polymer*, 1996, **37**, 5755-5759.
8. J. N. Israelachvili, D. J. Mitchell, B. W. Ninham, *J. Chem. Soc. Faraday Trans.*, 1976, **72**, 1525-1568.
9. S. P. Moulik, M. E. Haque, P. K. Jana, A. R. Das, *J. Phys. Chem.*, 1996, **100**, 701-708.
10. S. Soltanahmadi, A. Morina, M. C. P. van Eijk, I. Nedelcu, A. Neville, *J. Phys. D-Appl. Phys.*, 2016, **49**, 505302-505317.
11. S. Soltanahmadi, E. A. Esfahani, I. Nedelcu, A. Morina, M. C. P. van Eijk, A. Neville, *Tribol. Lett.*, 2019, **67**, 80-94.
12. J. Fan, M. Muller, T. Stohr, H. A. Spikes, *Tribol. Lett.*, 2007, **28**, 287-298.
13. M. Muller, K. Topolovec-Miklozic, A. Dardin, H. A. Spikes, *Tribol. Trans.*, 2006, **49**, 225-232.
14. Y. Shen, S. Zhu, F. Zeng, R. Pelton, *Macromolecules*, 2000, **33**, 5399-5404.
15. Y. Y. Mai, A. Eisenberg, *Chem. Soc. Rev.*, 2012, **41**, 5969-5985.
16. G. Riess, *Prog. Polym. Sci.*, 2003, **28**, 1107-1170.
17. J. Clayden, N. Greeves, S. Warren, *Organic Chemistry*, OUP Oxford, 2012.
18. T. Manouras, E. Koufakis, S. H. Anastasiadis, M. Vamvakaki, *Soft Matter*, 2017, **13**, 3777-3782.
19. Y. F. Pan, Q. Y. Xia, H. N. Xiao, *Polymers*, 2019, **11**, 1283-1298.
20. Y. H. Fu, C. L. Lin, L. F. Chen, Y. Song, H. C. Ma, *Preparation of Cationic Rice Husk Flocculant and its flocculating characteristics*, Trans Tech Publications Ltd, Stafa-Zurich, 2012.
21. M. H. Acar, K. Matyjaszewski, *Macromol. Chem. Phys.*, 1999, **200**, 1094-1100.
22. T. X. Song, Y. Li, C. Q. Zhang, A. L. Zhang, X. H. Wang, Y. R. Wang, *Acta Polym. Sin.*, 2010, **10**, 143-148.
23. F. L. Baines, N. C. Billingham, S. P. Armes, *Macromolecules*, 1996, **29**, 3416-3420.
24. M. Hillmyer, *Curr. Opin. Solid State Mat. Sci.*, 1999, **4**, 559-564.
25. S. Mahajan, B. K. Cho, A. Allgaier, L. J. Fetters, G. W. Coates, U. Wiesner, *Macromol. Rapid Commun.*, 2004, **25**, 1889-1894.
26. J. D. Tong, S. R. Ni, M. A. Winnik, *Macromolecules*, 2000, **33**, 1482-1486.
27. W. A. Braunecker, K. Matyjaszewski, *Prog. Polym. Sci.*, 2007, **32**, 93-146.
28. W. A. Braunecker, K. Matyjaszewski, *J. Mol. Catal. A-Chem.*, 2006, **254**, 155-164.
29. J. Lad, S. Harrisson, G. Mantovani, D. M. Haddleton, *Dalton Transactions*, 2003, 4175-4180.
30. F. Zeng, Y. Shen, S. Zhu, R. Pelton, *Macromolecules*, 2000, **33**, 1628-1635.
31. W. Tang, Y. Kwak, W. Braunecker, N. V. Tsarevsky, M. L. Coote, K. Matyjaszewski, *J. Am. Chem. Soc.*, 2008, **130**, 10702-10713.
32. Y. W. Pei, A. B. Lowe, *Polym. Chem.*, 2014, **5**, 2342-2351.
33. D. Benoit, V. Chaplinski, R. Braslau, C. J. Hawker, *J. Am. Chem. Soc.*, 1999, **121**, 3904-3920.

34. K. Matyjaszewski, T. P. Davis, *Handbook of Radical Polymerization*, Wiley, Hoboken, 2003.
35. R. A. Cordeiro, N. Rocha, J. P. Mendes, K. Matyjaszewski, T. Guliashvili, A. C. Serra, J. F. J. Coelho, *Polym. Chem.*, 2013, **4**, 3088-3097.
36. Y. T. Li, S. P. Armes, *Angew. Chem.-Int. Edit.*, 2010, **49**, 4042-4046.
37. A. Blanazs, A. J. Ryan, S. P. Armes, *Macromolecules*, 2012, **45**, 5099-5107.
38. L. P. D. Ratcliffe, B. E. McKenzie, G. M. D. Le Bouedec, C. N. Williams, S. L. Brown, S. P. Armes, *Macromolecules*, 2015, **48**, 8594-8607.
39. Y. Pei, L. Thurairajah, O. R. Sugita, A. B. Lowe, *Macromolecules*, 2015, **48**, 236-244.
40. S. L. Canning, V. J. Cunningham, L. P. D. Ratcliffe, S. P. Armes, *Polym. Chem.*, 2017, **8**, 4811-4821.
41. M. J. Derry, O. O. Mykhaylyk, S. P. Armes, *Angew. Chem.-Int. Edit.*, 2017, **56**, 1746-1750.
42. L. A. Fielding, J. A. Lane, M. J. Derry, O. O. Mykhaylyk, S. P. Armes, *J. Am. Chem. Soc.*, 2014, **136**, 5790-5798.
43. D. Zehm, L. P. D. Ratcliffe, S. P. Armes, *Macromolecules*, 2013, **46**, 128-139.
44. M. Bagheri, J. Bresseleers, A. Varela-Moreira, O. Sandre, S. A. Meeuwissen, R. M. Schiffelers, J. M. Metselaar, C. F. van Nostrum, J. C. M. van Hest, W. E. Hennink, *Langmuir*, 2018, **34**, 15495-15506.
45. M. A. De Jesús-Téllez, D. M. Sánchez-Cerrillo, P. Quintana-Owen, U. S. Schubert, D. Contreras-López, C. Guerrero-Sánchez, *Macromol. Chem. Phys.*, 2020, **221**, 1900543-1900549.
46. B. Bolto, J. Gregory, *Water Res.*, 2007, **41**, 2301-2324.
47. G. Couture, A. Alaaeddine, F. Boschet, B. Ameduri, *Prog. Polym. Sci.*, 2011, **36**, 1521-1557.
48. W. Jaeger, J. Bohrisch, A. Laschewsky, *Prog. Polym. Sci.*, 2010, **35**, 511-577.
49. R. J. Bruessau, *Makromol. Chem., Macromol. Symp.*, 1992, **61**, 199-218.
50. S. Sugihara, A. Blanazs, S. P. Armes, A. J. Ryan, A. L. Lewis, *J. Am. Chem. Soc.*, 2011, **133**, 15707-15713.
51. M. J. Derry, L. A. Fielding, S. P. Armes, *Polym. Chem.*, 2015, **6**, 3054-3062.
52. J. R. Howse, R. A. L. Jones, G. Battaglia, R. E. Ducker, G. J. Leggett, A. J. Ryan, *Nat. Mater.*, 2009, **8**, 507-511.
53. C. Gonzato, M. Semsarilar, E. R. Jones, F. Li, G. J. P. Krooshof, P. Wyman, O. O. Mykhaylyk, R. Tuinier, S. P. Armes, *J. Am. Chem. Soc.*, 2014, **136**, 11100-11106.
54. W. Zhou, Q. Qu, Y. Xu, Z. An, *ACS Macro Lett.*, 2015, **4**, 495-499.
55. W. J. Fan, L. Liu, H. Y. Zhao, *Angew. Chem.-Int. Edit.*, 2017, **56**, 8844-8848.
56. Y. Zhao, W. Fan, H. Zhao, *Mater. Chem. Front.*, 2019, **3**, 606-614.
57. B. Y. Shi, H. Zhang, Y. Liu, J. Wang, P. Zhou, M. Y. Cao, G. W. Wang, *Macromol. Rapid Commun.*, 2019, **40**, 9.
58. T. Sentoukas, S. Pispas, *J. Polym. Sci. Pol. Chem.*, 2018, **56**, 1962-1977.
59. M. Semsarilar, E. R. Jones, A. Blanazs, S. P. Armes, *Adv. Mater.*, 2012, **24**, 3378-3382.
60. M. J. Derry, L. A. Fielding, S. P. Armes, *Prog. Polym. Sci.*, 2016, **52**, 1-18.
61. S. Perrier, *Macromolecules*, 2017, **50**, 7433-7447.
62. A. P. Lopez-Oliva, N. J. Warren, A. Rajkumar, O. O. Mykhaylyk, M. J. Derry, K. E. B. Doncom, M. J. Rymaruk, S. P. Armes, *Macromolecules*, 2015, **48**, 3547-3555.
63. L. P. D. Ratcliffe, M. J. Derry, A. Ianiro, R. Tuinier, S. P. Armes, *Angew. Chem.-Int. Edit.*, 2019, **58**, 18964-18970.

5. Applications Testing of Polyisoprene-based Block Copolymers in Lubricant Formulations

5.1. Introduction

The use of copolymers as additives for lubricant formulations is common, with commercial products being widely used as viscosity modifiers, which offset the drop in viscosity experienced by the base oil as temperature increases during operation.[1-5] This helps to ensure a consistent performance of the lubricant over the full, operational temperature range. However, the use of copolymers as friction modifiers has been considerably less explored, perhaps because of the difficulties in preparing copolymers that are soluble in base oil whilst containing functional groups capable of binding to metal surfaces.[6, 7] The use of polymers as friction modifiers has several potential benefits such as low volatility and increased viscosity index. Generally, they are also benign to the environment, which is particularly important with ongoing environmental concerns over the presence of metals and high phosphorus levels due to the use of zinc dialkyldithiophosphate (ZDDP) as a friction modifiers in engine oils.[8-10] The use of polymeric friction modifiers (PFMs) offers the possibility for dual-functional lubricant additives that can act as a viscosity and friction modifiers. This would be desirable because formulations currently contain many individual additives for addressing each requirement. A particular difficulty with having multiple additives in a formulation is that they have the ability to interact with each other in solution which can hinder performance, especially for friction modification where interaction with the metal surfaces is critical.[11, 12]

The polyisoprene-based block copolymers discussed in the preceding chapters offer potential because they have been shown to be dispersible in non-polar solvents such as *n*-decane but contain polar, heteroatom-containing functional groups which previously formed the core of self-assembled micelles. These heteroatom-containing functional groups have the potential to bind to metal surfaces, enabling the copolymer to reduce the friction between the sliding metal parts.

Previous reports have concluded that block copolymers containing strongly Lewis basic functional groups (e.g alcohols in poly(hydroxyethyl methacrylate) (PHEMA) and

amines in PDMAEMA) are effective as friction modifiers for metal surfaces.[13-16] However, the conclusions from these studies are limited in several ways. Firstly, the chemical structures of block copolymers are commonly constrained by the synthetic protocols that were used for their synthesis, typically RDRP. The polymerisation of non-polar dienes by RDRP is complicated by slow kinetics and poor control over the molar mass and dispersity of the polymer. The non-polar, lipophilic block for promoting solubility in base oil is therefore typically a long-chain methacrylate or acrylate. Secondly, the reported investigations into friction modification were carried out using neat solutions of the copolymers in base oil, rather than in full lubricant formulations. The performance of additives in neat base oil and full formulations is generally expected to differ greatly because of the (sometimes unfavourable) interactions with other, surface-active ingredients. In the current project, block copolymers were tested in both neat base oil for comparison with the academic literature and in full formulations to assess actual commercial potential.

Herein, block copolymers of PI-*b*-PMMA and PI-*b*-PDMAEMA were investigated as lubricant additives for friction modification by the use of a mini traction machine (MTM). The copolymers were initially tested in base oil as neat solutions, so as to remove the effect of the other additives present in full formulations. Following this, the block copolymers were tested in a variety of full formulations, including Motul 0W20, Motul 0W16, Motul 5W30 and Mobil Delvac 5W30. These formulations vary significantly, both in their ingredients and the typical end-use. The performance of the block copolymers in these standard lubricants will be compared against 'neat formulations' where no extra friction modifier is added and also against commercial friction modifiers to fully assess the performance against the state-of-the-art lubricant additives.

5.2. Results and Discussion

Non-polar, lipophilic homo- and copolymers have been used in lubricant formulations as viscosity modifiers for the past century.[1] Moreover, these viscosity modifiers can also have an appreciable effect as friction modifiers because of shear thinning during mechanical motion.[6, 7] Further to this, more polar, heteroatom-containing polymers have been shown by optical interferometry to form thick tribofilms on metal surfaces, which provide further friction reduction.[17, 18] Despite this, there are few

commercially-available heteroatom-containing PFMs, most probably because of the difficulties in preparing amphiphilic copolymers (on an industrial scale) that remain soluble in non-polar media.[19-21] This area is starting to gain more interest because of the massive potential of such additives, and the environmental restrictions of standard friction modifiers such as zinc dialkyldithiophosphates (ZDDP).[9] The recent development of RAFT-mediated PISA in non-polar solvents has offered some potential for the preparation of useful copolymers, however there are significant practical limitations for the scale-up to a commercial scale.[22, 23] The block copolymers described in the current Chapter were prepared by the same change-of mechanism polymerisation (CHOMP) process as described in Chapters 3 and 4. In this chapter, the testing of polyisoprene-based block copolymers for industrial applications will be discussed along with their potential as lubricant additives.

5.2.1. Poly(Isoprene-*block*-(methyl methacrylate)) (PI-*b*-PMMA) Copolymers for Friction Modification

In chapter 3, it was shown that PI-*b*-PMMA block copolymers self-assemble when dispersed in non-polar solvents such as *n*-decane. This dispersibility in non-polar media makes them suitable for use in lubricant oils where the solvent is a highly non-polar base oil. The lone pair of the oxygen of the carbonyl in the ester functionality of PMMA has the potential to bind to metal surfaces. At present, it is unclear if the PI-*b*-PMMA samples will self-assemble in base oil as was previously observed for *n*-decane, however the variation in block copolymer composition and total molar mass was previously shown to result in clear differences in the self-assembly behaviour and concurrent thermal properties. For this reason, a wide variety of samples was prepared and tested as friction modifiers in order to see if these properties also affect the lubrication performance.

5.2.1.1. Scale-up of Polymer Synthesis

PI-*b*-PMMA samples were prepared for applications testing by the same change of mechanism polymerisation (CHOMP) procedure, previously discussed in chapter 3, albeit scaled-up for the preparation of approximately 20 g batches, which were necessary for full applications testing. Similar results were observed for conversion, yield and dispersity in both polymerisation steps. Molar mass data for the PI-*b*-PMMA block copolymers are shown below in Table 5.3. An image of the polymers following their dispersion by solvent-switching in Yubase 4 at 5 wt% is shown below in Figure 5.1.

Table 5.3: Molar mass data for the first family of PI-b-PMMA block copolymers prepared by ATRP of MMA from PI-Br macroinitiators.

Sample	M_n/ kg mol^{-1}			Đ^d	wt% PI^e
	PI Block^a	PMMA Block^b	Total^c		
PI$_{29}$-*b*-PMMA$_{63}$	1.98	6.27	8.25	1.35	24
PI$_{29}$-*b*-PMMA$_{127}$	1.98	12.7	14.7	1.35	13
PI$_{29}$-*b*-PMMA$_{158}$	1.98	15.8	17.8	1.23	11
PI$_{79}$-*b*-PMMA$_{200}$	5.38	20.0	25.4	1.26	21
PI$_{79}$-*b*-PMMA$_{256}$	5.38	25.6	31.0	1.25	17
PI$_{79}$-*b*-PMMA$_{386}$	5.38	38.7	44.1	1.13	12
PI$_{147}$-*b*-PMMA$_{312}$	10.0	31.3	41.3	1.24	24

[a] M_n(PI) from triple detection SEC of PI sample from living anionic polymerisation of PI-*OH*
[b] M_n(PMMA) calculated from NMR spectra of PI-*b*-PMMA block copolymers using the same method described in chapter 3
[c] M_n(PI-*b*-PMMA) calculated from M_n(PI) + M_n(PMMA)
[d] Dispersity from triple detection SEC of PI-*b*-PMMA
[e] wt% PI calculated from M_n(PI)/M_n(PI-*b*-PMMA) x 100
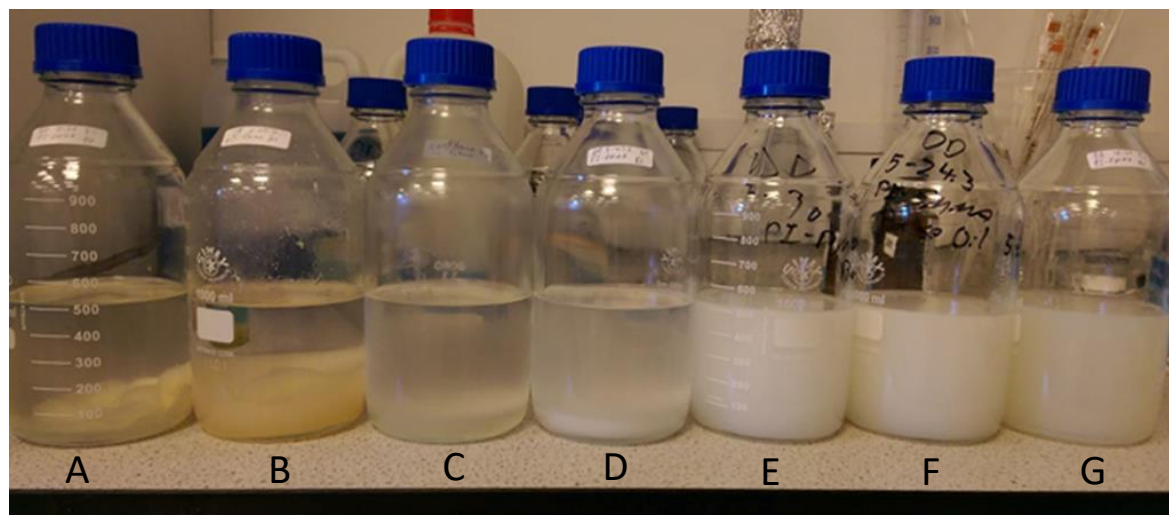
Figure 5.1: Images of PI-b-PMMA (from Table 5.3) dispersed in Yubase 4 at 5 wt% by solvent-switching. A: PI$_{29}$-b-PMMA$_{158}$, B: PI$_{29}$-b-PMMA$_{127}$, C: PI$_{79}$-b-PMMA$_{386}$, D: PI$_{29}$-b-PMMA$_{63}$, E: PI$_{79}$-b-PMMA$_{256}$, F: PI$_{79}$-b-PMMA$_{200}$, G: PI$_{147}$-b-PMMA$_{312}$

The data in Table 5.3 are for a family of PI-b-PMMA block copolymers with variations in the total molar mass of the block copolymer and the composition, and the image in Figure 5.1 shows each of these dispersed in Yubase 4 at 5 wt% by solvent-switching. However, Figure 5.1 shows that many of these block copolymers (PI$_{29}$-b-PMMA$_{158}$ (Figure 5.1A), PI$_{29}$-b-PMMA$_{127}$ (Figure 5.1B), PI$_{79}$-b-PMMA$_{386}$ (Figure 5.1C) and PI$_{29}$-b-PMMA$_{63}$ (Figure 5.1D)) were insoluble in Yubase 4. Interestingly, all block copolymers with $M_{n, PI}$ of 1.98 kg mol^{-1} were insoluble in Yubase 4 despite PI$_{29}$-b-PMMA$_{63}$ being 24 wt% PI, which is considerably higher than that of P$_{79}$-b-PMMA$_{256}$ (Figure 5.1E, 17 wt% PI) which was dispersed to give an opaque white liquid. This suggests that composition of PI-b-PMMA block copolymers is not the sole factor in determining if the block copolymer is dispersible, and that a higher molar mass of PI is needed to stabilise the PMMA block. For this reason, a new family of PI-b-PMMA block copolymers was prepared, where each had a comparatively higher molar masses of PI-Br macroinitiators. One of the key benefits of block copolymers, particularly in comparison to small molecule organic friction modifiers (OFMs), in lubricant formulations, is the ease with which the structure can be tailored. Even within the confines of two discrete, constituent polymer blocks, there are many properties that can be varied to obtain a broader picture of the performance of the block copolymers in applications, with a view towards optimisation. Within this study, several samples of PI-b-PMMA were prepared, to allow the observation of any potential correlation between structure and performance, with the following structural parameters being investigated:

- Varying total molar mass at constant mole fraction of blocks

- Varying molar mass of PI at constant molar mass of PMMA

- Varying molar mass of PMMA at constant molar mass of PI

The last of these is particularly straightforward when using a PI-macroinitiator of fixed molar mass - an approach previously exploited in chapter 3. The molar mass data for the PI-*b*-PMMA block copolymers used in this study are illustrated graphically in Figure 5.2 and tabulated values are shown in Table 5.4.
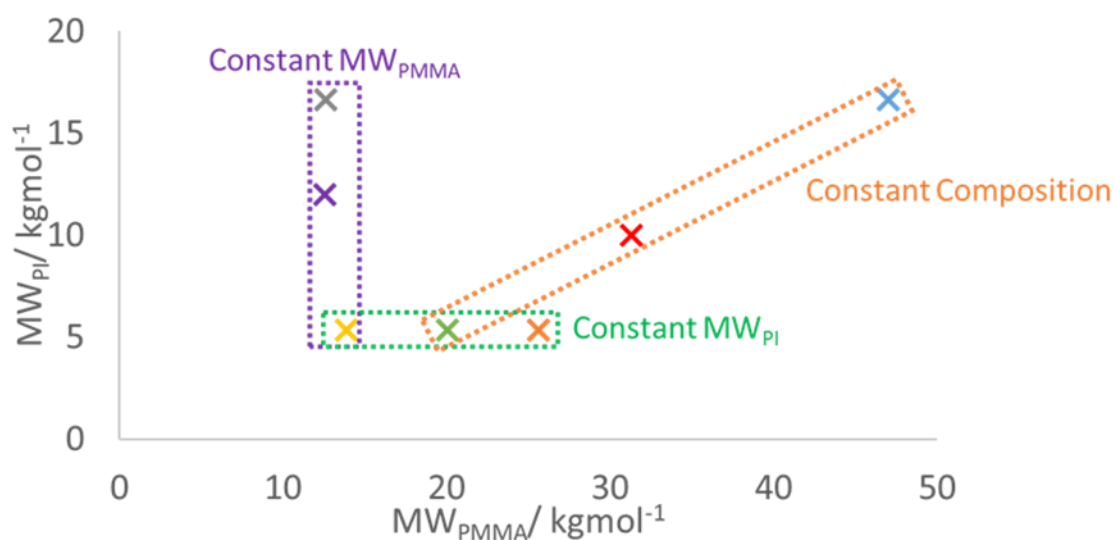
Figure 5.2: Graph showing the variation in molecular weight of PI and PMMA in PI-b-PMMA block copolymers prepared for application testing. Trends to be investigated highlighted in dashed boxes and labelled. Each sample numbered and colour-coded for future reference

Table 5.4: Molar mass data for the second family of PI-b-PMMA block copolymers prepared for applications

Sample	M_n/ kg mol^{-1}			$Đ$[d]	wt% PI[e]
	PI Block[a]	PMMA Block[b]	Total[c]		
PI$_{79}$-b-PMMA$_{138}$	5.38	13.8	19.2	1.29	28
PI$_{79}$-b-PMMA$_{200}$	5.38	20.0	25.4	1.26	21
PI$_{79}$-b-PMMA$_{256}$	5.38	25.6	31.0	1.25	17
PI$_{147}$-b-PMMA$_{312}$	10.0	31.3	41.3	1.24	24
PI$_{176}$-b-PMMA$_{125}$	12.0	12.5	24.5	1.31	49
PI$_{244}$-b-PMMA$_{131}$	16.6	13.1	29.7	1.25	56
PI$_{244}$-b-PMMA$_{469}$	16.6	47.0	63.6	1.16	26

[a] M_n(PI) from triple detection SEC of PI sample from living anionic polymerisation of PI-*OH*
[b] M_n(PMMA) calculated from NMR spectra of PI-*b*-PMMA block copolymers using the same method described in chapter 3
[c] M_n(PI-*b*-PMMA) calculated from M_n(PI) + M_n(PMMA)
[d] Dispersity from triple detection SEC of PI-*b*-PMMA
[e] wt% PI calculated from M_n(PI)/M_n(PI-*b*-PMMA) x 100

The data in Figure 5.2 and Table 5.4 show that for the 7 block polymers prepared, the 3 trends described above can be investigated drawn with 3 'data points' within each trend (as highlighted by the dotted boxes on the graph).

The PI-*b*-PMMA block copolymers reported in Figure 5.2 and Table 5.4 were dispersed at 5 wt% in Yubase 4, using solvent-switching, by first dissolving in DCM, a common solvent for both blocks, which was then removed by evaporation once added to the oil. For friction testing, the dispersions were diluted to 1 wt% with a further addition of base oil. Figure 5.3 shows a photograph of all dispersions of PI-*b*-PMMA at 5 wt% in Yubase 4, ordered with increasing PI content within the block copolymer.
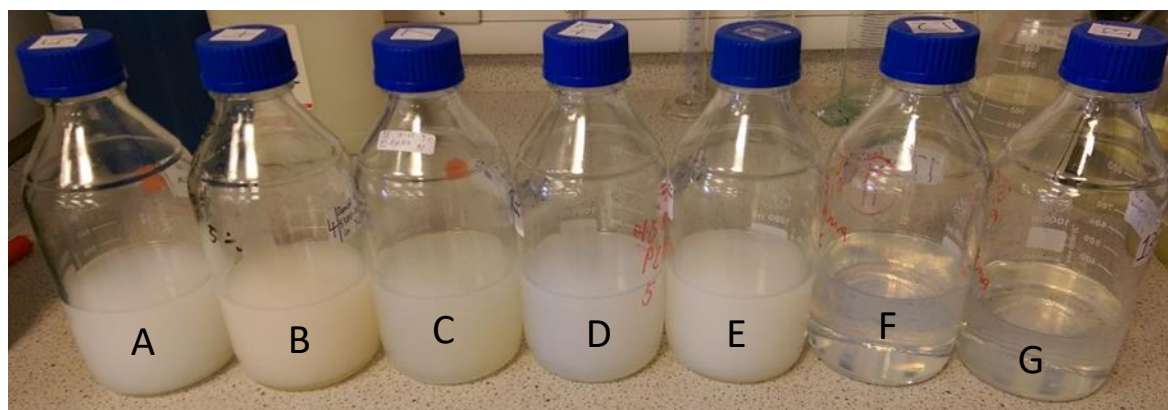
Figure 5.3: Photograph of PI-b-PMMA block copolymers described in Figure 5.2 and Table 5.4, dispersed at 5 wt% in Yubase 4 base oil. From left to right (the proportion of soluble polyisoprene in the block copolymers increases): A: PI_{79}-b-$PMMA_{256}$, B: PI_{79}-b-$PMMA_{200}$, C: PI_{147}-b-$PMMA_{312}$, D: PI_{244}-b-$PMMA_{469}$, E: PI_{79}-b-$PMMA_{138}$, F: PI_{176}-b-$PMMA_{125}$ and G: PI_{244}-b-$PMMA_{131}$

Figure 5.3F and G clearly show that the 2 block copolymers with the highest PI content (PI_{176}-*b*-$PMMA_{125}$ and PI_{244}-*b*-$PMMA_{131}$) with 49 and 56 wt% PI respectively, form clear, colourless dispersions in the base oil. This suggests excellent dispersibility within the non-polar oil. The remaining 5 dispersions are all opaque white which suggests a decreased solubility within the base oil. Alternatively, the white colour of the dispersions could be due to light scattering, suggesting self-assembly into micelles with dimensions comparable to (or greater than) the wavelength of visible light. It was not possible to investigate the self-assembly of PI-*b*-PMMA block copolymers in Yubase 4 by DLS or TEM because of the high viscosity and low purity of the industrial base oil. The opacity of the dispersions was not deemed to be concerning because the dispersions illustrated in Figure 5.3 are at 5 wt% whereas friction testing would be carried out after dilution to a maximum of 1 wt%. It should also be noted that commercial friction modifiers are often prepared so that they are barely soluble in the oil, because the high Lewis basicity helps with binding to metal surface, and can therefore aid lubrication. The compromise between solubility and effective friction modification often requires considerate balancing and can cause problems in the long-term stability of lubricant formulations. However, the dispersions discussed herein were all stable with no sedimentation after 6 months.

5.2.1.2. Friction Testing of PI-*b*-PMMA Block Copolymers in Neat Yubase 4

The evaluation of the coefficient of friction for 1 wt% dispersions of PI-*b*-PMMA in Yubase 4 was carried out using a mini-traction machine (MTM) (for diagram and

explanation, see experimental chapter). At first, a preliminary test was run on some of the dispersions and three Stribeck curves were measured immediately in sequence under identical conditions (36 N, 80 °C and entrainment speed from 3000 – 3 mm s^{-1}), however the data generated were very noisy and the 3 repeats for each sample were highly variable with respect to each other. This irreproducibility in the Stribeck curves was hypothesised to be the result of the slow diffusion of the polymers to the metal surfaces. To investigate this, the friction coefficient of the 1 wt% dispersion of PI$_{147}$-*b*-PMMA$_{313}$ in Yubase 4 was measured over 2 hours at a constant entrainment speed (50 mm s^{-1}), pressure (30 N) and temperature (60 °C), and the results are shown below in Figure 5.4.
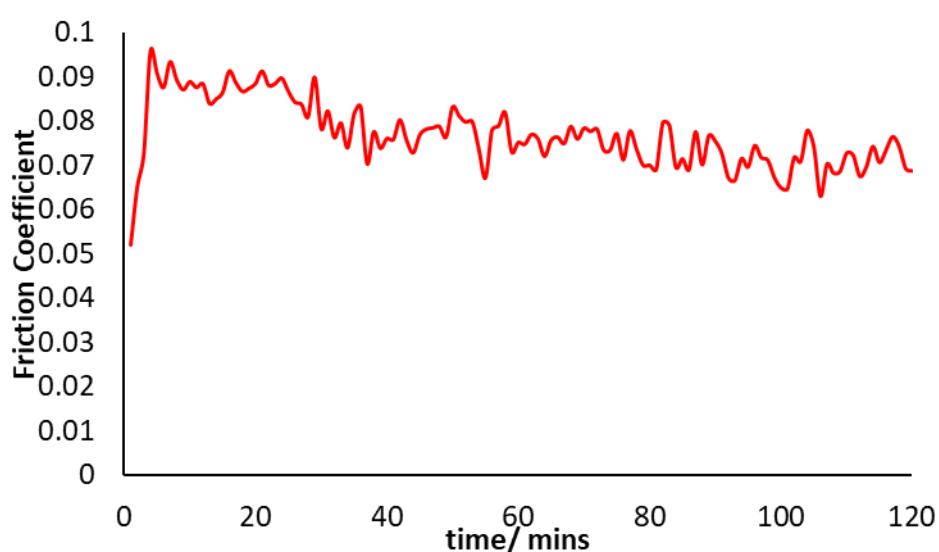
Figure 5.4: Measurement of the friction coefficient across 2 hours of a 1 wt% dispersion of PI$_{147}$-b-PMMA$_{313}$ in Yubase 4 held at 60 °C, 30 N and 50 mm s^{-1}

Figure 5.4 shows that, after an initial increase from 0.05 to approximately 0.09 caused by the MTM accelerating to 50 mm s^{-1}, the friction coefficient shows a steady decrease from 0.09 to 0.07 over the first 60 minutes of the experiment before a plateau from 60 minutes onwards. The gradient of the decrease is steepest in the first 40 minutes. This is significant because it was during this time that the 3 Stribeck curves in the previous test were recorded. This confirms that the irreproducible results previously noted are the result of the system requiring an extended period of time to fully reach 'steady-state'. From 40 – 120 minutes, Figure 5.4 shows no dramatic change in the friction coefficient. The time taken for each PI-*b*-PMMA block copolymer to reach this 'equilibration' could vary depending on the composition and total molar mass. Therefore, each dispersion was

allowed to equilibrate for 2 hours under the same conditions described above, before the friction coefficient was measured at varying entrainment speed for the Stribeck curve.

Another observation of the data in Figure 5.4 is the level of noise. This is typical of MTM measurements, and is most commonly the result of slight fluctuations in the pressure and entrainment speed of the MTM during the measurement. It can also be the result of slight differences in roughness across the surfaces of the disc and ball which are in contact. While the level of noise did not prevent the 'equilibration' being identified in Figure 5.4, it could be problematic in subsequent comparisons of PI-*b*-PMMA block copolymer dispersions. To mitigate for this, 10 repeats of the friction coefficient measurement were taken at each entrainment speed with the average friction coefficient being recorded and the standard deviation for the error. The friction coefficient of each polymer dispersion was measured at entrainment speeds from 3000 – 3 mm s^{-1} at 80 ^{o}C and 36 N. The results for each PI-*b*-PMMA dispersion and a sample of neat Yubase 4 are shown in Figure 5.5.

Figure 5.5: Results of friction testing for all neat PI-b-PMMA dispersions at 1 wt% in Yubase 4. All samples are colour-coded in accordance with the graph in Figure 5.2. A neat sample of Yubase 4 containing no other additive was also tested and is shown in black for comparison.

The results in Figure 5.5 show a reduction in friction coefficient (compared to neat base oil) for all polymer dispersions, especially at entrainment speeds <200 mm s^{-1}. The reduction is particularly significant towards the boundary regime (<30 mm s^{-1}), where metal

components are generally closer together, causing frictional forces to be at their highest. This is encouraging and suggests that all PI-*b*-PMMA block copolymers prepared have the potential to be effective friction modifiers in lubricant formulations.

Above in Figure 5.2 sets of three polymers were identified, to allow an investigation of the impact of varying one particular structural parameter on performance as a friction modifier. However, the data in Figure 5.5 does not suggest a clear structure-property correlation. There is perhaps a suggestion that the block copolymers with a lower total molar mass (PI_{79}-*b*-$PMMA_{200}$ – 25400 g mol^{-1} (green data) and PI_{79}-*b*-$PMMA_{138}$ – 19200 g mol^{-1} (yellow data)) and block copolymers with a higher fraction of PMMA (PI_{79}-*b*-$PMMA_{200}$ – 79 wt% (green data) and PI_{147}-*b*-$PMMA_{313}$ – 76 wt% (red data)) show an improved performance at the boundary regime. However, the trends investigated are clearly not linear which means that not too much should be read into the individual variations in polymer structure. In the lubricant industry, it is well-known that it is often impossible to linearly correlate friction reduction with the structure of friction modifiers. The fact that Stribeck curves most often show non-linear performance between entrainment speed and friction coefficient further complicates this issue.[24-26] Because, it is not possible to predict friction performance based on the composition or molar mass of PI-*b*-PMMA block copolymers, it is likely that a design of experiments methodology would not be entirely suitable as a future method, and that preparing many samples may be necessary to explore the parameter space.

Another interesting feature of the Stribeck curves is that several samples (PI_{79}-*b*-$PMMA_{200}$ (green data), PI_{147}-*b*-$PMMA_{313}$ (red data) and PI_{79}-*b*-$PMMA_{138}$ (yellow data)) show a peak in friction coefficient at a specific entrainment speed. The position of the peak (U_{max}) for the block copolymer dispersions in base oil, varies widely, from 250 – 30 mm s^{-1}. Interestingly, the samples that showed a peak, all had the lowest friction coefficient of the PI-*b*-PMMA samples in the boundary regime (<30 mm s^{-1}). The presence of a peak has previously been reported by Zheng *et al* for self-assembled poly((2-ethylhexyl acrylate)-*ran*-(*tert*-butyl acrylate))-*block*-(2-hydroxyethyl acrylate)) (P(EXA-*r*-tBA)-*b*-PHEA) block copolymers in neat base oil.[15] The self-assembly of their block copolymers into spherical micelles was proven by TEM which was carried out by reacting the hydroxyl groups of PHEA with cinnamoyl chloride to yield poly(2-cinnamoyloxyethyl acrylate) (PCEA) in the core

which was UV-crosslinked. The crosslinked micelles were dialysed to remove the base oil and leave the micelles dispersed in THF. From this, the dispersion was sprayed onto carbon-coated copper grids. The micelles were stained with osmium tetroxide for contrast and the THF was allowed to evaporated off before imaging. They observed a correlation between the U_{max} and the diameter of spherical micelles which itself appeared to correlate with the total molar mass of the block copolymers. While they suggested the presence of a peak is indicative of spherical micelles in base oil, they were not able to definitively conclude a reason for this phenomenon. However, they suggest that the friction between the 2 surfaces spaced by spherical micelles, should mostly result from the force required to shear the micelles, and that the number of micelles entrained between surfaces decreases with entrainment speed. This could suggest that the PI-*b*-PMMA samples described above, which show a peak in Figure 5.5 are undergoing self-assembly into micelles within the base oil. Unlike, the aforementioned paper, the position of U_{max} in Figure 5.5 does not correlate with total molar mass of the block copolymer. An attempt was made to investigate any self-assembly of PI-*b*-PMMA by TEM, however the high viscosity of Yubase 4 made it impossible to image the samples by standard TEM. Further investigation would be needed to explore any self-assembly of PI-*b*-PMMA in Yubase 4.In order to further judge how effective the block copolymers were as friction modifiers, their performances were compared to two commercial friction modifiers. Thus, 1 wt% dispersions of commercial friction modifiers - glycerol monooleate (GMO) and Perfad 3050 - in Yubase 4 were prepared and tested under the same conditions. GMO is a widely-studied organic friction modifier that forms tribofilms at metal surfaces with the carbon chain directed away from the metal surface, similarly to polymer brushes.[27-30] Perfad 3050 is a Croda-produced, PFM and as such offers a useful comparison to the block copolymers prepared in this study. The Stribeck curves for the best performing PI-*b*-PMMA block copolymers are shown in Figure 5.6, along with data for the 2 commercial friction modifiers.
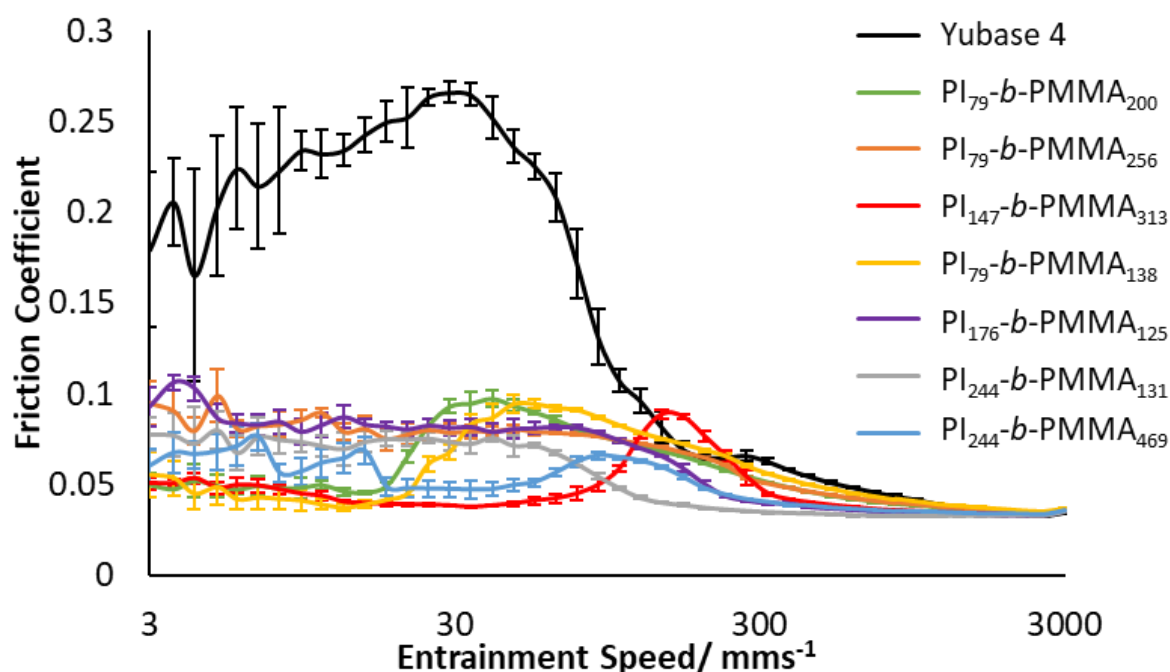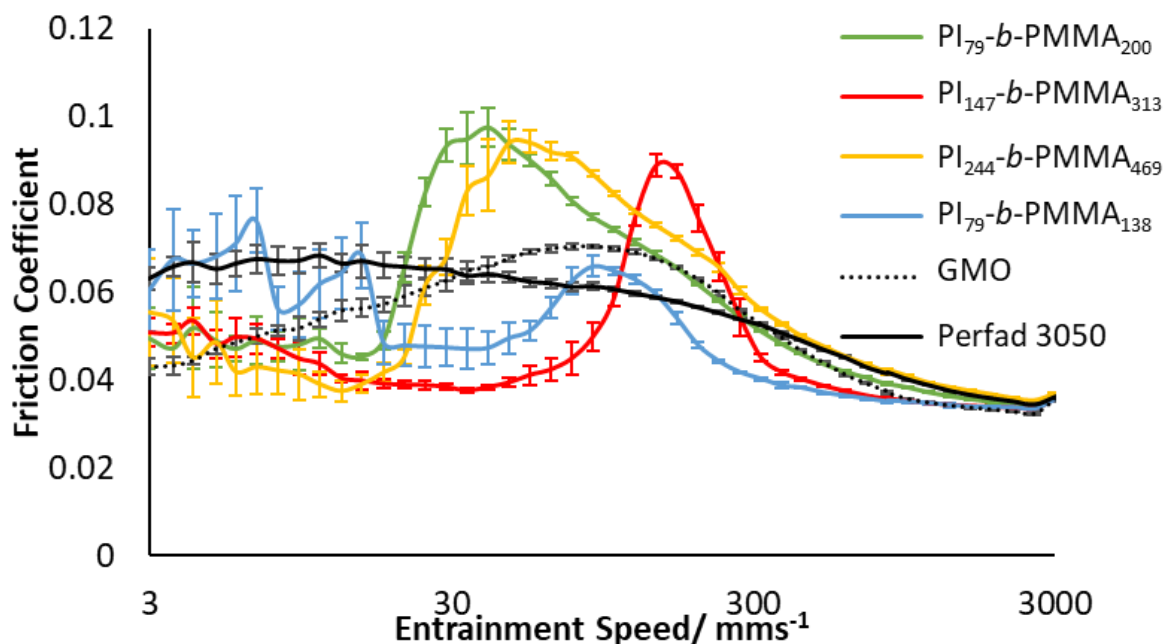
Figure 5.6: Results of friction testing for the best performing PI-b-PMMA dispersions at 1 wt% in Yubase 4. All samples are colour-coded in accordance with the graph in Figure 5.2. The results for the identical test with 2 commercially available friction modifiers, GMO and Perfad 3050, are also shown.

It can be seen from the friction curves in Figure 5.6 that the PI-*b*-PMMA samples compare reasonably well with the commercial friction modifiers. At the boundary conditions (<30 mm s^{-1}), PI$_{79}$-*b*-PMMA$_{200}$ (green data), PI$_{147}$-*b*-PMMA$_{313}$ (red data) and PI$_{79}$-*b*-PMMA$_{138}$ (blue data) have a significantly lower friction coefficient (<0.05) than Perfad 3050 (>0.06) and are close to the curve of GMO (<0.06). This suggests that the PI-*b*-PMMA samples are acting as effective friction modifiers in neat base oil. The competitive performance with Perfad 3050 is particularly important because the latter is a commercial polymeric friction modifier, and as such may be the more useful comparison in predicting formulations which could be used for PI-*b*-PMMA block copolymers.

As mentioned previously, the best performing PI-*b*-PMMA samples at the boundary regime (all displayed in Figure 5.6) showed a peak in friction coefficient at a specific entrainment speed. The result for GMO also showed a broad peak, however, Perfad 3050 did not. The reasons for the peak in GMO are difficult to elucidate without further *in-situ* analysis during the friction test, however, it could suggest some self-assembly of the amphiphilic molecule in base oil as has been reported in the literature.[15]

The performance of the PI-*b*-PMMA block copolymers in neat base oil is encouraging and suggests that these block copolymers could perform effectively as friction

modifiers. However, demonstrating effectiveness in neat base oil is no guarantee of performance in a full lubricant formulation which will contain a wide variety of additives, many of which will be amphiphilic/surface-active and are added to fulfil a variety of functions (e.g. wear reduction, corrosion inhibition).[31, 32] It is necessary for friction modifiers to compete strongly with these other additives in reaching the metal surface and forming tribofilms with the surface-active ingredients.[33]

5.2.1.3. Friction Testing of PI-*b*-PMMA Block Copolymers in Full Lubricant Formulations

As well as friction reduction, there are several other key functions that a lubricant formulation must fulfil, including preventing wear and corrosion and all of these properties must also continue to be effective across all operational temperatures.[31, 32] To achieve these properties, many different ingredients are introduced, which make lubricant formulations highly complicated. Furthermore, a high proportion of formulation additives are surface-active molecules (e.g. ZDDP, GMO etc.). Consideration of interactions of these molecules with one another, both in solution and at the metal surfaces, is critical to ensuring the optimal performance for each specific application.[33]

Previously, all PI-*b*-PMMA block copolymers prepared were found to significantly reduce the friction coefficient in comparison to neat Yubase 4 (see Figure 5.5) and several of the samples were also found to be competitive with the commercial products GMO and Perfad 3050 (see Figure 5.6). In order to understand how the PI-*b*-PMMA samples perform in the presence of other additives, full commercial formulations were prepared containing 1 wt% each of the 4 best performing copolymers (PI$_{79}$-*b*-PMMA$_{200}$, PI$_{147}$-*b*-PMMA$_{313}$, PI$_{79}$-*b*-PMMA$_{138}$ and PI$_{244}$-*b*-PMMA$_{131}$). In this instance Motul 0W20 was used as the base formulation to assess the performance of the PI-*b*-PMMA block copolymers. The 0W20 formulation is particularly useful for engines starting at very cold temperatures because the viscosity remains low enough to be poured and pumped easily. Once prepared, these formulations were then subjected to friction testing with a different procedure to the one previously used for neat solutions. The new test was more industrially relevant, in that measurements of friction coefficient are made during 2 hours of rubbing the metal surfaces in the presence of the lubricant at 80 °C. In contrast to the neat solutions, repeat measurements of friction coefficient at each entrainment speed were not made, therefore error analysis was not carried out, as previously. Stribeck curves were measured

sequentially for the same sample at increasing time intervals of 0, 5, 10, 15, 30 and 60 minutes. Figure 5.7 shows the sixth and final Stribeck curve, measured after the full 2 hours of rubbing for the PI-*b*-PMMA and the 2 commercial friction modifiers.
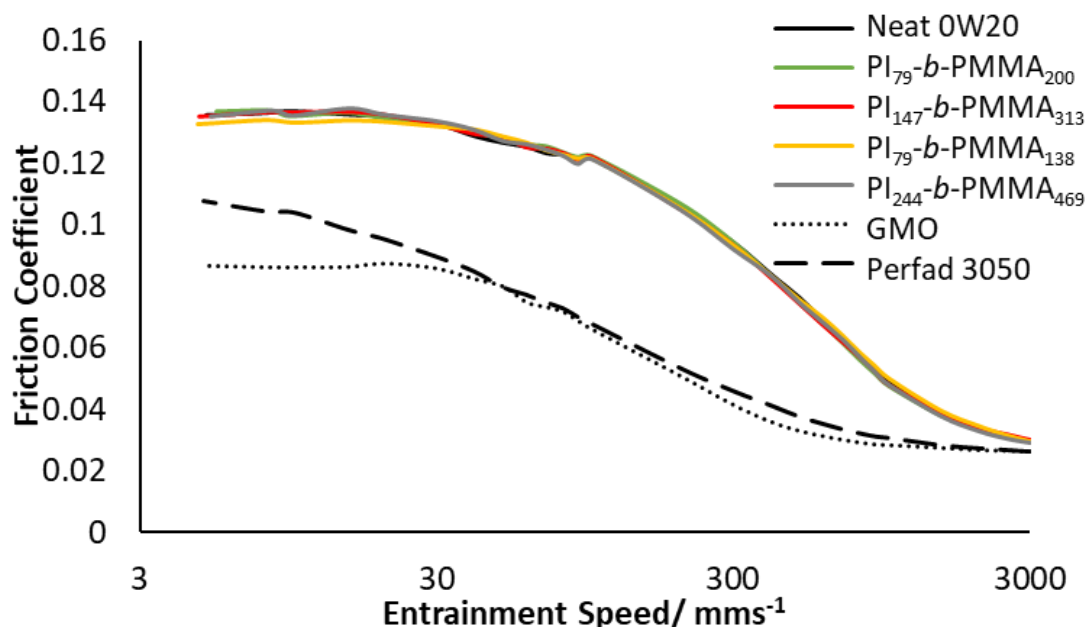
Figure 5.7: The final Stribeck curve obtained after 2 hours of rubbing at 80 °C for full 0W20 formulations containing 1 wt% best performing PI-b-PMMA samples in neat base oil. Also included are data for a neat 0W20 formulation (in black) and equivalent samples containing the 2 commercially available friction modifiers (dashed black).

Figure 5.7 shows that all PI-*b*-PMMA samples perform identically (badly) when added to the 0W20 formulation and identically to 0W20 with no additional friction modifier (termed 'neat' henceforth). These results demonstrates that the PI-*b*-PMMA block copolymers have no impact at all on friction when in a full formulation with multiple other additives. It had already been established (Figure 5.5) that the block copolymers are highly effective friction modifiers in neat base oil, so the lack of impact in full formulation is most likely caused by other surface-active agents reaching the metal surface and adsorbing preferentially. If the block copolymers cannot displace these surface-active agents or cooperatively form a tribofilm to reduce friction, there will be no difference in performance to that of the full formulation with no added friction modifier. The interactions between the multiple ingredients within a lubricant formulation are poorly understood and because of the high degree of complexity there are few examples of studies into these phenomena.[11] Generally such studies rely on the use of simulations and molecular dynamics because of the complexity of the multicomponent systems and the challenge of

in-situ experimental analysis. Even so, the few reports on the nature of such interactions have based their studies on highly simplified formulations, often focussing on only 2 or 3 key additives such as friction modifiers and dispersants. To fully study these effects, it is also important to optimise the loading of each additive in turn because this can also affect the likelihood of competition with all other ingredients.

The commercial friction modifiers performed much better in this test across all entrainment speeds. The reason for this presumably lies in the chemical structure of these additives. The functional groups in GMO and Perfad 3050 are known to interact strongly with metal surfaces. The ester group in PMMA is not highly Lewis basic, meaning that there is likely to be a lower affinity for metal surfaces. In order to improve the ability of the block copolymers to adsorb to the metal surface (and then not desorb upon at high temperature and shear), it was decided to synthesise analogous block copolymers with an amine-containing monomer – dimethylaminoethyl methacrylate (DMAEMA).

5.2.2. Friction Testing of PI-*b*-PDMAEMA Block Copolymers

The disappointment of PI-*b*-PMMA block copolymers failing to reproduce the excellent friction reduction results in neat base oil, when added to a full formulation suggests that a block copolymer containing a more Lewis basic substituent could be necessary in order to adsorb to the metal surface and reduce friction. PDMAEMA is similar in structure to PMMA, however, the 'R' group on the ester is a *tert*-amine rather than a methyl group. This significantly increases the Lewis basicity and could allow for the polymer to reach, and interact strongly with, the metal surface. Statistical and block copolymers of PDMAEMA (polymerised with lipophilic alkyl methacrylates) have previously been investigated as friction modifiers in neat solutions of base oil and have been shown to reduce friction significantly in comparison with less Lewis basic methacrylates.[34, 35] Amines are well-known to interact strongly with metallic elements and are commonly used as ligands for transition metals used in inorganic chemistry.

5.2.2.1. Molar Mass Properties of PI-*b*-PDMAEMA Block Copolymers

As with the PI-*b*-PMMA samples prepared for applications testing, the scaled-up synthesis (>20 g) of PI-*b*-PDMAEMA was attempted by the ATRP of DMAEMA from PI-*Br* macroinitiators. Because of the previously observed solubility issues for PI-*b*-PMMA block

copolymers in the non-polar base oil, and the increased Lewis basicity of the PDMAEMA compared to PMMA, the synthesis was only attempted with PI-*Br* macroinitiators with a number average molar mass ≥ 5 kg mol^{-1}. For the ATRP of DMAEMA, an identical set of conditions was used (i.e. THF solvent, PMDETA ligand, CuBr activator, 30 $^{\circ}$C and a target solids content of ≈10 wt% for the final block copolymer) to those previously found to be effective in chapter 4. For the preparation of PI$_{79}$-*b*-PDMAEMA$_{58}$, the synthesis proceeded as expected and gave a molar mass of PDMAEMA which was in line with expectations based on the previously reported results in Chapter 4. However, when using the PI$_{244}$-*Br* macroinitiator, the molar mass measured by SEC did not increase following the ATRP, suggesting that DMAEMA was not polymerised. Initially this was hypothesised to be purely the result of a slow rate of initiation because of the far greater molar mass of the macroinitiator. However, repeating the reaction at 90 $^{\circ}$C did not result in any polymerisation of DMAEMA being observed. Performing the reaction under the dilute conditions used (≈10 wt%) decreases the likelihood of monomer insertion steps taking place for the active chain end and, as such, it is likely that the failed reactions were carried out too dilute for the polymerisation to take place. Song *et al* have previously reported the preparation of polybutadiene-*b*-PDMAEMA block copolymers by ATRP of DMAEMA from a PB-*Br* macroinitiator, prepared by living anionic polymerisation.[36] The conditions they used for the ATRP were almost identical (PMDETA, CuBr, THF), and the molar mass of PB-*Br* macroinitiator was 5.7 kg mol^{-1}. The only obvious difference in their reaction protocol was the target solids content for the final PB-*b*-PDMAEMA block copolymer which was 50 wt% rather than 10 wt%. By use of these conditions they were able to prepare a block copolymer with a total molar mass of 44.2 kg mol^{-1} and a dispersity of 1.27. A modelling study by Johnston-Hall *et al* has suggested that both the RAFT and free radical polymerisations of MMA have a lower rate of termination when the reaction is carried out at higher concentrations because the medium is higher in viscosity which limits the diffusion of the polymer chains.[37] Although their report was for alternative mechanisms of radical polymerisation for the polymerisation of MMA, they explicitly state that the model would be expected to be consistent for ATRP and other monomers. Therefore, the reaction was repeated on a smaller scale (yield <10 g) with PI$_{244}$-*Br* as a macroinitiator and a higher target solids content in THF (≈50 wt%) at 60 $^{\circ}$C. Following this reaction, the molar mass was found

to increase significantly by SEC, suggesting the successful polymerisation of DMAEMA from PI$_{244}$-*Br* (molar mass data shown below in Table 5.5).

Table 5.5: Molar mass data for PI-b-PDMAEMA block copolymers prepared by ATRP of DMAEMA from PI-Br macroinitiators

Sample	M_n/ kg mol^{-1}				
	PI Block[a]	PDMAEMA Block[b]	Total[c]	Đ[d]	wt% PI[e]
PI$_{79}$-*b*-PDMAEMA$_{58}$	5.38	9.14	14.5	1.21	37
PI$_{244}$-*b*-PDMAEMA$_{145}$	16.6	22.8	39.4	1.25	42
PI$_{244}$-*b*-PDMAEMA$_{208}$	16.6	32.7	49.3	1.24	34

[a] M_n(PI) from triple detection SEC of PI sample from living anionic polymerisation of PI-*OH*
[b] M_n(PDMAEMA) calculated from NMR spectra of PI-*b*-PDMAEMA block copolymers using the same method described in chapter 4
[c] M_n(PI-*b*-PDMAEMA) calculated from M_n(PI) + M_n(PDMAEMA)
[d] Dispersity from triple detection SEC of PI-*b*-PDMAEMA
[e] wt% PI calculated from M_n(PI)/M_n(PI-*b*-PDMAEMA) x 100

The molar masses of PI and PDMAEMA in the block copolymers, reported in Table 5.5 are similar to those previously investigated in applications testing of PI-*b*-PMMA (from Figure 5.2 and Table 5.4), allowing a direct evaluation of the impact of the more Lewis-basic PDMAEMA block on friction modification. The effect of molar mass of PDMAEMA in block copolymers with lipophilic 'poly(non-functionalised alkyl methacrylates) (PNFAMA)' on friction reduction in base oil has previously been explored by Fan *et al.*[34] With a fixed molar mass of PNFAMA, they found that increasing the molar mass of PDMAEMA (from 23.1 – 146 kg mol^{-1}) resulted in a reduction in friction coefficient (from <0.055 for 23.1 kg mol^{-1} PDMAEMA, to <0.035 for 146 kg mol^{-1} PDMAEMA across all entrainment speeds from 2500 - 5 mm s^{-1}). They suggested this was due to an increased number of sites for the polymer to bind to the metal surface. With this in mind, it might be expected that, in the current study, PI$_{244}$-*b*-PDMAEMA$_{208}$ which has the highest PDMAEMA composition (66 wt%) and $M_{n, PDMAEMA}$ (32.7 kg mol^{-1}) would perform best in the friction testing. However, it is also worth noting that Fan did not investigate the effect of varying the molar mass of the soluble, PNFAMA block, which will be investigated in our study using the 2 different molar masses of the PI block (5.38 and 16.6 kg mol^{-1}, respectively).

5.2.2.2. Friction Testing of PI-*b*-PDMAEMA Block Copolymers in Yubase 4

All PI-*b*-PDMAEMA samples reported in Table 5.5 were dispersed in Yubase 4 at 5 wt%, by solvent switching, whereby they were first dissolved in DCM, a common solvent for PI and PDMAEMA blocks. This method gave stable dispersions with no obvious solid settling out, even after 6 months. For friction testing in neat Yubase 4, the dispersions were diluted to 1 wt% and the results from the MTM testing are shown in Figure 5.8.
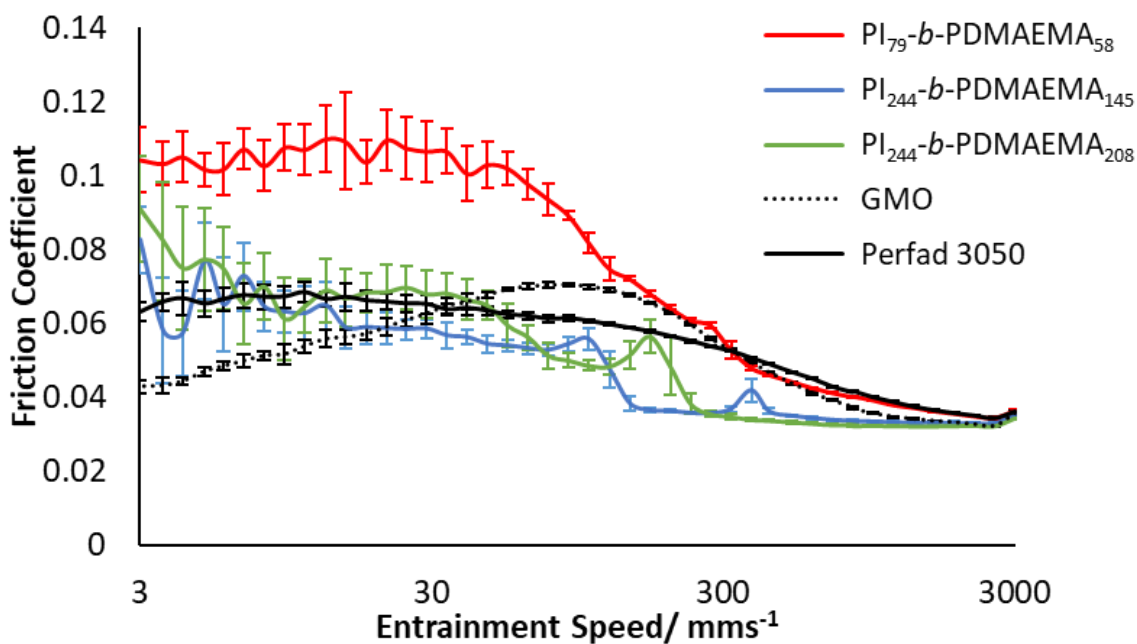
Figure 5.8: Friction results for neat solutions of 1 wt% PI-b-PDMAEMA and commercial friction modifiers , GMO and Perfad 3050, in Yubase 4

The results in Figure 5.8 show that PI_{244}-*b*-$PDMAMEA_{145}$ (blue data) and PI_{244}-*b*-$PDMAEMA_{208}$ (green data) reduce the friction of Yubase 4 to a far greater extent than PI_{79}-*b*-$PDMAEMA_{58}$ (red data), across all entrainment speeds. The most likely cause of the difference in performance is the polymer structure. While PI_{79}-*b*-$PDMAEMA_{58}$ has a similar weight fraction of PDMAEMA to PI_{244}-*b*-$PDMAMEA_{145}$ and PI_{244}-*b*-$PDMAEMA_{208}$ (37, 42 and 34 wt% PDMAEMA, respectively), the former has a much lower total molar mass (14500, 39400 and 49300 g mol^{-1}, respectively). This could suggest that the total molar mass of PI-*b*-PDMAEMA block copolymers or the molar mass of the PDMAEMA block, alone, has a significant impact on the ability of the block copolymer to perform as a friction modifier, although further data would clearly be required to be certain.

The friction coefficient data for the 1 wt% dispersions of PI-*b*-PDMAEMA in Yubase 4, (Figure 5.8) are similar to those of PI-*b*-PMMA (Figure 5.6) in so much that, in common with the PI-*b*-PMMA samples, the PI-*b*-PDMAEMA samples all show a reduction in friction compared to neat Yubase 4 (data shown previously in Figure 5.5). For PI_{244}-*b*-$PDMAMEA_{145}$ and PI_{244}-*b*-$PDMAEMA_{208}$, the friction coefficient at the boundary region (<30 mm s^{-1}) is below 0.08 with a slight increase at 3 mm s^{-1} in both cases. Previously, the best performing PI-*b*-PMMA samples (see Figure 5.6) all showed a friction coefficient of below 0.06 in the boundary regime, however, these samples also had peaks in the friction coefficient between 30 − 250 mm s^{-1} where the friction coefficient reached close to 0.1. PI_{244}-*b*-$PDMAMEA_{145}$ and PI_{244}-*b*-$PDMAEMA_{208}$ do not show peaks in the friction coefficient, meaning that there are significant portions of the Stribeck curves where these samples give lower friction than the PI-*b*-PMMA samples mentioned above. PI_{244}-*b*-$PDMAMEA_{145}$ and PI_{244}-*b*-$PDMAEMA_{208}$ also showed very similar friction performance to Perfad 3050 which, again suggests that the PI-*b*-PDMAEMA block copolymers are effective friction modifiers, however, the performance in the full formulation needs to be assessed before confirming this.

5.2.2.3. Friction Testing of PI-*b*-PDMAEMA Block Copolymers in Full Lubricant Formulations

Having established that PI_{244}-*b*-$PDMAEMA_{145}$ and PI_{244}-*b*-$PDMAEMA_{208}$ appear to be particularly effective friction modifiers in Yubase 4, the performance of the 3 PI-*b*-PDMAEMA block copolymers was assessed in a full 0W20 formulation. Figure 5.9 shows the results for the final Stribeck curve after 2 hours rubbing at 80 $^{\circ}$C for all PI-*b*-PDMAEMA samples dispersed at 1 wt% a full 0W20 formulation.
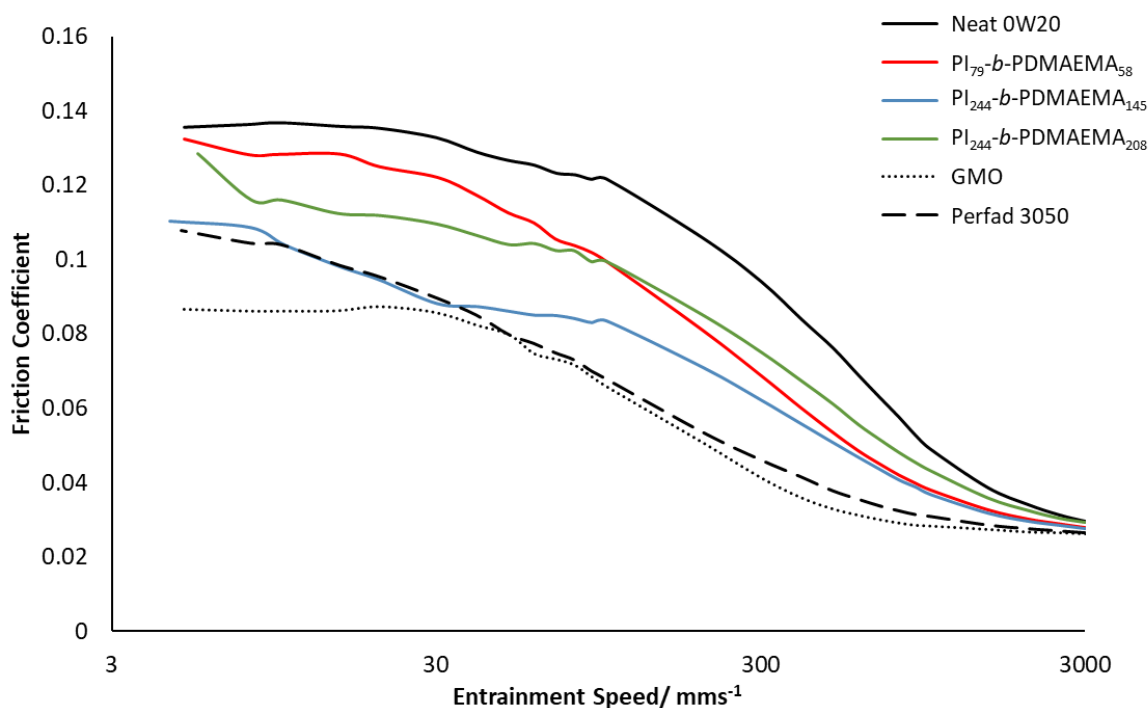
Figure 5.9: The Stribeck curve from the 2 hours rubbing at 80 °C of full 0W20 formulations, containing 1 wt% PI-b-PDMAEMA samples, 2 commercial friction modifiers and data for a neat 0W20 formulation containing no friction modifier.

The results of the friction testing in Figure 5.9 for full formulations show that all PI-*b*-PDMAEMA dispersions reduce the friction coefficient in comparison to the neat 0W20 at all entrainment speeds. The reduction in friction is particularly notable for PI_{244}-*b*-PDMAMEA$_{145}$ (blue data) which significantly reduces the friction coefficient from 0.14 (for neat OW20) at the boundary regime (<30 mm s^{-1}) to below 0.11. The results for PI_{79}-*b*-PDMAMEA$_{58}$ (red data) and PI_{244}-*b*-PDMAEMA$_{208}$ (green data) also show a reduction in the friction coefficient compared to neat 0W20, however the reduction is less significant than PI_{244}-*b*-PDMAMEA$_{145}$, particularly in the boundary condition where the friction was approximately 0.13 and 0.12 for PI_{79}-*b*-PDMAMEA$_{58}$ and PI_{244}-*b*-PDMAEMA$_{208}$, respectively. Previously, it was observed that in neat Yubase 4, PI_{79}-*b*-PDMAMEA$_{58}$ also gave the highest friction coefficient. As discussed above, this block copolymer had the lowest total molar mass and the lowest molar mass of PDMAEMA. Either of these suggest a correlation between the molar mass properties of PI-*b*-PDMAMEA block copolymers and their ability to perform as friction modifiers. However, in this instance, this was not the case for PI_{244}-*b*-PDMAMEA$_{145}$ and PI_{244}-*b*-PDMAEMA$_{208}$ where the former gave a greater reduction in

friction despite being a lower total molar mass (albeit with a far smaller difference in total molar mass than the difference from PI$_{79}$-b-PDMAMEA$_{58}$). This observation could suggest that the higher weight fraction of PI in the block copolymer helps to reduce friction. The reason for the performance of the different polymers as friction modifiers is difficult to conclude without the use of *in-situ* observation to probe the mechanism of adsorption to the metal surfaces. One could speculate that the molar mass of the PDMAEMA block is critical for adsorption to the metal surfaces because a greater DP$_{PDMAEMA}$ results in a greater number of potential binding sites between the polymer and the metal surface. Because the strongly non-polar base oil is a good solvent for polyisoprene, the PI block would be expected to be oriented perpendicular to the metal surface into the base oil (see diagram in Figure 5.10a for a typical, surface-bound polymer). Hence, a greater DP$_{PI}$ (as shown in Figure 5.10c) would result in a thicker polymer brush bound to the metal surface which would act to sterically repel the metal surfaces, thus reducing friction. However, there are also other considerations such as diffusion of PI-b-PDMAEMA through the base oil to the metal surface. The polyisoprene block is necessary for the solubility within the base oil and, as such, a very high DP$_{PI}$ could be expected to keep the block copolymer dispersed within the base oil, thus preventing adsorption to the metal surface. Further samples would need to be prepared and studied for this trend to be fully elucidated.
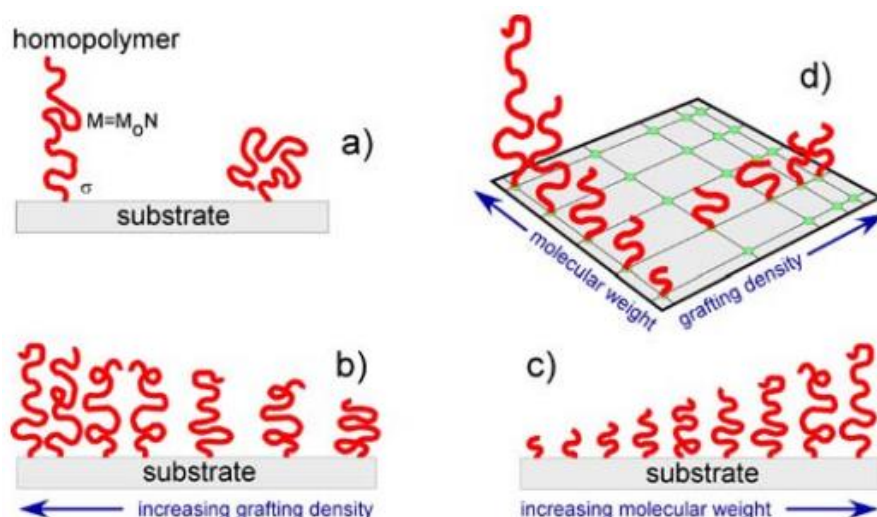
Figure 5.10: Diagram showing the changes in conformation of standard, surface-bound polymers (a)) with b) an increased grating density, c) an increased molecular weight and d) a variation in both grafting density and molecular weight. Reprinted with permission from reference[38], copyright (2021)

These results for the PI-*b*-PDMAEMA samples are highly encouraging, in contrast to the previous results for PI-*b*-PMMA in full formulation, which all overlaid exactly with the neat formulation (Figure 5.7). These encouraging results suggest that, as hypothesised, the introduction of an amine functionality increases Lewis basicity such that the block copolymers can more strongly interact with the metal surface.

The data presented in Figure 5.9 also shows that the best performing block copolymer sample (PI$_{244}$-*b*-PDMAMEA$_{145}$) compares very well to Perfad 3050, at all entrainment speeds, but less well against GMO especially at the boundary condition (<30 mm s^{-1}). In the current study, comparisons in performance against Perfad grades are considered more relevant because Perfad is a PFM and as such may have similar areas of application in the future. The use of GMO is often limited in lubricant formulations because it is strongly suspected to undergo hydrolysis, producing oleic acid and glycerol.[39] Although the products of hydrolysis can reduce friction themselves, they are more volatile than GMO which can lead to loss of containment and damage to the engine under the high operational temperature. Moreover, the resulting fatty acid can lead to corrosion of the metal surface, increasing wear and surface roughness over time.[8]

As illustrated in Figure 5.4, the performance of PI$_{147}$-*b*-PMMA$_{313}$ in neat base oil was found to change significantly over the course of 2 hours. The experimental procedure for full 0W20 formulations measures 6 Stribeck curves from 3000 – 5 mm s^{-1} at increasing time intervals of 0, 5, 15, 30, 60 and 120 minutes rubbing. Previously, only the 6th and final Stribeck curve has been reported because this generally gives the highest friction coefficient at all entrainment speeds, and is therefore the most useful in comparing between different friction modifiers. However, the 6 Stribeck curves together can also give further information on performance and, in particular, if there, is any time dependence on the friction coefficient. Figure 5.11 shows Stribeck curves measured at 0, 15, 30, 60 and 120 minutes rubbing for PI$_{244}$-*b*-PDMAMEA$_{145}$ (Figure 5.11a), GMO (Figure 5.11b) and Perfad 3050 (Figure 5.11c) in 0W20.
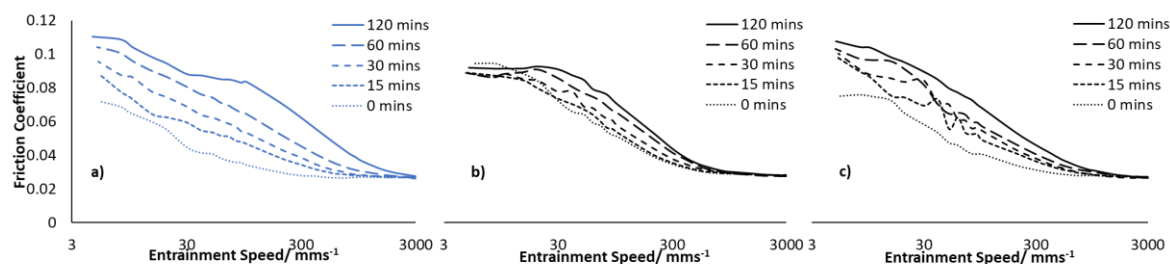
Figure 5.11: Stribeck curves measured at various time intervals during the 2 hours rubbing at 80 °C of full 0W20 formulations containing either: a) PI$_{244}$-b-PDMAMEA$_{145}$ b) GMO or c) Perfad 3050.

It can be seen from the data in Figure 5.11a that there is a reasonably significant increase in friction across all entrainment speeds for PI$_{244}$-*b*-PDMAMEA$_{145}$ as rubbing time increases. Initially, PI$_{244}$-*b*-PDMAMEA$_{145}$ shows significantly lower friction than GMO (Figure 5.11b) and Perfad 3050 (Figure 5.11c) at all entrainment speeds with the friction coefficient remaining below 0.07 at all entrainment speeds. However, after each rubbing interval, the friction increases at all entrainment speed with PI$_{244}$-*b*-PDMAMEA$_{145}$ reaching 0.11 at 5 mm s^{-1} in the final measurement. GMO does not experience a similar increase over time with the friction coefficient in the boundary regime (<30 mm s^{-1}) remaining fairly constant between 0.07 and 0.09. The reason for this is difficult to rationalise because of the complex nature of the full lubricant formulation. It could be caused by the nature of the tribofilm formed at the surface of the metal. As the tribofilm is sheared, the interface can become rougher which increases the friction.[40] Roughness of the metal surfaces being lubricated is well known to increase friction, so the roughness of the tribofilm can also be expected to have a detrimental effect on the lubrication.[41] Another potential reason could be the transfer of adsorbed lubricant additives from one metal surface to the other. Bahadur previously discussed this phenomena that can occur between sliding solid surfaces.[42] Generally the transfer of material, particularly polymers between surfaces in contact, can shield the metal-metal interface further to lower the friction. Material transfer has previously been investigated by use of IR spectroscopy and thermal analysis of surfaces.[43] This transfer often equilibrates over time, however, over longer periods the transfer can cause loss of material from the surfaces due to peeling off by the metal asperities. This leads to an increased surface wear, which increases the friction significantly over time. Certain filler particles such as graphite and copper monosulphide can be introduced to the polymer matrix and have been found to decrease the wear of the

surfaces over time.[44, 45]. Interestingly, PI_{244}-b-$PDMAMEA_{145}$ and Perfad 3050 perform significantly better than GMO in the initial test (0 mins rubbing) across all entrainment speeds. However, the performance of GMO across the 2 hours of the test is more stable (particularly in the boundary regime) which means it performs far better in the final test. GMO is clearly the most unaffected across the tests which could suggest that GMO protects the metal surfaces against wearing for longer. The fall-off in performance for PI_{244}-b-$PDMAMEA_{145}$ and Perfad could also signify a chemical degradation in the polymers or detachment from the surface, both of which could happen at high shear. As effective as GMO is in this test, it is less desirable than PFMs in modern lubricant formulations because its moderately high volatility can lead to loss of containment at high temperature and shear, and the formation of corrosive products upon hydrolysis of the ester functionality.[8]

5.2.2.4. Friction Testing of PI-b-PDMAEMA Block Copolymers in Multiple Different Full Lubricant Formulations

PI_{244}-b-$PDMAMEA_{145}$ showed significant friction reduction when added to 0W20 formulation and it was therefore decided to broaden the scope of the investigation by testing a nearly identical block copolymer in further commercial lubricant formulations, each designed for different applications. Motul 0W16 is a 'US-style' lubricant formulation for hybrid automotive engines where the engine temperature is cooler. Typically, the emission regulations are less strict for hybrid engines and oil drainage intervals can typically be shorter. Although PI_{244}-b-$PDMAMEA_{145}$ was previously shown to be the best performing PI-b-PDMAEMA sample, none of this sample remained so a new batch of block copolymer was synthesised with the same target molar mass and composition. The new sample (PI_{244}-b-$PDMAMEA_{156}$) was prepared from the identical PI_{244}-Br macroinitiator and had a similar molar mass of PDMAEMA (24500 g mol^{-1}) to that of PI_{244}-b-$PDMAMEA_{145}$ (22800 g mol^{-1}). The final Stribeck curve from 2 hours rubbing for the 0W16 formulation containing 1 wt% of (the new) PI_{244}-b-$PDMAMEA_{156}$ is shown below in Figure 5.12.
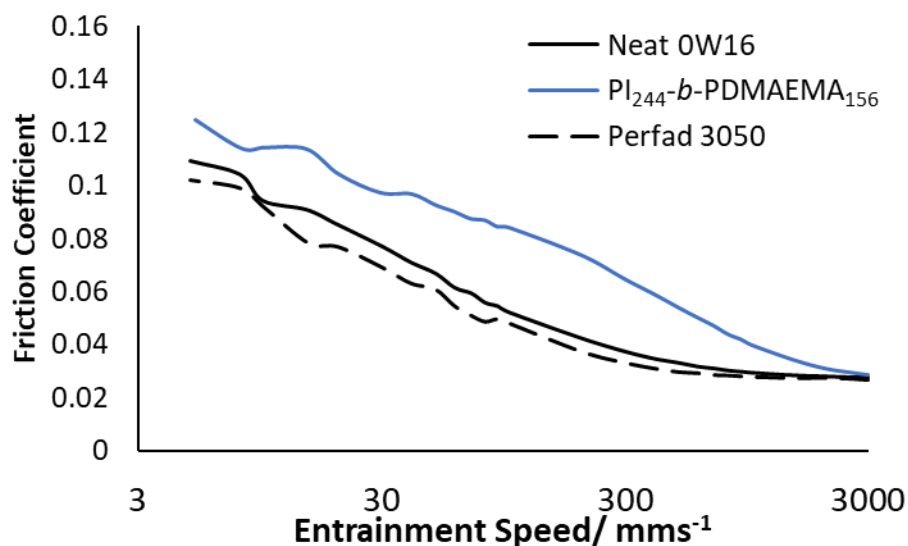
Figure 5.12: Stribeck Curve from 2 hours rubbing of the Motul 0W16 formulation containing 1 wt% PI$_{244}$-b-PDMAMEA$_{156}$ (blue) or Perfad 3050 (dashed black) as friction modifiers, measured at 80 °C. The solid black line is that of the neat 0W16 formulation with no extra friction modifier. NOTE: The data for the neat 0W16 formulation was not collected as part of this investigation because the test had previously been run

Despite the encouraging results for PI$_{244}$-*b*-PDMAMEA$_{145}$ in 0W20, the results from Figure 5.12 show a poor performance for PI$_{244}$-*b*-PDMAMEA$_{156}$ in Motul 0W16 (blue data). In comparison to the neat formulation (solid, black data), there was actually an increase in friction coefficient at all entrainment speeds when PI$_{244}$-*b*-PDMAMEA$_{156}$ was added. The performance of 0W16 containing Perfad 3050 (dashed, black data) was not significantly better than the neat formulation but was still better than PI$_{244}$-*b*-PDMAMEA$_{156}$ at all entrainment speeds. It is worth noting that another Croda-supplied PFM, Perfad 3006 (data not shown), also causes an increase in friction coefficient in the 0W16 formulation which would suggest that this lubricant is formulated very differently to the 0W20 formulation and the polymeric friction modifiers seem to be ineffective. The variability in design and composition of different lubricant formulations (for different applications) means that designing a generic friction modifier to work effectively in multiple lubricant formulations is extremely challenging but, in principle, would clearly be highly desirable.

PI_{244}-b-PDMAMEA$_{156}$ was added to two further formulations - Mobil Delvac 5W30 and Motul 5W30 and Stribeck curves were obtained. These formulations are designed for use in heavy vehicles such as lorries and diggers which are expected to have longer intervals between oil drainage. As such these products are formulated with high concentrations of surfactant to solubilise any particulates such as soot which, if left to accumulate, could damage the engine during long-term use. These harder-wearing oils were tested at a higher temperature (135 ^{o}C) to better reflect the stringent, long-term wearing conditions that they will experience in real applications. Figure 5.13 shows the final Stribeck curves for the 2 formulations after 2 hours rubbing at 135 ^{o}C.
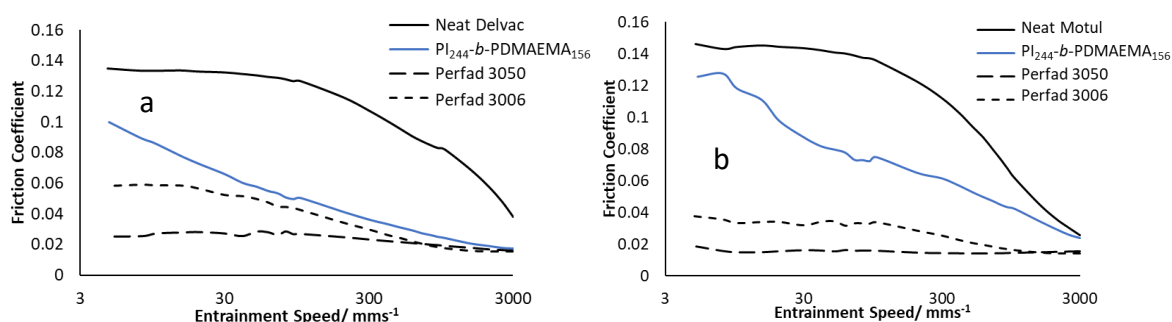
Figure 5.13: Stribeck curves for 2 different formulations containing 1 wt% of different friction modifiers after 2 hours rubbing at 135 ^{o}C. a) The full formulations of Mobil Delvac 5W30, b) Full formulations of Motul 5W30. In each case, the solid black line indicats the result for the neat formulation with no extra friction modifier. NOTE: The data for all formulations apart from those containing PI$_{244}$-b-PDMAMEA$_{156}$ were collected as part of a previous investigation.

The results for the Mobil Delvac 5W30 (Figure 5.13a) show that the addition of PI_{244}-b-PDMAMEA$_{156}$ (blue data) resulted in a significant reduction in friction, compared to the formulation with no friction modifier (solid, black data), at all entrainment speeds. This is particularly clear in the boundary regime (entrainment speed <30 mm s^{-1}) where the friction coefficient of PI_{244}-b-PDMAMEA$_{156}$ was 0.07 at 30 mm s^{-1} and 0.1 at 5 mm s^{-1} with a steady gradient in between, while the neat formulation had a nearly constant friction coefficient of 0.14 between 5 and 30 mm s^{-1}. This is a very significant decrease in the friction at entrainment speeds where the metal surfaces are typically in close contact and the friction is highest. Figure 5.13a also shows that the Stribeck curve of PI_{244}-b-PDMAMEA$_{156}$ also performs similarly to the commercial PFM, Perfad 3006 (dotted, black data), however, there is a divergence in performance in the boundary regime where the friction coefficient of Perfad 3006 remains fairly constant at 0.06. Another commercial PFM, Perfad 3050

(dashed, black data) significantly outperforms PI_{244}-b-$PDMAMEA_{156}$ at all entrainment speeds where the friction coefficient remains below 0.03 with very little change from 3000 – 5 mm s^{-1}. However, while these results for the commercial PFMs are apparently impressive, both Perfad 3006 and Perfad 3050 are known to have poor long-term solubility in this formulation and as such are not supplied commercially as friction modifiers for the Mobil Delvac 5W30 formulation. The poor solubility of the commercial friction modifiers is thought to be due to the high concentration of surfactants in the formulations, necessary to solubilise particulates such as soot during intensive, long-term use which can cause damage to the engine. Surfactants are known to have an effect on the solubility of amphiphilic block copolymers, because of their ability to bind with the insoluble block of the copolymers. A high concentration of surfactant (relative to the block copolymer) is known to inhibit the formation of block copolymer micelles.[46] The poor solubility of friction modifiers in this formulation means Mobil Delvac 5W30 is most commonly used without any additional friction modifier (i.e. as neat Mobil Delvac 5W30). Although a quantitative study on the long-term stability of PI_{244}-b-$PDMAMEA_{156}$ in Mobil Delvac 5W30 was not carried out, qualitatively, there did not appear to be any solubility problems and there was no visible sediment from the 1 wt% dispersion after 6 months of storage at room temperature. Therefore, the improvement in performance of PI_{244}-b-$PDMAMEA_{156}$ in Mobil Delvac 5W30 shown in Figure 5.13a compared to the neat formulation (which is how the lubricant is currently used commercially) is significant, and could present a commercial opportunity.

Figure 5.13b shows that the neat Motul 5W30 formulation (solid, black data) performs similarly to that of the neat Mobil Delvac 5W30 formulation (from Figure 5.12a), with a large increase in the friction coefficient from 3000 – 100 mm s^{-1} - from 0.04 to 0.14. Following this increase, the friction coefficient remains fairly constant at 0.14 throughout the boundary regime from 30 – 5 mm s^{-1}. At 1 wt% in the Motul 5W30 formulation, PI_{244}-b-$PDMAMEA_{156}$ (blue data) does reduce the friction compared to the neat lubricant across all entrainment speeds with an observed increase from 3000 – 5 mm s^{-1} of from 0.04 to 0.12. While this represents a modest improvement in the friction coefficient, Figure 5.13b also shows that the commercial PFMs clearly reduce the friction by a far greater amount across all entrainment speeds. Perfad 3006 (dotted, black data) has a friction coefficient of

0.02 at 3000 mm s^{-1} and increases up to 0.04 at 150 mm s^{-1} where it remains constant down to 5 mm s^{-1}. Meanwhile, the friction coefficient of Perfad 3050 (dashed, black data) remains below 0.02 from 3000 – 5 mm s^{-1} and remains fairly constant across all entrainment speeds. The excellent performance of the commercial PFMs was expected and Perfad 3050 is supplied as a commercial friction modifier for this formulation. The commercial products are stable in this formulation, meaning that a great level of improvement would be necessary for PI$_{244}$-*b*-PDMAMEA$_{156}$ to compete with the current state of the art for this formulation.

5.2.2.5. Investigating the Influence of Composition of PI-*b*-PDMAEMA Block Copolymers on Friction Reduction

With encouraging friction coefficient results for PI$_{244}$-*b*-PDMAMEA$_{145}$ in Motul 0W20 and PI$_{244}$-*b*-PDMAMEA$_{156}$ in Mobil Delvac 5W30, it was decided to see if variation in the molar mass/composition of the block copolymer could improve/optimise the friction performance. The relative performance of the three block copolymers tested in Motul 0W20 (Figure 5.9) showed that both PI$_{244}$-*b*-PDMAMEA$_{145}$ and PI$_{244}$-*b*-PDMAEMA$_{208}$ significantly out-performed PI$_{79}$-*b*-PDMAMEA$_{58}$. This suggests that a higher molar mass of the block copolymer (and in particular the PI block) is important for friction reduction, perhaps because of the larger brush layer of PI formed on the metal surfaces. A comparison of PI$_{244}$-*b*-PDMAMEA$_{145}$ and PI$_{244}$-*b*-PDMAEMA$_{208}$ revealed that the former gave lower friction. This suggests that a higher fraction of PI is important for friction reduction. A likely explanation for this is an increasing density of the polymer brush layer adsorbed to the metal surface. With this in mind, two more block copolymers were synthesised using the same PI$_{244}$-*Br* macroinitiator (M$_n$ 16.6 kg mol^{-1}) but with lower molar mass PDMAEMA blocks. The molar mass data for the family of five block copolymers with identical PI blocks and varying PDMAEMA blocks are shown in Table 5.6.

Table 5.6: Molar mass data for PI-b-PDMAEMA block copolymers prepared for optimisation in full lubricant formulations.

Sample	M_n/ kg mol^{-1}				
	PI Block[a]	PDMAEMA Block[b]	Total[c]	Đ[d]	wt% PI[e]
PI$_{244}$-*b*-PDMAEMA$_{33}$	16.6	5.25	21.9	1.06	76
PI$_{244}$-*b*-PDMAEMA$_{70}$	16.6	11.0	27.6	1.13	60
PI$_{244}$-*b*-PDMAEMA$_{145}$	16.6	22.8	39.4	1.25	42
PI$_{244}$-*b*-PDMAEMA$_{158}$	16.6	24.5	41.1	1.29	40
PI$_{244}$-*b*-PDMAEMA$_{208}$	16.6	32.7	49.3	1.24	34

[a] M_n(PI) from triple detection SEC of PI sample from living anionic polymerisation of PI-*OH*
[b] M_n(PDMAEMA) calculated from NMR spectra of PI-*b*-PDMAEMA block copolymers using the same method described in chapter 4
[c] M_n(PI-*b*-PDMAEMA) calculated from M_n(PI) + M_n(PDMAEMA)
[d] Dispersity from triple detection SEC of PI-*b*-PDMAEMA
[e] wt% PI calculated from M_n(PI)/M_n(PI-*b*-PDMAEMA) x 100

Previously, in Figure 5.9 and Figure 5.13, it was shown that samples of PI-*b*-PDMAEMA performed particularly well as a friction modifier in 0W20 and Mobil Delvac 5W30 lubricant formulations. For this reason, the investigation into the impact of changing the molar mass of the PDMAEMA block on performance of the block copolymers as friction modifiers again focussed on the same two formulations. The Stribeck curves for four of the PI$_{16}$-*b*-PDMAEMA$_x$ block copolymers in Motul 0W20 are reported in Figure 5.14.
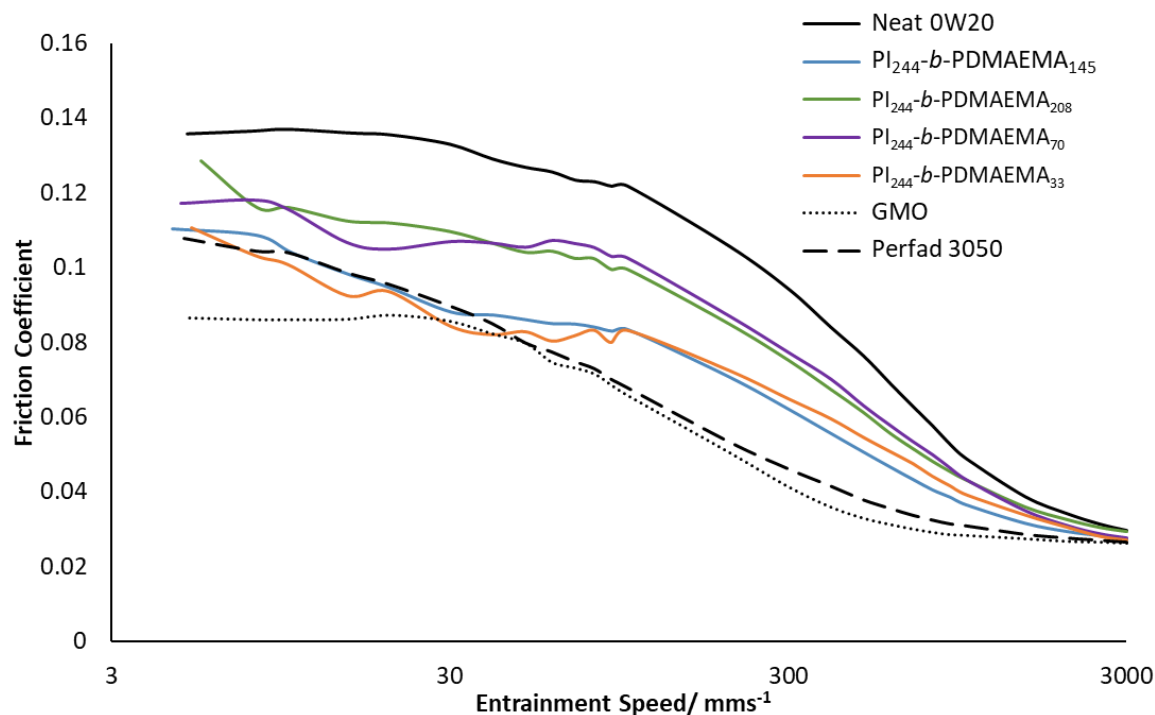
Figure 5.14: Stribeck curves from 2 hours rubbing at 80 °C of the Motul 0W20 formulation containing 1 wt% PI-b-PDMAEMA of specified molecular weight.

Previously in Figure 5.9, PI_{244}-*b*-PDMAMEA$_{145}$ and PI_{244}-*b*-PDMAEMA$_{208}$ were shown to reduce the friction of Motul 0W20 compared to the neat formulation. The data in Figure 5.14 shows that all four PI-*b*-PDMAEMA block copolymers reduce the friction compared to the neat formulation (solid, black data). For all samples, the friction increases significantly from 3000 – 100 mm s^{-1}, before the gradient becomes much shallower down to 5 mm s^{-1}. However, there does not appear to be an obvious trend in performance with respect to molar mass of the PDMAEMA block. The best performing samples were PI_{244}-*b*-PDMAMEA$_{145}$ (blue data, $M_{n, PDMAEMA}$ = 22.8 kg mol^{-1}) and PI_{244}-*b*-PDMAEMA$_{33}$ (orange data, $M_{n, PDMAEMA}$ = 5.25 kg mol^{-1}) which, in the boundary regime (<30 mm s^{-1}), both showed a friction coefficient below 0.11. PI_{244}-*b*-PDMAEMA$_{208}$ (green data, $M_{n, PDMAEMA}$ = 32.7 kg mol^{-1}) and PI_{244}-*b*-PDMAEMA$_{70}$ (purple data, $M_{n, PDMAEMA}$ = 11.0 kg mol^{-1}) had higher friction coefficients across all entrainment speeds with the friction coefficient in the boundary regime being below 0.13 in both cases. It should be noted that the differences between the two pairs of PI-*b*-PDMAEMA block copolymers discussed above are modest at all entrainment speeds and as such, the differences in the results are generally insignificant. However, given the previous two data sets obtained for PI_{244}-*b*-PDMAMEA$_{145}$ and PI_{244}-*b*-

PDMAEMA$_{208}$ did show significant differences in friction coefficient, the lack of a significant, linear change in friction coefficient is noteworthy. The lack of a clear trend between M$_{n,}$ $_{PDMAEMA}$ and friction coefficient was not entirely unexpected because in testing commercial PFMs, trends between molecular structure and friction coefficient are rarely observed during MTM testing. It is thought that the complex nature of the interactions with other ingredients and the solubility within the oil are the most likely reason that trends cannot be easily elucidated. Without a greater understanding of *in situ* interactions between all of the additives, it is not possible to predict the effects of changing the polymer structure on friction performance.

It should also be noted that whilst Figure 5.14 shows that PI$_{244}$-*b*-PDMAMEA$_{33}$ does not reduce the friction coefficient in comparison to PI$_{244}$-*b*-PDMAMEA$_{145}$, the greater fraction of PI (76 wt% compared to 45 wt%) appeared to greatly improve the solubility of the polymer in the base oil during formulation. Generally, the dispersion of all PI-*b*-PDMAEMA block copolymers in full formulations required mechanical stirring at 110 °C for 1 hour. However, PI$_{244}$-*b*-PDMAMEA$_{33}$ appeared to form a clear, homogeneous dispersion at 1 wt% in Motul 0W20 even at room temperature. For consistency in this set of testing, the dispersion was stirred for 1 hour at 110 °C, however, this behaviour could suggest that the formulation of PI$_{244}$-*b*-PDMAMEA$_{33}$ may be possible under very mild conditions whilst maintaining all the friction performance of the best performing PI-*b*-PDMAEMA block copolymer. The ease of dispersion into this formulation would also suggest that PI$_{244}$-*b*-PDMAMEA$_{33}$ is likely to be compatible with a broad range of lubricant formulations, a feature which is rarely the case for commercial friction modifiers.

The PI$_{244}$-b-PDMAMEA$_{33}$ and PI$_{244}$-b-PDMAEMA$_{70}$ block copolymers were also tested in the Mobil Delvac 5W30 formulation where, previously, PI$_{244}$-b-PDMAMEA$_{156}$ was found to be particularly effective in reducing the friction compared to the neat formulation. The commercial Perfad additives are known to demonstrate poor long-term solubility in this formulation whereas, qualitatively, PI$_{244}$-b-PDMAMEA$_{156}$ appeared to remain stable for a period of 6 months. As previously mentioned, a higher weight fraction of PI should enhance the compatibility of the block copolymer within lubricant formulations and enhance long-term stability. The Stribeck curves for PI$_{244}$-b-PDMAEMA$_{33}$, PI$_{244}$-b-PDMAEMA$_{70}$ and PI$_{244}$-b-PDMAEMA$_{156}$ are shown in Figure 5.15.
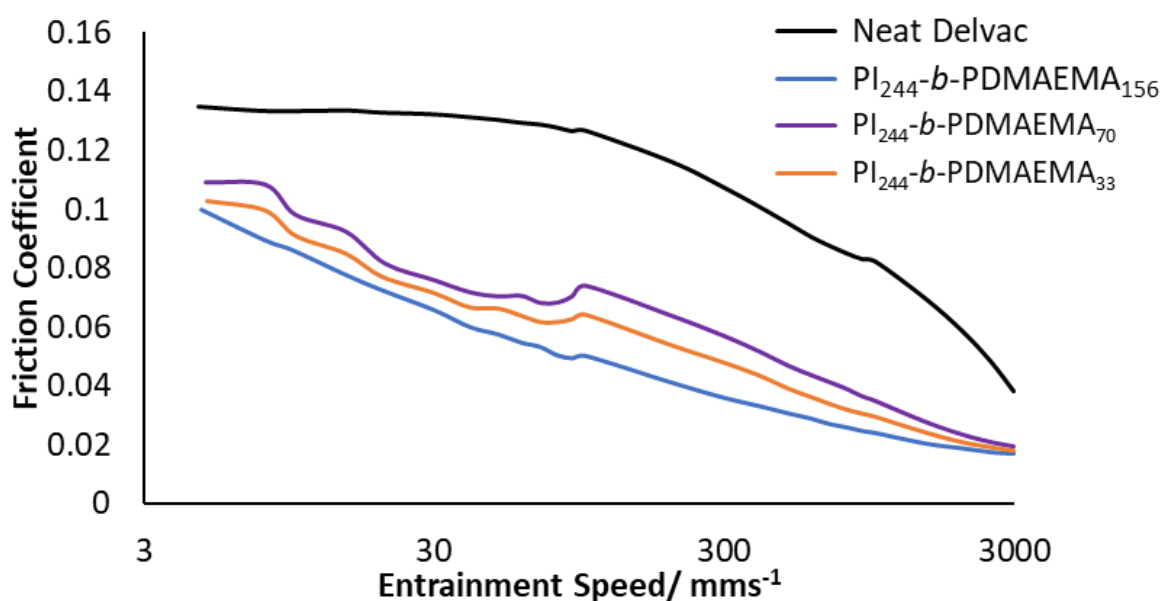
Figure 5.15: Stribeck curve form 2 hour rubbing at 135 °C of the Mobil Delvac 5W30 formulation containing 1 wt% of the specified PI-b-PDMAEMA additives.

As previously observed for the Motul 0W20 formulation (Figure 5.14), the Stribeck curves in Figure 5.15 show no clear correlation between the friction coefficient and molar mass (M_n) of the PDMAEMA block. All PI-b-PDMAEMA block copolymers had a friction coefficient close to 0.02 at 3000 mm s^{-1} and, from 3000 - 5 mm s^{-1}, the friction steadily increased in all cases. At 5 mm s^{-1}, the friction coefficients for PI$_{244}$-b-PDMAMEA$_{156}$ (blue data), PI$_{244}$-b-PDMAMEA$_{33}$ (orange data) and PI$_{244}$-b-PDMAEMA$_{70}$ (purple data) were 0.10, 0.10 and 0.11, respectively. The differences in friction at all entrainment speeds between the samples were very small and as such any differences are not significant. There is a slight suggestion in Figure 5.15 that PI$_{244}$-b-PDMAMEA$_{156}$, gave the lowest friction coefficient at all entrainment speeds. This block copolymer had the greatest $M_{n, PDMAEMA}$ (24.5 kg mol^{-1}),

but there is little correlation with the other PI-*b*-PDMAEMA block copolymers and it is likely that many more samples with different $M_{n, PDMAEMA}$ would need to be prepared to further explore this effect. Although no trend was elucidated from the data in Figure 5.15, the results for all PI-*b*-PDMAEMA block copolymers in Mobil Delvac 5W30 show an improvement in performance compared to the neat formulation. It is worth recalling that Mobil Delvac 5W30 is sold without added friction modifier, due to the aforementioned poor long-term solubility of commercially-available PFMs. It is possible that slight improvements in performance with the addition of the block copolymers, coupled with long term block copolymer solubility, could (if confirmed) prove to be of significant interest. Since this family of block copolymers show reasonably consistent performance with varying molar mass of the PDMAEMA block, this suggests that solubility could be optimised by varying the composition with no apparent loss in friction reduction. This is particularly the case for PI$_{244}$-*b*-PDMAMEA$_{33}$ which had the highest fraction of PI (76 wt%) and as such could be readily dispersed in the non-polar base oils.

5.3. Conclusions

PI-*b*-PMMA and PI-*b*-PDMAEMA block copolymers have been investigated extensively for their potential use as friction modifiers within lubricant formulations. PI-*b*-PMMA was found to be effective in reducing the friction of neat base oil. However, when dispersed into a full Motul 0W20 lubricant formulation, there was no difference in friction in comparison to the neat formulation. This suggests that, while PMMA can reach metal surfaces, it does not bind strongly enough to interact competitively or cooperatively when in the presence of other surface-active additives, common to lubricant formulations.

PI-*b*-PDMAEMA was also found to reduce friction in neat base oil. However, unlike the PMMA block copolymers, the PI-*b*-PDMAEMA copolymers were also found to be effective additives when tested in a full 0W20 formulation. The molar masses of both sets of block copolymers were similar, meaning that the improvement in performance can be ascribed to the introduction of the more Lewis basic tertiary amine functionality of DMEAMA in comparison to the carbonyl of the repeat unit in PMMA. As expected, the amine can interact with the metal surface more strongly, which is expected to form cooperative tribofilms with other surface-active additives, thus reducing friction. Moreover, the PI-*b*-PDMAEMA block copolymers were found to reduce friction in multiple

formulations, suggesting that it has the potential to be a useful additive with a broad scope. Attempts to further optimise the additive by varying the molar mass of PDMAEMA in the block copolymers did not reveal any clear correlation. However, the performance of each additive was maintained even at low molar masses of PDMAEMA, meaning that the solubility of the block copolymer in base oil and formulations was improved without a significant detriment to the friction.

While the performance of the PI-*b*-PDMAEMA in full lubricant formulations is encouraging, it may ultimately be futile if these additives (or something similar in structure) cannot be prepared on an industrial scale. The current change of mechanism polymerisation (CHOMP) procedure for preparing block copolymers in this investigation is not viable for commercialisation because it is over-complicated and requires multiple steps. Therefore, the following chapter describes an investigation into other possible routes towards the synthesis of similar functional polymer additives. The choice of synthetic routes will be highly influenced by the chemical structures found to be effective in applications testing within this chapter.

5.4. References

1. A. Martini, U. S. Ramasamy, M. Len, *Tribol. Lett.*, 2018, **66**, 1-14.
2. G. Verstrate, M. J. Struglinski, *ACS Symp. Ser. Am. Chem. Soc.*, 1991, **462**, 256-272.
3. N. N. Petrukhina, O. N. Tsvetkov, A. L. Maksimov, *Russ. J. Appl. Chem.*, 2019, **92**, 1179-1189.
4. P. Ghosh, A. V. Pantar, U. S. Rao, A. S. Sarma, *Indian J. Chem. Technol.*, 1998, **5**, 309-314.
5. D. Erickson, F. Z. Lu, D. Q. Li, T. White, J. Gao, *Exp. Therm. Fluid Sci.*, 2002, **25**, 623-630.
6. E. Okrent, *ASLE TRANSACTIONS*, 1961, **4**, 97-108.
7. E. Okrent, *ASLE TRANSACTIONS*, 1961, **4**, 257-262.
8. H. Spikes, *Tribol. Lett.*, 2015, **60**, 1-26.
9. J. S. Tse, Y. Song, Z. X. Liu, *Tribol. Lett.*, 2007, **28**, 45-49.
10. A. Somayaji, P. B. Aswath, *Tribol. Trans.*, 2008, **51**, 403-412.
11. G. Tsagkaropoulou, C. P. Warrens, P. J. Camp, *ACS Appl. Mater. Interfaces*, 2019, **11**, 28359-28369.
12. Z. Pawlak, *Tribochemistry of lubricating oils*, Elsevier, Amsterdam, 2003.
13. R. H. Zheng, G. J. Liu, T. C. Jao, *Polymer*, 2007, **48**, 7049-7057.
14. R. H. Zheng, J. D. Wang, G. J. Liu, T. C. Jao, *Macromolecules*, 2007, **40**, 7601-7608.
15. R. H. Zheng, G. J. Liu, M. Devlin, K. Hux, T. C. Jao, *Tribol. Trans.*, 2010, **53**, 97-107.
16. M. J. Derry, T. Smith, P. S. O'Hora, S. P. Armes, *ACS Appl. Mater. Interfaces*, 2019, **11**, 33364-33369.
17. M. Smeeth, H. Spikes, S. Gunsel, *Tribol. Trans.*, 1996, **39**, 726-734.
18. G. Guangteng, H. A. Spikes, *Tribol. Trans.*, 1996, **39**, 448-454.
19. D. Baskaran, *Prog. Polym. Sci.*, 2003, **28**, 521-581.
20. V. Jitchum, S. Perrier, *Macromolecules*, 2007, **40**, 1408-1412.
21. J. Wootthikanokkhan, M. Peesan, P. Phinyocheep, *Eur. Polym. J.*, 2001, **37**, 2063-2071.
22. F. D'Agosto, J. Rieger, M. Lansalot, *Angew. Chem.-Int. Edit.*, 2020, **59**, 2-27.
23. S. L. Canning, G. N. Smith, S. P. Armes, *Macromolecules*, 2016, **49**, 1985-2001.
24. R. Stribeck, *Z. Ver. Dtsch. Ing.*, 1902, **46**, 1341-1348.
25. R. Stribeck, *Z. Ver. Dtsch. Ing.*, 1902, **46**, 1432-1438.
26. R. Stribeck, *Z. Ver. Dtsch. Ing.*, 1902, **46**, 1463-1470.
27. J. L. Bradley-Shaw, P. J. Camp, P. J. Dowding, K. Lewtas, *Phys. Chem. Chem. Phys.*, 2018, **20**, 17648-17657.
28. J. L. Bradley-Shaw, P. J. Camp, P. J. Dowding, K. Lewtas, *Langmuir*, 2016, **32**, 7707-7718.
29. J. L. Bradley-Shaw, P. J. Camp, P. J. Dowding, K. Lewtas, *J. Phys. Chem. B*, 2015, **119**, 4321-4331.
30. H. Okubo, S. Watanabe, C. Tadokoro, S. Sasaki, *Tribol. Int.*, 2016, **94**, 446-457.
31. T. Mang, W. Dresel, *Lubricants and lubrication*, John Wiley & Sons, Weinheim, 2007.
32. D. Bonneau, A. Fatu, D. Souchet, *Internal combustion engine bearings lubrication in hydrodynamic bearings*, Wiley Online Library, 2014.
33. D. M. Pirro, M. Webster, E. Daschner, *Lubrication fundamentals, revised and expanded*, CRC Press, Boca Raton, 2016.
34. J. Fan, M. Muller, T. Stohr, H. A. Spikes, *Tribol. Lett.*, 2007, **28**, 287-298.

35. M. Muller, K. Topolovec-Miklozic, A. Dardin, H. A. Spikes, *Tribol. Trans.*, 2006, **49**, 225-232.
36. T. X. Song, Y. Li, C. Q. Zhang, A. L. Zhang, X. H. Wang, Y. R. Wang, *Acta Polym. Sin.*, 2010, **10**, 143-148.
37. G. Johnston-Hall, M. J. Monteiro, *Macromolecules*, 2007, **40**, 7171-7179.
38. R. R. Bhat, M. R. Tomlinson, T. Wu, J. Genzer, *Surface-grafted polymer gradients: Formation, characterization, and applications*, Springer-Verlag Berlin, Berlin, 2006.
39. Z. L. Tang, S. H. Li, *Curr. Opin. Solid State Mat. Sci.*, 2014, **18**, 119-139.
40. J. Dawczyk, N. Morgan, J. Russo, H. Spikes, *Tribol. Lett.*, 2019, **67**, 34-48.
41. G. Fernandes, P. Zanotto, A. Sinatora, *Lubricants*, 2016, **4**, 18-27.
42. S. Bahadur, *Wear*, 2000, **245**, 92-99.
43. V. K. Jain, S. Bahadur, *Wear*, 1978, **46**, 177-188.
44. S. Bahadur, D. Tabor, *Wear*, 1984, **98**, 1-13.
45. S. Bahadur, D. L. Gong, J. W. Anderegg, *Wear*, 1992, **154**, 207-223.
46. N. V. Sastry, H. Hoffmann, *Colloid Surf. A-Physicochem. Eng. Asp.*, 2004, **250**, 247-261.

6. Preparation of Maleinised and Imidised Polybutadiene for Lubricancy Applications

6.1. Introduction

In the previous chapter, the applications testing of two classes of polyisoprene-based block copolymers, for potential use as lubricant additives was discussed. PI-*b*-PMMA block copolymers were found to act as effective friction modifiers in neat base oil, however they did not exhibit any friction reduction in a full lubricant formulation, which contains many other surface-active additives. PI-*b*-PDMAEMA was found to be effective as a friction modifier both in neat solutions of base oil, and in several full lubricant formulations. However, whilst the Change of Mechanism Polymerisation (CHOMP) procedure (described in Chapters 3 and 4) used for their synthesis was useful as a means of quickly preparing several different families of block copolymers, it is industrially unfeasible because of the multiple steps required, some of which are likely to be costly and complicated. Therefore, it was considered important to explore more commercially viable routes towards preparation of these (or chemically similar) additives.

In order to devise a commercially viable route for the polymer synthesis, an alternative approach was adopted in which a single polymerisation mechanism was used. Therefore, in this chapter, the selective maleinisation of polybutadiene is described, which introduces functionality onto the polybutadiene, thus avoiding the polymerisation of a second polar monomer, such as DMAEMA, by a second mechanism. 1,3-butadiene is a cheap monomer that is commonly polymerised on an industrial scale by LAP.[1, 2] The polymerisation has been extensively studied and as such is well understood. Butadiene may polymerise with 4 different microstructures: 1,4-trans, 1,4-cis, 1,2-vinyl and cyclic (see structures in Figure 6.1)[3] and the proportion of each can be varied by careful control of the reaction conditions (e.g. reaction temperature, solvent polarity, additives etc.) and a different ratio of microstructures can deliver different physical properties (e.g. viscosity and glass transition temperature).[4-6] The 1,4 and 1,2 microstructures (Figure 6.1a-c) are formed from a single repeat unit of butadiene while the cyclic microstructure (Figure 6.1d) arises via the backbiting reaction of a propagating poly-1,2-butadienyl chain end with the

penultimate 1,4 unit. This was first identified by Quack *et al.* by use of proton and carbon NMR spectroscopy.[7]
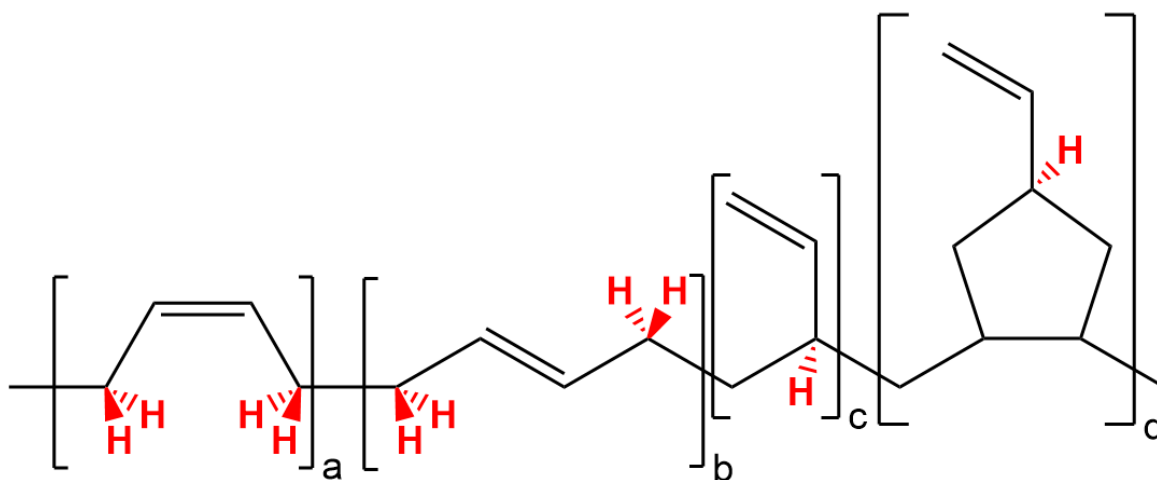
Figure 6.1: Chemical structure of polybutadiene showing the 4 different, commonly produced microstructures: a) 1,4-cis, b) 1,4-trans, c) 1,2-vinyl and d) cyclic. α-protons are highlighted in red for subsequent discussion.

All microstructures shown in Figure 6.1 give polybutadiene with double bonds either in or pendant to the polymer backbone. These alkene bonds can act as a reactive group that may be exploited to introduce polar functional groups into the otherwise non-polar polymer. Double bonds can be reacted with a variety of molecules to give polar products. One common example is epoxidation, the products of which can be reacted further by ring-opening to introduce other, different functional groups.[8] The different microstructures shown in Figure 6.1 have double bonds with different degrees of substitution, with the double bonds in the 1,4-repeat unit being 1,2-disubstituted and double bonds in the 1,2-vinyl and cyclic repeat units being monosubstituted. These differences mean the double bonds have different reactivities which can be exploited to exploit selectivity in the functionalisation of polybutadiene.[9]

The 'ene' reaction occurs between an electron-deficient alkene and an alkene containing an allylic hydrogen.[10, 11] Although similar to the Diels-Alder reaction, the 'ene' reaction is distinctive because of the breaking of the C-H bond α to the alkene[12] (highlighted red in Figure 6.1), which typically means a higher reaction temperature is required to drive the reaction to high conversion (see mechanism in Scheme 6.2). One of the more common reagents used as the electron-deficient alkene is maleic anhydride. The relative rates of

reaction for maleic anhydride with 'small molecule' alkenes and polydienes has been discussed in the literature. Benn *et al.* investigated the reaction of maleic anhydride with various 1-alkenes, cis-5-decene, and trans-5-decene. The reactions were carried out with a 1:1 molar ratio of the reagents in different solvents at different temperatures. The products were analysed with gas liquid chromatography (GLC) to measure the rate constant at various temperatures. The reaction was found to be first order with respect to both the alkene and the maleic anhydride. It was concluded that the energy of activation was similar for cis-5-decene and trans-5-decene (75.5 and 77.1 kJ mol^{-1}, respectively) which was lower than the 1-alkenes (90.0 kJ mol^{-1}); a result of the increased electron density of the disubstituted alkenes. Moreover, the entropy of activation was calculated to be lowest for cis-5-decene (-191 J mol^{-1} K^{-1}) and highest for the 1-alkenes (-152 J mol^{-1} K^{-1}) with trans-5-decene being -178 J mol^{-1} K^{-1}. The highly negative entropies of activation indicate an ordered transition state. They went on to predict that the reaction rate would be slowest for the 1-alkenes at below 371 K, but fastest above 481 K. They concluded that the reaction must proceed through an *exo* transition state rather than *endo* which is likely a consequence of the sterically hindrance of the latter. The 'ene' reaction of maleic anhydride with polybutadiene has been exploited industrially for improving the compatibility of polybutadiene with different materials. The different rates of the 'ene' reaction for the different types of alkenes has also been discussed (to some extent) in the literature, in particular by Ferrero, who investigated thermal maleinisation for 3 polybutadienes, each with a different microstructure. Ferrero established first order reaction kinetics for the reaction of maleic anhydride with polybutadiene and a greater reactivity of the 1,4 microstructure.[13] Ferrero went on to use DSC to show that polybutadiene with a higher 1,4 content had a lower activation energy for maleinisation than those with a high 1,2 content which further indicated the selectivity for maleinisation, which is consistent with the findings of Benn *et al*.[14] They also investigated the effect of different solvents when the thermal maleinisation was not carried out in bulk, albeit there is a limited choice of solvents with both a sufficiently high boiling point and capable of solubilising polybutadiene before and after maleinisation - o-xylene and decahydronapthalene being suitable solvents.[15] In this investigation, they showed that higher yields (up to 80.6 %) could be achieved with the latter solvent even after 1 hour at just 130 °C (c.f. 49.2 % yield for the comparable reaction in o-xylene). No reason was suggested for this observation.

The selectivity for the 1,4 microstructures in polybutadiene perhaps seems counter-intuitive given the steric hindrance of the double bond in the backbone in comparison to the more available pendant double bond in the 1,2- repeat unit. However, there are several key factors which can favour the reaction with the 1,4 microstructures instead of the 1,2 microstructures. Firstly, the disubstituted alkenes in the 1,4 microstructures are more nucleophilic than the monosubstituted alkenes in the 1,2 and cyclic microstructure because of the electron-donation of the alkyl substituents. This would increase the rate of the nucleophilic attack onto the electron-deficient alkene of maleic anhydride in a similar fashion to the nucleophilic attack of alkenes in an epoxidation reaction. Furthermore, The 1,4-microstructures also contain 4 α protons compared with only 1 in the 1,2 and cyclic microstructures. This would increase the likelihood of an α-hydrogen reacting with maleic anhydride and therefore the rate of the reaction. Further to this, the α-hydrogen in a 1,2 repeat unit is somewhat more sterically hindered than the 1,4 microstructure, which is not in close proximity for the microstructure (see mechanism in Scheme 6.2).
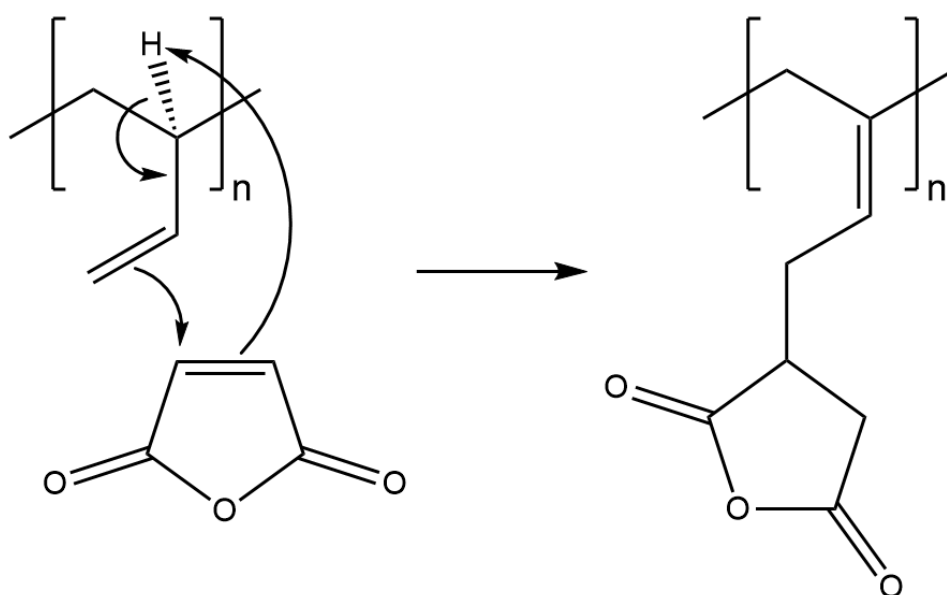
Scheme 6.2: Reaction mechanism for the maleinisation of 1,2-polybutadiene

As described in the previous chapters, block copolymers appear to perform better as friction modifiers than analogous statistical copolymers.[16] In this chapter, we will describe how the selectivity of the maleinisation reaction can be manipulated to prepare

'blocky' copolymers from polybutadiene. Thus, by controlling and changing the reaction conditions during the polymerisation of polybutadiene, a sample can be prepared with blocks comprising differing proportions of the microstructures. The selectivity of the maleinisation reaction results in an amphiphilic copolymer which has a higher fraction of anhydride contained within one of the 'blocks'. Subsequently, in order to mimic the chemical structure of PDMAEMA in block copolymers, the selectively introduced maleic anhydride will be used to introduce a tertiary amine functionality by an imidisation reaction with 3-(dimethylamino)-1-propylamine (DMAPA).

6.2. Results and Discussion

The use of polymeric friction modifiers (PFMs) is often limited by the commercial challenges in synthesising amphiphilic copolymers that are soluble in non-polar base oils and capable of lubricating metal surfaces.[17, 18] Commercially, the synthesis is generally only possible by free radical polymerisation which limits the structures to statistical copolymers with a monomer sequence that is dictated by the reactivity ratios.[19] However, block copolymers have previously been shown to be more effective as friction modifiers than chemically equivalent statistical copolymers.[16] The discussion in the previous chapter showed that PI-*b*-PDMAEMA block copolymers are particularly effective PFMs in both neat solutions of base oil and full lubricant formulations. Herein, the preparation and testing of chemically-analogous polymers is described, by use of a single polymerisation mechanism (living anionic polymerisation) and facile post-polymerisation modifications (maleinisation and imidisation).

6.2.1. Polymer Synthesis and Post-Polymerisation Modification

The change of mechanism polymerisation (CHOMP) procedure described previously for the preparation of polyisoprene-based block copolymers is not considered feasible on an industrial scale. With the aim of developing a more commercially-viable approach, a procedure was devised whereby polybutadiene with a controlled block-like distribution of varying microstructure could be prepared by living anionic polymerisation. The difference in the reactivity of the different alkenes in the (different microstructures of the) final polymer could then be exploited during post-polymerisation selective maleinisation reactions, to introduce Lewis basic functionalities, which have been shown in chapter 5 to be vital for binding to the metal surfaces in applications testing.

6.2.1.1. Preparation of Microstructural-Block Copolymers of Polybutadiene

The first step in the preparation of the polymers discussed herein was the living anionic polymerisation of 1,3-butadiene. Unlike the polymer syntheses described in previous chapters, where conventional trap-to-trap distillation under reduced pressure was used for LAP, the preparation of polybutadiene was carried out in the R&D labs at Synthomer, using a more 'commercial' synthetic protocol. The LAP was carried out above ambient temperature in a non-polar solvent.

The aim was to prepare polybutadiene such that a first 'block' was rich in the 1,4 microstructures and the second 'block' was rich in the 1,2-microstructures. Following this, a post-polymerisation maleinisation reaction, which is selective towards 1,4-repeat units, could be used to prepare amphiphilic copolymers with the first (high 1,4-microstructure) block becoming maleinised in preference to the second block. The synthesis of the block-like polybutadiene with blocks of different microstructure composition was achieved by controlling the conditions of the two stages of the polymerisation. The polymerisation of the first 'block' was carried out in a non-polar solvent which gives a high 1,4 content.[20] For the preparation of the second 'block', a commercial polar modifier was added into the reactor, which results in the polymerisation of butadiene with a high(er) content of the 1,2 microstructure.[3] The temperature for the polymerisation of the second block was lower for PBD2 and PBD3 than PBD1, the reason for which is discussed in more detail below. As well as the 3 'blocky' polybutadienes, a commercial grade (PBD4) was included for comparison. The molar mass data for all of these polymers is reported in Table 6.7.

Table 6.7: Molecular weight data from the triple detection SEC in THF of polybutadienes prepared by anionic polymerisation.

Polymer	1st Block			Final Polymer		
	$M_{n, Target}$/ g mol^{-1}	$M_{n, SEC}$/ g mol$^{-1 a}$	Đ [b]	$M_{n, Target}$/ g mol^{-1}	$M_{n, SEC}$/ g mol$^{-1 a}$	Đ [b]
PBD1	2500	3170	1.05	10000	7700	1.34
PBD2	5000	6060	1.03	10000	11090	1.05
PBD3	2500	3430	1.09	10000	12110	1.07
PBD4	-	-	-	9000	9650	1.04

a: $M_{n,SEC}$ calculated using dn/dc = 0.124 mL g^{-1},
b: Dispersity from $M_{w,SEC}/M_{n,SEC}$

The target molar masses for the final product of PBD1, PBD2 and PBD3 was 10000 g mol^{-1} which was chosen to be similar to the commercial grade (PBD4) . The data in Table 6.7, reveals that the M_n for PBD1 was 7700 g mol^{-1} which is significantly lower than the target. The dispersity for this polymer was 1.34 which is also far broader than would be expected for living anionic polymerisation. The first block of PBD1 had a target molar mass of 2500 g mol^{-1}, which was chosen because this would be the 1,4-rich block and as such would be expected to be preferentially maleinised over the second block. The actual M_n for the first block was 3170 g mol^{-1} which is in good agreement with the target and the dispersity was 1.05 which also suggests that the polymerisation was controlled. This suggests that the problems arose during the polymerisation of the second block of PBD1. The polymerisation of the second block was carried out with the addition of the polar modifier which is well known to change the proportions of the microstructure.[3] SEC traces for PBD1 polymerised under these conditions are shown below in Figure 6.2.
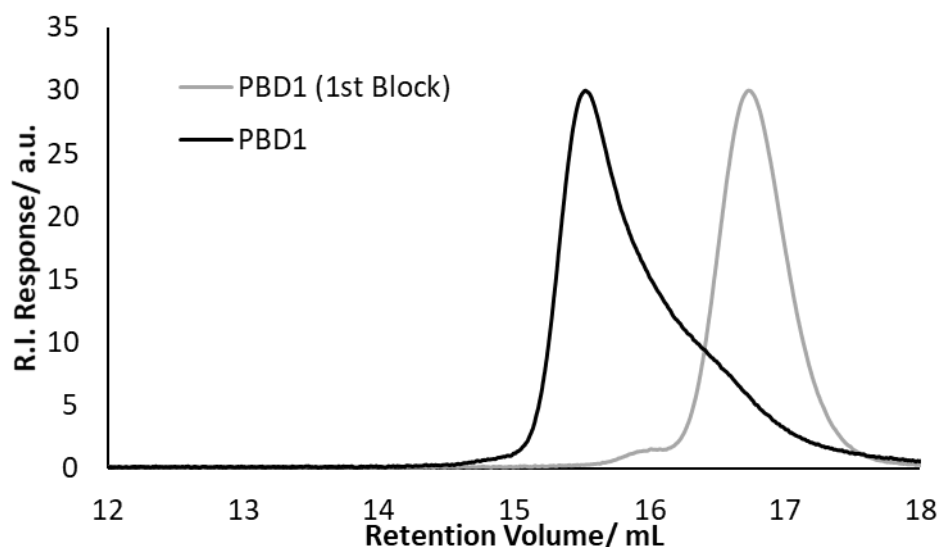
Figure 6.2: Refractive index signal from SEC traces of the 1st block and the final product of PBD1

The SEC traces of PBD1 (Figure 6.2) confirm that the dispersity broadened significantly during the polymerisation of the second block. The most likely reason for the broad dispersity is chain transfer.[3] Although a broad dispersity itself is not necessarily problematic for friction modification, chain transfer would prevent the sole formation of microstructural blocks and result in the presence of 1,2-rich homopolybutadiene. It is likely that the chain transfer we have observed could be reduced/eliminated by decreasing the amount of polar modifier in the reaction, however, this would also significantly decrease the 1,2 content in the second 'block'.

The conditions for the synthesis of PBD2 were therefore changed in an attempt to eliminate/reduce chain transfer. PBD2 had the same target molar mass for the final polymer (10000 g mol^{-1}), however, the target molar masses for the different blocks were changed to 5000 g mol^{-1} for each, such that any effect of different block lengths on friction performance could be elucidated (in a similar fashion to the CHOMP mechanism explored for PI-*b*-PMMA and PI-*b*-PDMAEMA in Chapters 3-5). The conditions for the polymerisation of the first block were identical to the first block of PBD1 which previously showed no chain transfer and once again, this resulted in a molar mass (M$_n$ 6060 g mol^{-1}) which was in good agreement with target molar mass and a narrow dispersity (1.03). However, for the synthesis of the second block the reaction temperature was reduced. In spite of being the most likely cause of chain transfer, the polar modifier was maintained at the same level of molar equivalents w.r.t initiator because decreasing this would be expected to reduce the

1,2-content.[3] The results in Table 6.7 show that these new conditions were successful in controlling the polymerisation of the second block, with the final polymer having M_n of 11090 g mol^{-1}, which is close to the target of 10000 g mol^{-1}, and also a narrow dispersity of 1.05. This suggests that the lower reaction temperature is sufficient to reduce/eliminate the effect of chain transfer during the polymerisation. Figure 6.3 shows the SEC traces for the first block and the final polymer of PBD2 which confirms that PBD2 has a much narrower dispersity than PBD1. Following the optimisation of the conditions in PBD2, PBD1 was repeated (as PBD3) using the same conditions as for PBD2 and this also showed good control in the M_n (12110 g mol^{-1}) and dispersity (1.07) which further demonstrates that chain transfer was no longer an issue.

PBD4 will act as an alternative to the other polybutadiene polymers because the 1,4 microstructure should be randomly distributed along the chain and, as such, maleinisation should take place indiscriminately along the polymer to give a random copolymer. PBD4 had a molar mass which was close to the other polymers (9650 g mol^{-1}) and a similarly narrow dispersity (1.04) so should be a useful comparison during friction testing.

6.2.1.2. Determination of Microstructure in Polybutadiene

A key property of the polybutadiene samples in this study (Table 6.7) is the microstructure of the first and second block, because the maleinisation reaction is selective towards the 1,4 microstructure rather than the 1,2 and cyclic polybutadiene. The microstructure can be calculated from the proton NMR spectra. An exemplar proton NMR
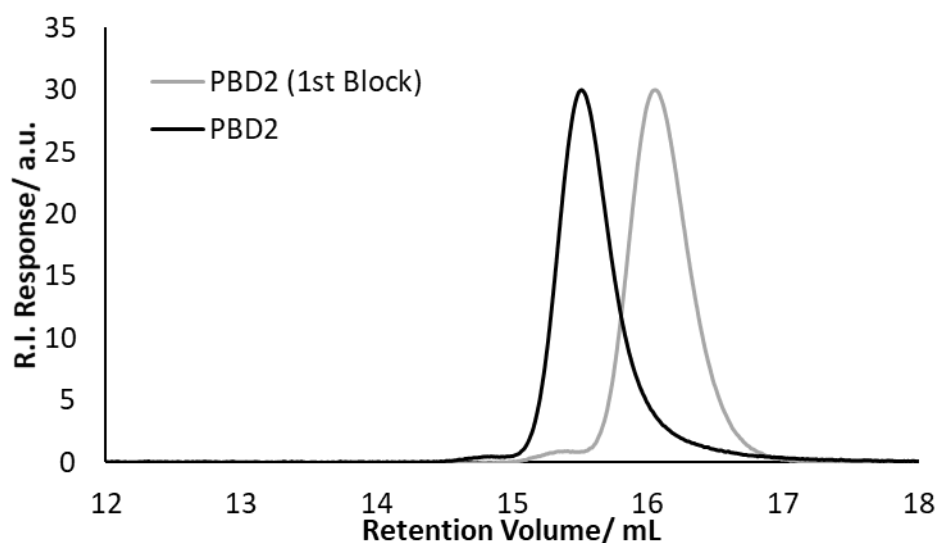
Figure 6.3: Refractive index signal from SEC traces of the 1st block and the final product of PBD2

for the first 'block' of PBD2 is shown in Figure 6.4. Below this is an example equation showing the method for calculating the relative % of the 1,4 microstructure.
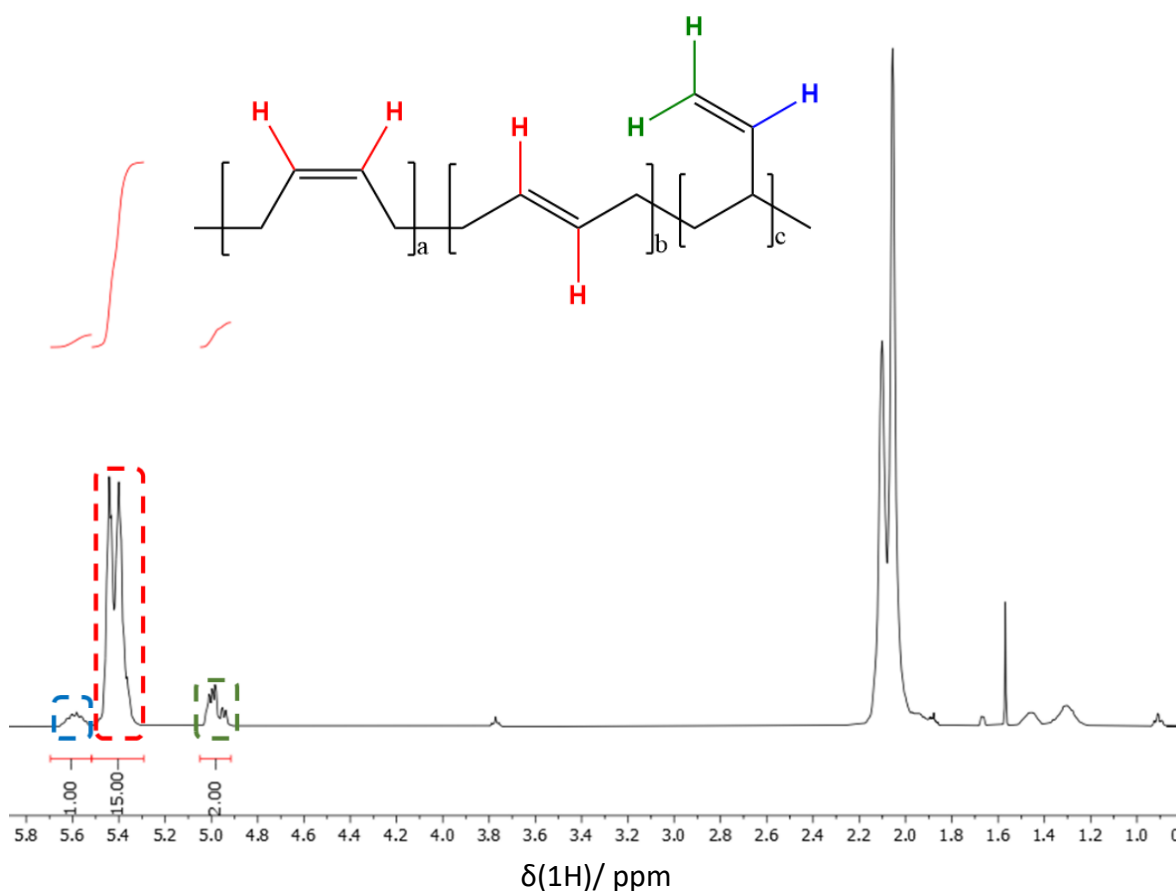
Figure 6.4 Proton NMR used for microstructure determination for the first 'block' of PBD2

$$\%(1,4) = \frac{\int_{5.29-5.52\ ppm}}{2} \div \left(\frac{\int_{5.29-5.52\ ppm}}{2} + \int_{5.52-5.70\ ppm} \right) = 7.5 \div (7.5 + 1) = 88\ \%$$

Figure 6.4 shows all of the expected peaks for polybutadiene.[21] The first 'block' contains no cyclic microstructure because the polar modifier, which promotes its formation, was not present. The peaks above 4.8 ppm can be ascribed to the various alkene protons and can therefore be used to determine the percentage of each microstructure as is shown in the calculation. Following polymerisation of the first 'block', the second 'block' was polymerised in the presence of the polar modifier which is known to promote the formation of a higher proportion of the 1,2 and cyclic microstructures. A proton NMR spectrum for the final polymer of PBD2 is shown below in Figure 6.5 with the equations used for the calculation of the percentage of each microstructure.
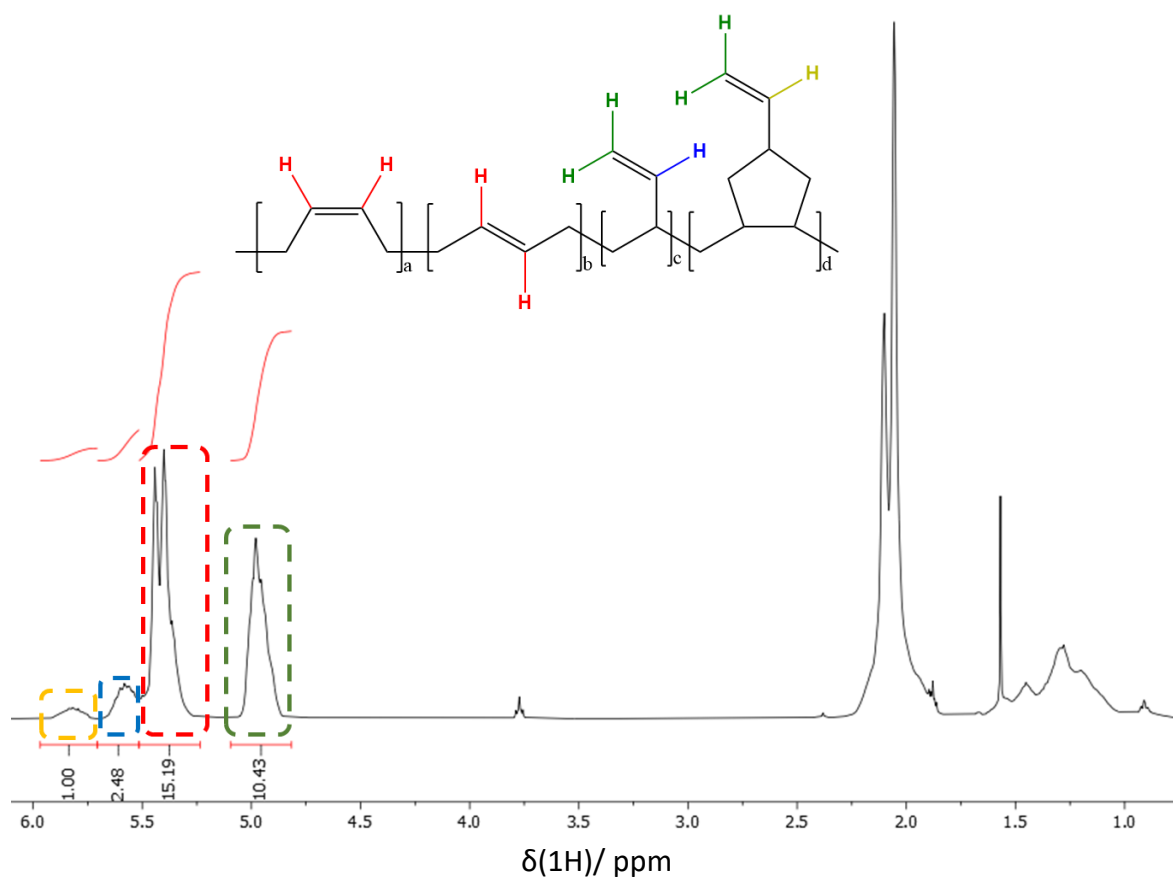
Figure 6.5: Proton NMR for the final polymer of PBD2

$$\%(1,4) = \frac{\int_{5.29-5.52\,ppm}}{2} \div \left(\frac{\int_{5.29-5.52\,ppm}}{2} + \int_{5.52-5.70\,ppm} + \int_{5.70-5.97\,ppm} \right)$$

$$= 7.60 \div (7.60 + 2.48 + 1.00) = 69\,\%$$

$$\%(1,2) = \int_{5.52-5.70\,ppm} \div \left(\frac{\int_{5.29-5.52\,ppm}}{2} + \int_{5.52-5.70\,ppm} + \int_{5.70-5.97\,ppm} \right)$$

$$= 2.48 \div (7.60 + 2.48 + 1.00) = 22\,\%$$

$$\%(Cyclic) = 100\,\% - \%(1,4) - \%(1,2) = 100\,\% - 69\,\% - 22\,\% = 9\,\%$$

The key difference between the NMRs of the first 'block' of PBD2 (Figure 6.4) and the final product (Figure 6.5) is the emergence of the peak at 5.80 ppm which is characteristic of the cyclic microstructure of polybutadiene.[7] The percentages for the microstructures can then be combined with the molar mass data for the first block and the final polymer to calculate the microstructure of the second block. An example calculation is shown below for the calculation of %(1,4) in the second block of PBD2. The same calculation was applied to the 1,2 and cyclic microstructures using the values calculated

above. The data for the microstructures of all polybutadienes prepared is tabulated below in Table 6.8.

$$M_{n,(1,4\ 1st\ Block)} = \%(1,4\ 1st\ Block) \times M_{n,1st\ Block} = 88\ \% \times 6060\ gmol^{-1}$$
$$= 5330\ gmol^{-1}$$

$$M_{n,(1,4\ 2nd\ Block)} = \left(\%(1,4\ Total) \times M_{n,Total}\right) - M_{n,(1,4\ 1st\ Block)}$$
$$= (69\ \% \times 11090\ gmol^{-1}) - 5330\ gmol^{-1} = 2320\ gmol^{-1}$$

$$\%(1,4\ 2nd\ Block) = M_{n,(1,4\ 2nd\ Block)} \div \left(M_{n,Total} - M_{n,1st\ Block}\right) \times 100\ \%$$
$$= 2320\ gmol^{-1} \div (11090\ gmol^{-1} - 6060\ gmol^{-1}) \times 100\ \% = 46\ \%$$

Table 6.8: Data for the microstructures of polybutadienes prepared by anionic polymerisation. Calculated from the 1H NMR spectra (example shown in Figure 6.5)

Sample	1st Block		2nd Block			Total		
	1,4	1,2	1,4	1,2	Cyclic	1,4	1,2	Cyclic
PBD1	88 %	12 %	25 %	41 %	34 %	51 %	29 %	20 %
PBD2	88 %	12 %	46 %	34 %	20 %	69 %	22 %	9 %
PBD3	87 %	13 %	45 %	38 %	17 %	57 %	31 %	12 %
PBD4	-	-	-	-	-	88 %	12 %	0 %

The data in Table 6.8 shows that the microstructures of PBD4 and the first blocks of PBD1-3 which were all polymerised under identical conditions, are almost equal. They all have a 1,4 content of approximately 88 % which is in excellent agreement with previous results for polybutadiene prepared in non-polar solvents using a *s*-BuLi initiator.[3] This is also identical to the microstructure of polyisoprene prepared in the preceding chapters, in which the living anionic polymerisation was also carried out in a non-polar solvent.

The final microstructures of PBD1-3 have much lower 1,4 contents which is to be expected because of the presence of the polar modifier during the polymerisation of the second block.[3] For PBD1, the percentage of 1,4 microstructure in the second block is 25 %. Because this polymer was previously shown by SEC to have poor control in the molar mass and the dispersity in the second block (see Table 6.7), the second block of PBD2 and PBD3

was carried out at a lower temperature than PBD1. This gave better control in the molar mass and dispersity for the polymers (see Figure 6.3), however, the data in Table 6.8 shows that this also means that the 1,4 content for the 1,2-rich second block has increased (46 % and 45 % for PDB2 and PBD3, respectively), which is in agreement with the literature.[3] In all cases, this still represents a significant amount of the 1,4 microstructure distributed along the second block. This will mean that, in spite of the blocky design of PBD1, PBD2 and PBD3, the maleinisation reaction, which is selective for 1,4-repeat units can occur at sites along the entire polymer rather than being confined wholly to the 1,4-rich block. However, statistically, the maleinisation reaction should still be more likely in the 1,4-rich block. The experimental conditions chosen for the anionic polymerisation reactions were based on a single standard industrial method. It would be possible to increase the 1,4-content in the 1,4-rich block and the 1,2-content in the 1,2-rich block by investigating other reaction conditions i.e., different solvent, polar modifier. For example, Poshyachinda *et al.* prepared blocky copolymers of polybutadiene with rich 1,4 and 1,2 blocks by living anionic polymerisation in cyclohexane, with the second block proceeding in the presence of 1,2-dipiperidinoethane (DIPIP); an additive which complexes strongly with the living polybutadienyllithium chain end to favour formation of the 1,2 vinyl microstructure.[22] By use of Raman spectroscopy, they were able to calculate a microstructure of 91 % 1,4 in the 1st block and 94 % 1,2 in the 2nd. For their block copolymers, the preference of the maleic anhydride for the 1,4 microstructure would likely result in far more 'block-like' amphiphilic block copolymers. However, given that the aim of this chapter is to develop more commercially-viable synthetic strategies (and noting the extremely high cost of DIPIP), this was not pursued herein. Due to time constraints, other reaction conditions were not priorities for investigation. It was hoped that, for the polymers described in Table 6.8, the higher 1,4 content in the 1,4-rich block would be sufficient to increase the degree of maleinisation in that block relative to the 1,2-rich block, resulting in an amphiphilic, blocky copolymer.

6.2.1.3. Maleinisation of Polybutadiene

Maleinisation is a commonly used industrial process for introducing polar functionality to non-polar dienes.[23, 24] This can be carried out for a number of different applications but is primarily to improve the compatibility of polybutadiene with polar

materials.[25, 26] Once reacted onto the polymer backbone, the anhydride can act as a platform to introduce many other easily accessible functional groups depending on the application. The maleinisation reaction is known to be selective towards the 1,4 microstructure of polybutadiene, due to the increased nucleophilicity of the disubstituted alkenes. Several blocky copolymers of polybutadiene with 1,4-rich and 1-2-rich blocks have been prepared and they can be selectively maleinised to produce an amphiphilic, gradient copolymer where, following maleinisation, one 'block' will become maleic anhydride-rich.

The maleinisation reaction was carried out at high temperature according to the common industrial practice. This process is known to reach extremely high conversion, which is important because unreacted maleic anhydride can be environmentally harmful and hazardous to health. For this project, the maleinisation was carried out to targets of 5 wt% and 10 wt% w.r.t total mass of polybutadiene (equivalent to 3 and 6 mol% w.r.t. diene repeat units), which are both common levels of maleinisation for commercially available products. Variation in the level of maleinisation could be useful in balancing the level of Lewis basicity necessary for friction reduction and dispersibility in the non-polar base oil; an issue that was important to consider in the previous chapter when considering the mole fraction of the blocks in PI-*b*-PMMA and PI-*b*-PDMAEMA. SEC traces for PBD2 before and after maleinisation, to both 5 and 10 wt%, are shown below in Figure 6.6.
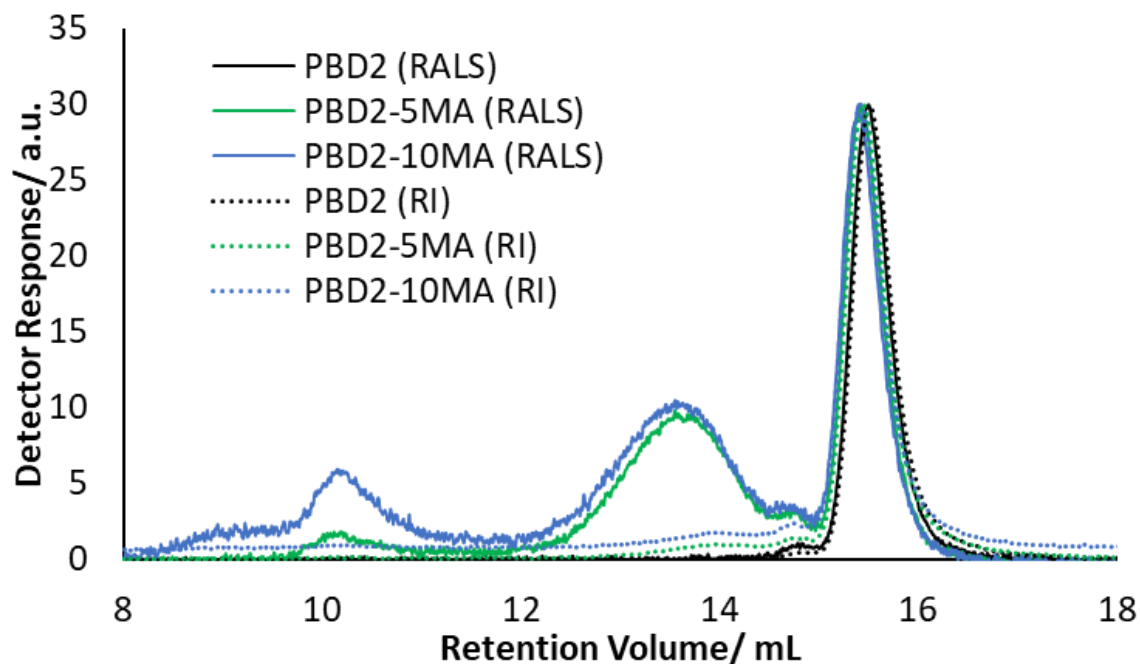
Figure 6.6: SEC (RI and RALS) chromatograms for PBD2 and the subsequent maleinised analogues to 5 wt% (PBD2-5MA) and 10 wt% (PBD2-10MA)

Figure 6.6 shows some clear differences in the polymers following maleinisation. The signal from the RI and RALS detectors shows that there is a slight shift in the 'main peak' (at 15.4 mL) to lower retention volume. This is consistent with an increase in the M_n which is expected upon maleinisation of the polymer. Furthermore, PBD2-10MA eluted slightly before PBD2-5MA which also indicates a higher molar mass of the polymer with a higher target degree of maleinisation. This is also indicated by the M_n calculated from triple detection SEC (with dn/dc of 0.124 mL g^{-1}) where PBD2-5MA and PBD2-10MA had molar masses of 12500 g mol^{-1} and 13100 g mol^{-1}, respectively. The main peak also appears to be a similar breadth in all cases which, for the most part, indicates similar dispersity properties of the polymer. However, in the RALS trace, the maleinised polymers also show 2 significant peaks at 13.5 mL and 10.1 mL. This suggests the presence of some higher molar mass species following the maleinisation reactions. This is not entirely unexpected because the maleinisation reaction was carried out at high temperature, which can oxidatively degrade polybutadiene.[27] Similar observations have previously been made by Pucci *et al.* where the ene reaction was carried out between poly(styrene-butadiene-styrene) (SBS) triblock copolymer and varying amounts of diethyl maleate (DEM) at 200 °C with different Lewis acid catalysts.[28] They reported a decrease in the M_n and an increase in M_w by SEC (without

showing the traces). The changes were variable depending on the reaction conditions with the unreacted SBS having a dispersity of 1.2 and those reacted with a higher target mol% of DEM reaching as high as 2.9. Interestingly, in the same paper, they had previously used maleic anhydride for the ene reaction with polyisobutylene (PIB) oligomers, however they mention that the reaction of maleic anhydride with SBS resulted in crosslinked materials. They suggest the increased dispersity was a result of 'degradation and crosslinking reactions' which they go on to suggest could be attributed to the complex formation between the Lewis acid catalysts and the exo alkenes of the 1,2-microstructure of PBD in SBS. The RI signal intensity for the PBD2-5MA and PBD2-10MA chromatograms is very low at the elution volumes where the peaks occur in the RALS, which suggests that the high molar mass polymers are present at a very low concentration in the polymer, which should mean they have little impact on the friction performance in the friction testing.

The extent of maleinisation was ascertained from the FTIR and the NMR of the maleinised polymers. The FTIR spectrum for PBD2-10MA is shown in Figure 6.7 overlaid with the spectrum for the 'unmaleinised' precursor PBD2 (first block and final polymer).
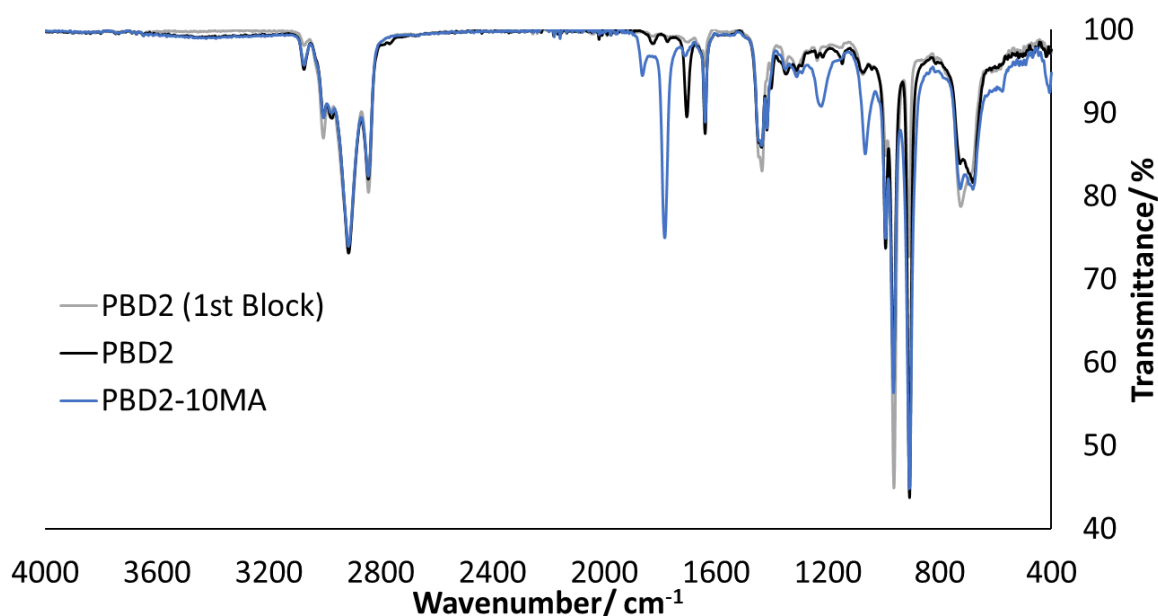
Figure 6.7: Overlaid FTIR spectra for PBD2 (1st block and final polymer) and the 10 wt% maleinised analogue (PBD2-10MA)

The FTIR data in Figure 6.7 for PBD2 shows some slight differences between the FTIR for the first block and the final polymer of PBD2. The key peak that emerges for the final polymer is at 1705 cm^{-1}. This is likely to be caused by the increased percentage of the monosubstituted alkene (1,2 microstructures) which are present in far greater proportions in the second block than the first (see Table 6.8). PBD2-10MA shows the emergence of a strong peak at 1784 cm^{-1} which is characteristic of the asymmetric stretch of the carbonyls in an anhydride, whilst the peak at 1863 cm^{-1} is likely to be the symmetric stretch of the carbonyls in an anhydride. As is expected for a saturated, cyclic anhydride, the latter is a weaker peak. This is in excellent agreement with FTIR results of maleinised polybutadiene published by Öztürk *et al*. who reported the carbonyl stretches at 1862 and 1783 cm^{-1}.[29] These peaks strongly suggest a successful maleinisation of polybutadiene.[30, 31] Also, PBD2-10MA shows a peak at 1067 cm^{-1} which is characteristic of an anhydride functional group. Furthermore, there is a peak at 1224 cm^{-1} which is typical of a C-O stretch, also present in anhydrides. Whilst the FTIR is useful for qualitative analysis, it cannot be used for accurately determining the percentage of maleinisation. Therefore, the proton NMR spectra of all maleinised polymers were obtained, and a typical example (for PBD2-10MA) is shown below in Figure 6.8. An example calculation for the degree of maleinisation is shown below.
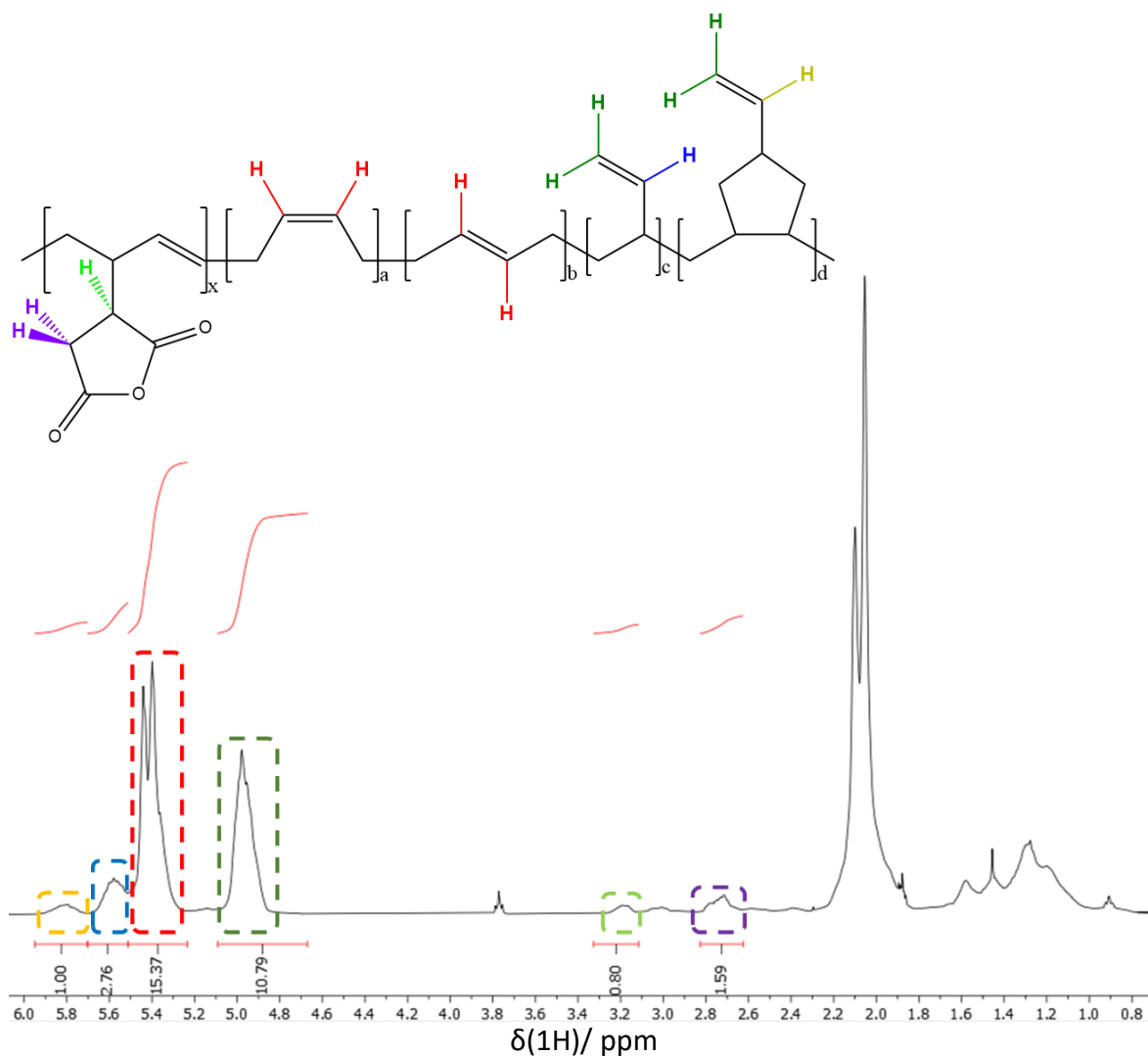
Figure 6.8: Characteristic ^1H NMR spectrum for PBD2-10MA prepared by maleinisation of PBD2. NMR spectrum referenced to the solvent, CDCl₃, peak at 7.26 ppm

$$mol\% \ (MAL) = \int_{3.19 \ ppm} \div \left(\frac{\int_{4.98 \ ppm} + \int_{5.35-5.51 \ ppm}}{2} + \int_{3.19 \ ppm} \right)$$

$$= 0.80 \div \frac{10.79 + 15.37}{2} + 0.80 = 5.83 \ mol\%$$

The NMR spectrum in Figure 6.8 shows all of the characteristic peaks for polybutadiene that were previously observed for precursor PBD2 in Figure 6.5.[21] The key difference in this spectrum is the emergence of peaks at 2.72 ppm and 3.19 ppm which are for those of the anhydride bound to the polymer backbone.[31, 32] The calculation below Figure 6.8 shows how the mol% of maleinisation was calculated. For this reaction, the

target degree of maleinisation was 10 wt%. From the masses used for the reactions and the molar mass of the PBD repeat unit (54.09 g mol^{-1}), the target mol% can be calculated to be 5.93 mol%. Therefore, Figure 6.8 suggests a 98 % conversion during the maleinisation reaction. This was expected for the ene reaction which is known to reach high conversion for polybutadiene under these reaction conditions, which is important for not leaving unreacted maleic anhydride which is a known health hazard.

The NMR spectrum in Figure 6.8 suggests that the maleinisation reaction could be selective for the 1,4 microstructure. However, the protons attached to the double bond formed as a result of maleinisation will have a similar chemical shift to the alkene protons of the unmaleinised PBD. Upon re-calculating the microstructure using the equation described previously in Figure 6.5, PBD2-10MA has a 1,4 content of 67 % which is slightly decreased from the value of 69 % for PBD2, which could indicate a selectivity for the 1,4 microstructures, albeit with the calculations likely having some error because of the expected overlap of the alkenes in the maleinised product with the unreacted alkenes of PBD. This would be in agreement with the work of Ferrer *et al.*, who have previously used DSC to show a greater rate of reaction for 1,4-rich polybutadienes with maleic anhydride and also a lower activation energy.[14] However, the result from the NMR is likely to be within reasonable experimental error for the calculation, particularly considering the likelihood of overlapping peaks for the alkenes in the product. It would be recommended that a study on small molecule alkenes be carried out to determine the true selectivity of the ene reaction of maleic anhydride with the different microstructures of polybutadiene.

6.2.1.4. Imidisation of Maleinised Polybutadiene

In the previous chapter it was reported that tertiary amines, such as those found in PDMAEMA, are a useful functional group for friction reduction because their Lewis basicity allows for adsorption to metal surfaces. This was in contrast to ester functionalities of PMMA which were found to be useful in neat base oil, but were not Lewis basic enough to bind to metal surfaces in the presence of other amphiphilic molecules in full lubricant formulations. The maleinisation of polybutadiene opens up the possibility for further chemical derivatisation to the polymer chain in an attempt to introduce the tertiary amine functionality. Specifically, an imidisation reaction was carried out using 3-(dimethylamino)-

1-propylamine (DMAPA) (Scheme 6.3), according to previous reports of analogous imidisation reactions.[33, 34]
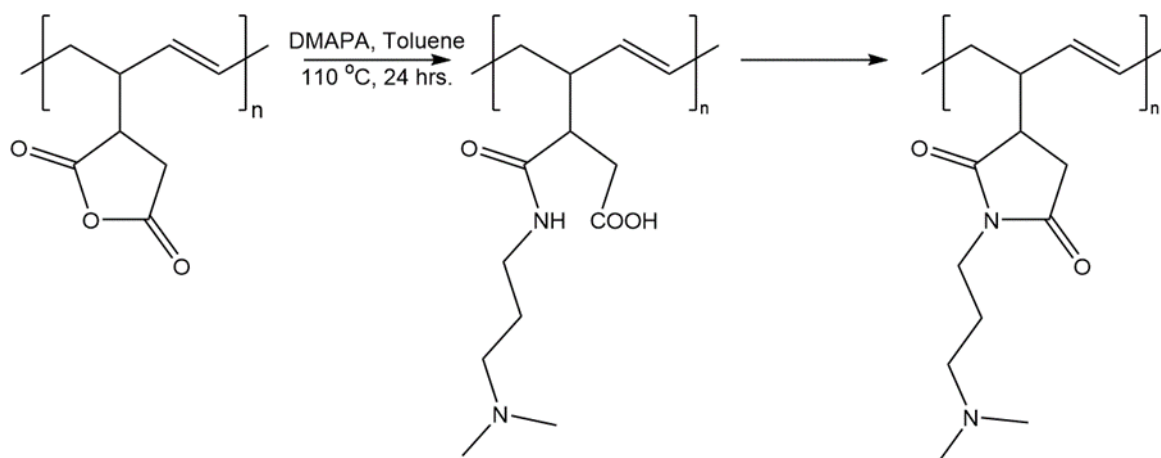
Scheme 6.3: Reaction scheme for the imidisation of maleinised polybutadiene with N,N-dimethylaminopropyl amine

Scheme 6.3 shows how the imidisation reaction of maleinised polybutadienes with DMAPA should leave a tertiary amine functionality pendant to the polymer chain, which is analogous to that of PDMAEMA, described in the previous chapter. Imidisation reactions are relatively facile, however they commonly lead to mixtures of amide and imide if the reaction does not go to completion (as illustrated in Scheme 6.3).[33] In this case, the presence of amide would not present a significant problem for the aim of preparing a polymeric friction modifier because it would still result in the tertiary amine being bound to the polymer. The imidisation reaction was carried out with a 1:1 molar ratio of anhydride
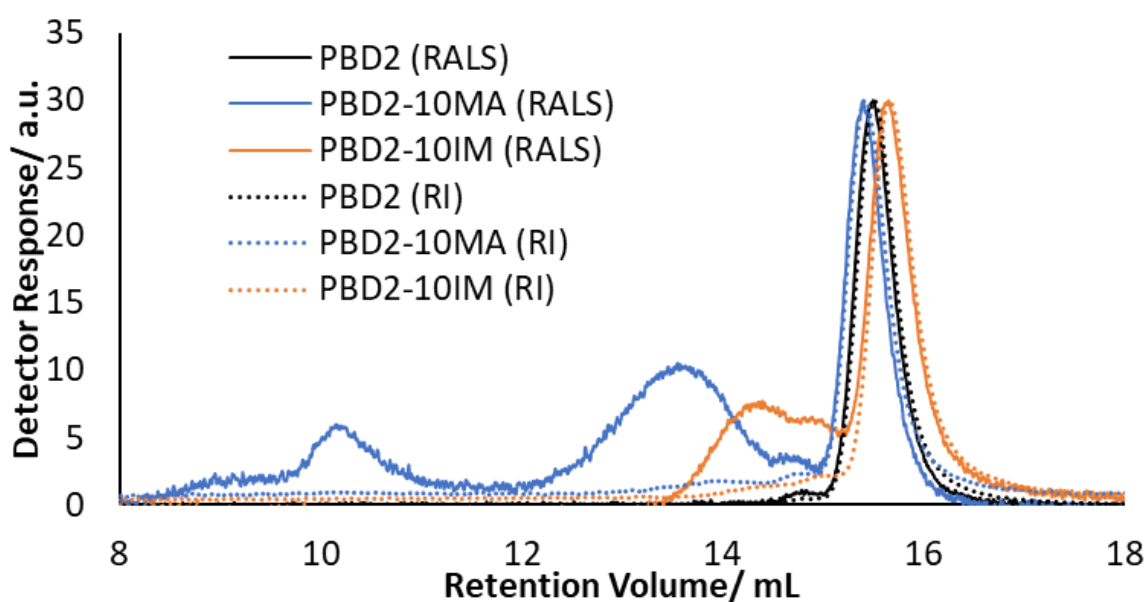

Figure 6.9: SEC chromatograms (RI and RALS) for PBD2 (1st block and final) , PBD2-10MA and PBD2-10IM

to DMAPA (assuming quantitative maleinisation) under reflux in toluene at 110 °C, and an inert nitrogen atmosphere, for 24 hours. Overlaid SEC traces for PBD2 before maleinisation, after maleinisation (PBD-10MA) and after imidisation (PBD-10IM) are shown below in Figure 6.9.

The SEC data illustrated in Figure 6.9 shows that some clear differences occur following the imidisation reaction. Firstly, the 'main peak' of PBD2-10IM eluted at 15.5 mL which is slightly higher than PBD2 and PBD2-10MA (both approximately 15.4 mL). Generally, this would indicate a decrease in the number-average molar mass which is unexpected because the imidisation reaction should result in an increase in the molar mass (of approximately 1230 g mol^{-1} if the conversion of the imidisation reaction was 100 %). The reason for this is unclear but could be caused by weak interactions between the amines of the product and the SEC column. The success of the reaction is discussed in further detail below based on data obtained by FTIR and NMR. The RALS trace for PBD2-10IM shows a large shoulder at 14.3 mL which was not present in PBD2 or PBD2-10MA. Surprisingly, the extra peaks at 13.5 mL and 10.1 mL in the RALS data for PBD2-10MA do not appear in the RALS data for PBD2-10IM, which suggests that they are no longer present. The product of the imidisation reaction was purified by precipitation into methanol, however this would not be expected to remove high molar mass polymers. The RI signal for PBD2-10IM shows that, as with the additional peaks from the RALS of PBD2-10MA, the concentration of the higher molar mass species is very low in comparison to the main peak for the polymer which suggests that this will not significantly influence the friction testing. The dispersity of PBD2-10IM remains very low (1.04) and is similar to PBD2 (1.05) and PBD2-10MA (1.10), which suggests that there is no significant amount of chain scission or oxidative degradation during the imidisation reaction.

To determine the success and extent of the imidisation reaction, FTIR and NMR spectroscopy were used. FTIR spectra for the maleinised and imidised analogues of PBD2 are shown in Figure 6.10 and show some clear differences. In particular, the strong carbonyl peak shifts from 1784 cm^{-1} to 1701 cm^{-1} upon imidisation, which is consistent with a successful reaction of the anhydride.[34] The value following the reaction is more likely to be an imide because the carbonyl stretch of secondary amides typically show at approximately 1680 cm^{-1}. This suggests a high conversion of the anhydride to the imide rather than there

being a mixture of amide and imide in the final product. Another indication of the high conversion of the reaction is the absence of peaks for the carboxylic acid which would also form alongside the amide. In particular, the carbonyl peak for the carboxylic acid would be expected appear at 1760 cm^{-1}. Other peaks that emerge in Figure 6.10 for the product are found at 1149 cm^{-1} and 1031 cm^{-1} which are characteristic of C-N stretches. There is also a broad peak centred on approximately 3340 cm^{-1}, which is most likely to be residual methanol from the precipitation to purify the product.
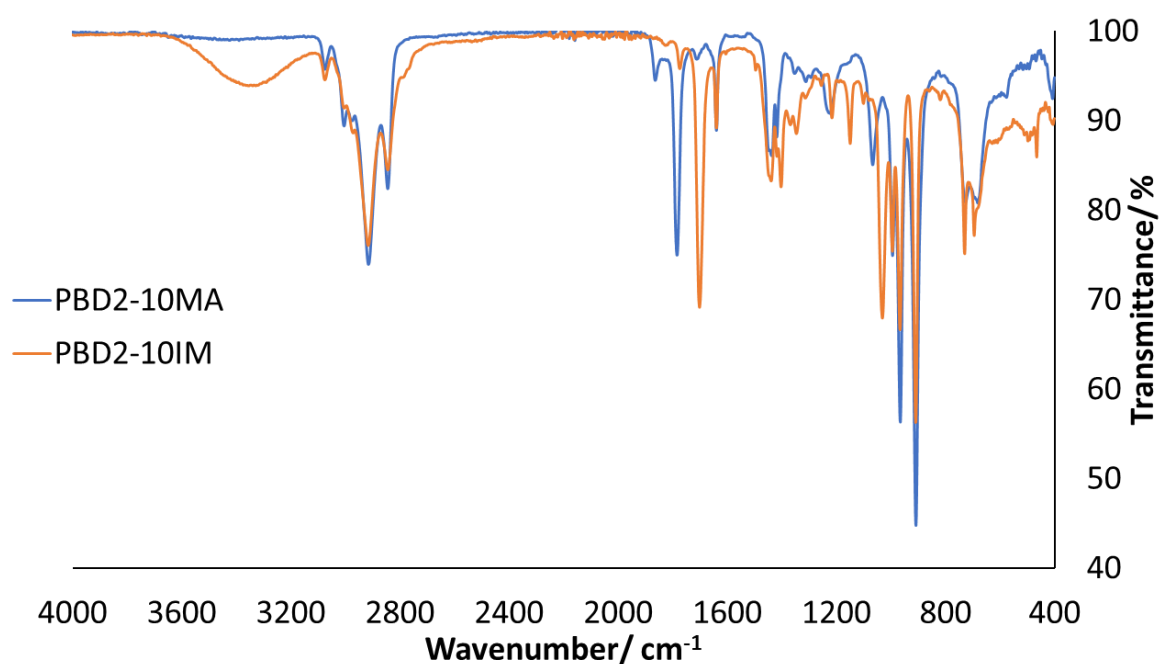
Figure 6.10: Overlaid FTIR spectra for PBD2-10MA and PBD2-10IM

The proton NMR spectrum for PBD2-10IM is shown below in Figure 6.11 along with a worked example used for calculating the degree of imidisation.
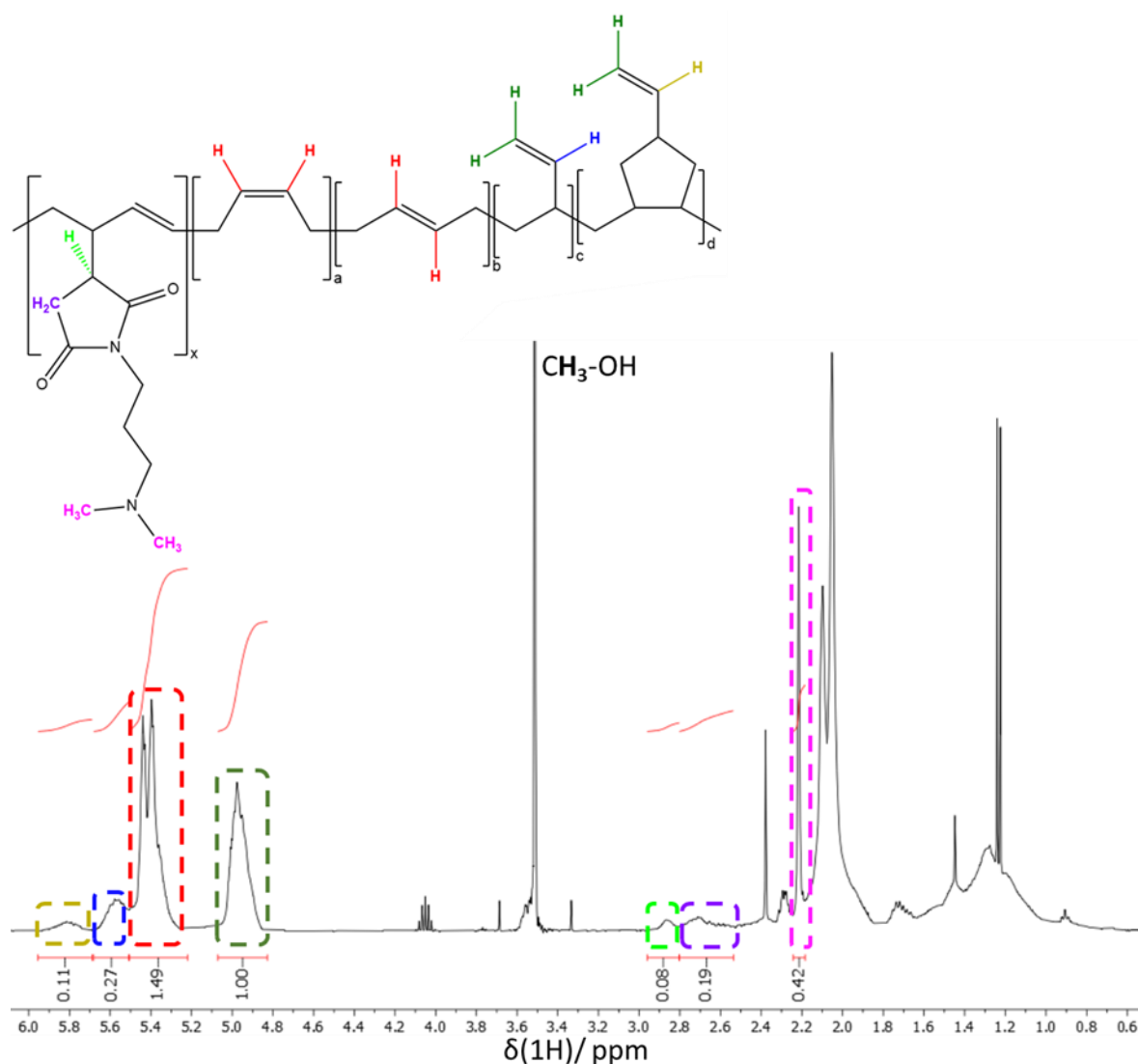
Figure 6.11: ^{1}H NMR spectrum for PD2-10IM prepared by imidisation of PBD2-10MA. NMR spectrum referenced to the solvent, CDCl$_3$, peak at 7.26 ppm

$$mol\% \, (IM) = \frac{\int_{2.22 \, ppm}}{6} \div \left(\frac{\int_{4.98 \, ppm} + \int_{5.35-5.51 \, ppm}}{2} + \frac{\int_{2.22 \, ppm}}{6} \right)$$

$$= \frac{0.42}{6} \div \left(\frac{1.00 + 1.49}{2} + \frac{0.42}{6} \right) = 5.32 \, mol\%$$

The NMR spectrum for PBD2-10IM in Figure 6.11 shows some clear differences to the spectrum for PBD2-10MA (Figure 6.8). In particular, the new sharp singlet at 2.22 ppm (highlighted in pink) can be ascribed to the −CH$_3$ protons of the dimethyl amino functional group of DMAPA. The assignment of the peak can be rationalised according to the analogous peak for the unreacted DMAPA (^{1}H NMR also run in CDCl$_3$, but not shown) which

can be found at 2.23 ppm. Furthermore, it is strongly reminiscent of the analogous peak in the NMR spectra for PI-*b*-PDMAEMA reported in the previous chapters, which occurred at 2.30 ppm.[35] Because the polymer was purified by precipitation into methanol, the presence of this peak strong suggests a covalent attachment between DMAPA with maleinised polybutadiene (rather than the presence of unreacted DMAPA which would be washed away during the precipitation). Using the peak ascribed to the dimethyl amino CH_3 protons and the alkene peaks for the polybutadiene (specifically, the peaks at 4.98 ppm (green) and 5.35-5.51 ppm (red)), the degree of imidisation for this sample was calculated to be 5.32 mol%, which is similar to the degree of maleinisation of polybutadiene previously calculated. This suggests the imidisation reaction has also gone to a conversion of 90 %, meaning a high degree of tertiary amines bound to the polymer backbone which should result in the PBD becoming more Lewis basic. Further to the previous observations, there is also a large solvent peak at 3.51 ppm from methanol used in the precipitation of the product, which also aligns with the observation of the broad peak in the FTIR at 3340 cm^{-1}.

6.2.3. Applications Testing of Functionalised Polybutadienes

In order to see if the functionalised-polybutadiene samples perform as friction modifiers, in a similar fashion to the PI-*b*-PDMAEMA samples, applications testing was carried out on the samples described above. The polymers prepared for testing are summarised below in Table 6.9.

Table 6.9: Summary of all samples prepared for applications testing, including polybutadiene, maleinised polybutadiene and imidised polybutadiene.

Sample	1st Block M_n (g/mol)	1st Block 1,4-content	Total M_n (g/mol)	Total 1,4-content	Maleinisation (Experimental)	Imidisation (Experimental)
PBD1	3170	88 %	7700	51 %	-	-
PBD1-5MA	-	-	-	-	3.17 mol%	-
PBD1-10MA	-	-	-	-	5.78 mol%	-
PBD1-10IM	-	-	-	-	-	5.78 mol%
PBD2	6060	88 %	11090	69 %	-	-
PBD2-5MA	-	-	-	-	3.18 mol%	-
PBD2-10MA	-	-	-	-	5.83 mol%	-
PBD2-10IM	-	-	-	-	-	5.32 mol%
PBD3	3430	87 %	12110	57 %	-	-
PBD3-5MA	-	-	-	-	2.92 mol%	-
PBD3-10MA	-	-	-	-	5.63 mol%	-
PBD3-10IM	-	-	-	-	-	5.47 mol%
PBD4	-	-	9650	88 %	-	-
PBD4-5MA	-	-	-	-	3.17 mol%	-
PBD4-10MA	-	-	-	-	5.71 mol%	-
PBD4-10IM	-	-	-	-	-	5.27 mol%

Table 6.9 shows all samples of polybutadiene which were prepared for friction testing. Henceforth, the sample codes for the respective polybutadienes prepared by living anionic polymerisation (e.g., PBD1) also encompass the target wt% maleinisation (e.g., PBD1-10MA) or the target wt% imidisation (PBD1-10IM). The 5 and 10 wt% targets for the reactions are equivalent to a target of 5.93 and 3.17 mol%, respectively. Compared to the target, all maleinised polymers in Table 6.9 had a conversion of at least 92 % (as calculated from the NMR spectra) which shows that each maleinisation reaction was close to completion. Of the maleinised polymers, the 10 wt% samples were reacted with DMAPA to produce 10 wt% imidised polybutadienes (which also had a target degree of imidisation of 5.93 mol%). For these reactions, the conversion was above 89 % in all cases, which again shows that the reactions were close to completion. Because of time constraints, the samples submitted for applications testing were prioritised, meaning that only the PBDX-10MA and PBDX-10IM polymers were tested. The unfunctionalised polybutadienes contain no heteroatoms meaning that they are highly unlikely to offer any friction reduction and

were not tested. The PBDX-10MA samples were chosen ahead of PBDX-5MA because of the increased proportion of heteroatoms which should offer a greater number of binding sites to metal surfaces. The 5 wt% maleinised samples could be useful in future if there is a need to reduce polarity for improving solubility in the non-polar base oil. Similarly, only the 10 wt% imidised polybutadienes were synthesised and submitted for applications testing along with the 10 wt% maleinised analogues.

6.2.3.1. Friction Testing of Functionalised Polybutadienes in Neat Base Oil

As with the PI-*b*-PMMA and PI-*b*-PDMAEMA described in the previous chapter, the first stage of assessing friction performance was to test the functionalised polybutadiene samples in neat Yubase 4 base oil containing no other additives. This allows for the elucidation of performance in the absence of other surface-active compounds, which can compete for adsorption to metal surfaces. The polymers were dispersed at 1 wt% in the base oil by direct dissolution at 110 ^{o}C in the presence of Irganox L135, an antioxidant to limit any thermal degradation of the polymer. In all cases, this gave a transparent, colourless solution which indicates good solubility of the polymers. This is encouraging, particularly for the highly polar, imidised polymers and the functionalised analogues of PBD4 which are maleinised at random points along the polymer chain. The testing procedure for the polymers in neat Yubase 4 at 80 ^{o}C was identical to that described in the previous chapter and the results for the maleinised polymers overlaid with neat Yubase 4 are shown below in Figure 6.12.
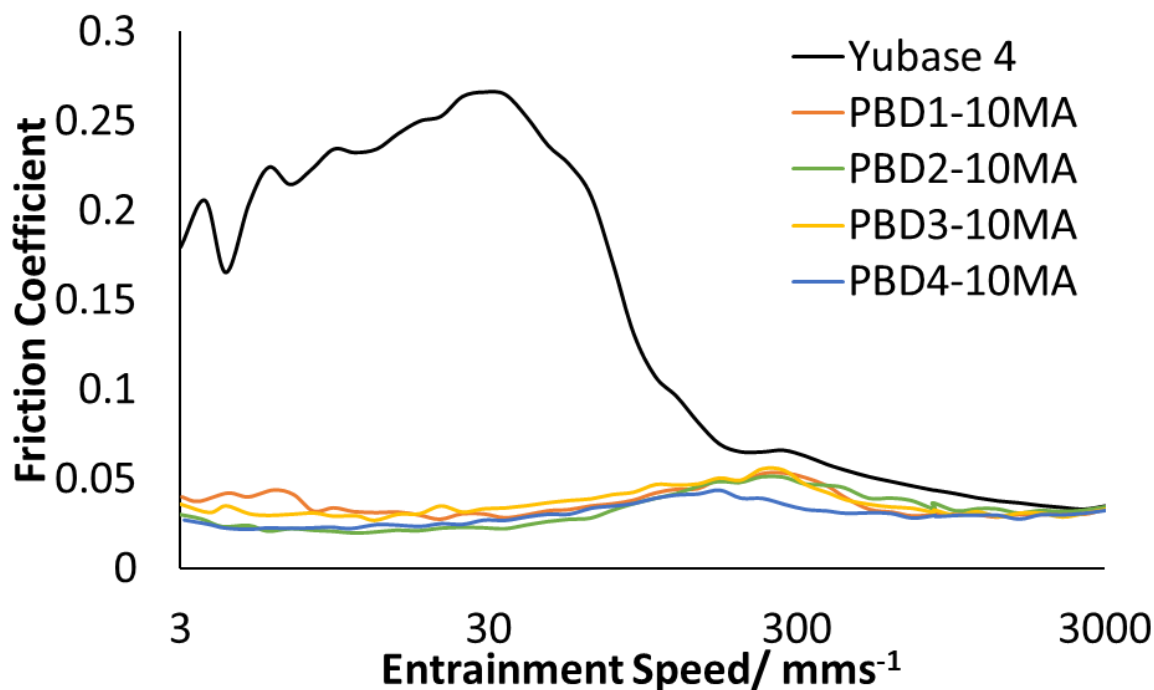
Figure 6.12: Results of friction testing for neat maleinised polybutadiene dispersions at 1 wt% in Yubase 4. A neat sample of Yubase 4 containing no other additive was also tested and is shown in black for comparison.

Figure 6.12 shows that all maleinised polybutadienes significantly reduce the friction compared to the neat Yubase 4 base oil, across all entrainment speeds. This suggests that the (Lewis basic) carbonyls of the anhydride groups bound to polybutadiene, adsorb to the metal surface. This behaviour is encouraging, given that the polymers had not yet been imidised and because the maleinised samples are commercially relevant. All samples reported in Figure 6.12 out-performed all PI-*b*-PMMA and PI-*b*-PDMAEMA block copolymers previously discussed. This could also suggest an improved adsorption of the anhydride functional groups to the metal surfaces, however, this may change when tested in full lubricant formulations, because of the presence of dispersants and surfactants, as was the case previously for PI-*b*-PMMA in particular. To compare the performance to 2 commercial products, the results for the 4 maleinised polybutadienes are overlaid in Figure 6.13. This graph is on a smaller scale with respect to the y-axis for closer analysis of the performance.
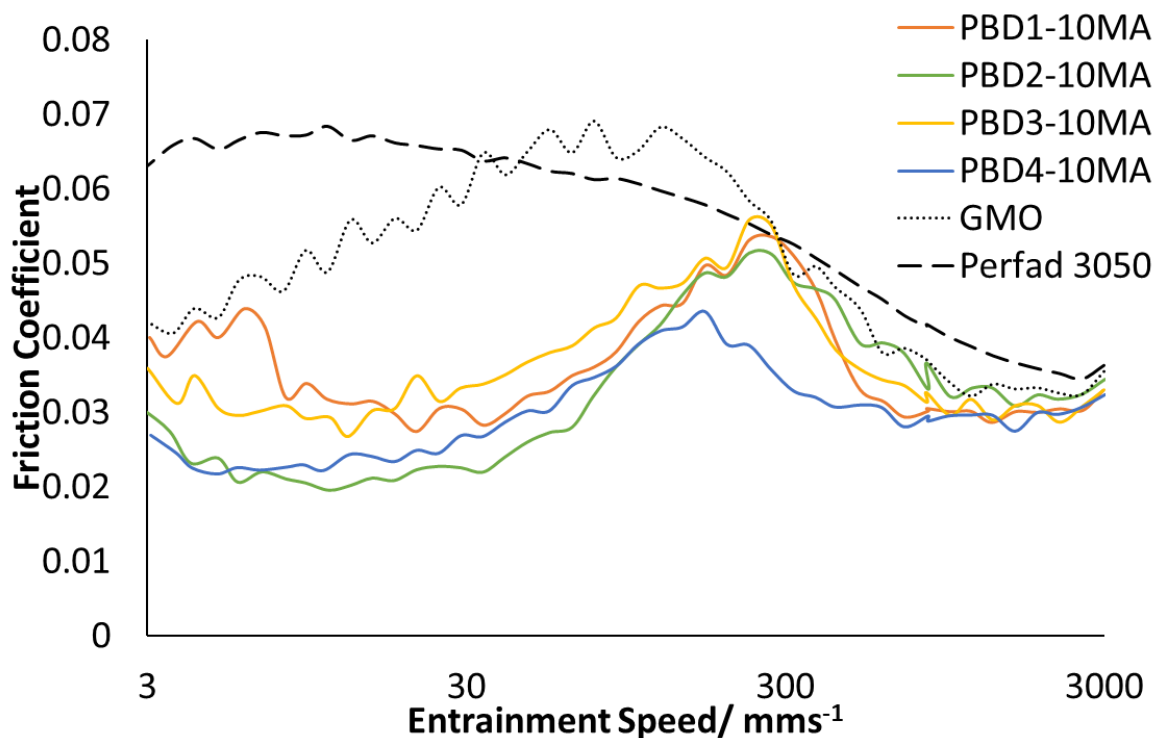
Figure 6.13: The results for the identical test with 2 commercially available friction modifiers, GMO and Perfad 3050, are also shown in black.

Figure 6.13 shows that the maleinised polybutadienes all perform similarly, at all entrainment speeds. The 2 samples with the lowest friction are PBD4-10MA (blue data) and PBD2-10MA (green data) which have a friction coefficient of below 0.03 in the boundary condition (<30 mm s^{-1}). PBD4-10MA is a maleinised version of the commercial grade polybutadiene (to give a randomly maleinised copolymer by design) and PBD2-10MA is one of the 'blocky' polybutadienes. The performance of the former is particularly interesting because this is already a commercial product and the path to market would be straightforward. However, these observations are not entirely consistent with the hypothesis that a block-like structure will deliver better performance than statistical copolymers with a random distribution of functional groups. This could be because the blocky maleinised polybutadienes are not as blocky as expected. As previously discussed, the microstructure of the constituent blocks is not 100 % 1,4 and 100 % 1,2 (see Table 6.8). Because of this, the 'blocky' copolymers may have a distribution of functional groups which is not very far from random. Another reason for the observation in Figure 6.13 could be that in neat base oil, a blocky architecture is not so important for adsorption to the surface. It could be that in the presence of other surface-active ingredients in full formulations, the

grouping of the Lewis basic groups in the blocky copolymers helps with the competitive adsorption of the polymer to the metal.

Figure 6.13 also shows that the maleinised polybutadienes perform very well in comparison to the commercial products at all entrainment speeds. In particular, they give a much lower friction (<0.045) at the boundary regime (<30 mm s^{-1}) in comparison to the commercial polymeric friction modifier, Perfad 3050 (black, dashed data; <0.06). This suggests that they are bound to the metal surfaces and acting to keep the surfaces apart, which is hoped to continue when tested in full lubricant formulations.

As with many of the friction measurements in neat base oil reported in the previous chapter, the data in Figure 6.13 shows a peak in the friction coefficient for the 3 'blocky' maleinised polybutadienes at an entrainment speed of approximately 270 mm s^{-1}. PBD4-10MA (the random, maleinised version of the commercial grade) has a smaller peak at the slightly lower speed of approximately 170 mm s^{-1}. The presence of peaks in the friction measurements of block copolymers has previously been discussed by Zheng *et al.* for block copolymers of poly((2-ethylhexyl acrylate)-*ran*-(*tert*-butyl acrylate)-*block*-(2-hydroxyethyl acrylate)) (P((EXA-*ran*-tBA)-*b*-CEA)).[36] They found that changes to the composition of the block copolymer caused the peak to move to different entrainment speeds. Given that the maleinised polybutadienes are not true 'block' copolymers, it is unlikely that there is a strong difference in the mole fraction of the maleinised:non-polar blocks as was the aim in preparing polybutadiene with 1,4-rich and 1,2-rich blocks.

Imidisation of the maleinised polybutadienes with DMAPA was carried out to introduce the tertiary amine functionality which has been shown to be particularly effective for friction modification in full formulations, because its increased Lewis basicity is suspected to help the copolymer adsorb to the metal surface. This was particularly so in comparison to the ester functionality of PMMA. The results for the 4 imides are shown below in Figure 6.14, overlaid with the 4 precursor anhydrides.
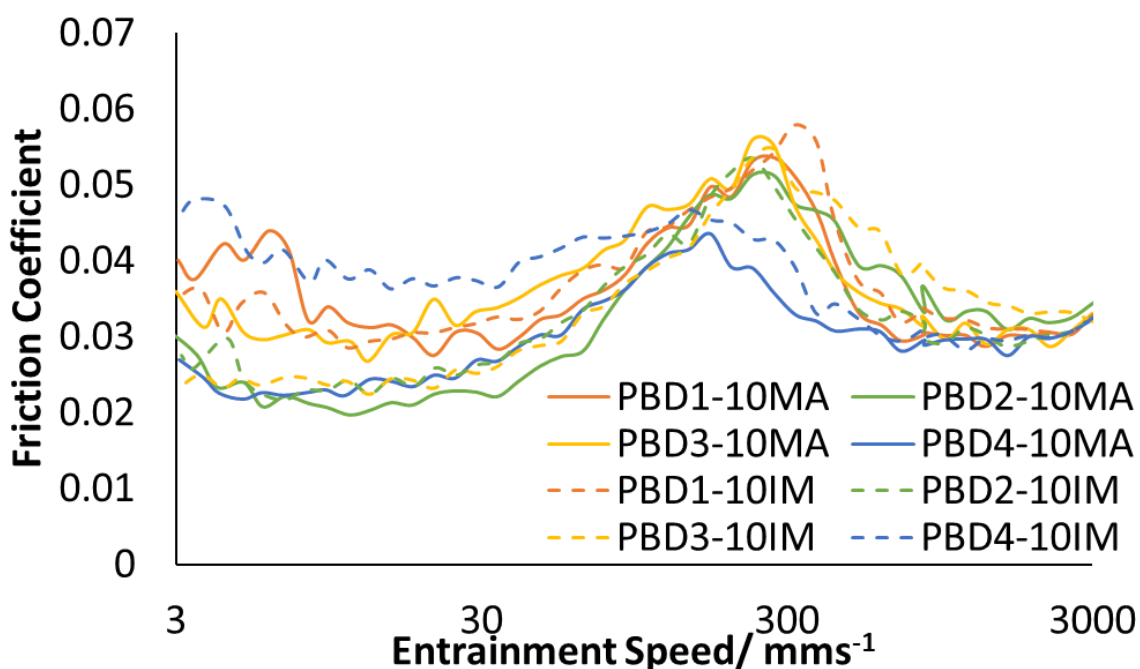
Figure 6.14: Results of friction testing for neat maleinised and imidised polybutadiene dispersions at 1 wt% in Yubase 4

Figure 6.14 shows that there is no clear and consistent difference between the performance of the samples before and after imidisation, in terms of friction reduction. PBD4-10MA (blue, solid data) performed better than PBD4-10IM (blue, dashed data), but PBD3-10IM (yellow, dashed data) performed better than PBD3-10MA (yellow, solid data) while the other samples performed similarly to each other before and after imidisation. In the data reported in the previous chapter, there were also no obvious trends in the results obtained upon systematic variation of molecular parameters such as total molar mass, relative mole fraction for the blocks and even the different polymers used (PMMA and PDMAEMA). The continuation of this trend (or lack thereof) makes it difficult to draw any conclusive correlation between structure and performance. However, in general, the low friction across all entrainment speeds is positive and these polymers were taken forward into full formulation testing.

PI-*b*-PDMAEMA block copolymers were found to be particularly effective for friction reduction in a full Mobil Delvac 5W30 formulation, where other commercial PFMs are typically insoluble. Because the imidised polybutadienes described in this chapter were designed to mimic the chemical structure of the PI-*b*-PDMAEMA block copolymers, they were also tested in this full formulation to see if friction reduction was observed. Figure 6.15 shows the Stribeck curves for the maleinised and imidised polybutadienes dispersed at 1 wt% in Mobil Delvac 5W30.
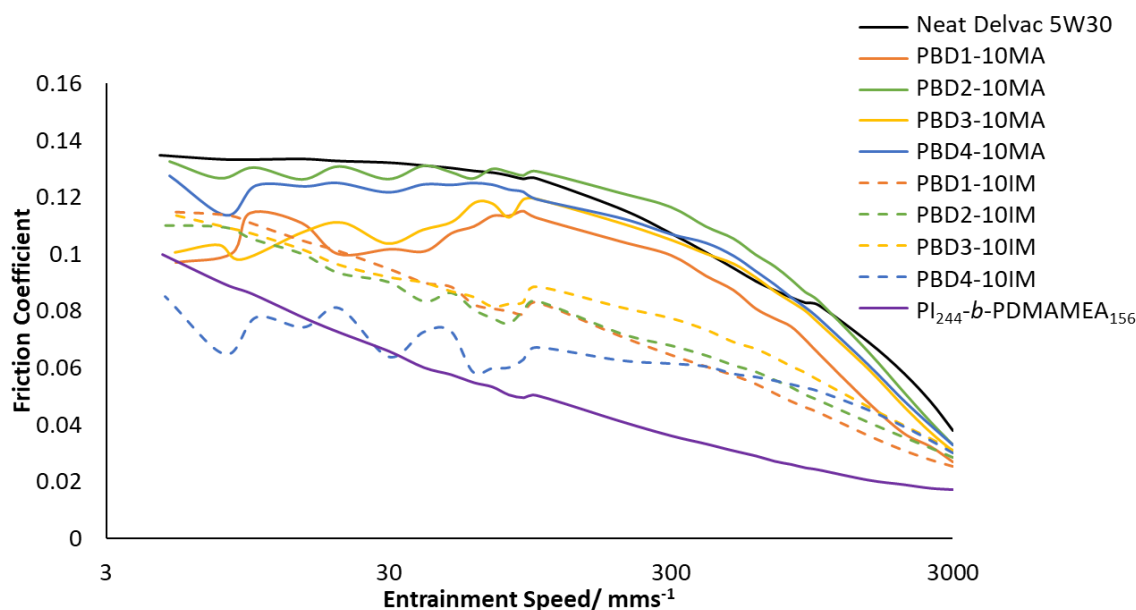
Figure 6.15: Stribeck curve following 2 hours rubbing at 135 ^{o}C for the Mobil Delvac formulation containing the specified additives at 1 wt%. 'Neat Delvac 5W30' refers to the result formulation with no extra additive

The results in Figure 6.15 show that in general, the imidised polybutadienes (dashed lines) reduce the friction to a greater extent than the maleinised polybutadienes (solid lines) across most entrainment speeds. This is particularly clear for PBD2 (green data) and PBD 4 (blue data) which reduce the friction from <0.14 and <0.13 to <0.11 and <0.09, respectively across all entrainment speeds. The same trend is mostly true for PBD1 (orange data) and PBD3 (yellow data), however there is a crossover in friction coefficient at ≈10 mm s^{-1} which suggests that the maleinised samples perform slightly better at low entrainment speeds. However, the difference in friction coefficient from 10 – 3 mm s^{-1} is very small (<0.1) and so is likely to be insignificant. The generally improved performance of the imidised polybutadienes is in excellent agreement with the results of the previous chapter which showed that the presence of the strongly Lewis basic, tertiary amine of PDMAEMA had a

far greater effect than the less Lewis basic PMMA for full formulations where many other surface-active ingredients are present. The tertiary amine is expected to adsorb more strongly to the metal surface which explains the improved performance of the imidised polymers in the presence of the other surface-active ingredients.

Of the imidised polymers, Figure 6.15 shows than PBD4-10IM (blue data) reduces the friction the most in comparison to the neat Delvac 5W30 (black data). Across all entrainment speeds the friction coefficient of PBD4-10IM was <0.09 which represents a significant decrease from the neat formulation which reached close to 0.14 from 30 – 3 mm s^{-1}. The performance of this polymer in comparison to the other samples is somewhat surprising given that PBD4 was the commercial grade of polybutadiene (i.e., with a random microstructure throughout the polymer backbone rather than targeted blocks). This could suggest that a blocky design for the copolymers upon maleinisation and imidisation is not crucial to the friction reduction, which was unexpected. The other significant difference in the polymer structure of PBD4 is the lack of the cyclic microstructure. For PBD1-3, the polymerisation of the second 'block' in the presence of the polar modifier resulted in up to 20 % of the total polymer being made up of this microstructure. Because PBD4 was prepared without the polar modifier, there was no cyclic microstructure present. Clearly it is not possible to draw conclusions from 1 data point and it is also unclear what effect (if any) the presence of cyclic polybutadiene could have on friction performance, however it could be an important consideration in future experiments. A useful comparison could be to repeat one of the 'blocky' polybutadienes with a different set of reaction conditions that promotes the 1,2 microstructure in the second block without also forming the cyclic microstructure. This polymer could then be compared to these results to further investigate any effect of the cyclic microstructure.

The data for the best performing sample from the previous chapter (PI_{244}-*b*-$PDMAEMA_{156}$) are also shown in Figure 6.15 (purple data). In comparison to PBD4-10IM (blue dashed data) the former shows a generally improved friction performance at 3000 – 30 mm s^{-1}, however, the latter shows similar performance at the boundary condition (<30 mm s^{-1}). This could suggest that at higher entrainment speeds where the surface experiences greater shear forces, the block-like structure of PI-*b*-PDMAEMA allows for the polymer to remain strongly adsorbed to the metal surface, whereas the less blocky PBD4-

10IM can be removed from the surface. However, the similarity in performance at low entrainment speeds is encouraging given this is where the metal surfaces are closest in contact such that frictional forces are generally at their highest and are therefore more likely to become damaged.

Although the performance of some of the imidised polybutadienes in a full, Mobil Delvac 5W30 formulation (Figure 6.15) is encouraging, it must be noted that there were some solubility issues noticed for these formulations. All maleinised and imidised polybutadienes gave turbid solutions which indicates a poor dispersibility in the formulation. This reduced solubility would likely be exacerbated with long-term storage, which is critically important for engine oil formulations. The solubility of PI-*b*-PDMAEMA block copolymers was good which could indicate the benefit of targeting more strictly defined block copolymers as PFMs. However, the set of functionalised polybutadiene samples tested in full formulations was relatively small and there are many potential ways to address the poor solubility of the imidised polybutadienes in the future. For example, all samples tested were the 10 wt% maleinised/imidised polybutadienes, however, 5 wt% samples were also prepared. The lower degree of maleinisation might be expected to give a more non-polar product which would in turn, be expected to exhibit improved solubility in base oil. The reduced polarity could also affect the friction performance, however, the friction of PBD4-10IM was already far below that of the neat formulation, so even a slight compromise on friction performance to aid solubility may result in better performance than the neat formulation. Furthermore, the molar mass of all samples was ≈10000 g mol^{-1}. This could easily be modified to give lower molar masses which would typically be expected to have an improved solubility. Another alternative could be to explore different lubricant formulations. Several commercial PFMs are already known to be insoluble in Delvac 5W30 which is thought to be a result of the high concentration of surfactants. Therefore, it could be expected that the imidised polybutadienes would show better solubility in other formulations, as is the case for the other PFMs. Unfortunately, because of time constraints, no further experimental investigation was undertaken.

6.3. Conclusions

In conclusion, a series of amphiphilic copolymers have been prepared by a commercially-viable synthetic protocol, comprising a single polymerisation mechanism and

post-polymerisation modifications. Using living anionic polymerisation, polybutadiene was prepared with 'blocks' of 1,4-rich and 1,2-rich microstructure with variation in the mole fraction of the 'blocks'. These polybutadiene samples were then reacted with maleic anhydride in a reaction that is expected to be selective for the 1,4 microstructure because of the increased nucleophilicity of the disubstituted alkene and the steric availability of the 4 α protons, resulting in the formation of a maleic anhydride-rich 'block'. To further derivatise the chemical structure, the maleinised polybutadienes were imidised with DMAPA. This reaction introduces a tertiary amine, pendant to the polybutadiene backbone; a functional group which was reported in the previous chapter to be particularly useful for friction reduction.

The maleinised and imidised polybutadienes were all found to be highly effective at reducing the friction at all entrainment speeds when dispersed into neat base oil. The performance was competitive in comparison to 2 commercial friction modifiers: GMO and Perfad 3050. However, there was no discernible difference in performance between maleinised and imidised polybutadienes. This is similar to the results seen in the previous chapter for PI-*b*-PMMA and PI-*b*-PDMAEMA and suggests that, without other amphiphilic ingredients present, the anhydride is sufficiently Lewis basic to adsorb to the metal surface and reduce the friction.

The samples were also tested in a full, Mobil Delvac 5W30 formulation, a lubricant in which PI-*b*-PDMAEMA was previously found to be an effective friction modifier. Several of the functionalised polybutadienes were also found to be effective friction modifiers in this formulation. In particular, PBD4-10IM, an imidised version of a commercial grade of polybutadiene, was found to be effective and compared well with the best performing PI-*b*-PDMAEMA block copolymer. However, all maleinised and imidised polybutadienes were found to have solubility issues in the formulation which would need to be rectified before commercialisation could be considered. The commercial PFMs investigated are also known to have poor solubility in this formulation.

6.4. References

1. M. Morton, E. E. Bostick, L. J. Fetters, R. A. Livigni, *J. Polym. Sci. A*, 1963, **1**, 1735-1747.
2. A. F. Johnson, D. J. Worsfold, *J. Polym. Sci. A*, 1965, **3**, 449-455.
3. H. Hsieh, R. P. Quirk, *Anionic Polymerization: Principles and Practical Applications*, Taylor & Francis, Boca Raton, 1996.
4. H. L. Hsieh, *J. Polym. Sci. A*, 1965, **3**, 181-190.
5. M. Lanzi, L. Paganin, F. P. Di-Nicola, C. Trombini, *J. Polym. Res.*, 2015, **22**, 208-218.
6. A. Forens, K. Roos, C. Dire, B. Gadenne, S. Carlotti, *Polymer*, 2018, **153**, 103-122.
7. G. Quack, L. J. Fetters, *Macromolecules*, 1978, **11**, 369-373.
8. R. Reeves, M. Lawrence, *Epoxides: Synthesis, Reactions, and Uses*, Nova Science Publishers, Incorporated, New York, 2018.
9. E. Brule, Y. R. de Miguel, K. K. Hii, *Tetrahedron*, 2004, **60**, 5913-5918.
10. H. M. R. Hoffmann, *Angew. Chem. Int.*, 1969, **8**, 556-577.
11. K. Alder, F. Pascher, A. Schmitz, *Ber. Dtsch. Chem. Ges.*, 1943, **76**, 27-53.
12. R. T. Arnold, J. S. Showell, *J. Am. Chem. Soc.*, 1957, **79**, 419-422.
13. F. Ferrero, M. Panetti, G. B. Saracco, *Chim. Ind.*, 1984, **66**, 3-6.
14. F. Ferrero, *J. Therm. Anal. Calorim.*, 2004, **76**, 1057-1067.
15. F. Ferrero, *Prog. Org. Coat.*, 2005, **53**, 50-55.
16. M. Muller, K. Topolovec-Miklozic, A. Dardin, H. A. Spikes, *Tribol. Trans.*, 2006, **49**, 225-232.
17. D. Baskaran, *Prog. Polym. Sci.*, 2003, **28**, 521-581.
18. K. Matyjaszewski, *Macromolecules*, 2012, **45**, 4015-4039.
19. J. W. Nicholson, *The Chemistry of Polymers*, Royal Society of Chemistry, London, 1997.
20. D. J. Worsfold, S. Bywater, *Can. J. Chem.-Rev. Can. Chim.*, 1964, **42**, 2884-2892.
21. X. Min, X. D. Fan, J. Liu, *R. Soc. Open Sci.*, 2018, **5**, 180516-180525.
22. S. Poshyachinda, H. G. M. Edwards, A. F. Johnson, *Polymer*, 1991, **32**, 334-337.
23. J. Saelao, P. Phinyocheep, *J. Appl. Polym. Sci.*, 2005, **95**, 28-38.
24. J. Sheng, X. L. Lu, K. D. Yao, *J. Macromol. Sci. A*, 1990, **A27**, 167-178.
25. L. Iancu, P. Ghioca, B. Spurcaciu, R. M. Grigorescu, C. A. Nicolae, R. A. Gabor, *Mater. Plast.*, 2013, **50**, 137-140.
26. W. J. Soer, W. Ming, C. E. Koning, R. van Benthem, J. M. C. Mol, H. Terryn, *Prog. Org. Coat.*, 2009, **65**, 94-103.
27. C. F. Cullis, H. S. Laver, *Eur. Polym. J.*, 1978, **14**, 571-573.
28. A. Pucci, C. Barsocchi, R. Rausa, L. D'Elia, F. Clardelli, *Polymer*, 2005, **46**, 1497-1505.
29. C. Öztürk, S. H. Küsefoğlu, *J. Appl. Polym. Sci.*, 2011, **120**, 116-123.
30. C. H. F. Maurano, L. L. Portal, R. Baumhardt Neto, R. S. Mauler, *Polym. Bull.*, 2001, **46**, 491-498.
31. Z. Mitov, R. Velichkova, *Eur. Polym. J.*, 1993, **29**, 597-601.
32. R. R. Qi, Z. F. Chen, C. X. Zhou, *Polymer*, 2005, **46**, 4098-4104.
33. H. Y. Liu, K. Cao, Y. Huang, Z. Yao, B. G. Li, G. H. Hu, *J. Appl. Polym. Sci.*, 2006, **100**, 2744-2749.
34. M. Szkudlarek, E. Heine, H. Keul, U. Beginn, M. Möller, *Int J Mol Sci*, 2018, **19**, 2617.
35. Y. W. Pei, A. B. Lowe, *Polym. Chem.*, 2014, **5**, 2342-2351.
36. R. H. Zheng, G. J. Liu, M. Devlin, K. Hux, T. C. Jao, *Tribol. Trans.*, 2010, **53**, 97-107.

7. Concluding Remarks

7.1. Conclusions

Throughout this project, the synthesis of diene-based block copolymers has been carried out with a view to allowing the dispersion of typically insoluble, polar functional groups in non-polar solvents. To reflect the 'academic' and 'industrial' aspects of the investigation, the following conclusions are split accordingly.

From an 'academic' point of view, poly(isoprene-*block*-(methyl methacrylate)) (PI-*b*-PMMA) block copolymers were prepared by a change of mechanism polymerisation (CHOMP). Living anionic polymerisation was used to prepare bromide-end-capped polyisoprene (PI-*Br*) which served as a macroinitiator for the atom-transfer radical polymerisation (ATRP) of MMA. This method allowed for several PI-*Br* macroinitiators to be prepared, all with different molar masses, from which homologous families of PI-*b*-PMMA block copolymers were prepared with a varied molar mass of PMMA. The block copolymers were dispersed into non-polar solvents at varying solids levels by solvent switching, resulting in self-assembly of the polymers to produce a variety of physical structures (i.e. free-flowing liquids, transparent gels and opaque gels) within each family of PI-*Br*. The dispersions were analysed by DLS and TEM to confirm that the different physical structures were comprised of self-assembled block copolymer micelles with different morphologies (i.e. spherical, wormlike and vesicles). Finally, the thermal-responsivities of the different self-assembled physical structures were investigated by rheology which revealed a temperature sensitivity that resulted in decreasing viscosity of the transparent gel, made up of wormlike micelles. TEM was used to show that an increase in dispersion temperature resulted in a change in morphology from wormlike to spherical micelles due to increased solvation of the insoluble PMMA core, which causes a change in the packing parameter of the block copolymer.

Building on the investigation into PI-*b*-PMMA block copolymers, a series of related poly(isoprene-*block*-(*N*,*N*-(dimethylamino)ethyl methacrylate)) (PI-*b*-PDMAEMA) block copolymers was prepared by a similar CHOMP procedure. Once again, the self-assembly of the block copolymers in *n*-decane was investigated by solvent-switching, resulting in free-flowing liquids, transparent gels and opaque gels, which were strongly reminiscent of those

formed by the self-assembly of PI-*b*-PMMA. The PI-*b*-PDMAEMA dispersions formed micelles of differing morphology (i.e. spherical, wormlike and vesicles) depending on molar mass and composition. One example of a PI-*b*-PDMAEMA block copolymer was subsequently quaternised with different alkyl iodides (forming PI-*b*-PQDMAEMA) to assess the differences in self-assembly behaviour with respect to both the molar mass of the alkyl iodide and the degree of quaternisation with respect to DP$_{PDMAEMA}$. During the quaternisation reaction with ethyl iodide, to varying degrees of quaternisation, in THF, changes in the physical properties of the reaction mixtures were observed. Some of the reaction mixtures formed transparent, soft gels, while others formed turbid solutions. The different dispersions were imaged by TEM which showed that the change in properties was the result of an *in-situ* quaternisation-induced self-assembly (QISA) of the block copolymers into spherical micelles, wormlike micelles and vesicles, respectively. It was concluded that QISA occurs because quaternisation of the previously soluble PDMAEMA block, renders the quaternised block insoluble in THF, which thus forms the core of micelles with PI at the corona. This is thought to be the first example of QISA, which has significant potential to be a useful tool for the facile preparation of different self-assembled micelles *in-situ*. Analogous quaternisation reactions with butyl iodide and octyl iodide showed no evidence of QISA which suggests that the process may only occur with very specific chemistries. The products of the quaternisation with octyl iodide (PI-*b*-PQDMAEMA(OI)) at varying mol% w.r.t the molar mass of PDMAEMA were subsequently dispersed in *n*-decane by solvent switching. This resulted in the formation of different physical structures in *n*-decane which were strongly reminiscent of the self-assembled block copolymers of PI-*b*-PMMA and PI-*b*-PDMAEMA. At 8 mol% quaternisation, a free-flowing liquid was formed, which is characteristic of spherical micelles. At 10 mol%, this morphology changed to a transparent gel, which was also seen for quaternisation with ethyl iodide and butyl iodide at all mol%. From 12-19 mol% the block copolymer self-assembled into opaque gels which were confirmed by TEM to be made up of vesicles. This demonstrates how a single block copolymer can be modified by quaternisation to change the tube diameter of the polymer which alters the Israelachvili packing parameter and, concurrently, changes the morphology formed upon self-assembly.

Following the 'academic' study, PI-based block copolymers were investigated in an 'industrial' context as friction modifiers in lubricant formulations. A series of PI-*b*-PMMA and PI-*b*-PDMAEMA block copolymers with varying molar masses of the constituent blocks was prepared by the same CHOMP procedures described in the preceding chapters. These block copolymers were dispersed into Yubase 4, a standard, commercial base oil, and first tested in neat solutions of base oil containing no other additives. Using a mini-traction machine (MTM), several PI-*b*-PMMA and PI-*b*-PDMAEMA block copolymers were found to significantly reduce the friction of the neat base oil, suggesting that the block copolymers interact well with the metal surfaces to reduce metal-metal contact. However, little correlation was found between the molar mass/composition of the block copolymers and their performance. The results were found to be strongly competitive with those of commercial friction modifiers (GMO and Perfad 3050) which were tested under the same conditions.

The PI-*b*-PMMA and PI-*b*-PDMAEMA additives which were found to be most effective as friction modifiers were also tested in a full Motul 0W20 lubricant formulation. Unfortunately, all examples of PI-*b*-PMMA additives which were investigated in full formulation were found to have no beneficial impact on friction in comparison with the neat formulation. It was concluded that this was most likely the result of poor surface-binding in the presence of, and in competition with, other surface-active additives present in the full formulation. In contrast, PI-*b*-PDMAEMA samples did reduce the friction (in full formulation) and were found to perform well in comparison to the commercial polymeric friction modifier, Perfad 3050. The PI-*b*-PDMAEMA block copolymers were found to also reduce the friction in several other full formulations, including Mobil Delvac 5W30, in which commercial friction modifiers typically have poor solubility. This not only suggests that PI-*b*-PDMAEMA could be an effective friction modifier, but also that it could have a broad scope with applicability in different formulations.

After finding an effective chemical motif for polymeric friction modifiers, comprising Lewis basic tertiary amines to promote adsorption to metal surfaces and a non-polar PI block for solubility in base oil, a new, commercially-viable synthesis route to produce analogous polymers was sought because of the likely difficulties in scaling up CHOMP. Living anionic polymerisation was used to prepare microstructural block

copolymers of polybutadiene comprising of a 1,4-rich 'block' and a 1,2-rich 'block'. Post-polymerisation maleinisation was then used to impart polar functionality to the polymer through an ene reaction between maleic anhydride and the alkenes present in all monomer repeat units of polybutadine. The ene reaction is selective towards the 1,4-microstructure, meaning the 1,4-rich 'block' in the microstructural block copolymer was preferentially reacted, thus resulting in an amphiphilic blocky copolymer. The anhydride functionality was then imidised with 3-(dimethylamino)-1-propylamine (DMAPA) to produce a polymer with a pendant tertiary amine, a functionality that was found to be effective in PI-*b*-PDMAEMA block copolymers. Maleinised and imidised polybutadienes were found to be excellent friction modifiers in neat solutions of base oil. The imidised versions were also found to be particularly effective in a full, Mobil Delvac 5W30 formulation, where PI-*b*-PDMAEMA was also found to perform well in comparison to the standard, neat formulation. However, the maleinised and imidised polymers gave turbid dispersions in the full formulation which suggests there were solubility issues.

7.2. Future Work

The work presented in this thesis offers many opportunities for future study. From an 'academic' point of view, the CHOMP procedure used in chapter 3 and chapter 4 has a unique versatility which means that a wide number of constituent blocks could be studied within the copolymers. This was already proven somewhat by the polymerisations of MMA and DMAEMA, but it could be of particular interest to investigate different lipophobic polymers. Slight differences in self-assembly were observed for PMMA and PDMAEMA so it would be interesting to explore differences in self-assembly with other lipophobic polymers. For example, different methacrylates (e.g. ethyl, butyl) would be expected to have a comparable solubility to methyl methacrylate, however, the different size of the alkyl moiety could change the tube diameter of the core-forming block which may result in differences to the Israelachvili packing parameter (and morphology formed upon self-assembly) at a comparable degree of polymerisation.

Changing the nature of the lipophilic block could also be of interest from an academic and industrial point of view. Polyisoprene was used throughout the academic study because there was more interest in varying the lipophobic block whilst maintaining a consistant lipophilic block. A simple modification would involve the use of polybutadiene

in place of polyisoprene. Whilst these polymers are very similar chemically, the slight change in molecular weight could give interesting differences upon self-assembly. Another, simpler, way to alter the tube diameter of the lipophilic block would be to prepare polyisoprene with a significantly different microstructure. In this thesis, polyisoprene was prepared by living anionic polymerisation in toluene which gave a predominantly 1,4 microstructure. By polymerising in a more polar solvent (e.g. THF) or with a polar additive, the 3,4 microstructure would become more prevalent. The 3,4 microstructure only has 2 carbon atoms in the backbone as opposed to 4 with the 1,4. Therefore it would be expected have a significantly different volume which should greatly impact on the nature of self-assembly. Other diene monomers which could be attractive for investigation are myrcene and farnesene which have the added benefit of being bio-derived monomers rather than fossil fuel-derived.

Another possible area of study with the lipophilic block is hydrogenation of the polydienes. This is a common industrial practice for improving oxidative stability of polydienes, which could be particularly beneficial for the high temperature lubricant applications which were investigated. The hydrogenation would also be likely to change certain physical and chemical properties, including crystallinity which could alter solubility of the polymer and affect the self-assembly behaviour. An alternative saturated, lipophilic polymer is polyisobutylene, which is generally prepared by cationic polymerisation. The preparation of end-capped polyisobutylene would offer a synthetic route via CHOMP towards analogous amphiphilic block copolymers which should also undergo self-assembly into micelles.

In the 'academic' study of PI-*b*-PDMAEMA, the tertiary amine of the methacrylate was quaternised with several different alkyl iodides. This was found to change the properties of the core-forming block sufficiently to change the morphology of micelles formed when dispersed into non-polar solvents. This investigation could be expanded greatly with, for example, different alkyl halides. Different isomers of the alkyl iodides should result in the formation of branched, quaternised species which could also have different impacts on the self-assembly behaviours. Moreover, different halogens could be used to determine their impact on the morphology of the micelles formed. Chloride anions are less bulky than iodides, so may have a smaller effect on the geometry of the polymers

being packed. Alternatively, the halide may not have a significant effect because they are not covalently bound to the polymer. These variations could also be applied to the quaternisation-induced self-assembly (QISA) of PI-*b*-PQDMAEMA in THF to broaden the understanding of the *in-situ* self-assembly.

During the applications testing of PI-*b*-PMMA and PI-*b*-PDMAEMA, the latter was found to be a particularly effective friction modifier for full lubricant formulations. This was believed to be because of the Lewis basic tertiary amine functionality which can adsorb strongly to the metal surfaces. Therefore, it could be useful to investigate methacrylic polymers containing other polar functional groups which have previously been shown to be effective for friction reduction such as morpholinylethyl methacrylate and ethylene urea methacrylate.[1] As discussed above, the versatility of the CHOMP procedure means that this can be easily changed with simple tweaks to the ATRP step.

The investigation into the synthesis and applications testing of polymeric friction modifiers culminated in the testing of maleinised and imidised polybutadienes which were prepared by a commercially-viable synthetic route. This novel synthetic route offers many opportunities for further investigation. The properties of maleinised polybutadiene could be altered by changes to the properties of the unfunctionalised polybutadiene. Most notably, it would be useful to vary the total molar mass of the polymer. This could be achieved by a simple variations to the polymerisation protocols but could result in an improved solubility in lubricant formulations and potentially an improved friction performance. An alternative method to improve solubility could be to decrease the wt% of maleinisation. During the investigation, only those polymers maleinised to 10 wt% were tested as friction modifiers, however, there could be a benefit to reducing this amount. This could be achieved simply by varying the amount of maleic anhydride used in the maleinisation reactions.

In an attempt to prepare blocky, maleinised polybutadienes, the microstructure was controlled during the living anionic polymerisation of butadiene. The selective maleinisation reaction was then attempted with the aim that the 1,4-rich block of polybutadiene would be maleinised in preference to the 1,2-rich block, thus enabling the preparation of amphiphilic blocky copolymers. Maleinisation has been shown to be selective for the 1,4 microstructures in the literature,[2, 3] however during this investigation,

the selectivity of the maleinisation was not definitively proven because of the overlapping of peaks in the NMR spectrum for the alkenes in polybutadiene before and after maleinisation. The selectivity of the maleinisation reaction could be further investigated. A simple way to investigate the selectivity would be to increase the degree of maleinisation from 10 wt% to 100 mol%. This would make any changes in the proton NMR much clearer which could then be used to elucidate the selectivity. This could then be used to infer how blocky the maleinised polybutadienes are.

Should the selectivity of the maleinisation reaction be confirmed, this should prove the formation of blocky maleinised polybutadiene. However, the actual microstructures of the microstructure block of polybutadiene were not 100 % in each block. The 1,4-rich block was 88 % 1,4 microstructure and the 1,2-rich block was 46 % 1,4. Therefore, the selectivity of the maleinisation reaction for the 1,4 microstructure resulted in the formation of random copolymers with maleinisation also taking place with the 1,4 microstructure in the 1,2-rich block. To enhance the formation of blocky copolymers, it may be necessary to synthesise microstructural block copolymers of polybutadiene with constituent blocks which are closer to 100 % 1,4 and 100 % 1,2, respectively. On a smaller scale, Polysachinda *et al.* have reported the preparation of blocks with 91 % 1,4 and 94 % 1,2 in the respective blocks of polybutadiene.[4] However, this route may not be feasible for commercial scale up because of the high cost of the 1,2-dipiperidinoethane additive necessary to promote a high 1,2 content in the latter block. Nevertheless, an investigation into the preparation of block copolymers by post-polymerisation maleinisation would be of considerable interest in an academic context, and also with a view towards potential industrialisation.

Following maleinisation, the anhydride functional groups bound to polybutadiene, were reacted with DMAPA for the preparation of imides with a pendant tertiary amine. DMAPA could be swapped for other reagents to give polymers with different pendant functional groups such as morpholine, which has previously been proven to be useful for friction reduction.[1] Morpholine could be introduced by reaction of the maleinised polybutadienes with *N*-(3-aminopropyl)morpholine to form imides in a similar fashion to the reaction with DMAPA described above. This method could allow for a simple investigation of the effect on friction reduction of different functional groups bound to polybutadiene, all of which could be prepared by commercially-viable synthetic methods.

Alternative strategies for preparing amphiphilic block copolymers in a more commercially-relevant fashion could include alternative polymerisation mechanisms used in CHOMP. Hydroxyl-end-capped polyisoprene used in the preparation of ATRP macroinitiators could themselves serve as macroinitiators for ring-opening polymerisation of cyclic esters such as ε-caprolactone or D,L-lactide. This would avoid the bromoacetylation step in CHOMP and also results in polyesters which are biodegradable.

Another synthetic route investigated was the ATRP of dienes, which is typically uncontrolled because of the poor solubility of the metal catalyst and the slow rate of propagation.[5-7] The low boiling point of 1,3-butadiene and 1,3-isoprene means that these issues cannot be addressed by carrying out the reactions at high temperatures. Myrcene is an alternative, bio-based diene that has frequently been investigated using living anionic polymerisation. It has a far higher boiling point which would allow for the ATRP to be carried out at high temperature. During this project, polymyrcene was produced by ATRP in bulk with a modest amount of control of the molar mass and dispersity. This could allow for the preparation of amphiphilic diene-based block copolymers by a single ATRP mechanism rather than CHOMP, however, further study would be required to control the synthesis of polymyrcene by ATRP and explore the potential for the preparation of block copolymers.

7.3. References

1. J. Fan, M. Muller, T. Stohr, H. A. Spikes, *Tribol. Lett.*, 2007, **28**, 287-298.
2. F. Ferrero, M. Panetti, G. B. Saracco, *Chim. Ind.*, 1984, **66**, 3-6.
3. F. Ferrero, *J. Therm. Anal. Calorim.*, 2004, **76**, 1057-1067.
4. S. Poshyachinda, H. G. M. Edwards, A. F. Johnson, *Polymer*, 1991, **32**, 334-337.
5. K. Matyjaszewski, *Macromolecules*, 2012, **45**, 4015-4039.
6. Y. F. Zhu, F. J. Jiang, P. P. Zhang, J. Luo, H. D. Tang, *Chin. Chem. Lett.*, 2016, **27**, 910-914.
7. J. Wootthikanokkhan, M. Peesan, P. Phinyocheep, *Eur. Polym. J.*, 2001, **37**, 2063-2071.